

White, Friend or Foe?

Understanding and predicting photocatalytic degradation of modern oil paintings

van Driel, Birgit

DOI

[10.4233/uuid:a64b7f31-a45b-4868-8978-70256e2ecb4f](https://doi.org/10.4233/uuid:a64b7f31-a45b-4868-8978-70256e2ecb4f)

Publication date

2018

Document Version

Final published version

Citation (APA)

van Driel, B. (2018). *White, Friend or Foe? Understanding and predicting photocatalytic degradation of modern oil paintings*. [Dissertation (TU Delft), Delft University of Technology].
<https://doi.org/10.4233/uuid:a64b7f31-a45b-4868-8978-70256e2ecb4f>

Important note

To cite this publication, please use the final published version (if applicable).
Please check the document version above.

Copyright

Other than for strictly personal use, it is not permitted to download, forward or distribute the text or part of it, without the consent of the author(s) and/or copyright holder(s), unless the work is under an open content license such as Creative Commons.

Takedown policy

Please contact us and provide details if you believe this document breaches copyrights.
We will remove access to the work immediately and investigate your claim.

Titanium white, Friend or Foe?

Understanding and
predicting photocatalytic
degradation of
modern oil paintings.

Proefschrift

ter verkrijging van de graad van doctor
aan de Technische Universiteit Delft,
op gezag van de Rector Magnificus
Prof. dr. ir. T.H.J.J. van der Hagen;
voorzitter van het College voor Promoties,
in het openbaar te verdedigen op
woensdag 9 mei 2018 om 15:00 uur

door Birgit Anne van DRIEL

Master of Science in Materials Science & Engineering
École Polytechnique Fédérale de Lausanne, Zwitserland
geboren te Heemstede, Nederland

This dissertation has been approved by the promotors:
Prof. dr. J. Dik and Prof. dr. K.J. van den Berg

Composition of the doctoral committee:

Rector Magnificus	chairman
Prof. dr. J. Dik	Delft University of Technology
Prof. dr. K.J. van den Berg	Cultural Heritage Agency of the Netherlands/University of Amsterdam

Independent members:

Prof. dr. E. Hendriks	University of Amsterdam
Prof. dr. I.M. Richardson	Delft University of Technology
Prof. dr. ir. J. Sietsma	Delft University of Technology
Dr. C. Miliani	CNR-ISTM, University of Perugia
Dr. A. Martins	Museum of Modern Art, New York

Other members:

Prof. A.N. Davies	AkzoNobel/University of South Wales
-------------------	-------------------------------------

The entire project was funded by AkzoNobel, as a sponsor of the Rijksmuseum, and supported by the staff and instrumentation at the AkzoNobel Specialty Chemicals research site in Deventer, the Netherlands.

Part of the research (chapter 2) was additionally funded by the European Union Horizon 2020 research and innovation programme under grant agreement No. 654148 Laserlab-Europe.

This Ph.D. is a joined project between the Rijksmuseum, Delft University of Technology, the Cultural Heritage Agency of the Netherlands and AkzoNobel. It is also an individual partner project of NICAS.

Prof. dr. P.J. Kooyman of University of Cape Town has contributed greatly to the preparation of this dissertation.

Designed by: Irma Boom Office
Printed by: Lenoirschuring

Copyright © 2018 by B.A. van Driel
ISBN/EAN: 978-94-6186-922-7

An electronic version of this dissertation
is available at <http://repository.tudelft.nl/>.

Summary/Nederlandse samenvatting	9	Part 3	225
Preface	17	Predicting degradation by titanium white pigments	
How to read this thesis?	21		
Introductions and project approach	25	Approach	227
A General introduction	27	Chapter 6	229
B Goal and project approach	39	A quick assessment of the photocatalytic activity of TiO ₂ pigments – From lab to conservation studio!	
C Introduction to part 1: Characterization of the properties and use of titanium white	43	Chapter 7	255
D Introduction to part 2: Understanding and monitoring of the degradation process	51	Determining the presence of photocatalytic titanium white pigments via paint sample staining: a proof of principle.	
E Introduction to part 3: Prediction of degradation	59	Conclusions, scientific outlook & impact on society	281
F Introduction to risk analysis and management	63	G General conclusions and discussions from this Ph.D.	283
References	65	H Scientific outlook, what's next?	291
Part 1	77	I Implications for conservation practice and collection care strategies	295
Characterization of the use and properties of titanium white pigments		J In the context of conservation science and beyond...	301
		Back matter	311
Approach	79	List of acronyms	313
Chapter 1	83	List of descriptions	315
The white of the 20th century – a broad XRF survey into Dutch modern art collections.		Description of supplementary material	323
Chapter 2	109	Dissemination of research	325
Investigating the complex photoluminescence behaviour of titanium white pigments.		TEDxDelft award talk	329
Part 2	133	Acknowledgements	333
Understanding and monitoring the degradation process of titanium white containing oil paints		Curriculum Vitae	339
Approach	135		
Chapter 3	139		
Determination of early warning signs for photocatalytic degradation of titanium white oil paints by means of surface analysis.			
Chapter 4	163		
Investigating the photocatalytic degradation of oil paint using ATR-IR and AFM-IR.			
Chapter 5	187		
Investigating the effect of artists' paint formulation on degradation rates of TiO ₂ -based oil paints.			
Chapter 5B	213		
Applicability of DoE for cultural heritage research.			

SUMMARY

This dissertation presents a study into the ultraviolet irradiation-initiated degradation phenomena occurring in titanium white containing oil paints, commonly referred to as photocatalytic degradation. The topic of this thesis can be summarized as: the (photocatalytic) properties of titanium white pigments in oil paints and their consequences for collections containing modern art. The thesis consists of three parts: 1) characterization of the use and properties of titanium white pigments, 2) understanding and monitoring the degradation of titanium white containing oil paints and 3) predicting degradation caused by titanium white pigments. Combining the results of these three parts leads to a risk management strategy for modern art collections presented as a conclusion of this thesis.

Titanium white pigments were introduced in the 20th century as an alternative for lead white and zinc white. The pigments underwent a gradual development resulting in a large variety of pigments available throughout history. This variety ranges from very photocatalytic or 'bad' pigments, which severely speed up degradation, to photostable or 'good' pigments which can protect their environment from UV irradiation. Both 'good' and 'bad' pigments found their way into artist materials and thus into paintings. Hence the question '*Titanium white, Friend or Foe?*'. The pigment's photocatalytic activity is highly dependent on the pigment's crystal structure (rutile or anatase) and (inorganic) surface treatment. When a pigment is photocatalytic, radicals can form upon

NEDERLANDSE SAMENVATTING

In dit proefschrift wordt een onderzoek gepresenteerd naar UV-geïnitieerde degradatie die plaatsvindt in titaanwittende olieverfschilderijen, beter bekend als fotokatalytische degradatie. Het onderwerp van mijn promotieonderzoek kan samengevat worden als: *de (fotokatalytische) eigenschappen van titaniumwitpigmenten en de gevolgen daarvan voor collecties van moderne kunst*. Het proefschrift is opgesplitst in drie delen: 1) het karakteriseren van het gebruik en de eigenschappen van titaanwit pigmenten, 2) het begrijpen en monitoren van degradatie in titaanwittende olieverven en 3) het voorspellen van degradatie door titaanwitpigmenten. De combinatie van de resultaten uit deze drie delen, leidt tot een risicomanagementstrategie voor collecties met moderne kunst.

Titaanwitpigmenten werden in de twintigste eeuw geïntroduceerd als alternatief voor loodwit- en zinkwitpigmenten. De ontwikkelingen van titaanwitpigmenten hebben als resultaat een grote variatie aan pigmenten op de markt, met verschillende eigenschappen. Deze variatie omvat zeer fotokatalytische ('slechte') pigmenten, die UV-degradatie kunnen versnellen, maar ook fotostabiele ('goede') pigmenten, die UV-degradatie kunnen voorkomen of vertragen. Zowel 'goede' als 'slechte' pigmenten zijn in kunstenaarsmaterialen, en daarmee in schilderijen, terechtgekomen, vandaar de vraag '*Titaanwit, Vriend of Vijand?*'. De fotokatalytische activiteit van het pigment is onder andere afhankelijk van de kristalstructuur (rutil of anatase) en van de (anorganische) oppervlaktebehandeling van het pigment. Als een

UV irradiation, which attack the oil binding medium and break it down to volatile components, leading to an effect called chalking: the pigment is unbound on the paint surface.

Interestingly, while we know that ‘bad’ TiO₂ pigments were used in modern oil paints, photocatalytic degradation problems have not been widely reported thus far. Several hypotheses for the lack of problems in collections are presented and investigated in this thesis. Additionally, characterization tools, predictive tools, and monitoring tools are developed, in order to provide solutions before it is too late. Simultaneously, analytical methods and research approaches, that are uncommon in the field of conservation science are explored to evaluate their applicability in answering cultural heritage research questions.

The tested hypotheses are:

- Photocatalytic titanium white was not commonly used in (oil) paintings {chapter 1}.
- The degradation process is slow due to low UV exposure in art collections {chapter 3-5, I}.
- Other components in the paint influence the degradation and perhaps slow it down or prevent it {chapter 5}.
- The degradation phenomena are not yet visible, conservators do not know what to look for, or both {chapter 3, 4}.

The developed tools are

- The absence of niobium in pXRF analysis as an indication for presence of rutile and as a dating tool {chapter 1}.
- Using the distinct photoluminescence of rutile and anatase as an

pigment fotokatalytisch is, kunnen radicalen worden gevormd door blootstelling aan UV-licht, waardoor het bindmiddel (gepolymeriseerde drogende olie) wordt afgebroken tot volatile componenten, wat zorgt voor een effect dat we verkrijting noemen: het pigment bevindt zich los op het verfloppervlak.

Ondanks dat we weten dat ‘slecht’ titaanwit is gebruikt in moderne olieverven, worden degradatieproblemen bij dit soort verven nog niet vaak gerapporteerd. Daarom hebben wij een aantal hypotheses opgesteld, die in dit proefschrift getoetst worden. Daarnaast worden een aantal monitorings- en voorspellingsmethoden ontwikkeld, zodat de eventuele degradatie vastgesteld of voorspeld kan worden voordat het te laat is. Tegelijkertijd worden in dit proefschrift analytische technieken en onderzoeksbenaderingen, die relatief onbekend zijn voor het onderzoeksveld betreffende het cultureel erfgoed, gebruikt en geëxploreerd met betrekking tot hun nut voor het beantwoorden van vragen uit het veld.

De getoetste hypotheses zijn:

- Fotokatalytisch titaanwit werd niet vaak gebruikt in (olieverf-) schilderijen {hoofdstuk 1}.
- Het degradatieproces verloopt langzaam door de lage blootstelling aan UV-licht in kunstcollecties {hoofdstuk 3-5, I}.
- Andere componenten in de verf beïnvloeden de degradatie. Deze wordt mogelijk vertraagd of voorkomen {hoofdstuk 5}.
- De degradatiefenomenen zijn nog niet zichtbaar, restauratoren weten niet precies waar ze op moeten letten, of beide {hoofdstuk 3, 4}.

De ontwikkelde methodes zijn:

- De afwezigheid van niobium in

alternative, highly sensitive, non-invasive characterization method {chapter 2}. The detection of early warning signs of degradation by AFM, XPS or IR {chapter 3, 4}.

- A photocatalytic activity test for dry pigment or paint scrapings {chapter 6}.
- A photocatalytic activity test for pigments in a paint cross-section {chapter 7}.

The explored analytical methods and research approaches are:

- Atomic Force Microscopy (AFM) {chapter 3}.
- X-ray Photoelectron Spectroscopy (XPS) {chapter 3}.
- Atomic Force Microscopy coupled Infrared Spectroscopy (AFM-IR) {chapter 4}.
- Design of Experiments (DoE) {chapter 5 and 5B}.
- Transmission Electron Microscopy (TEM) {chapter 1, 2 and poster}.

In this research oil paint was the focus. However, the results can be partly extrapolated to other binding media such as alkyds, acrylics, resin-coated photographic paper, plastics and others.

Chapter 1 illustrates that titanium white became popular rather late in the Netherlands. While this suggests that more ‘good’ pigments were used, as they were on the market at that time, examples of ‘bad’ pigments were also found in oil paintings. The survey, carried out with portable X-ray fluorescence spectrometry (pXRF), also indicates the detection of niobium as an interesting trace element. Niobium is only present in pigments produced by the sulfate process. The more recent (1959) chloride process is mainly used

pXRF analyse als indicatie voor de aanwezigheid van rutiel en te gebruiken als dateringsmethode {hoofdstuk 1}.

- Het gebruik van de onderscheidende fotoluminescentieprofielen van rutiel en anatase als alternatieve, gevoelige, non-invasieve karakteriseringsmethode {hoofdstuk 2}.
- Methodes voor de detectie van vroege tekenen van degradatie met AFM, XPS of IR {hoofdstuk 3, 4}.
- Een test voor de fotokatalytische activiteit van droog pigment of pigmenten in verfschraapsels {hoofdstuk 6}.
- Een test voor de fotokatalytische activiteit van pigmenten in een verfdwarsdoorsnede {hoofdstuk 7}.

De geëxploreerde analytische technieken en onderzoeksbenaderingen zijn:

- Atomic Force Microscopy (AFM) {hoofdstuk 3}
- X-ray Photoelectron Spectroscopy (XPS) {hoofdstuk 3}
- Atomic Force Microscopy coupled Infrared Spectroscopy (AFM-IR) {hoofdstuk 4}
- Design of Experiments (DoE) {hoofdstuk 5B}
- Transmission Electron Microscopy (TEM) {hoofdstuk 1, 2 en poster}

In dit proefschrift zijn de titaanwit-houdende olieverven onder de loep genomen; dit onderzoek kan echter gedeeltelijk geëxtrapolerd worden naar andere bindmiddelen zoals alkyd, acryl, fotopapier, plastics en andere.

for the production of rutile. Thus niobium may function as a marker for the pigment crystal structure (no niobium = rutile) and the date (no niobium = post 1959). This discovery illustrates an expansion of the current capabilities of pXRF. The importance of niobium is again noted in chapter 2 which presents the complex photoluminescence behavior of TiO₂ pigments. An interesting finding is that the presence of niobium in anatase pigments severely influences the photoluminescence spectrum. Furthermore, chapter 2 introduces an alternative, non-invasive method for the distinction between rutile and anatase.

During artificial aging experiments of simple pigment-binder paints in chapter 3 and 4, it became clear that the visible change (chalking) occurs suddenly and rapidly. Thus, it is likely that chemically the degradation process is ongoing, but that the visible phenomena are not discernible yet. Therefore, the chemical/physical changes that occur prior to visible changes were investigated with the aim to detect early warning signs of degradation. The changes were monitored with a range of analytical techniques such as gloss analysis, AFM, XPS, AFM-IR, ATR-FTIR. These methods all have their specific benefits and drawbacks mainly related to the need for sampling and to the measurement being absolute or comparative.

Chapter 5 reports an artificial aging study of titanium white oil paints with different compositions. This study reveals that the paint formulation has a strong influence on the photocatalytic degradation rate of the paints. Most formulations containing photocatalytic titanium white were found to eventually

Hoofdstuk 1 laat zien dat titaanwit pas redelijk laat, vanaf de jaren vijftig, populair werd in Nederland. Dit geeft aan dat het gebruik van 'goede' pigmenten, door schilders in die tijd, aannemelijk is, omdat deze toen al op de markt waren. Echter, voorbeelden van 'slechte' pigmenten zijn óók gevonden in olieverfschilderijen uit die tijd. De inventarisatie, uitgevoerd met draagbareröntgenfluorescentiespectrometrie (pXRF), leidde ook tot de identificatie van niobium als interessant sporenelement. Niobium is alleen aanwezig in pigmenten die geproduceerd zijn met het sulfaatproces. Het recentere (1959) chlorideproces wordt vooral gebruikt voor de productie van rutiel. Met andere woorden, niobium kan functioneren als een marker voor de kristalstructuur (geen niobium = rutiel) en als marker voor de datum (geen niobium = na 1959). Deze ontdekking breidt de huidige capaciteiten van pXRF uit. Het belang van niobium wordt ook aangestipt in hoofdstuk 2 over het complexe fotoluminescentiegedrag van titaanwitpigmenten. Een interessante vondst is dat niobium in anatase het fotoluminescentiespectrum sterk beïnvloedt. Daarnaast introduceert hoofdstuk 2 fotoluminescentie als alternatieve, non-invasieve methode voor het aantonen van rutiel of anatase.

Tijdens versnelde verouderingsexperimenten van simpele pigment-olieverven, in hoofdstuk 3 en 4, werd duidelijk dat de zichtbare verandering (verkrijting) plotseling en snel plaatsvindt. Het is daarom waarschijnlijk dat, chemisch gezien, de degradatie al plaatsvindt, maar dat de problemen lange tijd nog niet zichtbaar zijn. Daarom heb ik onderzoek gedaan naar de chemische/fysische veranderingen

degrade, with the exception of formulations containing enough photostable pigment, which acts as a UV scavenger.

With the knowledge that photocatalytic pigments have been used in oil paintings, that most formulations containing 'bad' TiO₂ will eventually chalk under UV exposure and that the developed monitoring methods {chapter 3 and 4} are expensive and high-tech; we aimed to develop a prediction test for photocatalytic activity. Two easy-to-use prediction tests for conservators are presented in chapter 6 and 7. The most promising method is described in chapter 7. This method is based on monitoring the color change of a photocatalytic activity indicator ink (PAII) applied on a paint cross-section. In the presence of a photocatalytic pigments, the ink changes color which can easily be recorded with a microscope. The method is spatially resolved, as only the paint layers containing photocatalytic pigments will show this color change. Thus, a tool is now available to quickly identify 'potential risk' paintings in modern art collections.

A risk assessment and management strategy is proposed in which identification of the 'potential risk' of objects is the first step, which is performed by assessing the vulnerability and value of objects. The vulnerability can be determined using pXRF and/or the ink test and the value is established by the stakeholders. Based on the 'potential risk', the composition of the collection and the aim of the collection corrective measures can be applied such as dark storage or UV removal on object or building level.

To conclude, although degradation is slower than expected and TiO₂ pigments

die plaatvinden voordat de verandering zichtbaar is. Dit is gedaan met verschillende analytische technieken zoals glansmetingen, AFM, XPS, AFM-IR en ATR-FTIR. Hiermee zijn verschillende veranderingen geïdentificeerd, die gemonitord kunnen worden als vroege detectie van degradatie. Alle methodes hebben voor- en nadelen. Deze zijn vooral gerelateerd aan de noodzaak om monsters te nemen van een schilderij en aan het verschil tussen absolute of vergelijkende metingen.

Hoofdstuk 5 toont aan dat verformulering (het recept) een sterke invloed heeft op degradatiesnelheden van de verf onder UV-licht. De meeste formuleringen waar fotokatalytisch titaanwit in zit, gaan uiteindelijk degraderen, met als uitzondering formuleringen die genoeg stabiel pigment bevatten, wat als UV-beschermers werkt.

Met de kennis dat fotokatalytische pigmenten gebruikt zijn in olieverven, dat de meeste formuleringen uiteindelijk leiden tot degradatie bij blootstelling aan UV en dat de methodes die ontwikkeld zijn in hoofdstuk 3 en 4 duur en hightech zijn, ontstond de wens (en de noodzaak) om een makkelijke voorspellingstest te ontwikkelen voor restauratoren. Twee ontwikkelde testen worden beschreven in hoofdstuk 6 en 7, waarvan de test in hoofdstuk 7 het meest veelbelovend is. Deze test gebruikt de zogenaamde 'photocatalytic activity indicator ink', eigenlijk ontwikkeld voor de analyse van zelfreinigende tegels en glas, op verfdwarsdoorsnede. Als een fotokatalytisch pigment aanwezig is, verandert de kleur van de inkt, wat simpel waargenomen kan worden met een microscoop. De methode is lokaal, omdat alleen verflagen waar het fotokatalytische pigment aanwezig is van

in the Netherlands were used later than expected, titanium white containing objects do form a potential risk in modern art collections. This research, especially due to the proposed risk assessment and management strategy, can contribute to the preservation of titanium white containing 20th century oil paintings for the future.

kleur veranderen. Hiermee is er nu een makkelijke test om snel schilderijen die kwetsbaar zijn te identificeren in collecties van moderne kunst.

Als synthese van alle resultaten stel ik een risicostrategie voor waarbij het toekennen van 'potentieel risico' de eerste stap is. Dit wordt gedaan door het vaststellen van de kwetsbaarheid en de waarde van objecten in een collectie. De kwetsbaarheid kan beoordeeld worden door gebruik te maken van pXRF en/of de inkttest en de waarde wordt vastgesteld door de verschillende belanghebbenden. Gebaseerd op het potentiële risico van objecten, de compositie van de collectie en het doel van de collectie kunnen corrigerende maatregelen getroffen worden zoals het opslaan van objecten in het donker of het reduceren van UV-straling op gebouw- of objectniveau.

Ondanks dat degradatie langzamer gaat dan we verwacht hadden en dat titaanwitpigmenten in Nederland later in gebruik zijn genomen dan we verwacht hadden, vormen titaanwit-houdende objecten toch een risico voor collecties van moderne kunst. Dit promotieonderzoek kan, met name door de voorgestelde methode voor risicoanalyse en management, ertoe bijdragen, dat titaanwithoudende kunstobjecten voor de toekomst ongeschonden behouden blijven.

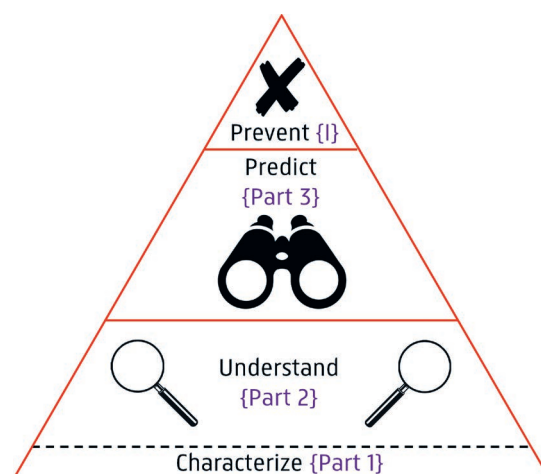
PREFACE

'Titanium white, Friend or Foe?' is an accurate title for this Ph.D. because titanium white pigments exist in a range of different qualities: from highly damaging to protective for their environment. The difference between these 'good' and 'bad' pigments ('Friends or Foes) is a recurring theme throughout this thesis.

The dissertation is divided into three parts: characterization of the use and properties of titanium white pigments, understanding and monitoring the degradation of titanium white containing oil paints and predicting degradation by titanium white pigments. This division followed naturally from a talk I held at the finals of the TEDxDelft awards (February 2016, back matter). In this talk, my main message was that rather than only researching known and manifested conservation problems, it is important to gain more insight into degradation processes, and with that into the risks that art collections face. I proposed the triangle, now referred to as the 'thesis triangle' to 'understand, predict and prevent' degradation, Figure 1. Before we can start understanding degradation processes, it is important to make an inventory of the materials used, which is why characterization plays an important role and was added to the triangle.

Prevention of titanium dioxide-mediated degradation is rather straightforward, and thus it is not described in a separate section of the thesis. As the process is initiated by ultraviolet irradiation, removing exposure will stop the degradation process from occurring. However, as this can be an expensive undertaking, which is a waste of resources in the case of 'good' TiO_2 , it is important to introduce a risk management strategy, which is discussed in the 'conclusions, scientific outlook and impact on society' section {I}. The thesis triangle will be a guide throughout the thesis.

Figure 1 Thesis triangle.



2 <https://www.nemokennislink.nl/publicaties/is-voorkomen-altijd-beter-dan-genezen/>

3 Bewer, F. G. (2010). A Laboratory for Art: Harvard's Fogg Museum and the Emergence of Conservation in America, 1900-1950, Harvard Art Museum.

4 <https://www.bcnepea.com/FindDoctorHospital/PreventiveDiagnostic.aspx>,

5 <https://www.hap.org/blog/2016/09/preventive-or-diagnostic>

6 <https://www.marketingfacts.nl/berichten/voorkomen-is-beter-dan-genezen-datainnovaties-in-de-gezondheidszorg>

7 <http://www.pbl.nl/dossiers/klimaatverandering/content/correctie-formulering-over-overstromingsrisico>

8 <https://www.vn.nl/dreiging-die-we-allemaal-onderschatten-wat-als-het-water-komt/>

9 <https://nos.nl/op3/artikel/2147604-ja-als-maar-kunnen-de-dijken-ook-echt-breken.html>

All URL's are accessed at 11-12-2017

The approach, illustrated in the thesis triangle, is built on the idea illustrated by the proverb that 'an ounce of prevention is better than a pound of cure'. In his Ph.D. thesis, Rik Peeters² places the introduction of preventive thinking in the Dutch government in the 1980s. Preventive thinking found applications in many aspects of our society, such as terrorism prevention, preventive health care, and flood prevention.

The analogy between health care and conservation science is not uncommon. Actually, the analogy was already used by Forbes in the beginning of the 20th century. Bewer states that '*He resorted to medical analogies [...] explaining, for instance, that in winter objects made of wood shrink in the dry air of heating systems just as our throats become dry when subject to cold*'. This analogy also led to the description of conservation problems in medical terms such as: tin pest, lead disease, glass sickness and ultramarine sickness³. Both fields are based on research into processes of change and the results are commonly used for diagnostics and treatment. Therefore we can extend this analogy to the theme of risk management. In health care, a distinction is made between preventive care and diagnostic care⁴. Preventive care can designate two different approaches. Either it indicates the use of simple tests or screening at the moment a patient is feeling healthy, or it relates to a healthy lifestyle to prevent illnesses. Diagnostic care, on the other hand, is performed to treat an existing condition. Interestingly, in the United States, a preventive visit is often completely covered by the insurance, while a diagnostic care visit often is not⁵. Another development notable in the health care field is the use of large datasets to get a better insight into illnesses. An example is recognizing dementia by machine learning which detects language issues by recognizing patterns. This method can identify (predict, if you will) dementia in an early stage, when several treatments may still be effective⁶. Thus, in other words, a combination of preventive measures, as well as early detection, are important aspects when it comes to our health and should be important in cultural heritage as well.

Another example is flood prevention. This is an important topic in the Netherlands, as 26% of the country is below sea level, and an additional 29% is sensitive for river floods⁷. The current policy is based on probability calculations accepting a break-through once in 10.000 years. However, developments of advanced mathematical models, which can predict floods and their consequences in a more accurate way, render flood defense more targeted. In the case of flood defense management, in addition to the preventive approach, procedures for disaster control, such as evacuation plans, are in place^{8, 9}. Similar to health care, prevention alone is

not enough: monitoring the current situation is of high importance as well. In the Netherlands, all water levels of the sea, rivers, and lakes are continuously monitored¹⁰. Furthermore, upcoming storms are forecast in order to take appropriate measures. Finally, the quality of the dykes themselves is monitored with modern sensing equipment, for example, to evaluate an effect called 'piping' wherein small channels and bubbles are formed in the dyke, compromising its integrity¹¹.

How does preventive thinking relate to cultural heritage preservation? In the Netherlands there are protocols in place to predict calamities that can occur unexpectedly, such as fire, floods, theft or vandalism. However, continuous problems such as wear or degradation are not covered by these guidelines for risk management and preventive measures. While several steps are being taken within the field of cultural heritage {F, J} in order to be more aware of slow risk, this is not in the same stage of maturity as it is in health care, flood prevention and other areas of society. Taking the cultural and financial importance of cultural heritage for society under consideration, it seems to me that preventive thinking needs to be incorporated more into cultural heritage science and management. For this type of change to take place, it is important to raise awareness. Thus, the translation between theory and practice and between high-tech and low-tech was very important to me during this Ph.D. research. In an applied field such as conservation science, the end users (of tools and information) always needs to be kept in mind. In my opinion, this does not mean dismissing all fundamental studies, nor does it mean only focusing on object diagnostics and phenomenology. Rather, it means both aspects should be kept in mind and, whenever possible, a bridge should be built between theory and practice, while keeping in mind that this is a two way street.

The thesis triangle, focusing on investigating the TiO₂ degradation process and proposing a risk management strategy, is the main approach of this Ph.D thesis. To achieve my goals, I was additionally motivated to explore a range of research approaches and analytical techniques less commonly used in our field of research. These methods were only available to me due to the highly collaborative nature of my project involving a museum (the Rijksmuseum), a university (Delft University of Technology), a research institute (the Cultural Heritage Agency of the Netherlands) and an industrial partner (AkzoNobel). I want to use this preface to motivate researchers in our field to think outside the box, to go out into the world and to start collaborations with university and industry because this will catalyze progress.

Enjoy!

10 <https://www.rijkswaterstaat.nl/water/waterbeheer/bescherming-tegen-het-water>

11 <https://www.nemokennislink.nl/publicaties/televisieserie-als-de-dijken-breken-zeer-realistisch/>

All URL's are accessed at 11-12-2017

HOW TO READ THIS THESIS

The thesis triangle, Figure 1, will be shown at the beginning of the different parts of the thesis, to highlight where you are. All chapters in this dissertation, except chapter 5B, are published papers or submitted manuscripts and therefore their reference list is formatted according to the requirements of the journal they were published in or submitted to. Because the chapters are directly related to published papers/submitted manuscripts, the thesis has repeated content. This is especially the case for the introductions and references. We chose to accept these repetitions in the thesis to make sure that the chapters and parts can be read as separate entities. In the front matter and sections G to J references are recorded in footnotes. Footnotes, figures, and tables are continuously numbered throughout A-J, paper specific numbering is used in the chapters.

A list of acronyms as well as a terminology list are included in the back matter of this thesis.

Given the length of this dissertation the supplementary material of the papers/manuscripts will not be printed in hard copy. As all chapters with supplementary material have been accepted for publication, the supplementary material can be accessed online.

Part 1, 2 and 3 all start with a specific project approach discussing the choices that were made for that part of the research. These sections are not numbered. The core of the dissertation (excluding front and back matter) has the following build up:

- Introductions and project approach
 - This part is numbered A-F and contains the general introduction {A}, the project approach {B}, the three part specific introductions {C-E} and an introduction to risk management {F}.
- Part 1: Characterization of the use and properties of titanium white pigments.
 - Part one contains chapter 1 and chapter 2.
- Part 2: Understanding and monitoring the degradation process of titanium white containing oil paints.
 - Part two contains chapter 3, chapter 4, chapter 5 and chapter 5B. Chapter 5B was not submitted for publication.
- Part 3: Predicting degradation by titanium white pigments.
 - Part three contains chapter 6 and chapter 7.

- Conclusions, scientific outlook and impact on society.
This part is numbered G-J and it contains an overview of all the most important results {G}, a scientific outlook {H}, a risk management strategy {I} and a discussion about the placement of my work within the scope of cultural heritage {J}.

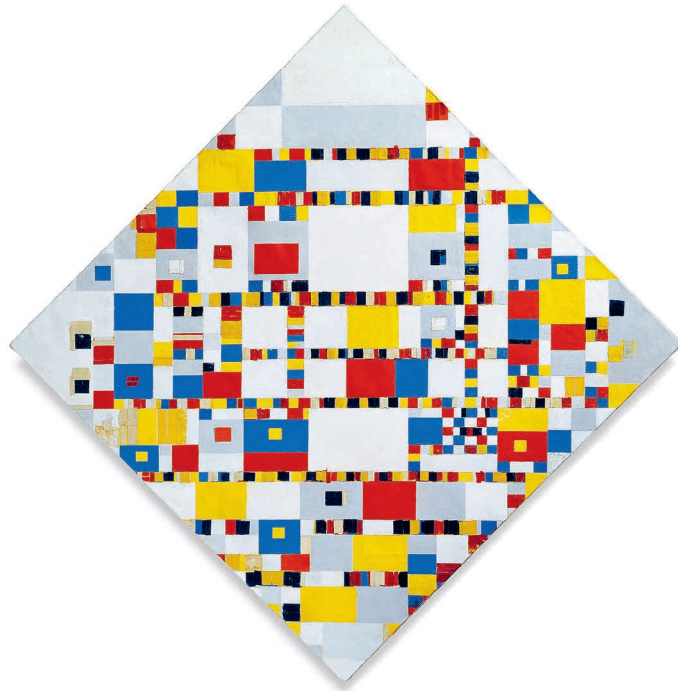
This dissertation is aimed to serve several audiences: friends, curators, conservators, and scientists. Thus aiming to bridge theory and practice, the thesis can be read in different ways:

- Reading the preface, the general introduction {A}, the project approach {B}, and the part of the conclusions {I and J} will give you a superficial but complete overview of the entire project.
 - Additionally reading conclusions part G will also illustrate all the main results.
- Depending on your interest (e.g. theory: part 2, practice: part 3) you may decide to read each of the three parts separately. The parts all have a specific introduction {C-E}.
- As the thesis is paper-based, each chapter includes its own introduction and conclusions. Thus the chapters can be read as separate entities.

INTRODUCTIONS & PROJECT APPROACH

A	TITANIUM WHITE, FRIEND OR FOE? GENERAL INTRODUCTION	27
A.1	Art & the meaning of white	27
A.2	Titanium white pigments	28
A.3	Titanium white oil paint	33
A.4	The photocatalyst at work	33
A.5	So what?	37
B	GOALS & PROJECT APPROACH	39
C	INTRODUCTION TO PART 1 Characterization of the use and properties of titanium white pigments	43
C.1	TiO ₂ market and occurrences in works of art and archives	43
C.2	Main characteristic properties influencing photocatalytic activity	44
D	INTRODUCTION TO PART 2 The understanding and monitoring of the degradation process of titanium white containing oil paints	51
D.1	Photocatalysis	51
D.2	The role of light in photocatalysis	52
D.3	Other environmental conditions and their role in photocatalysis	53
D.4	Components in oil paint	53
D.5	Paint film characteristics	56
D.6	Artificial aging studies	57
E	INTRODUCTION TO PART 3 Predicting degradation by titanium white pigments	59
E.1	Direct methods to test photocatalytic activity	59
E.2	Indirect methods to test photocatalytic activity	61
F	INTRODUCTION TO RISK ASSESSMENT AND MANAGEMENT	63

Figure 2 Piet Mondriaan, Victory Boogie Woogie, 1942-44, Gemeentemuseum, Den Haag.



13 Piero Manzoni – Reprinted in *Monochromes* p. 188 from *Malevich to the present* (Barbara Rose, eds: valeria varas, raul rispa) University of California press 2006 – From *Libera dimensione Azimuth no 2* (1960) unnumbered.

‘A white that is not a polar landscape, not a material in evolution or a beautiful material, but a sensation or a symbol or anything else; just a white surface that is simply a white surface and nothing else [...], or better still, a surface that simply is: to be [...].’¹³

– Piero Manzoni

14 Kazimir Malevich - Moholy-Nagy, Lazslo, *The new vision*, New York: B. Wittenborn, 1947, Reprinted in *Monochromes* p. 188 from *Malevich to the present* (Barbara Rose, eds: valeria varas, raul rispa) University of California press 2006.

‘I have transformed myself in the zero of form and have fished myself out of the rubbishy slough of academic art. I have destroyed the rig of the horizon and got out of the circle of objects, the horizon ring that has imprisoned the artist and the forms of nature.’¹⁴

– Kazimir Malevich

A. TITANIUM WHITE, FRIEND OR FOE? GENERAL INTRODUCTION

Titanium white is the whitest of white pigments [1-3]. The pigment was marketed in the early 20th century and was used abundantly ever since for a wide range of application. The pigments underwent a long development process, which resulted in a large variety of pigments available on the market. In 1985 there were no less than 580 individual grades of titanium white pigments for sale [4]. As a pigment, titanium white is said to have quickly replaced the toxic lead white and zinc white [4]. As a versatile material, not just for pigments, but for other applications as well {A.4.2}, titanium dioxide has been of significant research interest in the past century [5-12]. Depending on its characteristics, titanium dioxide can be a stable UV absorber or a photocatalyst (PC) {A.4, C.2, D.1}. For pigments used in paintings, high photocatalytic activity (PC activity) is a bad property since it can cause degradation. Different qualities of titanium white pigments found their way into artists materials and thus into paintings, hence the question *‘Titanium white, Friend or Foe?’*. In other words, titanium dioxide is a complex material, introduced in an age of rapid technological development which will possibly have detrimental effects on the material condition of modern art objects in the future. Therefore, this thesis focusses on *‘Understanding and predicting photocatalytic degradation of modern oil paintings’*.

A.1. Art & the meaning of white

The story of titanium white is linked to the story of the twentieth century. It was the century of Albert Einstein and great technological achievements, of shattering world wars and nationalism. On the other hand, it was also the century of modern art & architecture: *‘Art for the purpose of art’*.¹⁵ Within this framework, Le Corbusier popularized white in his modernist architecture of the 1920s and with Kazimir Malevich’s suprematism painting *‘White on white’* (1918), white became a defining icon of modernism [13, 14]. Several radical events that changed the art world can be identified such as the *‘invention of abstraction’* (1913) and the publication of Lucio Fontana’s *Manifesto Blanco* (1946), in which he states: *‘new art that is in greater harmony with the needs of the spirit in an age in which the painted canvas and the standing plaster figure no longer have any reason to exist’* [15]. From 1958 to 1966 the ZERO movement played an important role in the art scene. Their aim was to prevent any visible role of the artist in/on their art. The artwork was purely about the materiality and the world in which it exists [16]. In this objective context, white was a highly suitable color to use (Figure 3).

15 A 19th Century expression related to modernism - *‘L’art pour l’art’* in French.

Figure 3 Personal photograph, taken at 'ZERO, Let us explore the Stars' at the Stedelijk Museum Amsterdam (2015), illustrating the role of white in the ZERO movement.

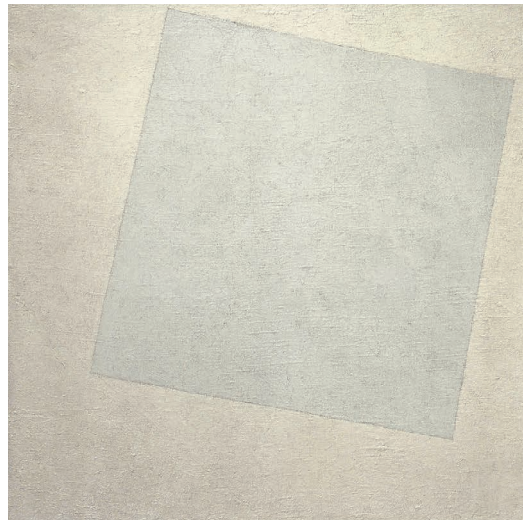


Because the clean and untouched surface of these paintings plays an important role for their meaning, natural aging, commonly accepted and even appreciated in earlier artwork, is a topic of discussion [17]. The acceptance of these aging effect, known as patina, in modern art and the ethics related to treating or accepting these changes fall outside the scope of this work but are interesting to keep in mind [18]. It is also in this setting, that the first modern American art movements came up, such as Abstract Expressionism with Jackson Pollock and Willem de Kooning, Color Field Painting with Barnett Newman and Mark Rothko and Pop Art with Jasper Johns, Roy Lichtenstein, and Andy Warhol: All known users of titanium white {C.1} [4].

A.2. Titanium white pigments

In November of the year that Kazimir Malevich painted 'White on white' (1918, Figure 4), industrial production of titanium white composite pigments began in Fredrikstad in Norway.

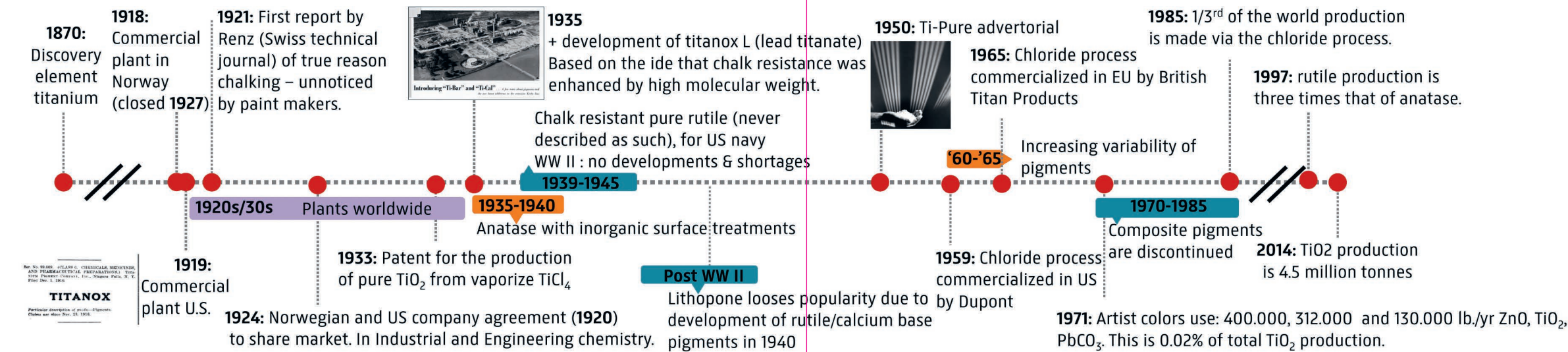
Figure 4 Kazimir Malevich, White on white, 1918, Museum of Modern Art, New York



A year later, in 1919, full scale production of composite TiO_2 pigments started in Niagara Falls, New York [4]. Around the same time, health and safety issues related to lead white were discovered, eventually leading to banning or restricting the use of lead white.¹⁶ However, a full ban of lead white for outdoor painting and artworks only came as late as 2009 in the Netherlands [19-21]. Additionally, war shortage of lead white forced artists to look into alternative white pigments, such as the recently developed titanium white [1, 22]. This is what Piet Mondriaan faced when he painted the Broadway Boogie Woogie and Victory Boogie Woogie (Figure 2) in the early 1940s in New York. Both paintings contain titanium white, despite Mondriaans complaints about its properties [22, 23]. The history of titanium white has been documented in detail [1, 4, 24-26] and while it is ambitious to visualize the complex TiO_2 development, Figure 5 presents a timeline of the main events towards developing the stable pigments available today. The most important developments were the ability to produce pure rutile pigments as opposed to the other common polymorph anatase, the development of the chloride process and the introduction of pigment coatings which significantly reduce photocatalytic activity {C.2} [25]. It cannot be stressed enough, that pigments with inferior properties are still on the market today and are for instance used in gouache [27]. It is interesting to note that in 1971 only 0.02% of the entire TiO_2 production was used for artists materials [4]. As a niche market, artists' materials, cannot be directly related to general pigment developments. Two statements to that end are included in artists pigments [4], referring to the 1930s. First Laver notes that 'Artists color makers were slow to introduce the new pigment in their productions.' and second she notes that 'Due to their greater whiteness early products based on anatase were retained for many years after rutile pigments were introduced' [4]. The latter statement is supported by personal contact with European color makers Winsor and Newton and Royal Talens, that make the transition from anatase to rutile for oil paints in the 1970s and 1990s respectively [28]. Finally, an important realization is that paint manufacturers do not produce titanium white themselves. Thus, the quality of the pigment they receive is dependent on the pigment manufacturer. As stated by Laver: 'In the early years of development of anatase and rutile-based pigments, production difficulties often resulted in [...] or a mixture of both forms' [4]. An example is that XRD showed the presence of both rutile and anatase in a 1980s Talens paint tube, while supposedly only anatase was used [27].

The discussion about which white is better has continued since the days and complaints of Mondriaan [22, 29]. Contemporary

Figure 5 TiO₂ development timeline based on [1, 4]



17 Often noted on the paint tube as PW6 + PW4. PW6 is TiO₂, PW4 is ZnO.

artist still do small test to compare paint characteristics [30, 31]. All pigments have their own benefits and drawbacks in oil paints. Lead white is toxic but has brilliance, a nice consistency and a faster drying time. Titanium white has high opacity, but is said to have a higher tendency to yellow, and zinc white is beneficial for its higher transparency and lower price but has the tendency to dry to a brittle film [3]. The price of pigments has likely played a role in the choice of white pigments and, considering the current price increase of titanium white, will play a role again. However, this falls outside the scope of this thesis. Combining titanium and zinc white leads to non-brittle and opaque formulations, additionally countering concerns about yellowing [32]. Therefore, most contemporary titanium white oil paints also contain zinc white¹⁷. Soap formation, a stabilizing as well as degrading phenomenon, in some lead and zinc whites [1, 33, 34] does not occur in titanium white [1, 4].

A.3. Titanium white oil paint

According to the Oxford dictionary, a paint is [35]:

‘A colored substance which is spread over a surface and dries to leave a thin decorative or protective coating’.

Paint in its most simple form contains pigment {A.2, D.4.3} and binder (or binding medium) {D.4.1}. Pigments need to be evenly dispersed into the binder and are used to give color and opacity to the paint. On the other hand, the binder is used to bind the pigment together and bind the pigment to the chosen surface such as the panel or the canvas [36]. This dissertation focusses on oil paints. Nevertheless, similar studies are of interest for other binders in which titanium white is used. In addition to pigment and binder, paint can contain other components such as secondary pigments, extenders, and additives which may influence the paint behavior {D.4}. Extenders are generally cheaper than pigments and are added to lower the price of paint or to adjust the tinting strength of the paint. Zinc white is often added to titanium white paints to reduce yellowing or improve drying behavior [37, 38]. Additionally, blue pigments are sometimes added as optical whiteners as is the case for Permalba titanium white, which contains ultramarine pigments [32]. Finally, additives can be added such as driers (bulk or surface driers, often based on transition metals), wetting agents, shelf life extenders, anti-flocculation agents and many others. Common additives to 20th century oil paints are metal stearates. Particularly aluminum stearate was used in the 20th century [39]. A metal stearate is composed of a long fatty acid chain, such as stearic acid, with a multivalent metal at the end [40]. In oil paints, these metal stearates or metal soaps can alternatively form on their own in the reaction of zinc or lead white with fatty acids [41].

A.4. The photocatalyst at work

Immediately after their introduction onto the market, titanium white pigments presented some, badly understood, degradation problems in paints [1, 42]. These problems are related to the pigments photocatalytic activity (PC activity) that originates from its semiconductor properties. Multiple inorganic pigments, including titanium white and zinc white, fall in the category of semiconductors based on their bandgap (which can be overcome by photons of at least that energy). For ZnO and TiO₂, the band gap lies in the UV region, and absorption of UV light can lead to the acceleration of several processes via photocatalysis [4, 43, 44].

A.4.1. Photocatalysis

The mechanism of photocatalysis {D.1}, Figure 6, is based on absorption of UV light, which causes the excitation of an electron to the conduction band and a remaining hole in the valence band. In other words, an e^-/h^+ pair is formed. The electron and hole may recombine and emit heat, in this case, the titanium dioxide acts as a UV scavenger/absorber. In an alternative process, the charge carriers can migrate to the particle surface, where reactions take place with surface absorbents such as H_2O and O_2 [45, 46]. Reactive radicals are formed by these reactions, which in turn can react with (organic) material present in their surrounding (e.g. pollutants, polymers, paint binder such as oil, organic colorants). The ratio of absorbed photons that lead to recombination, compared to those that lead to radical formation, determines the photocatalytic activity. If UV absorption leads to degradation or protection is dependent on the pigments photocatalytic activity as well as the UV sensitivity of the surrounding material.

Photocatalytic activity is dependent on many pigment characteristics such as crystal structure, surface treatment, particle size and surface area and defect structure {C.2}.

A.4.2. Applications of photocatalytic activity

Photocatalytic reactions can lead to degradation of the surrounding material, which for a paint can be problematic as the painting would attack itself {A.4.3, A.4.4}. Paint is not the only application in which photocatalytic activity is a drawback. TiO_2 is also a very common component in sunscreen [44] and many cosmetic products, in which it is also required to be UV stable, Figure 6. On the other hand, photocatalysis can also be exploited to our benefit, Figure 6. The industrial potential of TiO_2 as a catalyst motivated a lot of research and resulted in many possible applications such as self-cleaning paints (controlled chalking) [10, 11], water purification systems [47], air-purification [45, 48-50] and degradable TiO_2 -pigmented plastics [12, 51].

A.4.3. Potential problems in paint caused by photocatalytic activity

Photocatalytic pigments can accelerate the degradation of their surroundings upon UV irradiation. This can cause, among others, the degradation of surface dirt (Figure 7A, exploited in self-cleaning paint) or the degradation of the binding medium. While a self-cleaning painting may sound tempting, and controlled binder degradation (chalking) could lead to a continuously white

appearance of monochrome paintings, the loss of original material in artworks through photocatalytic degradation is undesirable.

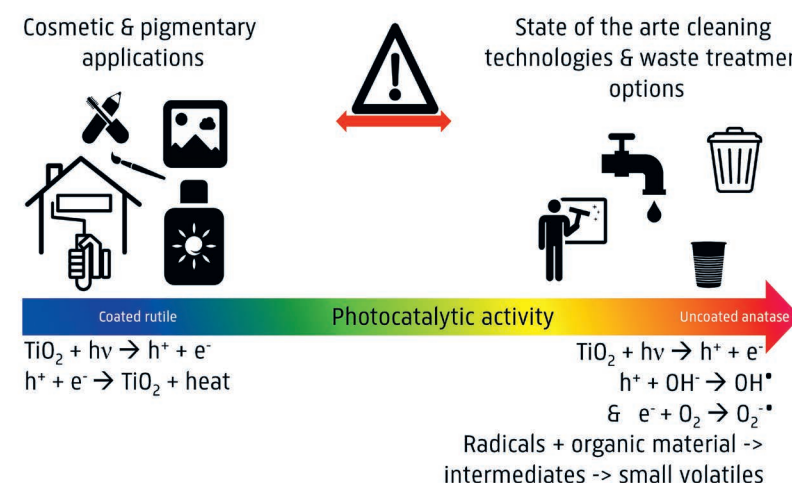
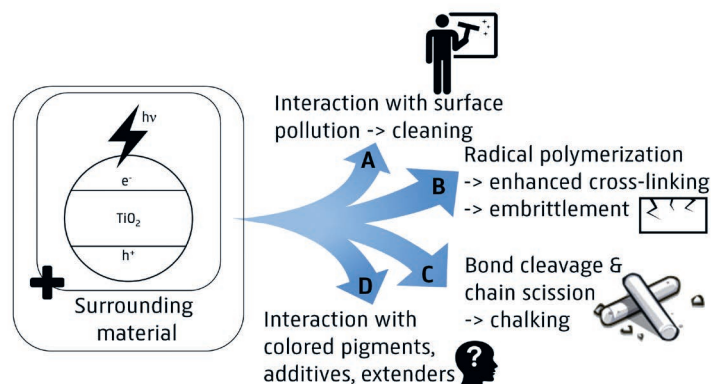


Figure 6 Overview of titanium dioxide photocatalytic activity and related applications. Using the TiO_2 powder for the wrong application can lead to problems.

The problems related to photocatalytic activity presented themselves, for industrial outdoor paints, soon after the pigment's introduction. The correct explanation for these problems was published as early as 1921 [52], but at the time went unnoticed by paint manufacturers. Work has been done on understanding the degradation mechanism by, among others, Jacobsen in 1949 [53], Voltz in 1974 [54], Pappas in 1975 [55] and Colling in 1981 [56]. Voltz et al. describe the problem of photocatalytic degradation of an alkyd medium leading to the most well-known problem in paintings: 'chalking' [57-61] (Figure 7C). In this thesis, chalking is the degradation phenomenon under investigation. However, chalking is not the only problem that can occur in an artwork, and the final degradation phenomena will be dependent on both the pigment and the surrounding material, Figure 7 and Scheme 1. If the surrounding material is prone to radical polymerization, embrittlement caused by extensive cross-linking [62] can occur (Figure 7B). Alternatively, as noted earlier, radicals may attack pollutants on the paint surface (Figure 7A) or they can break down the oil network (Figure 7C). It is unclear how degradation and self-cleaning processes compete with one another, which will also be dependent on the composition of the complete system. Finally, in competition or simultaneously with binder degradation, surrounding colored pigments [60, 63], or other paint components may be degraded (Figure 7D). The degradation of colored pigments or other paint components, caused by photocatalytic TiO_2 , has not been commonly been reported, nor was it the focus of this dissertation.

Titanium white may cause problems not only in original paint layers but also contained in restauration materials such as those used for retouches. Blanching of retouches has been noted by conservators, and thermal stability of TiO₂ containing retouches was subject of reported investigations. However, this falls outside the scope of the present study [64-66].

Figure 7 Degradation phenomena caused by titanium white photocatalysis.



Depending on the UV stability of the surrounding medium and the photocatalytic activity of the titanium dioxide, TiO₂ can also act as a UV protector by scavenging UV irradiation [4, 56, 67]. This protective behavior is stronger for less photocatalytic pigments. However, even photocatalytic pigments can have a positive influence if the surrounding material is very sensitive to UV irradiation. In other words, the entire system needs to be taken into account to understand the possible degradation phenomena, Scheme 1. In the scheme we distinguish between the intrinsic photocatalytic activity of the pigment, the photostability of the object and the exposure as important factors, dictating the material conditions or state of degradation at a certain point in time. Each factor is affected by a combination of things such as pigments characteristics, paint composition and different environmental properties.

Scheme 1 Model of degradation of TiO₂ containing films top {C.2}, mid-top {D.4, D.5}, mid-bottom {D.2, D.3}, bottom.

$$[\text{Crystal structure}] * [\text{Size}] * [\text{BET area}] * [\text{Surface treatment}] * [\text{Defect structure}] * [\text{Impurities}] = [\text{Intrinsic photocatalytic activity of the pigment}]$$

$$[\text{Binder}] * [\text{Intrinsic photocatalytic activity}] * [\text{Additives \& Extenders}] * [\text{Film properties}] = [\text{Photostability of object}]$$

$$[\text{O}_2] * [\text{H}_2\text{O}] * [\text{Light}] * [\text{Time}] * [\text{Temperature}] * [\text{Pollution}] = [\text{Exposure}]$$

$$[\text{Photostability of object}] * [\text{Exposure}] = [\text{State of Degradation}]$$

A.4.4. Reported problems in paint caused by photocatalytic activity

Problems with titanium white were reported in the 1920s for industrial paints [68-70]. These problems included slow drying, yellowing, and chalking, for instance of outdoor murals [4, 71]. Laver states, from personal communication, that problems such as anatase in acrylic color field paintings and TiO₂ with dammar for retouches have been reported [4]. Apart from that, no clear and unambiguous cases of photocatalytic degradation of paintings have been found. The only account that was found is that of painted metal shield in Denmark, which indicate different levels of chalking depending on their paint composition and distance to window [72]. Thus, while photocatalytic pigments were on the market and despite the fact that photocatalytic binder degradation is known to be able to occur, the expected problems in paintings are not yet reported or noticed.

A.5. So what?

The main discrepancy highlighted in the previous sections is that TiO₂-catalyzed degradation of oil paints is expected and to a certain degree understood, but it is not yet often noticed or reported. This realization triggered the formulation of several hypotheses which forms the basis of the research and motivated the focus on a preventive approach {B}.

B. GOALS & PROJECT APPROACH

The general introduction ends with the realization that: TiO₂-catalyzed degradation of oil paints is expected and to a certain degree understood, but it has not yet been noticed or reported {A.5}. In other words, this project was motivated by the idea that the clock is ticking and art collections may face severe TiO₂-catalyzed paint degradation problems in the near future. The discrepancy between theory and reality sparked several hypotheses that forms the basis for the preventive approach followed in this research:

- Photocatalytic titanium white pigments were not commonly used in (oil) paintings.
- The oil degradation process is slow due to low UV exposure in art collections.
- Other components in the paint such as additives and extenders influence the degradation and perhaps slow it down or prevent it.

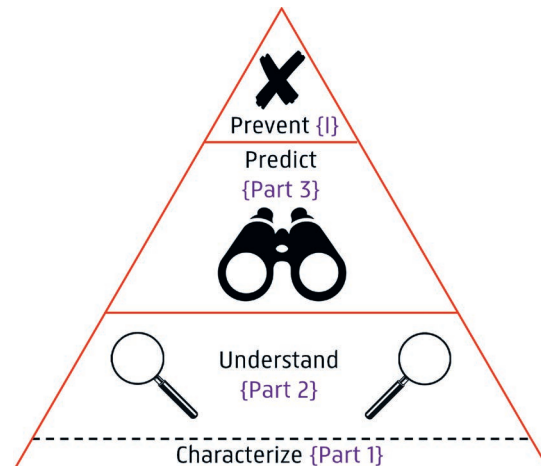
The degradation phenomena, such as chalking, are not yet visible, conservators do not know what to look for or both.

My research aims to test these hypotheses, with the broader set goal to understand, predict and prevent titanium white-catalyzed degradation of modern oil paints, Figure 8. This predictive or even preventive approach is novel in the field of conservation science {Preface, J} and was sparked by the lack of reported cases of degradation. Understanding the problem requires characterization of the use and the properties of the pigments as well as understanding the degradation process. Prevention can be done by removing all UV irradiation. However, this may be economically nonsensical, if most of the collection contains photostable TiO₂. Thus, prevention combines the development of predictive tools, to determine the vulnerability of objects, with a proposed risk assessment and management strategy for collections with TiO₂-containing objects.

The project has a secondary aim, which is a result of its collaborative nature and therefore the availability of many analytical techniques. Thus, I also set out to explore analytical methods and research approaches for the field of cultural heritage research.

This project made use of a large variety of different sources of information. These include: mid-20th century industrial literature, such as the Journal of the Oil and Colour Chemist Association; contemporary, industrial documentation from Kronos, Dupont and Tronox; archival sources such as those from Winsor&Newton,

Figure 8 Infographic of the preventive approach used during this Ph.D. (Thesis triangle).



Talens and Dupont; expert conversations with paint manufacturers; and research and review articles from the field of catalysis science and engineering as well as the fields of polymers, pigments, paints and coatings.

The thesis is divided into three main parts corresponding to the thesis triangle: part 1) Characterization of use and properties of titanium white pigments, part 2) Understanding and monitoring the degradation process of titanium white containing oil paints and part 3) Predicting degradation by titanium white pigments. The risk management strategy, is covered in a specific part of the conclusions {I}.

The first part of the thesis, about characterization, is made up of two chapters. Chapter 1 tests the first hypothesis by a broad elemental survey of white paints in Dutch collection, using the non-invasive method: X-ray fluorescence spectrometry. This research was performed with the aim to obtain an idea of the use of titanium white in paintings in the 20th century Netherlands. The second chapter, dives into the deep with the investigation of the complex photoluminescence behavior of different types of titanium white pigments. This work was performed in close collaboration with the Politecnico di Milano and received support from LaserLab-Europe. The second chapter aims to do a seminal explorative investigation of the photoluminescence properties of TiO₂ pigments with a method that is becoming more and more common in the field of heritage science.

The degradation process is investigated in part 2, with the aim to 1) determine early degradation signals and 2) understand the effect of paint formulation on degradation rates. In chapter 3 and 4, the aging mechanism is monitored with different analytical techniques such as gloss analysis, AFM and XPS (in close collaboration with TUDelft) and ATR-FTIR and AFM-IR (in close collaboration with the University of Manchester). Chapter 3 focusses on the inorganic components and morphological changes, such as 'TiO₂ surfacing', while chapter 4 focusses on changes in the organic component. Both studies aim to identify so-called '*early warning signs of degradation*': a useful tool to understand degradation rates and to predict future damage. Chapter 5 describes a different approach, namely comparing degradation rates of complex paint formulations, as opposed to simple pigment-binder systems {chapter 3 and 4} (in close collaboration with AkzoNobel). The work in chapter 5 is partly done using a Design of Experiments approach. The wider applicability of this approach to answer conservation science, and specifically formulation-based questions is discussed in chapter 5B. The three chapters in part 2,

investigate the three remaining hypotheses and follow the secondary aim of the project: to explore new methods.

The prediction part (part 3) presents two methods to predict the quality or PC activity of the TiO₂ pigments. Both methods are based on color change and can be carried out with limited analytical equipment, and are thus suitable for museum-based and private conservators. Chapter 6 describes a method usable for powdered pigments, while chapter 7 presents a method to be used on paint cross-sections. This part of the thesis bridges theory and practice and provides new tools, to further survey modern art collections and gain more information about the use of photocatalytic pigments. These tools will be important for vulnerability assessment of objects, the first step of risk management {I}.

The thesis is concluded with a synthesis of all the presented results and their meaning in relation to each other, in relation to risk management/collection care and in relation to their impact on conservation science.

C. INTRODUCTION PART 1: CHARACTERIZATION OF THE USE AND PROPERTIES OF TITANIUM WHITE PIGMENTS

The TiO₂ market and the documentation of occurrences of titanium white, as well as its important pigment characteristics, will be presented to introduce part 1 of this thesis

C.1. TiO₂ Market & occurrences in works of art and archives

Since the discovery of titanium dioxide, the market has expanded drastically. The biggest producers in the western world are Dupont, Cristal, Huntsman, Kronos and Tronox. In 2011 the market size of titanium dioxide was 5.4 million MT of which 85% is used by paints & coatings (60%) and plastics (25%) [73]. Much of the production, nowadays, has moved to China, to compensate for increasing prices of the raw material. Numbers resulting from market analysis do not directly relate to the use of titanium white in artists materials. In 1971, 1.4 kT of titanium dioxide (anatase and rutile) was used for artists colors; this accounted for just 0.02% of the entire pigment market [74].

Producers of artist oil paints introduced the new pigment at different rates [4]:

- Société Bourgeois, 1925
- Société Lefranc, 1927
- Winsor&Newton, ~1930
- Talens, 1937 (test batch). Commercial product marketed in France in 1950 and in the Netherlands after 1951 [9].

In the 1940s titanium white did not yet dominate other types of artist materials, such as pastels. A survey in 1940 shows two out of nine European producers used titanium dioxide in fine art pastels. Titanium dioxide as an opacifier for plastics was introduced at the same time as in artist pigments. The introduction of titanium white in resin-coated photographic paper occurred later, around the 1960s. This was preceded by titanium dioxide containing acetyl cellulose base material [4].

Although many dates of industrial developments are known, it is not straightforward to directly relate this to the real occurrence of titanium dioxide in art objects of a certain time. Therefore characterization of objects is important and was carried out during this project. Through several types of chemical analysis, titanium dioxide can be identified in works of art. A summary by Laver [4] provides the best overview, the list contains works of Picasso,

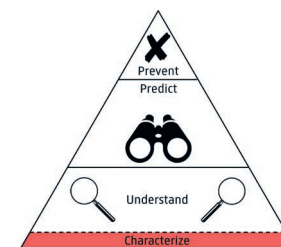


Figure 9 Thesis triangle highlighting part 1: Characterization of use and properties of titanium white pigments.

Willem de Kooning, Jackson Pollock [75], Barnett Newman, Hans Arp and others [4]. Furthermore, Mondriaan also used titanium white by the end of his career [22, 23, 29]. Next to reported occurrences in works of art, archival sources provide information concerning the use of titanium white pigments in the 20th century. The archives of Talens [32, 76], Weber [32, 77], Winsor&Newton [78] and Dupont [79], as well as patents [24, 80-86] proved to be very useful.

In other words, there is a wealth of information about the presence and use of titanium white pigments in the 20th century. However, this work is rather scattered, unorganized and not a structural survey of the use within a certain country or time frame. Considering the presence and popularity of multiple other white pigments popular at the time such as lead white, zinc white and lithopone [1], and the number of different grades of TiO₂-based pigments, it is challenging to make statements about the use of white pigments without chemical analysis.

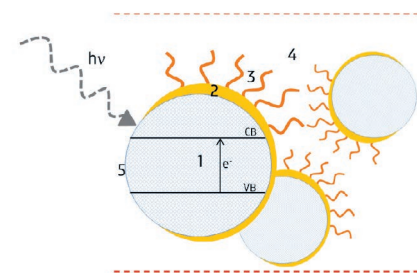
C.2. Main characteristic properties influencing photocatalytic activity

Several factors, detectable by chemical analysis, can influence the grade of titanium white and its intrinsic photocatalytic activity. In the following, the factors influencing the intrinsic photocatalytic activity will be discussed. While all the factors are of importance, the most important ones for pigment powders are the crystal structure and the presence/quality of an inorganic coating, Figure 10. In the case of catalyst powders, which are more commonly described in literature, more subtle differences in impurities, particles size, and others play an important role.

C.2.1. Crystal structures of TiO₂

Titanium dioxide exists in three different crystal structures: anatase, rutile and brookite. Due to its limited availability, brookite has never been used as a pigment [4]. The crystal structure has a large influence on the photocatalytic activity of the pigment {A.4, D.1}. The PC activity of anatase, despite the larger bandgap, has been shown to be higher than that of rutile [87-89]. Several explanations for this are proposed. According to Yang et al. [67], it is due to a higher density and a more narrow bandgap for rutile, yielding a much higher recombination probability. Thus, if more charge carriers recombine, fewer radicals can be formed. Voltz et al. [54] propose that, while rutile forms more excitons, due to its absorption edge, the difference stems from a more rigid bond with

the surface hydroxyl groups resulting in a slower reaction of the positive hole. Another aspect of the discussion about the activity of rutile and anatase is the type of hydroxyl radicals, which can be surface-bound or free. The surface-bound hydroxyl radicals, which are generated more on rutile, are restricted to degrade surface bound substrates. In the other hand, the free hydroxyl radicals, which are generated more on anatase, are more mobile and can thus additionally cause degradation in the bulk [90]. Mixed phase TiO₂ powders¹⁸ (e.g. Degussa P25) can have increased photocatalytic activity due to the charge carrier transfer between the phases which increases their lifetime [91].



18 Mixed phase TiO₂ is different than a mixture of anatase and rutile. In mixed phase powders bandgap coupling influenced the powder properties.

Figure 10 Schematic overview of titanium white pigments in a binding medium. 1=TiO₂, 2=Inorganic coating, 3=Organic coating, 4=Binding medium, 5=Inconsistencies in the treatment.

The assumption that rutile pigments are less photocatalytic than anatase is followed in this thesis. This assumption holds up because, in the case of pigments, it is likely that most rutile pigments are additionally surface treated to reduce photocatalytic activity even further. This is plausible since inorganic coatings {C.2.3} were well under development before the full scale production of rutile {A.2.1} [1, 4]. This assumption was not disproven during this research since no rutile pigments without surface coatings have been encountered during the characterization of reference powders or objects [27].

The crystal phase of titanium dioxide can be analyzed by several analytical techniques [4] of which X-ray diffraction and Raman spectroscopy are the most straightforward. FTIR can also distinguish between the crystal phases. However, the characteristic vibrations are at low wavenumbers which makes identification a challenge due to the spectral range of regular FTIR equipment.

C.2.2. Production processes of titanium white

Titanium white pigment can be produced by two different production processes: the sulfate process and the chloride process. The detailed specifications of both processes are well documented in the literature [1, 4, 92, 93]. The main characteristics are briefly summarized in the following.

C.2.2.1. Sulfate process

- First production (US):** 1914-1915: experimental;
1919: commercial plant
- First production (EU):** 1913: experimental;
november 1918: commercial
plant in Fredrikstad
- Ore/Feedstock:** ilmenite, titania slag produced
from ilmenite (70-90% TiO₂,
rich in Ca and Mg)
- Reaction mechanism:**
- $\text{FeTiO}_3 + 2 \text{H}_2\text{SO}_4 \rightarrow \text{TiSO}_4 + \text{FeSO}_4 + \text{H}_2\text{O}$
(dissolution feedstock)
 - $\text{TiOSO}_4 + \text{H}_2\text{O} \rightarrow \text{TiO}_{2n} \cdot \text{H}_2\text{O} + \text{H}_2\text{SO}_4$
(precipitation of TiO₂)
 - $\text{TiO}_{2n} \cdot \text{H}_2\text{O} \rightarrow \text{TiO}_2 + n\text{H}_2\text{O}$
(TiO₂ calcination)

Impurities: Nb₂O₅ (incorporated in the crystal),
P (on the surface, controls growth), Al, grinding aid

Type of pigments: Generally anatase, rutile (1940s, required
rutile seed crystals during the hydrolysis step)

C.2.2.2. Chloride process

- First production (US):** early 1950s: experimental;
1959: commercial plant by Dupont
- First production (EU):** 1965: commercial plant
- Ore/Feedstock:** natural rutile, synthetic rutile, high
grade ilmenite or slag: chloride slag
(85-87% TiO₂) or upgraded titania
slag (UGS, 95% TiO₂)
- Reaction mechanism:**
- $2 \text{TiO}_2 + 3 \text{C} + 4 \text{Cl} \rightarrow 2 \text{TiCl}_4 + 2 \text{CO} + \text{CO}_2$
 - TiCl_4 (impure gas) \rightarrow TiCl_4 (liquid)*
 - $\text{TiCl}_4 + \text{O}_2 \rightarrow \text{TiO}_2 + 2 \text{Cl}_2$

Impurities: reduced to 10-20 ppm, co-oxidant AlCl₃
(Al -> 1%), grinding aid

Type of pigments: Generally rutile (with a narrower particle
size distribution than sulfate process rutile), anatase is possible but
not commonly used (minor production between 1975 and 1985).

*Other metal chlorides
are separate out as solids.
Except Si and Zr, which
don't form chlorides and
accumulate as slags in
the reactor.

C.2.3. Surface treatments on TiO₂

Surface treatments were developed to enhance the durability of
pigments and to modify their wettability and other characteristics for
their use as pigments. Inorganic and organic treatments are applied to
achieve different goals and will, therefore, be discussed separately [94].

C.2.3.1. Inorganic surface treatment

Many different inorganic coatings have been used and patented over
time [81-83, 86, 95-97]. Contemporary stable pigments are coated
with silica and alumina in superimposed layers. Inorganic surface
treatments form a barrier between the charge carrier and the
adsorbent. Therefore, recombination is forced, and the radical
formation and with that PC activity is decreased {A.4, D.1} [98, 99].
Inorganic surface treatment often consists of (hydrated) metal oxides
such as Al(OH)₃, Al₂O₃, SiO₂ or ZrO₂. The coating can be applied as
separate layers or mixed. Typically, hydrated oxides are precipitated
on the pigment under controlled conditions. In the course of history,
other materials have also been used such as 'Boron, Barium, Magnesium,
zinc and tin compounds, and small amounts of cerium, chromium,
manganese or cobalt compound' [4]. Electron imaging shows coating
is not always even (Figure 11) [100]. According to Braun et al. 5%
alumina is typical for non-durable pigment grades. The hydrous
alumina may be stabilized with an anion (sulfate/phosphate). A silica
coating increases the chalk resistance and is about 2% (by weight).
Glassy silica sheet of more than 4% silica by weight is used in the
production of super durable pigment grades [92].

Inorganic surface treatments can be analyzed in different ways
[101]. STEM-EDX proved useful to analyze the inorganic pigment
coating on powders and in paint films (Figure 11 and Figure 12)¹⁹.
X-ray photoelectron spectroscopy (XPS) is another (surface)
method that may be employed to detect inorganic coatings on loose
material and possibly in a matrix. The problem is that XPS does not
provide spatial information, which makes it difficult to determine if
an element is present in the coating or as an additive [74, 102-104].

Specifically for silica coatings, the acid solubility test may be employed.
Due to the solubility differences between silica and titania in boiling
sulfuric acid, the integrity of the coating can be assessed [4, 105].

C.2.3.2. Organic surface treatment

To make pigments more suitable for their end application, an
organic coating can be applied to make the surface hydrophilic or
hydrophobic. Organic surface treatment may affect the photo-

¹⁹ Results obtained
using this technique and
illustrating the applicability
of the technique have been
reported on a poster at
ICOM-CC 2017. Other
results are discussed in
chapter 2 where STEM-EDX
was used as a supporting
technique. Presently (2017-
2018), a student project at
the Cultural Heritage
Agency of the Netherlands
(RCE) is looking into the
analysis of coatings on
different pigments.

catalytic activity by blocking absorbent sites. However, the effect is not nearly as effective as the presence of an inorganic surface treatment, and the goal of the treatment is clearly different [106]. Organic coating materials are among others silicones, amines, and polyols. Organic materials may also be added as additives. Additives can, among others, aid a processing step such as grinding or they can improve the flow properties [4, 92, 107].

Given the very low quantity and different bonding mechanisms (chemical bonding vs. adsorption) of organic surface treatment analysis is not straightforward. In general, the distinction between materials added as a coating or as production aid is difficult to make. When the organically coated pigment has been used in another organic material such as the binder, it becomes increasingly difficult to detect the organic coating. A combination of spectroscopic and chromatographic methods may be employed [92, 107].

Figure 11 STEM image (left) and STEM-EDX map (right) of a coated titanium dioxide pigment - Sample Tronox CR-826.

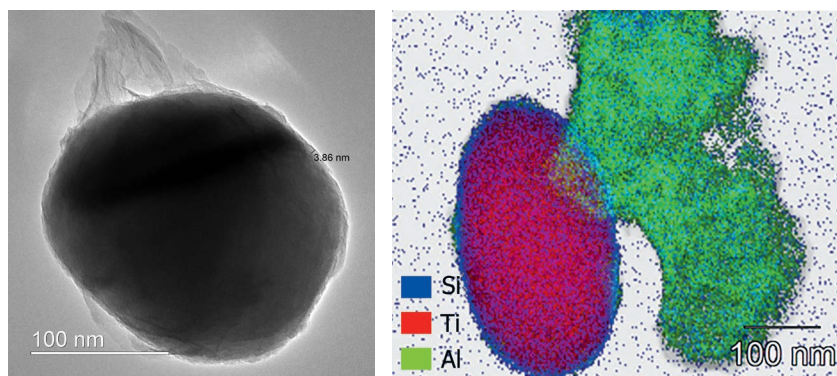
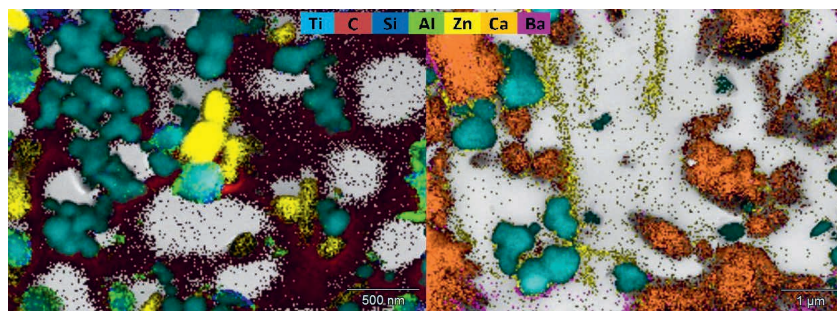


Figure 12 STEM-EDX map (left) of a self-made paint containing coated rutile, uncoated anatase and zinc oxide and (right) of a tube paint (Talens Amsterdam oil colours, dated: 1982-1986) containing anatase and CaCO_3 (XRD) clearly indicating zinc rich strands (carboxylates?) as well as an uneven and partly detached coating. Images reproduced from [100].



C.2.4. Particle size and surface area of titanium dioxide

Crystal structure and surface treatments are the most important characteristics determining photocatalytic activity of pigment powders. Photocatalytic activity of non-pigmentary TiO_2 powders, not containing a surface treatment can be additionally influenced by other pigments characteristic such as size, surface area and electronic structure.

It is suggested that particle size and surface area influence the photocatalytic activity by determining the number of absorption sites for H_2O and O_2 [108]. Carneiro et al. conclude that two competing parameters influence the relation between particle size and PC activity: the OH concentration on the surface and the availability of holes. Depending on the particle size, one of these parameters dominates the photocatalytic activity [109]. Du et al. describe the effect of particle size in an aqueous suspension. They show that decreasing the particle size, increases the degradation speed of methylene blue {E.2.1}, which is said to be caused by a higher absorption rate. The effect is greatest when the particle size drops below 30 nm [110]. Furthermore, Allen et al. describe the effect of particle size and surface area on dispersion and interaction with the matrix which can affect the degradation [108]. In general, small particle size combined with a high surface area is beneficial for the production of highly effective photocatalysts [111]. The size does not only influence the photocatalytic activity but also the color; nanopowders can result in transparent films, often used for self-cleaning materials [10].

C.2.5. Defects and impurities related to titanium dioxide

A defect is a structural imperfection in a crystal lattice. These imperfections can be point defects such as vacancies (missing atoms) and impurities or line defects such as dislocations (misalignment of some atoms in the crystal lattice). The defect structure affects the electronic properties of crystal and thus its photocatalytic activity. By adapting the electronic structure, traps can, for instance, form recombination centers, or they can inhibit recombination [87, 91, 111-113]. Two types of recombination may occur, surface and bulk recombination. There are several contradicting assumptions about the effect of charge traps on electron-hole recombination [87, 91, 114]. Ohtani proposes the following hypothesis in an attempt to unify contradicting statements: shallow traps enhance photocatalytic activity by migration of the electron through conduction band traps; while deep traps reduce photocatalytic activity by stimulating recombination of a charge carrier pair [9].

A differentiation should be made between ore or production defects and impurities and intentional changes to the structure, such as doping. Doping (e.g. nitrogen doping) can be used to move the catalytic activity of TiO_2 catalysts to the visible light region [115]. Another effect is demonstrated in composite semiconductors such as $\text{CdS}/\text{TiO}_2^{20}$. CdS has a low-energy bandgap absorbing a large portion of the light while the stable TiO_2 is used to further 'process' the formed charge carriers [87].

20 RCdS/TiO_2 composite semiconductors are different from simple mixtures of CdS and TiO_2 . Similar to mixed-phase TiO_2 , change in properties is related to bandgap coupling.

Doping with certain transition metals (molybdenum/vanadium) decreases the photocatalytic activity by acting as an electron donor and annihilating the high energy holes [116] while other transition metals (Pt) increase the photocatalytic activity by acting as an electron trap, leaving the hole free to migrate to the surface [87].

In this research, the electronic structure of pigments is investigated with time resolved photoluminescence spectroscopy (TRPL). This method is commonly reported for single crystal or nano-TiO₂ [117-120] and is increasingly used for the study of artists materials [121, 122].

D. INTRODUCTION PART 2: UNDERSTANDING AND MONITORING OF THE DEGRADATION PROCESS OF TITANIUM WHITE CONTAINING OIL PAINT.

The second part of the thesis will focus on understanding the degradation process. To introduce the two chapters on early warning signs for degradation and the chapter on the effect of paint formulation on degradation rates, I will first present the state of the art relating to photocatalytic degradation of pigment-binder systems. Each chapter will start with a specific introduction in addition to the context provided here.

D.1. Photocatalysis

The process of photocatalysis [6, 7, 9, 54, 123] can be summarized by the following reactions, Figure 14:

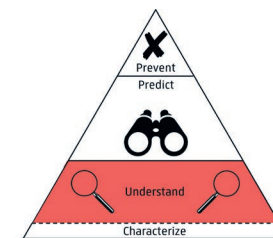
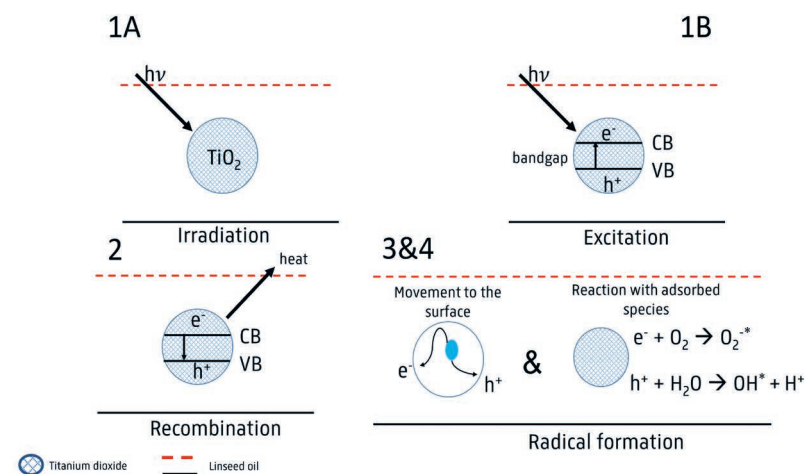
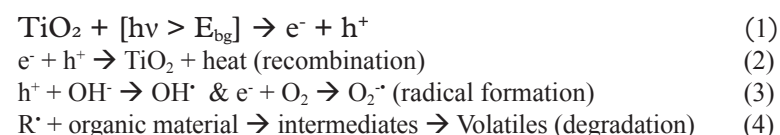


Figure 13 Thesis triangle highlighting part 2: Understanding and monitoring the degradation process of titanium white containing oil paint.

Figure 14 Photocatalytic cycle (numbered following reactions 1-4).

The wavelength of the light required to surpass the bandgap can be calculated by:

$$E_{\text{bandgap}} = (hc)/\lambda$$

h: Planck's constant, $6.63 \cdot 10^{-34}$ Js

c: light speed, $3 \cdot 10^8$ m/s

λ: wavelength of the light

$1 \text{ eV} = 1.6 \cdot 10^{-19}$ J

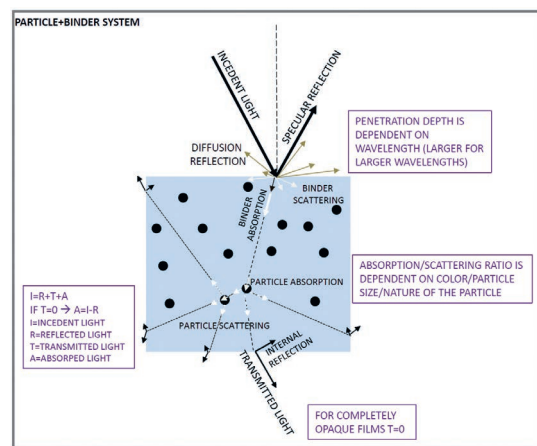
D.2. The role of light in photocatalysis

Due to its energy, light, and especially UV light can cause damage to materials (e.g. the skin). Degradation directly caused by light is called photochemical degradation. Radiation can also indirectly cause degradation, which is the case for the photocatalytic cycle. Light intensity, the duration of exposure and the spectral distribution influence both types of degradation processes [124, 125]. Indoor lamps can have a UV-content which should not be neglected. Window glass or specific filters can be used to block UV-radiation. However, in many (non-museum) environments these are not present. Furthermore, efficiency (the cut-off wavelength) of these filter may change during their service life [126].

It is assumed that direct photochemical degradation follows the reciprocity principle. This principle uses the fact that exposure is represented by the product of the intensity of radiation and the time of radiation. It predicts that the effect of the same exposure is identical. In other words, it states that the exposure and thus effect of 1h@500 Lux is identical to 2h@250 Lux. The total number of photons causing damage in both cases is the same [127]. It is named a principle, rather than a law because it is not always exactly accurate. A parameter that may cause deviation from the principle is temperature rise at high intensities, causing increased reaction rates [127, 128].

Indirect photo-processes such as photocatalytic degradation are less straightforward because photons, after being absorbed, can either recombine or cause radical formation {D.1} [127, 129, 130]. According to Egerton and King photocatalytic degradation speed at high intensity, is related to the square root of the intensity [68]. At low intensity, the intensity and degradation speed are directly related. The same square root relation has been found in a dummy reaction {E.2.1} [68] as well as for a degrading paint film [89].

Figure 15 Light interaction with a particle-binder system.



Absorption and scattering of light by the paint film govern the penetration depth of the light, Figure 15. The penetration of light is thus dependent on among others type of particles (size/refractive index/bandgap), type of binder and dispersion quality [123, 131]. The combination of small penetration depths of short wavelengths (UV) and the presence of a UV absorbing pigment (TiO_2/ZnO) will confine the PC degradation to the paints top surface [132, 133].

D.3. Other environmental conditions and their role in photocatalysis

Light is not the only parameter influencing the photocatalytic degradation cycle. The presence of oxygen and water is also needed for photocatalytic degradation. In the absence of water, the process stops but in the absence of oxygen an effect called photogreying occurs [54, 134, 135]. Sullivan concluded oxygen and water are not diffusion limited [136].

Air pollution can also play a role, TiO_2 can be used as photocatalyst for cleaning of waste water [47, 137] or air purification [50, 138]. Thus, the question of how these degradation reactions compete with degradation reactions of the binding medium, is an interesting one. Pollutants may be present as gasses and will penetrate the films as do water and oxygen.

Temperature and pH are conditions known to influence most reaction rates. The pH influences the surface charge of titanium. TiO_2 will be positively charged in acidic medium and negatively charged in basic medium. The surface charge of titanium dioxide changes the potential of the catalytic reaction, by modifying the electronic behavior which plays an important role in these reactions [139, 140].

The effect of temperature is not completely clear. In general, reactions proceed faster at high temperature. However, since there is a competition between recombination and radical formation, the temperature effect depends on the favored process. This results, according to Mills at al., in a limited temperature sensitivity [141]. On the other hand, Rauf et al. state that the photocatalytic activity decreases with temperature due to enhanced recombination [139].

D.4. Components in oil paint

Paints are much more complex than just the combination of a pigment and a binder. They contain several types of pigments, extenders, additives and the binding medium. To understand degradation processes, it is important to understand and take into

account the complete paint formulation. Research into the effect of paint formulation on degradation rate is presented in chapter 5.

D.4.1. Oil binder

The binding medium of oil paints is vegetable oil. Vegetable oils consist of a triglyceride with long chain fatty acids. Oils differ from each other based on the statistical distribution of fatty acids [142]. Vegetable oils are classified as drying oil or non-drying oil based on their ability to polymerize. Polymerization takes place through cross-linking of the double bonds. Auto-oxidation with atmospheric oxygen at the unsaturated bond leads to the formation of highly reactive peroxides that react with other unsaturated sites resulting in a higher molecular weight network [143-147]. In general, less double bonds result in slower polymerization. Furthermore, pigments and reaction condition can influence drying time of oil paints [142].

Next to polymerization, hydrolysis of the ester bonds may also take place, resulting in fatty acids and glycerol derivatives (di- and mono-glyceride) [143, 145, 147]. These free fatty acids can react further with heavy metals forming soaps [34, 148]. According to Lazzari et al. continuation of the curing reactions causes degradation [146]. In the first stages of curing peroxides are formed at preferential positions. These peroxides can form cross-links or cause beta-scission. Cross-linking is favored, however, with the hardening of the paint film cross-linking may be hindered, favoring the other pathways: mainly beta-scission. This results in the formation of small organic and volatile fragments. Additionally, oil paints are known to yellow over time [149]. In general, it is clear from the literature that drying, degradation, and yellowing of drying oils are complex and simultaneously occurring processes often governed by peroxides and influenced by many parameters.

D.4.2. Extenders and additives for oil paints

Paints contain extenders (also known as fillers) such as calcium carbonate and barium sulfate are added to the paint to bring the price down and/or adjust the tinting strength. Different absorption or scattering of light, caused by different particle sizes or the different nature of the extender, may play a role in photocatalytic degradation. For instance, as barium sulfate and calcium carbonate do not absorb UV light, the penetration depth will be enhanced, and degradation may occur deeper into the paint film [2].

Metal stearates are used in the coatings and plastic industry mainly as a wetting agent. Particularly aluminum stearate was used as an additive in the 20th century. By modifying the wettability of pigments aluminum stearate results in better application properties of the paint and in an economic benefit, since paint production is accelerated [39, 40]. Certain metal salts (ions) can interact with charge carriers of radicals to affect the photocatalytic degradation. Irick et al. show an increase in 'time to embrittlement' in the presence of zinc salts [150]. Furthermore, as a wetting agent the metal stearate forms some kind of organic surface treatment around the pigment {C.2.3} [151], which can influence the photocatalytic activity as well.

Other commonly used metallic compounds added to paints are driers. Especially oil paints need driers given their slow drying time [146]. Typical metal coordination compounds used as driers include cobalt, manganese, and iron. Drying and photocatalytic degradation are both free radical processes and are aided by the same chemicals. Catalytic TiO_2 will aid the drying process [152], but the drier may aid the catalytic degradation process. Driers exist as surface driers and bulk driers. Some driers help transport oxygen, which in the degradation phase will also have an effect [146].

D.4.3. Other (colored) pigments

Zinc oxide is a common admixed pigment to TiO_2 -based paint because it is believed to improve the properties of the paint film by decreasing the degree of yellowing in drying oil [37]. Furthermore, it should aid the compatibility of TiO_2 with oil [38]. ZnO is a photocatalytic semiconductor just as TiO_2 (bandgap 3.26 eV). Combining semiconductor pigments such as titanium dioxide, zinc oxide, vermilion (HgS) or cadmium yellow (CdS) [43, 153, 154] can lead to complex electronic structures. Photocatalytic activity can be enhanced when bandgap coupling occurs or when it acts as a 'composite semiconductor' {C.2.5}.

Other inorganic pigments may also be added and may affect the degradation. Samain et al. investigated the fading of Prussian blue with several different white pigments. No color change was observed during light exposure by Samain et al., due to the use of a (probably coated) rutile pigment, which exhibits a protecting effect. The combination with ZnO however, shows significant fading [63]. Zhang on the other hand [155] shows degradation of Prussian blue mixed with anatase. It is unclear what causes the change in color: real Prussian blue color change or optical scattering due to the degraded binder (chalking). Yamamoto et al. described the reduction of Prussian blue to Prussian white intercalated into

21 Unpublished research, presented at Technart 2015 by Elena Nazarenko. 'Resonant X-ray emission as a tool of Prussian blue Studies'. Site specific X-ray emission spectroscopy was carried out at the Paul Scherrer institute in collaboration with E. Nazarenko, C. Gervais and M.A. Languille. The unpublished results suggested the reduction from Fe³⁺ to Fe²⁺ in Prussian blue as the cause for anatase-mediated UV degradation.

titanium nanosheet ultrathin films [156]. Although in a very different setting this paper shows the possibility of titanium white induced Prussian blue degradation, which was confirmed in a paint film as well.²¹ Furthermore, it has been reported that titanium dioxide in combination with alizarin lake caused problems in the past [157]. However, limited literature exists on the topic. Johnston-Feller et al. reported fading of alizarin lake in a mixture of rutile titanium dioxide with PVAc binder [60]. On the other hand, Chen [158] showed with a test (TiO₂ + pigment in solution) that alizarin lake is much more stable (limited degradation within 50 hours) in combination with coated rutile than with uncoated anatase (complete degradation within 24 hours). Laver briefly mentions the fading of alizarin lake as well as Prussian blue in titanium dioxide (anatase grade) containing pastels [4].

Finally, other organic pigments or dyes may be present in paints. The degradation of the dye may compete with the degradation of the organic binder. The degradation of dyes in solution is commonly used as a 'dummy' reaction to probe photocatalytic activity {E.2.1} [139, 159-162]. Depending on location, mobility and competition with other organic materials (e.g. air pollutants) this may have unexpected effects that have not yet been investigated.

D.5. Paint film characteristics

In addition to its composition, a paint film is characterized by its film properties such as, thickness, pigment-volume-concentration (PVC), other layers (e.g. varnish) and dispersion quality. These properties affect the photocatalytic degradation rate or the perception of degradation. Perception is specifically related to the quality of dispersion: good dispersion temporarily inhibits the loss of gloss while the absolute degradation remains the same [56, 163].

The pigment content (or pigment-volume-concentration, PVC) described by the following equation:

$$PVC = (V_{\text{pigment}}/V_{\text{total}}) * 100\%$$

also affects the gloss of the paint surface and its degradation. The gloss decreases by increasing PVC of solid material (TiO₂, other pigments or extenders). This decrease becomes most apparent above the critical pigment-volume-concentration (CPVC, strongly influenced by the quality of dispersion) [56, 163, 164]. Another effect of the PVC on degradation relates to a higher UV absorption of a paint with a higher TiO₂ content. Depending on the photocatalytic activity of the pigment this results in higher radical formation or UV scavenging and thus accelerated or

inhibited degradation [56]. In an aqueous system, increasing the photocatalyst loading increases the dye degradation until the solution turns turbid blocking UV-radiation which decreases the speed of degradation [139]. UV-penetration is influenced not only by PVC, but also by particle size and dispersion, by the medium and its characteristic absorption and by the spectral distribution and angle of the incident light. Unbound pigment on the surface (caused by degradation), will significantly decrease the UV-penetration and stop the degradation process going deeper into the film. If the film is too thin, it risks being completely disintegrated, while a thicker film will have a protected bulk [56].

A covering layer such as varnish can also influence UV-penetration, as well as oxygen or water transport [165]. Depending on the material and the additives (possibly UV-blocking) varnishes have different effects on photocatalytic degradation. In general, a varnish will always diminish UV-penetration and transport of species (if only by increasing the film thickness) and can, therefore, be considered as a protective layer for photocatalytic degradation.

D.6. Artificial aging studies

Artificial aging studies of TiO₂ pigment-binder systems will be reviewed as a starting point to monitor aging and determine early warning signs as presented in chapter 3 and 4. Accelerated aging studies are studies in which pigmented polymeric films are prepared and naturally or artificially aged and subsequently analyzed [70, 89, 166-170]. Many methods of aging are available and used [127, 171], and many techniques to monitor the result of weathering have been employed. These include: visual techniques, such as evaluation of color or gloss; basic techniques, such as monitoring the weight [12]; surface imaging techniques, such as Scanning Electron Microscopy [54, 172]; chemical analysis of the film by FTIR or MS²² [173] or XPS [12, 174]; chemical analysis of the off gassing [48, 89, 168, 169]; and many other methods like an evaluation of thermal and mechanical properties [175-178].

One technique has been reported since 1999 and offers a fast/in-situ testing method with the artificial aging of paint samples. The group of Egerton has first described this method based on the evolution (off gassing) of CO₂ from degrading films by Fourier Transform Infrared Spectroscopy (FTIR) [168, 169]. A paint sample is irradiated in a special cell. Infrared spectroscopy is used to determine the evolution of CO₂, which is an end product of degradation of organic (binder) material). CO₂ evolution experiments show the expected difference between rutile pig-

22 E. van Dam (VU, RCE) developed an LC-ESI-MS method to investigate oil paint during her MSc. thesis (2015). In the scope of this work she also investigated aging TiO₂-oil paints and found preliminary indications that aging could be monitored successfully by LC-ESI-MS as well. However, this work was not pursued further in view of the complexity of the method. The method was published: Eliane P. van Dam, Klaas Jan van den Berg, Art Ness Proano, Gabor, Maarten van Bommel, Analysis of triglyceride degradation products in drying oils and oil paints using LC-ESI-MS, International Journal of Mass Spectrometry - <http://dx.doi.org/10.1016/j.ijms.2016.09.004>. Detailed results on the TiO₂ samples during aging are only reported in the master thesis (under the same name) in Chapter 6.

mented, anatase pigmented and unpigmented acrylic paint films. This difference is visible within 300 minutes making it much faster than traditional weathering experiments. The results correlate well with gloss evaluated traditional weathering tests. This method, while useful, is not practical to employ on real artwork and thus does not offer perspectives to detect early warning signs. Alternatively, FTIR can be a very useful method to monitor chemical changes in the polymer [166, 179, 180].

X-ray photoelectron spectroscopy (XPS) was reported to follow the degradation of polymeric films. So far this has been done by researchers at the National Institute of Standards and Technology (NIST) [174, 181], and by several groups researching TiO₂ mediated degradation of plastics (PE, PS, and PVC) [12, 51, 182]. Upon degradation, the amount of Ti measured at the surface is increasing indicating the chalking process [174, 181, 182]. The ability to indicate chalking by XPS provides a promising tool to follow the degradation of other paints/polymer in great elemental detail.

E. INTRODUCTION PART 3: PREDICTING DEGRADATION

Despite the fact that photocatalytic degradation is dependent on a variety of parameters, photocatalytic activity of the pigment remains the main driving force. Therefore, one part of this research is completely focussed on measuring photocatalytic activity.

Photocatalytic activity can be evaluated by what I refer to as direct or indirect methods. Direct methods are those measuring the direct effect of UV absorption. It includes measuring radical formation or measuring the charge carriers. Indirect tests evaluate the outcome of a secondary reaction. This may be a dummy reaction [53, 68, 69, 137, 139, 160-162, 174, 183-194] or an artificial aging experiment {D.6} [70, 89, 166-170]. An up to date overview of all the official ISO tests for photocatalytic activity was published by Mills et al. [195].

E.1. Direct methods to test photocatalytic activity

Photocatalytic processes are based on the formation, migration, and reactions of charge carriers. Electron-hole pairs are generated by UV-irradiation after which they follow several pathways such as migration to the surface and radical formation, recombination or several types of trapping {D.1}. Because the charge carriers are an essential part of the process, several techniques are available based on their presence and mobility. These techniques are very useful for the research of photocatalytic materials. However, due to their complexity, they are not so applicable for cultural heritage applications. Nevertheless, an overview of photocatalytic activity tests would not be complete without briefly discussing those techniques. In this section, I will discuss photoconductivity measurement, electron spin resonance techniques, and an electrochemical approach.

E.1.1. Photoconductivity

Conductivity is a measure of the ability of a material to transport electronic current. Photoconductivity is a phenomenon that refers to a change in conductivity due to light absorption. The increased number of charge carriers that are formed upon UV-irradiation in TiO₂ (semiconductor) cause an increase in conductivity. However, the effect is not as straightforward, due to the competition between charge carrier formation, recombination, and charge trapping. Conductivity measurements are used to study properties of semiconductors [196]. Starting in the 1970s, this method has been explored to understand photocatalytic processes such as the

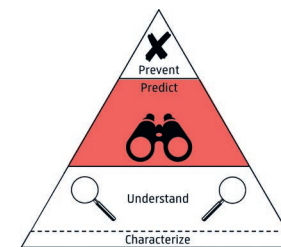


Figure 16 Thesis triangle highlighting part 3: Predicting degradation by titanium white pigments.

23 ESR was briefly investigated in collaboration with ESA-ESTEC. However, in-situ analysis of paints did not yield a sufficient signal, likely due to the wide variety of different short lived radicals. As using spin-traps severely alters the system under investigation ESR was not investigated further. Nevertheless, the technique may be highly suitable to answer more fundamental questions.

24 The electrochemical approach was evaluated in a student project by R. van der Linden for the master Chemical Engineering at Delft University of Technology. This project highlighted the difficulty to use the set-up and the high sensitivity of the set-up, making it challenging to use for the quick and easy assessment of photocatalytic activity.

oxidation from isobutane to acetone by Hermann et al. [197]. More recently researchers at the National Institute of Standards and Technology (NIST) have aimed to explore photoconductivity as a fundamental technique to determine the photocatalytic activity [174, 198]. The drawback of this method is that the instrumentation, as well as sample preparation, are quite complex [198].

E.1.2. Electron spin resonance spectroscopy

Electron spin resonance has been widely used in the field of semiconductor (and specifically TiO_2) investigations [174, 196, 199-203]. Electron spin resonance or electron paramagnetic resonance is a method, related to nuclei magnetic resonance (NMR), that can measure paramagnetic species. It is of major interest, as this method can investigate charge carriers and radicals, which are the most important species in photocatalytic degradation. In general, interesting species, such as radicals, are short lived and measuring them required techniques such as lowering the temperature, inclusion in a solid matrix or spin trapping. A spin trap reacts with the species of interest and with this reaction the ESR signal changes [174, 201]. A spin trap for examination of titanium dioxide pigments was used by Ceresa et al. in the early 1980s [202]. The drawback of this method is that the real situation is adapted by spin trapping, rendering the method indirect. Therefore, there is a second method which can be used: ESR in the solid state. To avoid problems with the wide variety of short lives species solid state ESR is carried out at 77 K [174, 204, 205]²³.

E.1.3. Electrochemical approach

An electrochemical approach, proposed by Anaf et al., was recently introduced to study semiconductor pigments [43, 206] and has been considered as a method to test photocatalytic activity. The idea is that amperometry can be used to measure the photo-generated current (electron), which is (at least partly) dependent on photocatalytic activity. This is done in a three electrode cell, where the working electrode is adjusted by depositing a thin layer of the semiconductor pigment on top (TiO_2). The working electrode is then irradiated by a suitable energy, depending on the pigment. In amperometry, a constant potential is applied to the electrodes, and the current is measured. A change in current indicates any ionic fluctuation in the electrolyte, thus, if photo-generated electrons are formed and transferred to the environment, this will be detected as a change in current. While the method has potential and is used in the investigation of other pigments [43, 206], it is not straightforward or easy-to-use and thus not suitable as a fast indication of photocatalytic activity.²⁴

E.2. Indirect methods to test photocatalytic activity

Dummy reactions are systems where the reactant is designed to react with the PC formed radicals. The conversion, dictated by the number of radicals present, provides information on the photocatalytic activity. Many indirect tests exist [174, 194, 195], but the most common tests are either a wide range of dye/ink degradation tests or the conversion of isopropanol to acetone. The tests involving color are most suitable to use in the field of cultural heritage because change is evident and can be evaluated by eye.

E.2.1. Dye degradation tests

Dye tests are based on the photocatalytic degradation of organic dyes. Commonly used dyes are methylene blue [186], rhodamine B [159] and several types of acid dyes [160-162, 184, 188, 190, 191, 193]. The degradation is usually monitored in an aqueous TiO_2 dispersion. However, dye tests have also been performed in solid state systems [192]. The idea of the test is simple: a dye is dissolved in water and titanium dioxide powder is dispersed in it; the dispersion is then irradiated, and at time intervals the degradation of the dye is monitored either by chemical analysis or by visual assessment of color change. The speed of degradation/discoloration provides information on the photocatalytic activity of the powder [139].

E.2.2. Photocatalytic activity indicator inks

In analogy with dye degradation tests, photocatalytic activity indicator inks were developed by the group of Andrew Mills [207-212]. The inks are fully tested, validated for their use on self-cleaning surfaces and commercially available {chapter 7} [213]. The ink test is based on a photocatalytic reduction of a dye (resazurin, Basic Blue 66 and others) causing a quickly noticeable color change. The main benefit of the inks is the speed of indication, the manner of application and the ease of use. Studies are now carried out to extend the test method towards powdered material [208].

E.2.3. Isopropanol to acetone

The isopropanol test measures the conversion of isopropanol to acetone [69]. The test shows that a good differentiation between a wide range of powders (not only catalysts) can be made. The experimental set-up is more complex compared to the dye degradation because a chemical change (rather than a color change) needs to be monitored. Egerton and King, as well as Irick, show that the results of isopropanol conversion correlate well to weathering of paints [68, 194].

F. INTRODUCTION TO RISK ANALYSIS AND MANAGEMENT

Preventive measures to avoid photocatalytic degradation are theoretically easy: removal of all UV irradiation will stop the degradation process. However, UV removal is not always practical, necessary nor economically viable. Based the results from this research, we propose a risk assessment and management strategy for modern art collections {I}, of which the basic principle are introduced in this section.

Several definitions of risk can be found in literature such as ‘consequences of the activity and associated uncertainties’ [214] or ‘the chance of something happening that will have a negative impact on our objectives’ [215]. In studies towards cultural heritage, the activities could be: display, transport or treatment; the consequences may be chemical degradation or damage; and the uncertainties can relate to surprise events during transport or display (‘black swans’) or limitations of our knowledge concerning composition, exposure and degradation processes.

Two important terms in risk assessment are consequence and likelihood [216]. These terms are complicated to use in risk assessment and management of cultural heritage. Therefore, in the QuickScan approach developed by Brokerhof and Bülow, risk to heritage collections is identified for objects of high value, vulnerability and exposure (Figure 18, left) [217]. Following this approach, we determine the ‘potential risk of impact’ of an art object by combining value and vulnerability of the object. Both terms can be classified as ‘high’ or ‘low’. Consequently, the ‘potential risk of impact’ is illustrated as a two by two matrix of both terms (Figure 18, right), similar to the traditional consequence-likelihood risk profile [216]. This classification results in low potential risk objects (low*low), high potential risk objects (high*high) and everything in between.

The value of the art object should be determined by all stakeholders and consists of a combination of cultural, social and economic value [218]. The vulnerability of the object is related to the paint composition and more specifically the pigment’s photocatalytic activity. This assessment of potential risk is independent of exposure. However, potential risk and exposure are related: for object with a low potential risk (bottom left corner of the diagram), the impact will be small upon exposure. But when an object with a high potential risk is exposed to UV-irradiation, photocatalytic degradation will cause damage and, eventually, an (un)acceptable loss of value (impact).

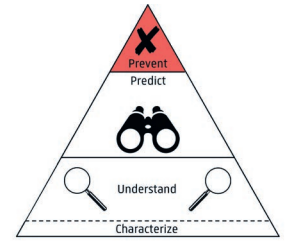
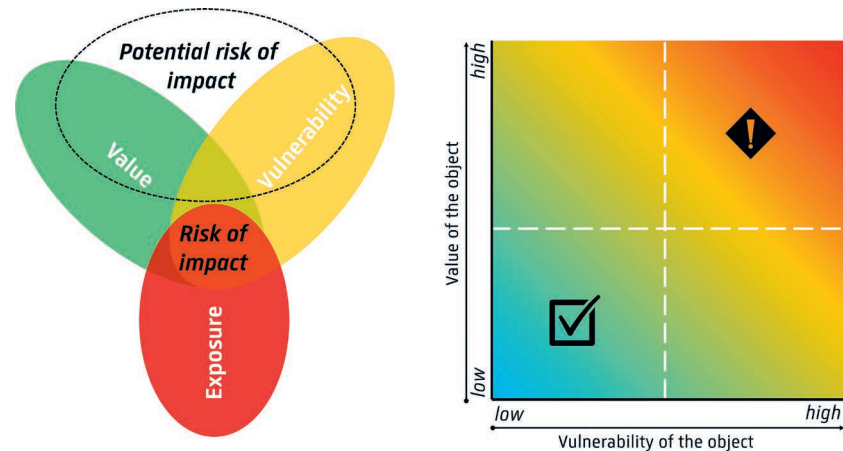


Figure 17 Thesis triangle highlighting prevention.

Determining the potential risk of objects (vulnerable value) in collections is a first step towards proper risk assessment. For high potential risk objects, that are exposed to damaging agents, risk management strategies (corrective actions) should be developed {section I}. In principle there are three general strategies for corrective actions: accept, transfer, and mitigate. Determining which strategy to follow can be done with tools such as cost-benefit analysis. Risk management is about balancing concerns, profits, health and safety, public perception, etc. For risk management to be sustainable it is important to continuously re-evaluate the situation after implementation of corrective actions.

Figure 18 Left: Value, Vulnerability, Exposure --> Effect. Right: Value-Vulnerability diagram (Potential risk of impact).



References for parts A-F

1. Stieg FB. Opaque White Pigments in Coatings. ACS Appl Polym Sc. 1985; 285: 1249-1269.
2. Feller RL and Roy A. Barium sulfate. In: Artists' Pigments: A Handbook of their History and Characteristics, Vol. 1. National gallery of Art, Washington. Londen:Archetype Publications. 1986; p. 47.
3. Eastaugh N, Walsh V, Chaplin T and Sidall R. Pigment compendium, a dictionary and optical microscopy historical pigments, Butterworth-Heinemann. 2004, Burlington: Elsevier.
4. Laver M. Titanium White. In: West FitzHugh E, editor. Artists' Pigments: A Handbook of their History and Characteristics, Vol. 3. National gallery of Art, Washington. Londen:Archetype Publications. 1997. 3: 295-355.
5. Hoffmann MR, Martin ST, Choi W and Bahnmann DW. Environmental Applications of Semiconductor Photocatalysis. Chem Rev. 1995; 95(1): 69-96.
6. Fujishima A, Rao TN and Tryk DA. Titanium dioxide photocatalysis. J Photochem Photobiol C. 2000. 1(1): p. 1-21.
7. Kazuhito H, Hiroshi I and Akira F. TiO₂ Photocatalysis: A Historical Overview and Future Prospects. JPN J Appl Phys. 2005; 44(12R): 8269.Xxx
8. Ohtani B. Photocatalysis A to Z—What we know and what we do not know in a scientific sense. J photochem photobiol. C. 2010; 11(4): 157-178.
9. Ohtani B. "Titania Photocatalysis beyond Recombination: A Critical Review. Catalysts. 2013; 3(4): 942-953.
10. Benedix R, Dehn F, Quaas J and Orgass M. Application of titanium dioxide photocatalysis to create self-cleaning building materials. 2000; p.157-168
11. Gunnarsson SG. Self-Cleaning Paint: Introduction of photocatalytic particles into a paint system. PhD thesis DTU. 2011.
12. Zhao X, Li Z, Chen Y, Shi L and Zhu Y. Solid-phase photocatalytic degradation of polyethylene plastic under UV and solar light irradiation." J Mol Cat A. 2007; 268(1-2): 101-106.
13. Wilk C, editor. Modernism: Designing a New world. Harry N. Abrams, publisher. V&A. 2008.
14. Whiter than white research report. Accompanying the whiter than white exhibition by Material Council (2012). Downloaded at: <https://www.materialscouncil.com/download-the-whiter-than-white-research-report/>. Accessed on January 3rd 2018.
15. Quote from: Lucia Fontana, Manifiesto Blanco. Buenos Aires 1946, reprinted in G. Celant, L'inferno dell'arte italiana materiali (1946-1964) Genoa:Costa&Nolan, 1990 – Reprinted in Monochromes from malevich to the present (Barbara Rose, eds: valeria varas, raul rispa). University of California press 2006 p.39
16. Asbury Brooks B. How the Zero movement became on the Art History's Most Viral Movements. 2014. URL: https://www.artspace.com/magazine/art_101/art_market/zero-group-52526. Accessed 2017.
17. Starn R. Three Ages of "Patina" in Painting. Representations (Spring). 2002; p. 86-115.
18. Van de Vall R, Beerkens L and van den Berg KJ. Questioning patina in modern art. Unpublished project proposal 2012.
19. Crijns B. Loodwit symposium - Geen witte onschuld, een blik op internationale loodwit regelgeving. URL: <http://www.collectiewijzer.nl/2012/01/12/loodwitsymposium-geen-witte-onschuld-een-blik-op-internationale-loodwit-regelgeving-2/>. Accessed 2017.
20. Markowitz G, Rosner D. History and Perspective on Lead
21. Crijns B and Contant I. Dodelijk mooi. In: Magazine of the Cultural Heritage Agency of the Netherland. 2012; vol 1. URL: http://www.kleurenvisie.nl/db/upload/documents/kleur_in_de_media/Dodelijk_mooi_RCE_1_2012.pdf. Accessed 2017.

22. van Bommel MR, Janssen H, Sponk R. Victory Boogie Woogie uitgepakt. 1st edition. Haags Gemeentemuseum and Amsterdam University press. 2012.
23. Martins A, Albertson C, McGlinchey C, Dik J. Piet Mondrian's Broadway Boogie Woogie: non-invasive analysis using macro X-Ray fluorescence mapping (MA-XRF) and multivariate curve resolution-alternating least square (MCR-ALS). *Herit Sci.* 2016; 4.
24. de Keijzer M. The history of modern synthetic inorganic and organic artists' pigments. In: Contributions to conservation at the Netherlands Institute for Cultural Heritage, James & James (Science Publishers) Ltd. 2002
25. De Keijzer M. The colourful twentieth century. In: *Modern Art: the restoration and techniques of modern paper and paints.* 1998; p 13-20.
26. de Keijzer M. Apropos of Titanium white. *Restaur.* 1989; 95(3): 214-217
27. van Driel BA. Unpublished characterization of object in the scope of this dissertation. 2017.
28. Archival information in the Talens Archive and the Winsor&Newton archive supported by personal communication of van Driel B and van den Berg KJ with Bert Klein-Ovink (Royal Talens) and van den berg KJ with Ian Garret (Winsor&Newton). 2014-2018.
29. Cooper H and Spronk R. *Mondrian: the Transatlantic Paintings.* 2001. Yale University Press.
30. Linton J. The white test... 5 years in the making. URL: <http://blog.jonathanlinton.com/2010/05/white-test-5-years-in-making.html>. Accessed November 2014.
31. Mancini-Hresko L. White test. 2013 URL: <http://leomancinihresko.com/white-test-2013/>. Accessed: November 2014.
32. Phenix A, van den Berg KJ, Soldano A, van Driel BA. The Might of White: formulations of titanium dioxide-based oil paints as evidenced in archives of two artists' colourmen mid-twentieth century. In: ICOM-CC Triennial conference 2017, Copenhagen. 2017.
33. Hermans JJ. Metal Soaps in oil paint, structure mechanisms and dynamics. PhD thesis at Van 't Hoff Institute for Molecular Sciences, Universiteit van Amsterdam. 2017. ISBN: 978-94-629-5578-3. URL: <http://hdl.handle.net/11245.1/53663926-183c-40aa-b7b3-e6027979cb7d>. Accessed September 2017.
34. Keune K, Kirsch K and Boon J. Lead soap efflorescence in a 19th C Painting: Appearance, Nature and Sources of Materials. 2006; AIC annual meeting Providence, Rhode Island.
35. URL: <https://www.oxforddictionaries.com/>. Accessed 2017.
36. Schuerman G and Bruzan R. Chemistry of paint. *J Chem Ed.* 1989; 66(4): 327.
37. Levison HW. Yellowing and Bleaching of paint films. *JAIC.* 1985; 24(2): 69-76.
38. Feller RL and Roy A. *Artists' Pigments: A Handbook of Their History and Characteristics*, 1997, National Gallery of Art.
39. Osmond G, Boon JJ, Puskar L and Drennan J. Metal stearate distributions in Modern Artists' oil Paints: Surface and Cross-Sectional investigation of reference paint films using conventional and synchrotron infrared microscopy. *Appl Spectroscopy.* 2012; 66(10).X
40. Baerlocher additives. Metallic stearates. Industrial brochure. URL: <http://bqp.pt/images/Baerlocher%20PDF/Brochure%20Metallic%20Stearates.pdf>. Accessed 2017.
41. Boon JJ. Metal Soaps. URL: <http://www.jaap-enterprise.com/metal-soaps/>. Accessed 2017.
42. Goodeve CF. The absorption spectra and photo-sensitising activity of white pigments. *Transactions Faraday Soc.* 1937; 33(0): 340-347.
43. Anaf W, Trashin S, Schalm O, van Dorp D, Janssens J and de Wael K. Electrochemical Photodegradation Study of Semiconductor Pigments: Influence of Environmental Parameters. *Anal Chem.* 2014; 86(19): 9742-9748.
44. Smijt TG and Pavel S. Titanium dioxide and zinc oxide nanoparticles in sunscreens: focus on their safety and effectiveness. *Nanotech Sciand Applications.* 20121; 4: 95-112.X
45. Haque MM, Detlef B and Muneer M. Photocatalytic degradation of organic pollutants: mechanism and kinetics. In: Rashe MN, Editors. 2012. *Organic Pollutants – Monitoring, risk and Treatment.* Chapter 12.
46. Ohtani B. Preparing Articles on Photocatalysis; Beyond the Illusions, Misconceptions, and Speculation. *Chem Let.* 2008; 37(3): 216-229.
47. Umar M and Abdul Aziz H. Photocatalytic degradation of organic pollutants in water. In: Rashed MN, editor. *Organic pollutants – monitoring, risk and treatment.* 2013. Chapter 8. ISBN: 978-953-51-0948-8
48. Auvinen J and Wirtanen L. The influence of photocatalytic interior paints on indoor air quality. *Atmos Env.* 2008; 42(18): 4101-4112.
49. Papiiaka ZE, Wendland N, Evangelia AV. The protective role of titanium dioxide pigments on pictorial artworks in contaminated indoor environments. In: Rosenberg E, editor. *e-preservation science.* 2010; 7, 48-54. URL: <http://www.morana-rtd.com/e-preservation-science/2010/Papiiaka-13-05-2008.pdf>. Accessed 2017.
50. Costa A, Chiarello GL, Selli E and Guarino M. Effects of TiO₂ based photocatalytic paint on concentrations and emissions of pollutants and on animal performance in a swine weaning unit." *J Environmental Management.* 2012; 96(1): 86-90.
51. Shang J, Chai M and Zhu Y. Solid-phase photocatalytic degradation of polystyrene plastic with TiO₂ as photocatalyst. *J Sol State Chem.* 2003; 174(1): 104-110.
52. Renz C. *Helv. Chim. Acta.* 1921; 4(961).
53. Jacobsen AE. Titanium Dioxide Pigments: Correlation between Photochemical Reactivity and Chalking. *Industrial Eng Chem.* 1949; 41(3): 523-526.
54. Völz HG, Kaempf G, Fitzky HG, Klaeren A. The Chemical Nature of Chalking in the Presence of Titanium Dioxide Pigments. *ACS Photodegrad Photostabil Coat.* 1981; 151: 163-182.
55. Pappas SP and Fischer RM. Photo-chemistry of pigments. Studies on the mechanism of chalking." *Pigment Resin Technol.* 1975; 4(1): 3-10.
56. Colling JH and Dunderdale J. The durability of paint films containing titanium dioxide — Contraction, erosion and clear layer theories. *Prog Org Coat.* 1981; 9(1): p. 47-84.
57. Spathis P, Karagiannidou E, Magoula A-E. Influence of Titanium Dioxide Pigments on the Photodegradation of Paraloid Acrylic Resin. *Stud Conserv.* 2003; 48(1): 57-64.
58. Braun JH, Baidins A, Marganski RE. TiO₂ pigment technology: a review. *Prog Org Coat.* 1992; 20(2): 105-138.
59. Gaumet S, Siampiringue N, Lemaire J, Pacaud B. Influence of titanium dioxide pigment characteristics on durability of four paints (acrylic isocyanate, polyester melamine, polyester isocyanate, alkyd). *Surf. Coat. Int.* 1997; 80(8): 367-372.
60. Johnston-Feller R, Feller RL, Bailie CW, Curran M. The Kinetics of Fading: Opaque Paint Films Pigmented with Alizarin Lake and Titanium Dioxide. *JAIC.* 1984; 23(2): 114-129.
61. Coupry C, Le Marec J, Corset J Duval A, Lahanier C, Rioux et al. Analyses de pigments blancs appliquées à l'étude chronologique des peintures de chevalet - blanc de titane. ICOM-CC: 8th triennial meeting. Sydney. 1987.
62. Decker C. Kinetic Study and New Applications of UV Radiation Curing." *Macromol Rapid Comm.* 2002; 23(18): 1067-1093.
63. Samain L, Silversmit G, Sanyova J, Vekemans B, Salomon H, Gilbert B, et al. Fading of modern Prussian blue pigments in linseed oil medium. *J Anal Atom Spectrom.* 2011; 26(5): 930-941.
64. Marconi BL. Chalking or Fading of Retouches. Whitish appearance of Retouches on Flesh Parts. 6th Joint Meeting of the ICOM committee of museum laboratories and the sub-committee for the treatment of paintings. Brussels. 1967.
65. Feller RL. Problems in Retouching: Chalking of Intermediate Layers. In: *Bulletin of the American Group. International Institute for Conservation of Historic and Artistic Works.* Maney Publishing. 1966; 7(1): 32-34.

66. Kuznetsov VN and Malkin MG. Basic Mechanisms of Thermal Degradation of the Compositions of Synthetic Restoration Polymers With Metal Oxides. *J Appl Spectroscopy*. 2000; 67(5): 763-769.
67. Yang H, Zhu S and Pan N. Studying the mechanisms of titanium dioxide as ultraviolet-blocking additive for films and fabrics by an improved scheme. *J Appl Polym Sci*. 2004; 92(5): 3201-3210.
68. Egerton TA and King CJ. the influence of light intensity on photoactivity in TiO₂ pigmented systems. *JOCCA*. 1979; 62: 386-391.
69. Cundall RB, Hulmet B, Rudham R and Salim S. The photocatalytic oxidation of liquid phase propan-2-ol by pure rutile and titanium dioxide pigment. *JOCCA*. 1978; 61: 351-355.
70. Wilska S. Testing of titanium dioxide pigments in paints for dispersion, weathering resistance and optical properties. *JOCCA*. 1967; 50: 911-941.
71. Conservation Management Plan Volume 2: The Keith Haring Mural, Former Collingwood Technical School. 2011.
72. Lauridsen CB, Sanyova J, Simonsen KP. "Analytical study of modern paint layers on metal knight shields: The use and effect of Titanium white. *Spectrochim Acta A*. 2014; 124: 638-645.
73. De Bondt R. TiO₂, the technical and the rational. Tronox presentation. Personal communication.
74. Erdem B, Hunsicker RA, Simmons GW, Sudol ED, Dimonie VL and El Aasser MS. XPS and FTIR Surface Characterization of TiO₂ Particles Used in Polymer Encapsulation." *Langmuir*. 2001; 17(9): 2664-2669.
75. Martins A, Coddington J, van der Snickt G, van Driel BA, McGlinchey C, Dahlberg D, Janssens J, Dik J. Jackson Pollock's Number 1A, 1948: a non-invasive study using macro-x-ray fluorescence mapping (MA-XRF) and multivariate curve resolution-alternating least squares (MCR-ALS) analysis." *Her Sci*. 2016; 4(1): 33.
76. Burnstock A, van den Berg KJ, van der Gorp F, Bayliss S, Klein-Ovink B. Making paint in the 20th Century: the Talens Archive. In: Eyb-Green S, Townshend JH, Pilz K, Kroustallis S, van Leeuwen I, editors. *Sources in Art Technology, Back to Basics*. Pp. 43-50. Archetype. 2016
77. Gibbs J. F. Weber & Company, Inc. Records. The Getty Research Institute. Access can be requested at URL: <http://archives2.getty.edu:8082/xtf/view?docId=ead/950018/950018.xml>. Accessed 2017.
78. The Winsor&Newton Archive. URL: <https://www.hki.fitzmuseum.cam.ac.uk/archives/winsor-and-newton>. Accessed 2017.
79. Dupont Magazine digital Archive.
80. URL: <http://digital.hagley.org/islandora/object/islandora%3A1979489>. Accessed 2017.
81. Lederle E, Gunther M and Brill R. White pigment, Google Patents. 1938.
82. Werner AJ. Titanium dioxide pigment coated with silica and alumina. Google Patents. 1969
83. Bettler CR, Jacobson HW, Baloga MR and Lewis MH. Titanium dioxide pigment coated with boron-modified silica and alumina, Google Patents. 1998.
84. Albert D. Titanium dioxide of improved chalk resistance, Google Patents. 1972.
85. Gregor B and Roemelt WF. Novel pigment compositions, Google Patents. 1962.
86. Nelson WK. Chalk-resistant titanium dioxide pigment and method for preparing the same. Google Patents. 1944
87. Linsebigler AL, Lu G and Yates JT. Yates, Photocatalysis on TiO₂ Surfaces: Principles, Mechanisms, and Selected Results. *Chem Rev*. 1995. 95(3): p. 735-758.
88. Sclafani A and Herrmann JM. Comparison of the Photoelectronic and Photocatalytic Activities of Various Anatase and Rutile Forms of Titania in Pure Liquid Organic Phases and in Aqueous Solutions. *J Phys Chem*. 1996; 100(32): 13655-13661.
89. Christensen PA, Dilks A, Egerton TA and Temperley J. Infrared spectroscopic evaluation of the photodegradation of paint Part II: The effect of UV intensity & wavelength on the degradation of acrylic films pigmented with titanium dioxide. *J Mater Sci*. 2000; 35(21): 5353-5358.
90. Odling G and Robertson N. Why is Anatase a Better Photocatalyst than Rutile? The Importance of Free Hydroxyl Radicals. *ChemSusChem*. 2015; 8(11): 1838-1840.
91. Carneiro JT, Savenije TJ, Moulijn JA and Mul G. How Phase Composition Influences Optoelectronic and Photocatalytic Properties of TiO₂. *J Phys Chem C*. 2011; 115(5): 2211-2217.
92. Braun JH, Baidins A, Marganski RE. TiO₂ pigment technology: a review. *Prog Org Coat*. 1992; 20(2): 105-138. Double
93. Gazquez MJ, Bolivar JP, Garcia-Tenorio, R and Vaca Federico. A review of the production cycle of titanium dioxide pigment. *Mater Sci Appl*. 2014.
94. Schroder J. Surface treatment of pigments." *Prog Org Coat*. 1988;16: 3-17.
95. Brand JR. Encapsulated by layers of alumina and both dense and voluminous silica, Google Patents. 1980.
96. Jacobson HW. Light-stable titanium dioxide pigment composition. Google Patents. 1980
97. Iler RK. Product comprising a skin of dense, hydrated amorphous silica bound upon a core of another solid material and process of making same, Google Patents. 1959.
98. Schiller M, Muller FW and Damm C. Photo-physics of surface-treated titanium dioxides. *J Photochem Photobiol A*. 2002; 149(1-3): 227-236.
99. Furlong DN. Surface Chemistry of Silica Coatings of Titania. *Colloid Chem of Silica, ACS*. 1994; 234: 535-559.
100. Van Driel BA, van den Berg KJ, Steyn L, Dik J and Rossenaar B. Visualizing the invisible. Poster ICOM-CC triennial conference Copenhagen. 2017.
101. Day RE and Egerton TA. Surface studies of TiO₂ pigment with especial reference to the role of coatings. *Colloid Surface*. 1971; 23(1-2): 137-155.
102. Jensen H, Soloviev A, Li Z and Sogaard EG. XPS and FTIR investigation of the surface properties of different prepared titania nano-powders. *Appl Surf Sci*. 2005; 246(1-3): 239-249.
103. Johansson LS. "Analysing coated powders with XPS." *Surf Interface Anal*. 1991; 17(9): 663-668.1991
104. Diebold U and Madey TE. TiO₂ by XPS. *Surf Sci Spectra*. 1996; 4(3): 227-231.
105. Diebold MP, Kwoka RA, Mehr SR and Varga RW. Rapid assessment of TiO₂ pigment durability via the acid solubility test. *JCT Research*. 2004; 1(3): 239-241.
106. Kobayashi M, Kalriess W. Photocatalytic Activity of Titanium Dioxide and Zinc Oxide. *Cosmetics & Toiletries magazine*. 1997; 112: 83-85.
107. Watts JF and Falla NAR. The analysis of surface coatings and raw materials." *Analytical Proceedings* 1984; 21(7): 255-261.
108. Allen NS, Edge M, Ortega A, Sandoval G, Liauw CM, Verran J, et al. Degradation and stabilisation of polymers and coatings: nano versus pigmentary titania particles." *Polym Degrad Stabil*. 2004; 85(3): 927-946.
109. Carneiro JT, Savenije TJ, Moulijn JA and Mul G. Toward a Physically Sound Structure-Activity Relationship of TiO₂-Based Photocatalysts. *J Phys Chem C*. 2009; 114(1): 327-332.Xxx
110. Xu N, Shi Z, Fan Y, Dong J, Shi J and Hu MZC. Effects of Particle Size of TiO₂ on Photocatalytic Degradation of Methylene Blue in Aqueous Suspensions. *Industrial Eng Chem Res*. 1999; 38(2): 373-379.
111. Henderson M. A surface science perspective on TiO₂ photocatalysis. *Surf Sci Reports*. 2011; 66(6-7): 185-297.
112. Diebold U. The surface science of titanium dioxide." *Surf Sci Reports*. 2003; 48(5-8): 53-229.
113. Wang X, Shui M, Li R and Song Y. Correlation of lattice distortion with photocatalytic activity of titanium dioxide. *Mater Res Bull*. 2007; 43(8-9): 2476-2484.

114. Colbeau-Justin C, Kunst M and Huguenin D. Structural influence on charge-carrier lifetimes in TiO₂ powders studied by microwave absorption. *J Mater Sci*. 2003; 38(11): 2429-2437.
115. Cong Y, Zhang J, Chen F and Anpo M. Synthesis and Characterization of Nitrogen-Doped TiO₂ Nanophotocatalyst with High Visible Light Activity. *J Phys Chem C*. 2007; 111(19): 6976-6982.
116. Luo Z and Gao QH. Decrease in the photoactivity of TiO₂ pigment on doping with transition metals." *J Photochem Photobiol A*. 1992; 63(3): 367-375.
117. Fujihara K, Izumi S, Ohno T and Matsumara M. Time-resolved photoluminescence of particulate TiO₂ photocatalysts suspended in aqueous solutions. *J Photochem Photobiol A: Chem*. 2000; 132(1): 99-104.
118. Mercado C, Seeley Z, Bandyopadhyay A, Bose S, McHale JL. Photoluminescence of Dense Nanocrystalline Titanium Dioxide Thin Films: Effect of Doping and Thickness and Relation to Gas Sensing. *ACS Appl Mater Interface*. 2011; 3(7): 2281-2288.
119. Pallotti DK, Passoni L, Maddalena P, Di Fonzo F and Lettieri S. Photoluminescence Mechanisms in Anatase and Rutile TiO₂. *J Phys Chem C*. 2017; 121(16): 9011-9021.
120. Dozzi MV, D'Andrea C, Ohtani B, Valentini G and Selli E. Fluorine-Doped TiO₂ Materials: Photocatalytic Activity vs Time-Resolved Photoluminescence. *J Phys Chem C* 2013; 117(48): 25586-25595.
121. Nevin A, Cesaratto A, Bellei S, D'Andrea C, Toniolo L, Valentini G and Comelli D. Time-resolved photoluminescence spectroscopy and imaging: new approaches to the analysis of cultural heritage and its degradation. *Sensors*. 2014; 14.
122. Artesani A, Bellei S, Capogrosso V, Cesaratto A, Mosca S, Nevin A, Valentini G, Comelli D. Photoluminescence properties of zinc white: an insight into its emission mechanisms through the study of historical artist materials. *Appl Phys A* 2016; 122(12): 1053.
123. Egerton T. UV-Absorption—The Primary Process in Photocatalysis and Some Practical Consequences. *Molecules*. 2014; 19(11): 18192.
124. Cuttle C. Damage to museum objects due to light exposure. *Lighting Research and Technology*. 1996; 28(1): 1-9.
125. MaterialsTechnology. UV-Degradation Mechanisms. URL: <http://www.drbrmattech.co.uk/uv%20degradation.html>. Accessed 2014.
126. Boye C, Preusser F and Schaeffer T. UV-bloking window films for use in museums – revisited. *WAAC Newsletter*. 2010; 32(1): 13-18.Xx
127. Feller RL. Accelerated aging: Photochemical and thermal aspects. In: Berland D, editor. *Research in Conservation*. Getty conservation institute. 1994. ISBN: 0-89236-125-5.
128. Martin JW, Chin JW and Nguyen T. Reciprocity law experiments in polymeric photodegradation: a critical review." *Prog Org Coat*. 2003; 47(3-4): 292-311.
129. Hare CH. The degradation of coatings by ultraviolet light and electromagnetic radiation. *Journal of Protective coatings & Linings*. 1992.
130. Klemchuk PP. Influence of pigments on the light stability of polymers: A critical review." *Polym Photochem*. 1983; 3(1): 1-27.
131. Thomson G. Penetration of Radiation into Old Paint Films. In *National Gallery Technical Bulletin*. 1979; Vol 3, pp 25-33. URL: <http://www.nationalgallery.org.uk/technical-bulletin/thomson1979>. 15-12-2017.
132. Creagh DC and Bradley D. *Physical Techniques in the Study of Art, Archaeology and Cultural Heritage*. Elsevier Science, editor. 2007; Vol 2: p 203.
133. Pfaff G. *Inorganic Pigments*. De Gruyter, editor. 2017. ISBN: 978-3-11-048451-9
134. Egerton TA, The Influence of Surface Alumina and Silica on the Photocatalytic Degradation of Organic Pollutants. *Catalysis*. 2013; 3(1): 338-362.
135. Gesenhues, U. Influence of titanium dioxide pigments on the photodegradation of poly(vinyl chloride)." *Polym Degrad Stabil*. 2000; 68(2): 185-196.
136. Sullivan WF. Weatherability of Titanium-Dioxide-Containing Paints. *Prog Org Coat*. 1972; 1: 157-203.
137. Muneer M, Philip R and Das S. Photocatalytic degradation of waste water pollutants. Titanium dioxidedmediated oxidation of a textile dye, Acid Blue 40. *Res Chem Intermediat*. 1997; 23(3): p. 233-246.
138. Julson AJ. Photocatalytic decolorization of organic dyes in titanium dioxide-air systems. Masterthesis at North Carolina State University. 2005. URL: <https://repository.lib.ncsu.edu/handle/1840.16/600>. Accessed 2017.
139. Rauf MA and Ashraf SS. Fundamental principles and application of heterogeneous photocatalytic degradation of dyes in solution. *Chem Eng J*. 2009; 151(1-3): 10-18.
140. Gaya UI and Abdullah AH. Heterogeneous photocatalytic degradation of organic contaminants over titanium dioxide: A review of fundamentals, progress and problems. *J Photochem Photobiol C*. 2008; 9(1): 1-12.
141. Mills A. and Le Hunte S. An overview of semiconductor photocatalysis." *J Photochem Photobiol A*. 1997; 108(1): 1-35.
142. Juita, Dlugogorski BZ, Kennedy EM and Mackie C. Low temperature oxidation of linseed oil: a review. *Fire Science Rev*. 2012; 1(1): 1-36.
143. Van den Berg JDJ. Analytical chemical studies on traditional linseed oil paints. PhD thesis Universiteit van Amsterdam. URL: <https://dare.uva.nl/search?identifier=45f7355e-79aa-43be-b6a3-b38cc4ab983f>. Accessed 2017.
144. Van den Berg JDJ, van den Berg KJ and Boon JJ. Identification of non-cross-linked compounds in methanolic extracts of cured and aged linseed oil-based paint films using gas chromatography-mass spectrometry. *J Chromatography A*. 2002; 950(1-2): 195-211.
145. de Viguerie L, Payard PA, Portero E, Walter P and Cotte M. The drying of linseed oil investigated by Fourier transform infrared spectroscopy: Historical recipes and influence of lead compounds. *Prog Org Coat*. 2016; 93: 46-60.Xx
146. Lazzari M and Chiantore O. Drying and oxidative degradation of linseed oil. *Polym Degrad Stabil*. 1999; 65(2): 303-313.
147. Mallégol J, Lemair J and Gardette JL. Drier influence on the curing of linseed oil. *Prog Org Coat*. 2000; 39(2-4): 107-113.
148. Wang X, Rackaitis M. Gelling nature of aluminum soaps in oils. *J Colloid Interf Sci*. 2009; 331(2): 335-342.
149. Mallégol J, Lemair J and Gardette JL. Yellowing of Oil-Based Paints. *Studies Conserv*. 2001; 46(2): 121-131.
150. Irick G, Newland GC and Wang RHS. Effect of Metal Salts on the Photoactivity of Titanium Dioxide. *Photodegrad Photostabil Coat ACS*. 1981; 151: 147-162.
151. *Modern paints uncovered*. In: Learner T, Smithen P, Krueger JW, Schilling MR, editors. *Proceedings from the modern paints uncovered symposium, May 16-19, 2006. Tate Modern, London. Los Angeles: The Getty Conservation Institute; 2008.*
152. Mukherjee D, Barghi S and Ray Ajay. Preparation and Characterization of the TiO₂ Immobilized Polymeric Photocatalyst for Degradation of Aspirin under UV and Solar Light. *Processes*. 2013; 2(1): 12-23.
153. Penot G, Arnaud R and Lemaire J. Cadmium sulphide photocatalytic oxidation of crosslinked polyethylene. *Polym Photochem*. 1982; 2(1): 39-53.
154. de Keijzer M, de Groot S, Megens L and van Keulen H. *Schildertechnisch onderzoek aan Mondriaans Compositie met rood, zwart, geel en grijs uit 1920, Instituut collectie Nederland*. 2008.
155. Zhang A. Photocatalytical Effect of TiO₂ pigments on the surface of Paint films. Master thesis Delft University of Technology. 2013. URL: <https://repository.tudelft.nl/islandora/object/uuid:940a74cf-2f11-45af-a4d5-d66218632535?collect ion=education>.
156. Yamamoto T, Saso N, Umemura Y and Einage Y. Photoreduction of Prussian Blue Intercalated into Titania Nanosheet Ultrathin Films. *JACS*. 2009; 131(37): 13196-13197.
157. Personal communication with Pieter Keune and Klaas Jan van den Berg at Aterliergebouw in 2015.

158. Chen Z. Photo-catalytic activity test for titanium dioxide with artist's pigments and dyes of the 20th century, Master thesis Delft University of Technology. 2013. URL: <https://repository.tudelft.nl/islandora/object/uuid%3Ac14ab687-deca-4eb4-badf-564743a47a84>
159. Asiltürk M, Salilkan F, Erdemoglu S, Akarsu M, Salilkan H, Erdemoglu M and Arpac E. Characterization of the hydrothermally synthesized nano-TiO₂ crystallite and the photocatalytic degradation of Rhodamine B. *J Hazardous Mater.* 2006; 129(1-3): 164-170.
160. Jank M, Koser H, Lucking F, Martienssen M and Wittchen S. Decolorization and Degradation of Erioglaucine (Acid Blue 9) Dye in Wastewater. *Environmental Technology.* 1998; 19(7): 741-747.Xx
161. Dias M and Azevedo E. Photocatalytic Decolorization of Commercial Acid Dyes using Solar Irradiation. *Water, Air, and Soil Pollution.* 2009; 204(1-4): 79-87.
162. Bianco Prevot A, Baiocchi C, Brussino MC, Pramauro E, Savarino P, Augugliaro V, et al. Photocatalytic Degradation of Acid Blue 80 in Aqueous Solutions Containing TiO₂ Suspensions." *Environmental Sci Technol.* 2001; 35(5): 971-976.
163. A Comprehensive Understanding of TiO₂ Pigment Durability. *Paint & Coating Industry.* 2005. URL: <http://www.pcimag.com/articles/a-comprehensive-understanding-of-tio2-pigment-durability>. Accessed 2017.
164. Pigment Volume Concentration. MPI online training. a. URL: <http://www.mpi.net/mpitraining/level1/Coatings/Pigments2.asp>. Accessed 2014.
165. Blackman C. Choosing varnishes, in between the concept and the reality falls the practising conservator. 2007. URL: <http://www.e-conservationline.com/content/view/568/145/>. Accessed 2014.
166. Jin C. FTIR Studies of TiO₂ - Pigmented Polymer Photodegradation. PhD thesis University of Newcastle upon Tyne. 2004. URL: <http://ethos.bl.uk/OrderDetails.do?uin=uk.bl.ethos.405309>. Accessed 2017.
167. Worsley DA and Searle JR. Photoactivity test for TiO₂ pigment photocatalysed polymer degradation. *Mater Sci Technol.* 2002; 18(6): 681-684.Xxx
168. Christensen PA, Dilks A, Egerton TA and Temperley J. Infrared spectroscopic evaluation of the photodegradation of paint Part I. The UV degradation of acrylic films pigmented with titanium dioxide. *J Mater Sci.* 1999; 34(23): 5689-5700.Xx
169. Jin C, Christensen PA, Egerton TA, Lawson EJ and White JR. Rapid measurement of polymer photo-degradation by FTIR spectrometry of evolved carbon dioxide. *Polym Degrad Stabil.* 2006; 91(5): 1086-1096.
170. Robinson AJ, Searle JR and Worsley DA. Novel flat panel reactor for monitoring photodegradation. *Mater Sci Technol.* 2004; 20(8): 1041-1048.
171. Ellinger ML. Weathering tests. *Prog Org Coat.* 1977; 5: 21-35.
172. Kampf G, Papenroth W, Voltz G and Weber G. Quick-Motion observation of Chalking under the electron microscope.
173. Meilunas RJ, Bentsen JG and Steinberg A. Analysis of Aged Paint Binders by FTIR Spectroscopy. *Studies Conserv.* 1990; 35(1): 33-51.Xx
174. Watson SS, Tseng IH, Forster A, Chin J and Sung LP. Investigating Pigment Photoreactivity for coating applications: method development. In: *Service life prediction of polymeric materials.* Springer. 2009; Chapter 29, 423-456.
175. Izzo, F. C., et al. (2011). "TG-DSC analysis applied to contemporary oil paints." *Journal of Thermal Analysis and Calorimetry* 104(2): 541-546.
176. Spyros A and Anglos D. Study of Aging in Oil Paintings by 1D and 2D NMR Spectroscopy. *Anal Chem.* 2004; 76(17): 4929-4936.
177. Ploeger R, Musso S and Chantore O. Contact angle measurements to determine the rate of surface oxidation of artists' alkyd paints during accelerated photo-ageing. *Prog Org Coat.* 2009; 65(1): 77-83.
178. Mills JS. The Gas Chromatographic Examination of Paint Media. Part I. Fatty Acid Composition and Identification of Dried Oil Films. *Studies in Conserv.* 1966; 11(2): 92-107.X
179. Duce C, Della Porta V, Tine MR, Spepi A, Ghezzi L, Colombini MP and Bramanti E. FTIR study of ageing of fast drying oil colour (FDOC) alkyd paint replicas. *Spectrochimica Acta Part A.* 2014; 130(0): 214-221.X
180. Van der Weerd J, van Loon A and Boon JJ. FTIR Studies of the Effects of Pigments on the Aging of Oil." *Studies in Conserv.* 2005; 50(1): 3-22.
181. Dilks A. An XPS study on the effect of pigment on the UV degradation of an Epoxy system." *Degrad stabil polym.* 1983; 1: 601-628.
182. Cho S and Choi W. Solid-phase photocatalytic degradation of PVC-TiO₂ polymer composites. *J Photochem Photobiol A.* 2001; 143(2): 221-228.
183. Khataee AR and Kasiri MB. Photocatalytic degradation of organic dyes in the presence of nanostructured titanium dioxide: Influence of the chemical structure of dyes. *J Mol Catal.* 2010; 328(1-2): 8-26.Xx
184. Cortes JA, Alarcon-Herrera MT, Perez Robles JF, Vollicana-Mendez and Gonzalez-Hernandez J. Kinetic degradation of acid blue 9 through the TiO₂/UV advanced oxidation process. Conference and trade. 2007. URL: http://iwra.org/congress/resource/abs774_poster.pdf. Accessed 2017.
185. Gustavsson AK. Solar Photocatalytic degradation of rhodamine B by TiO₂ nanoparticle composites, Master thesis University of Gothenburg. 2010. URL: https://radfys.gu.se/digitalAssets/1305/1305320_Rapport_Emil.pdf. Accessed 2017.
186. Lakshmi S, Ranganathan R and Fujita S. Study on TiO₂-mediated photocatalytic degradation of methylene blue. *J Photochem Photobiol A.* 1995; 88(2-3): 163-167.X
187. Yan X, Ohno T, Nishijima K Abe and Ohtani B. Is methylene blue an appropriate substrate for a photocatalytic activity test? A study with visible-light responsive titania. *Chem Phys Let.* 2006; 429(4-6): 606-610.
188. Saquib M, Abu Tariq M, Faisal M and Muneer M. Photocatalytic degradation of two selected dye derivatives in aqueous suspensions of titanium dioxide. *Desalination.* 2008; 219(1-3): 301-311.
189. Shahmoradi B, Maleki A and Byrappa K. Photocatalytic degradation of Amaranth and Brilliant Blue FCF dyes using in situ modified tungsten doped TiO₂ hybrid nanoparticles. *Cat Sci Technol.* 2011; 1(7): 1216-1223.
190. Tang WZ and Huren A. Photocatalytic degradation kinetics and mechanism of acid blue 40 by TiO₂/UV in aqueous solution. *Chemosphere.* 1995; 31(9): 4171-4183.
191. Bouzaida I, Ferronato C, Chovelon JM Rammah ME and Herrmann JM. Heterogeneous photocatalytic degradation of the anthraquinonic dye, Acid Blue 25 (AB25): a kinetic approach. *J Photochem Photobiol A.* 2004; 168(1-2): 23-30.
192. Doushita K and Kawahara T. Evaluation of Photocatalytic Activity by Dye Decomposition. *J Sol-Gel Sci Technol.* 2001;22(1-2): 91-98.
193. Daneshvar N, Salari D, Niaei A and Khataee AR. Photocatalytic degradation of the herbicide erioglaucine in the presence of nanosized titanium dioxide: comparison and modeling of reaction kinetics." *J Environ Sci Health B.* 2006; 41(8): 1273-1290.X
194. Irick G. Determination of the photocatalytic activities of titanium dioxides and other white pigments. *Jf Appl Polym Sci.* 1972; 16(9): 2387-2395.
195. Mills A, Hill C and Robertson PKJ. Overview of the current ISO tests for photocatalytic materials. *J Photochem Photobiol A.* 2012; 237: p. 7-23
196. Runyan WR and Shaffner TJ. *Semiconductor Measurements and Instrumentation*, McGraw Hill. 1998.
197. Herrmann JM, Disdier J, Mozzanega MN and Pichat P. Heterogeneous photocatalysis: In situ photoconductivity study of TiO₂ during oxidation of isobutane into acetone. *J Catalysis.* 1979; 60(3): 369-377.
198. Chin J, Scierka S, Kim T and Forster A. Photoconductivity Technique for the Assessment of Pigment Photoreactivity. Federation of Societies for Coatings Technology (FSCCT) Technical Program Annual Meeting, 81st. 2003. Philadelphia.
199. Coronado JM, Maira AJ, Conesa JC, Yeung KL, Augugliaro V and Soria J. EPR Study of the Surface Characteristics of Nanostructured TiO₂ under UV Irradiation. *Langmuir.* 2001; 17(17): 5368-5374.
200. Howe RF and Gratzel M. EPR study of hydrated anatase under UV irradiation. *J Phys Chem.* 1987; 91(14): 3906-3909

201. Lund A, Shimida S and Shiatani M. Principles and Applications of ESR Spectroscopy, Springer. 2011.
202. Ceresa E, Burlamacchi L and Visca M. An ESR study on the photoreactivity of TiO₂ pigments." J Mater Sci. 1983; 18(1): 289-294.
203. Schlick S, Kruczala K, Motyakin MV and Gerlock JL. Spectral profiling of radicals in polymer degradation based on electron spin resonance imaging (ESRI). Polym Degrad Stabil. 2001; 73(3): 471-475.
204. Rasmussen K, Grampp G, van Eesbeek M, Rohr T. Thermal and UV Degradation of Polyimides and Silicones Studied In Situ With ESR Spectroscopy. 2009. 11th International Symposium on Materials in a Space Environment, Aix-en-Provence, France.
205. Rasmussen K, Grampp G, van Eesbeek M and Rohr T. Thermal and UV Degradation of Polymer Films Studied In situ with ESR Spectroscopy. ACS Appl Mater Interfaces. 2010; 2(7): 1879-1883.
206. Vermeulen M, Sanyova J, Janssens K, Nuyts G, de Meyer S and de Wael K. The darkening of copper- or lead-based pigments explained by a structural modification of natural orpiment: a spectroscopic and electrochemical study. JAAS. 2017; 32(7): 1331-1341.
207. Mills A, O'Rourke C and Wells N. A smart ink for the assessment of low activity photocatalytic surfaces. Analyst. 2014; 139(21): 5409-5414.
208. Mills A, Wells N and O'Rourke C. Probing the activities of UV and visible-light absorbing photocatalyst powders using a resazurin-based photocatalyst activity indicator ink (Rz Paii). J Photochem Photobiol A. 2017; 338: 123-133.
209. Mills A and Wells N. Indoor and outdoor monitoring of photocatalytic activity using a mobile phone app. and a photocatalytic activity indicator ink (paii). J Photochem Photobiol. 2015; 298(Supplement C): 64-67.
210. Mills A, Wells N and O'Rourke C. Correlation between the photocatalysed oxidation of methylene blue in solution and the reduction of resazurin in a photocatalyst activity indicator ink (Rz Paii). J Photochem Photobiol A. 2016; 330: 86-89.
211. Church AH. The Chemistry of Paints and Painting, Seeley, Service. 1915.
212. Mills A, O'Rourke C, Lawrie K and Elouali S. Assessment of the Activity of Photocatalytic Paint Using a Simple Smart Ink Designed for High Activity Surfaces. ACS Appl Mater Interfaces. 2014; 6(1): 545-552.
213. Mills A. Ink Intelligent. URL: <http://www.inkintelligent.com/>. Accessed 2017.
214. Aven T. Risk assessment and risk management: Review of recent advances on their foundation. European Journal of Operational Research. 2016; 253(1): 1-13.
215. Pedersoli JL Jr, Antomarchi C and Michalski S. A Guide to risk management of cultural heritage. ICCROM publication. 2016. URL: http://www.iccrom.org/sites/default/files/2017-12/risk_management_guide_english_web.pdf. Accessed: 2017.
216. 31000. International standard Risk management – principles and guidelines. 2009
217. Brokerhof AW and Bulow AE. The QuickScan – a quick risk scan to identify value and hazards in a collection. J Institute of Conservation. 2016; 39(1): 18-28.
218. Cultural Heritage Agency of the Netherlands. Assessing museum collections. 2014. ISBN: 9789057992247.

PART 1



pXRF analysis. Photo credit: K.J. van den Berg

Characterization of use and properties of titanium white pigments

*‘There are two possible outcomes:
if the result confirms the hypothesis,
then you’ve made a measurement.
If the result is contrary to the
hypothesis, then you’ve made
a discovery.’²⁵*

²⁵ Enrico Fermi, https://www.brainyquote.com/quotes/quotes/e/enricofermi125836.html?src=t_measurement, accessed 11-12-2017.

APPROACH PART 1

The current state of knowledge on the use and occurrence of TiO_2 pigments is scattered, unorganized, and does not constitute a structural record of the use within a certain country or time frame. Thus, the main question under investigation in this part is: how widespread was the use of titanium white in the Netherlands in the 20th century? Addressing this question is urgent to get an idea of the extent of the TiO_2 problem.

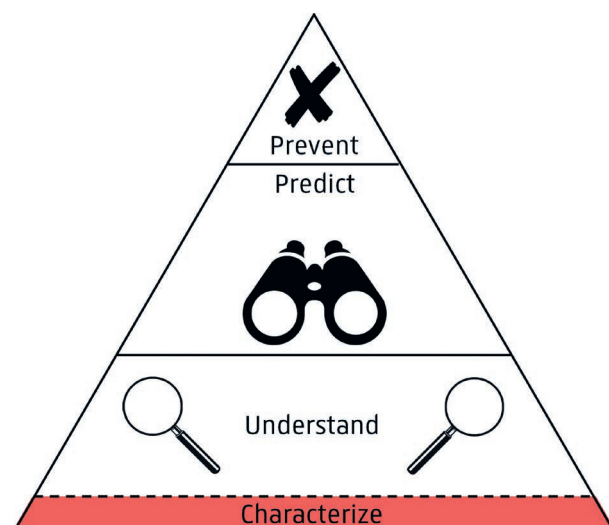
In chapter 1, an extensive (180 paintings) survey carried out at Dutch modern art institutes is presented to gain insight into the white pigments used between 1920 and 2000 in the Netherlands. This survey was carried out continuously over the course of three years. X-ray fluorescence spectrometry (XRF) was chosen as the method of analysis, given its element sensitivity for the elements of interest (Ca, Ba, Ti, Pb, Sr, Zn), the instrument availability and transportability, its non-invasive character, and its ease of use. These properties are important, considering the need to gain access to collections, as well as the future aim to extend the survey {H}. The drawback of this choice is that XRF does not provide information about crystal structure and surface treatment of the pigments {C.2}. Micro-sample analysis carried out by X-ray diffraction (XRD) and Scanning Transmission Electron Microscopy coupled with Energy Dispersive Spectroscopy (STEM-EDX)²⁶ supports the XRF analysis to compensate for this lack of information.

With the introduction of Macro X-ray fluorescence spectrometry (MA-XRF), portable X-ray fluorescence spectrometry (pXRF) seems to be currently viewed as a less useful method²⁷. Even though the method is still common as a simple 'point and shoot' diagnostic tool, it often does not reach its full potential in the way it is currently used. Thanks to the investigation of a medium-sized dataset of different paintings and references, and consequently the use of several types of data-analysis, an interesting discovery was made relating to a trace element marker, thus extending the current capability of pXRF.

The effects of crystal structure and coating on photocatalytic activity are reasonably well understood and relatively straightforward to characterize {C.2.1 and C.2.3}. However, this is not the case for the electronic structure of titanium white pigments {C.2.5}. While photoluminescence is being used more and more to investigate semiconductor pigments, the lack of knowledge concerning the photoluminescence behaviour of TiO_2 pigments was a clear gap. This is especially striking considering that the luminescence behaviour of other white pigments has been under

26 Unfortunately only a minor amount of case study analysis can be discussed in chapter 1. Other (diagnostic) analysis was performed in the scope of my study such as analysis of the white Rietveld chair in the Rijksmuseum collection or analysis of a white retouch from two van Gogh paintings. My vision of the field {J} would entail collecting such data in an international database, as they usually do not fit in specific papers but nevertheless are very valuable.

27 Personal opinion from four years in the field. pXRF is valued as a direct characterization tool but not as a tool to answer in depth research questions.



investigation, and that the luminescence behaviour of non-pigment grade TiO₂ powders also have been subjected to in-depth research. Thus, through a shared interest in this research question between myself and the Politecnico di Milano (A. Nevin and D. Comelli) and our different expertise (pigment and technique respectively), a proposal was submitted and granted via Laserlab-Europe. Chapter 2 presents the first explorative study into the photoluminescence of titanium white pigments.

Chapter 1

The white of the 20th century – A broad XRF survey into Dutch modern art collections.

White pigments were abundantly used in 20th century paintings, and relate to several degradation risks such as titanium white mediated photocatalytic binder degradation or zinc soap formation. Knowledge about the white pigments that were used is essential for risk assessments of 20th century collections. In this study, a representative set of 179 paintings in Dutch modern art collections were analyzed by portable X-ray fluorescence spectrometry. Subsequent explorative data analysis was performed, supported by qualitative findings from 140 home-made reference samples. Micro-samples were further investigated by X-ray diffraction and scanning transmission electron microscopy to gain information about crystal structure and surface coating.

This study reveals that Dutch 20th century artists were hesitant to use titanium white. In the Netherlands, the use of this pigment is observed convincingly from the 1970s onward and initially mostly in non-oil binders. Additionally, lead white was used until late in the 20th century for paints and grounds but rarely mixed with titanium white in paints. The study also indicated that many CoBrA artists used zinc white, underlining the risk of degradation due to soap formation.

Furthermore, this study highlights the different production processes of titanium white. Through the association of titanium with niobium, an impurity only present for sulfate processed pigments, the production process can be identified. The absence of niobium indicates the presence of rutile and is thus a sign of paint stability, as well as a 'post 1959' dating.

This explorative study illustrates the value of a combination of data analysis approaches, which includes assessment of spectra as well as descriptive, bivariate and multivariate analysis, for medium-sized datasets gathered at similar conditions.

Based on the published paper: B.A. van Driel, K.J. van den Berg, J. Gerretzen and J. Dik (2018), *Heritage Science* 6:16.

Note This manuscript includes a document with supplementary material (in the text referred to as 'SI') which can be downloaded (link is provided in the back matter).

1.1. Introduction

This study investigates the use of different white pigments in the Netherlands during the 20th century. The 20th century was a century of great technological achievements, of shattering world wars and of modern art and architecture: ‘art for the purpose of art’.^{1,1} Within this era, Le Corbusier popularized white in his modernist architecture of the 1920s and with Kazimir Malevich’s painting ‘White on white’ (1918), white became a defining icon of modernism. Almost simultaneously, in November of 1918, industrial production of titanium white composite pigments began in Fredrikstad, Norway [1]. Around the same time, health and safety problems related to lead white were discovered, leading to a ban or restriction (Geneva White Lead Convention) of the use of lead white for interior painting between 1905 and 1930 in most countries [2]. Although lead white was on the market (pure or mixed) in the 20th century, Bacci et al. report, based on literature, that its presence dropped from 100% in the early 20th century to 10% by 1945, and it nearly disappeared after the second world war [3, 4]. Less effective earlier alternatives to lead white such as lithopone (a co-precipitate of barium sulfate and zinc sulfide) were eventually and after heavy competition [5], replaced by the new and superior calcium-based rutile titanium white [2].

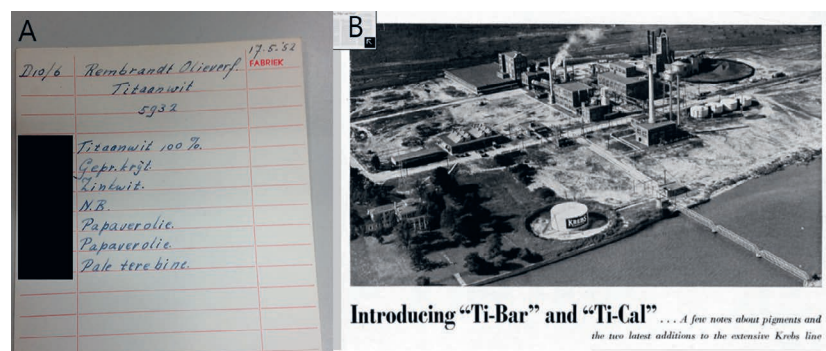
Zinc white was marketed by Winsor & Newton in 1834 and was thus an earlier alternative for lead white. However, initially zinc white was not very popular. This is due to the price difference (zinc white being more than four times more expensive than lead white at the turn of the 18th century), as well as the lack of hiding power. Zinc white only became popular after 1850 [6]. After the introduction of titanium white, zinc white continued to be used as a pure pigment. Additionally, it is used in titanium white paints and colored paints to adjust the tinting strength [7].

In the early 1940s, Piet Mondriaan painted his famous Broadway Boogie Woogie and Victory Boogie Woogie, reportedly using Permalba [8, 9], a renowned American titanium white [7]. However, Mondriaan complained about the properties of titanium white, and he is assumed to have preferred lead white [10]. The discussion about the best choice of white has continued since the days and complaints of Mondriaan. Present day artists still wonder and do small tests to compare paint characteristics of white paints [11, 13]. The white pigments all have their specific benefits and drawbacks. Lead white oil paint is toxic but has brilliance, a nice consistency and a faster drying time. Titanium white oil paint has high opacity but is said to have a higher tendency to yellow and

1.1 A 19th Century expression related to modernism - ‘L’art pour l’art’ in French.

zinc white oil paint dries to a brittle film, although it is beneficial due to its transparency and price. Combining titanium and zinc white makes successful formulations and is often found in recipes in the United States as well as in Europe, see Figure 1A [7].

Figure 1.1 A - 1952 Recipe for titanium white from the archive of Royal Talens (Apeldoorn, the Netherlands) and B - An article concerning titanium white composite pigments from the Dupont magazine 1935 [14].



In the 1920s most commercial titanium white pigments are composite pigments from the plant in Fredrikstad or Niagara Falls, see Figure 1B {SI table 1}. After 1926, the production of pure anatase pigments is reported [1]. In the 1940s, surface treatments and rutile pigments enter the market, but the main pigments continue to be composite pigments until they are eventually discontinued, around 1970 [5], due to their incompatibility with water-borne paints [15].

The evolution of the use of white pigments is undoubtable country dependent, related to novel developments and patents and connected to marketed pigments as well as artist preference. While trends of white pigment use have been identified, they seem to have a geographical bias toward the United States [1, 5].

This study intends to geographically specify and extend information about the use of white pigment by non-invasive and micro-invasive analysis of 20th century paintings mainly by Dutch artists. The driving force was the need to know the extent of use of titanium white in relation to its risk of photocatalytic degradation [16-18]. The timing of titanium white becoming popular amongst artists is important, as it possibly relates to the quality of those pigments. Similarly, knowing how much zinc white has been used may help us understand and estimate the extent of the zinc soap degradation risks of modern collections [19].

In this study, portable X-ray fluorescence spectrometry (pXRF) was used to investigate the white pigments used in modern paintings in Dutch art collections. Portable XRF was chosen for its general availability (both to the authors and also increasingly for museums), for its ease of use and its completely non-invasive character. The

main drawback of XRF is that the distinction between rutile or anatase pigments cannot be made [20, 21]. Furthermore, pigment coating materials, such as alumina and silica, cannot be detected. To account for the limitations of pXRF on paintings, a selection of titanium containing micro-samples are investigated by X-ray diffraction (XRD) and scanning transmission electron microscopy with energy dispersive spectroscopy (STEM-EDX).

Portable XRF, while being widely used for the investigation of paintings [21-24], should be interpreted with care as physical processes such as attenuation, absorption and matrix effects can influence the outcome. Furthermore, so-called escape peaks, scatter peaks, peaks originating from the instrument as well as overlapping peaks can complicate interpretation, which is especially challenging when investigating non-homogeneous multilayer materials such as paintings. Given these limitations, while peak areas are used to facilitate interpretation, the results of this study should be considered as qualitative, showing merely trends. A notorious difficulty, applicable to white paint, is the overlap between Ti K-lines and Ba L-lines [21]. This overlap can challenge the identification of titanium when barium is also present [7]. Hence, in this study, the applicability of PyMCA (Python MultiChannel Analyzer) [25] for deconvolution of these overlapping peaks is evaluated with self-made reference paints. As a comparison of XRF spectra can be challenging, more and more accounts of additional multivariate data analysis are reported [26-29]. It is in this scope that, Principal Component Analysis (PCA) has been used in this chapter to enhance the interpretability of the pXRF dataset.

To summarize, the goal of the present study is to gain insight into the use of 20th century white pigments in Dutch collections. This is performed using a combination analytical techniques and data analysis approaches. To that end, we use pXRF on paintings and reference samples, supported by XRD and STEM-EDX on particular micro-samples. The data analysis approaches includes spectral assessment, as well as descriptive, bivariate and multivariate methods. The gained insight is useful for risk assessment of paintings at modern art institutions, especially in relation to degradation phenomena occurring in paints containing the different white pigments.

1.2. Experimental

1.2.1. Dataset

In total, the dataset contains 189 paintings, 179 of which were analyzed by pXRF. Micro-samples were taken from nine out of

these 179 paintings. Ten paintings could not be analyzed by pXRF due to accessibility to the artwork and are only available as micro-samples. The micro-samples (19 in total) were analyzed by XRD and/or STEM-EDX. Data for this study was gathered over the course of three years at several art institutions aiming to gather a representative dataset of 20th century paintings. The data gathering procedure is representative for painting specific analysis performed in museum studios. The art institutes include Dutch company art collections as well as several Dutch modern art museums (see Table 1.1), resulting in a geographical focus towards the Netherlands. The goal when building the dataset was to avoid bias towards specific artists or towards a specific artistic movement. This was achieved by arbitrarily choosing 20th century paintings containing white, spread between 1920 and 2000. The selection of artworks was left to the discretion of the collection keepers under the conditions that the paintings have white areas, are unframed and were painted after 1920. Each collection keeper approached this differently. For instance the collection database was searched for the word ‘white’ and filtered for the time period. In other instances, physically accessible paintings in a collection or office buildings were chosen, taken into account radiation safety. The number of works that could be measured was limited by the time the institutions allowed access to the collections (mostly 1-3 days) and by whether the paintings were collected in a single room or hanging throughout a building.

Table 1.1 Overview of the artwork dataset.

**Indicates the paintings that were analyzed with pXRF and XRD or STEM-EDX.*

Art collection	Number of investigated paintings	
	XRF	XRD and or STEM-EDX
AMC art collection	6	0
Cobramuseum Amstelveen	35	1*
Gemeentemuseum Den Haag	30	1*
ING art collection	11	0
Museum Prinsenhof Delft	16	0
Bouwfonds art collection	16	8
RCE art collection	35	1
Stedelijk museum Schiedam	25	0
Other	5	8*
Total	179	10*+9

While being balanced over time, with more than 20 paintings per decade from the 1940s to the 1980s, and geographically focused on the Netherlands, the dataset is unavoidably art historically limited. Some art historically significant artists or artistic movements, such as Mondriaan or the neo-realistic movement, are missing from the pXRF dataset. However, our selection does reflect a continuous chronology of whites used between 1920 and 2000. In other words, while not being art-historically complete our selection is chronologically and geographically representative.

The size of the dataset allowed for a combination of data analysis approaches. It is small enough to assess the spectra individually and large enough to identify interesting trends. A second data set (the reference set), composed of self-made paints, was analyzed in this study. It was built with the aim to reach better spectral interpretation following qualitative guidelines specifically related to peak ratios, peak overlap and layering effects. The need for improved spectral interpretation is due to the large number of non-expert users in museums and was highlighted by a pXRF round robin in 2009. The round robin indicated that while 65% of the laboratories identified the correct elements, only 40% reached a correct interpretation [21].

The reference set was based on readily available paints from other studies containing mixtures of different types of titanium white, titanium white mixed with zinc white, barium sulfate or calcium carbonate [16, 18], as well as combinations of single-pigment layers (unpublished study). The dataset was extended with several crucial samples including layer combinations and mixtures with lead white and a calibration set for the Ba-L/Ti-K deconvolution. The reference samples were painted either on melinex or on modern prepared canvas board and attached with double-sided tape to a Perspex board for pXRF analysis to limit background detection.

Both complete datasets are summarized in the Supplementary Information in Tables 2 and 3.

1.2.2. Analysis

1.2.2.1 Portable X-ray fluorescence spectrometry

The paintings were analyzed using a Bruker III-SD pXRF. Two different instruments of the same type were used due to instrument availability during the project. Measurements were taken in two slightly different settings for the two instruments suitable for the detection of the elements of interest in paintings:^{1,2}

- Bruker Tracer III-SD (1) 40 kV, 10µA, air, 10 s, no contact, Ti/Al filter.
- Bruker Tracer III-SD (2) 40kV, 15µA, air, 30 s, no contact, Ti/Al filter.

The Ti/Al filter was used because it renders pXRF more suitable for the analysis of elements from titanium to silver. Using the filter provides a reduced background in the low energy region and eliminates, for instance, the Rh-L and Ar-K lines originating from the tube and the air {SI Figure 1}.

1.2 The use of different instrument settings was an unintended error. The time between using the first and the second instrument was substantial, due to the malfunctioning of the first instrument. Since time of analysis can easily be corrected and 10 or 30 s is both appropriate for the detection of the elements of interest, changing the time from 10 to 30 seconds was a minor concern. Furthermore, the second instrument had a glitch and only functioned in the 40 kV, 15 µA setting.

1.3 To return the favor of allowing us access we offered collections analysis to answer questions about specific paintings.

Depending on the number of artworks to be measured in one day, and on specific questions from the collection,^{1,3} we measured a different number and selection of areas per painting. For each painting, at least two different areas of white paints were analyzed. Additionally, the following areas were occasionally analyzed: impasto areas, areas of paint ground, the back of the painting and colored areas. Furthermore, in some cases, additional measurements were performed without the Ti/Al filter. Therefore the number of spectra per artwork is variable and averaging of peak areas is performed before data analysis.

The reference samples were all measured two times, some of which were additionally analyzed without the Ti/Al filter.

1.2.2.2. X-ray diffraction & STEM-EDX

The crystalline phases of individual micro-samples were analyzed by XRD using a Discover D8 microdiffractometer with a general area detection diffraction system (GADDS) two dimensional detector (Bruker AXS, Karlsruhe, Germany). The samples were measured without preparation on a concave microscope slide. Diffractograms were acquired in reflection mode using Cu-K α 1 as primary radiation (40 kV, 30 mA). The GADDS software was used for azimuthal integration of the two-dimensional XRD pattern in order to obtain a one-dimensional 2theta diffractogram suitable to perform a PDF library search on, using the Bruker AXS Eva software, for phase identification.

Bright field images of the powders were collected on a JEOL 2010F FEG-TEM equipped with a STEM unit and ThermoNoran EDX detector for elemental mapping. Samples were prepared by dipping a lacey C coated Cu TEM grid in the powder and subsequently removing the excess of powder.

1.2.3. Data exploration

Data analysis was performed with the primary aim to investigate when titanium white became popular among artists working in the Netherlands in the 20th century. The exploration of the data was performed using a semi-quantitative approach which combines spectral investigation of paintings and references, with descriptive, bivariate and multivariate analysis. The qualitative results or trends obtained with principal component analysis in this study could be obtained and confirmed by descriptive and bivariate analysis as well. However, PCA is used here mainly as a visualization tool, because it is able to provide an interpretable summary of the data in two dimensions.

Data analysis was performed on the deconvoluted elemental peak areas. This method was chosen because it is easily interpretable and physically relevant. Data analysis on (corrected) raw spectra, which contain more information, as well as the use of other types of multivariate analysis, may result in more detailed differentiation of paints. However, these methods fall outside the scope of our study at this explorative stage.

1.2.3.1. Deconvolution

PyMCA was used for batch spectral deconvolution. An iterative approach was followed to find a suitable deconvolution configuration, starting with all of the known parameters and subsequently testing and adjusting the configuration {SI, figure 2 to 10}. The goal was to find an appropriate deconvolution for the overlapping barium L-lines and titanium K-lines. Evaluation of the deconvolution, performed on reference paint outs of TiO₂/BaSO₄/oil mixtures showed to be very accurate {SI figure 11-13}.

In this study we analyzed the peak areas calculated through spectral deconvolution. In other words, each variable is a peak area related to a specific element. The peak area is the sum of the areas under all elemental K-peaks or L-peaks respectively [25]. Using the peak area, rather than the height, is preferential because it is not affected by the spectrometer resolution but only by the number of X-ray photons detected. Ideally, the peak area, while related to the concentration in homogeneous samples, needs to be adjusted using an element specific calibration constant and a matrix specific correcting term which accounts for the matrix effects such as absorption and enhancement. Elemental concentration were not calculated in this study, given the mistakes it would inherently cause, because we are dealing with inhomogeneous and layered structures [20].

1.2.3.2. Post-treatment

Time and threshold correction:

Before data analysis, all peak-areas produced by PyMCA were corrected for the measurement time and for a manually set threshold value. The threshold values were determined by identifying the minimum peak area for which a peak was still visible in the spectrum. This was done with the intention only to analyze variables that conservators and scientists in museums could visually extract from the spectrum. A list of the used threshold values can be found in the SI Tables 5 and 6.

1.4 Another approach is to average the spectra prior to deconvolution. Additionally, for the future a smart averaging algorithm could be developed separating the different types of paint on one painting and only averaging those similar to one another.

Averaging:

The full dataset contains about 1000 spectra including multiple spectra from the same artworks. The approach in this explorative study was to average the peak areas of multiple spectra from the same artwork. In different data subsets, the spectra of all the white areas, the spectra of all the colored areas, the spectra of all the white impastos or the spectra of all the areas of ground were averaged. This procedure may go at the expense of information such as the presence of different white paints on the same painting which could be of interest for a follow up study.^{1,4}

Normalization:

The average counts per second can vary drastically per element depending on the energy of the emitted photons. In order to make the values more comprehensible, they were normalized by division by the maximum peak area, for selected subset analyses. This results in normalized peak areas where '1' is the main peak of the spectrum, and the other values are the fraction of the main peak. Hence, a peak area of '1' for titanium and '0.9' for zinc indicates that visually (raw spectrum) the peaks are nearly equal in size. This procedure was performed to enhance the interpretability of the results. It is important to remember that XRF is not quantitative in terms of elemental concentration and peak areas are also influenced by element sensitivity of the instrument and instrument settings.

Error:

The measurement error is negligible in comparison with the induced error originating from paint heterogeneity and post-processing. All the samples in the reference set were measured twice in order to get a better understanding of the size of this induced error. Between each measurement, the instrument was removed from the paint surface and repositioned, to induce the expected variability in measurement distance. This procedure leads to an error between 5 and 20% of the peak area, based on the average of the standard deviations of the titanium K peak area of each set of two measurements. The same error holds for elemental detection limits that were investigated for an instrument from the same manufacturer as used in this study by Van der Snickt et al. [30].

1.2.4. Data analysis

In this study, we used a combined data analysis approach to explore the data with the main aim to determine when titanium white became popular among artists in the Netherlands. This approach involves descriptive, bivariate and multivariate analysis and has an explorative rather than exhaustive character. These

analyses were performed in an iterative, back and forth process between descriptive or bivariate analysis and multivariate analysis. The full dataset, at different stages of post-processing, as well as subsets of the data were explored, until the research question could be answered in an satisfying way.

Descriptive & Bivariate analysis:

Descriptive and bivariate analyses were performed either by counting paintings with specific elements in specific decades or by investigating the relation between two specific elements of a data (sub)set in scatterplots.

Principal component analysis:

Principal component analysis (PCA) was performed using a Python script in Jupyter notebook. All data have been mean centered prior to analysis. Principal component analysis of the full dataset indicated that the variance between the two different instruments is negligible if corrected for the time of analysis. This was done by visually comparing the shape of the PCA scores in the first two dimensions when PCA was applied to the data of both instruments separately. Because the datasets were randomly chosen by collections, both sets represent a similar group of paintings with a limited bias towards a decade, paint type or artist and may thus be compared.

1.2.5. Reference paint outs

Qualitative insights were gained from the spectral investigation of the reference paint outs {SI Figure 14-19} which can be used to interpret the paintings results. These insights are already detailed in the current section, given their applicability for data interpretation of the paintings dataset.

One of the main guidelines originates from the different element sensitivity of titanium and zinc. For pure metals the sensitivity for titanium was shown (L. Megens, Unpublished research) to be five times less than the sensitivity for zinc, using the Bruker III-SD instrument. The sensitivity is further distorted when the Ti/Al filter is used, as this affects the sensitivity for titanium stronger than for zinc. Reference paint outs of equal volume titanium white, zinc white mixtures indicate that the titanium peak area is ten times lower than the zinc peak area {SI figure 11}. This was shown by the analysis of six different mixtures resulting in the following linear fit: $[Ti/(Ti+Zn)]_{measured} = 0.2[Ti/(Ti+Zn)]_{real}$, which can be solved by a peak area ratio of 0.11 [Ti] to 1 [Zn]. This is important information when interpreting an XRF spectrum visually and will be important information for the clustering of the PCA score plot.

1.5 In this study we did not quantify the layer thicknesses of our references given their qualitative assessment. Thin indicates a single brushstroke, while thick indicates an obvious impasto with a thickness in the mm range. The authors underline the value that an indepth quantified reference dataset for XRF interpretation by non-experts would have, however this falls outside the scope of this work.

A combination of both peaks can also be caused by a layered paint structure with a thin^{1.5} brushstroke of titanium white on top of a zinc white layer. The intensity of the signal from the underlying zinc layer depends on the thickness and pigment content of both layers. The references show that when the titanium top layer reaches ‘impasto’ thickness (mm range), the zinc signal is completely absorbed. On the other hand, the combination of titanium and zinc in one spectrum cannot be caused by a layer of ZnO paint on top of TiO₂ paint. This was shown by reference samples with a thin brushstroke of zinc white (or lead white) that show complete absorption of the sublayer Ti signal. Given that, at this explorative stage, we work with averages of spectra from different white areas, the combination of Ti and Zn in an artwork in this study can also relate to the use of different white paints in different areas of the painting.

1.3. Results and Discussion

The trends resulting from the data exploration are discussed in relation to their impact on degradation risk and in relation to material/market knowledge acquired at several archives and in discussion with paint manufacturers. The use of white pigments in the 20th century will first be discussed based on general trends and specific artists. The results section will be concluded with the identification of characteristic trace elements of interest.

1.3.1. Acceptation of TiO₂ by Dutch artists

It was commonly assumed, based on the occurrence of TiO₂ in artworks from the United States [1, 5, 7], that TiO₂ was used by artists almost as soon as it was taken into production. However, the present dataset suggests that a different trend was followed by Dutch artists. Figure 1.2 shows the number of paintings containing different peak areas of titanium, zinc and lead over the decades. As discussed in the previous section, a normalized Ti peak area of 0.1, with a main peak of Zn relates to a mixture, a layered structure or the use of multiple different paints. Figure 1.2 shows the convincing introduction of titanium white in the 1970s, while the pigment was already in production since the twenties. Earlier, starting in the fifties, mixtures or layers of titanium and zinc white can be found. The timing is in line with findings from the Royal Talens archive in Apeldoorn [31], where it was found that artists’ oil paints containing titanium white were only marketed after 1951 for the Dutch market, while the first test batch was already produced in the thirties [7]. For the French market, Royal Talens marketed titanium white oil paints already in 1950, possibly as competition for LeFranc Bourgois, that sold titanium white paints

since the twenties [1]. While the relative absence of early titanium white in Dutch oil paints can be considered to be a good sign regarding degradation risk, it does not directly mean stable pigments were used from the seventies onward [1, 5]. An example is paint manufacturer Royal Talens, that only switched to rutile for oil paints in the nineties (personal communication with Bert Klein-Ovink, Royal Talens) and still uses anatase for gouache today (confirmed by XRD analysis). Furthermore, Laver notes that ‘*Due to their greater whiteness early products based on anatase were retained for many years after rutile pigments were introduced.*’ [1]. However, it is important to realize that treated anatase pigments were also brought to the market and may have been used in late 20th century paints again reducing the degradation risk [32]. For instance, the pigment ‘Tiofine A20’ is often reported as titanium white pigment in Royal Talens recipes. The reference collection of the Cultural Heritage Agency of the Netherlands has a pigment labelled ‘Tiofine’, and while this may not be the same pigment, it does come from the same manufacturer. This pigment, shown to be anatase by XRD analysis, showed in TEM-EDX analysis to have a partial Al/Si coating which would reduce the pigments photocatalytic activity.

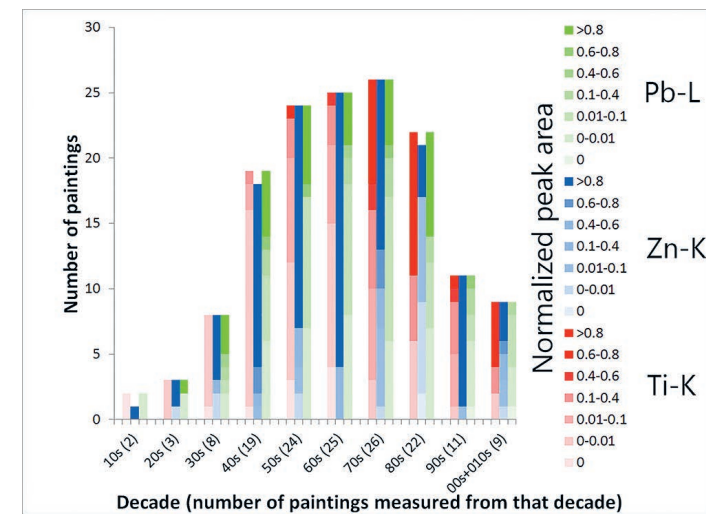


Figure 1.2 Number of paintings containing a certain normalized content of zinc, titanium and lead, plotted by decade.

We can only speculate about the reason for the slow rise of titanium white in Dutch oil paintings. Warnings were published about the yellowing of titanium white in oil paints [1, 33-35] possibly creating some reluctance for the use by artists. In the meantime, the yellowing problems were partly resolved by mixing titanium white with zinc white. Manufacturers such as Weber in the United states used zinc white additions early on and marketed their product ‘Permalba’ as ‘*Brilliant...Permanent...and easy to handle*’.

Titanium white is not only absent in the white paints but also in the colored paints. Due to the high refractive index of titanium white, zinc white was preferred at Royal Talens to adjust the hue of a color paint tube (personal communication Bert Klein-Ovink). This is confirmed in the present dataset. Of all the (averaged) measurements of colored paints, 25 have lead as the main peak, 50 have zinc as the main peak and only 10 have titanium as the main peak. The latter are likely related to non-oil paintings. This suggests that, while white oil paints may be at risk for photocatalytic degradation, this risk is minor for TiO₂-induced color fading. Furthermore, most of the paintings with Ti-K as the main peak are made with non-oil binding media such as acrylics, tempera and gouache. This is in line with XRD analysis of reference gouache, acrylic and tempera paint outs containing for the most part titanium white and fillers. It is understandable since both zinc white and lead white are not stable in, e.g. acrylic emulsion paints [1]. Furthermore, additional confirmation is found in archival recipes at Royal Talens of pure titanium white water-borne paints without the addition of any zinc white (van den Berg, unpublished research).

Figure 1.3 Scatter plot of non-normalized lead-L vs titanium-K peak areas of all grounds, labelled by year.

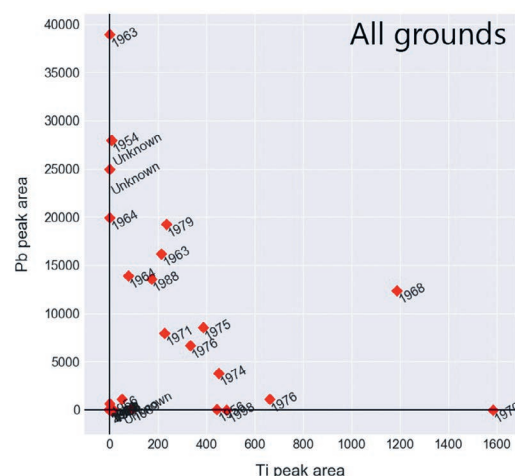


Figure 1.2 does not only shows the slow rise of titanium white and the ubiquitous use of zinc white, it also indicates the slow decrease of lead white. Until the eighties, it is found as the main element in some paints. This is in stark contrast with reports stating that lead white nearly disappears after World War 2 [3]. Additionally, analyzing a subset of painting grounds (Figure 1.3) further confirms the use of lead white for grounds far into the twentieth century. In the Netherlands, lead white was banned from interior painting as early as 1939 [36, 37]. However, protective regulations for people working with lead white were only implemented in 1988, and a full ban of lead white for outdoor paintings and artworks came as late

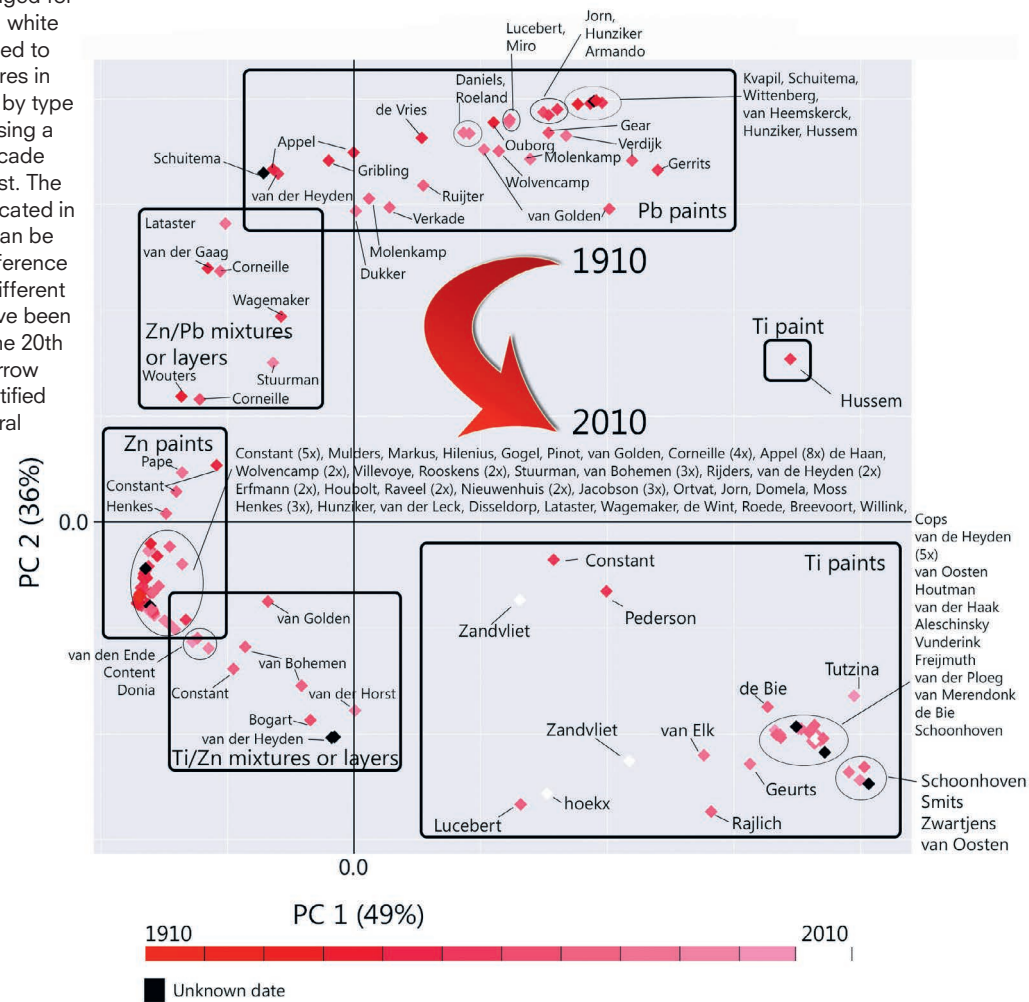
as 2009 [36, 37]. It is clear that due to its unmistakable popularity, despite the known health hazards, lead white was hard to ban from Dutch 20th century oil paintings. Low counts of lead may originate from an added drier rather than from the lead white pigment. Zinc white and titanium white are a common mixture, and zinc white with lead white is also found possibly as leaded zinc oxide [6]. On the other hand, the combination of lead white and titanium white is only found in grounds (Figure 1.3), which may originate from multiple ground layers or mixtures. The subset of impastos does not show a single case of a titanium white/lead white mixture. This is in line with investigated recipes in the Royal Talens and Weber archives [7], where only one recipe called 'mixed white' contains all three white pigments. In this, 1956, Talens recipe titanium white is present as a minor component of the oil paint (ten times less by weight than lead white and zinc white). This finding indicates that if lead and titanium peaks are both identified in an XRF spectrum these elements are likely originating from different layers, with titanium white most likely present in the top layer.

1.3.2. The developments in white paint composition in the 20th century

Figure 1.4 shows the PCA scoreplot of the average of the white areas from all paintings, normalized to the maximum peak area. The figure can be interpreted as a reference roadmap for researchers and conservators doing XRF on modern paintings. Figure 1.5 presents the associated loadings for principal component 1 and 2, which describe 85% of the variation in the post-processed dataset. The PCA scoreplot shows interesting chronological features discussed below. Before doing so, we would like to underline a number of important caveats. Firstly, clusters based on paint type have been manually defined after coloring the plot for normalized Ti peak areas, normalized Zn peak areas, normalized Pb peak areas and normalized ratio: $Ti/(Ti+Zn)$, taking into account the signal distortion between Zn and Ti peak areas {SI Figure 20-21}. Secondly, this analysis does not provide insight into painting stratigraphy, hence combination groups are labelled: mixture or layers.

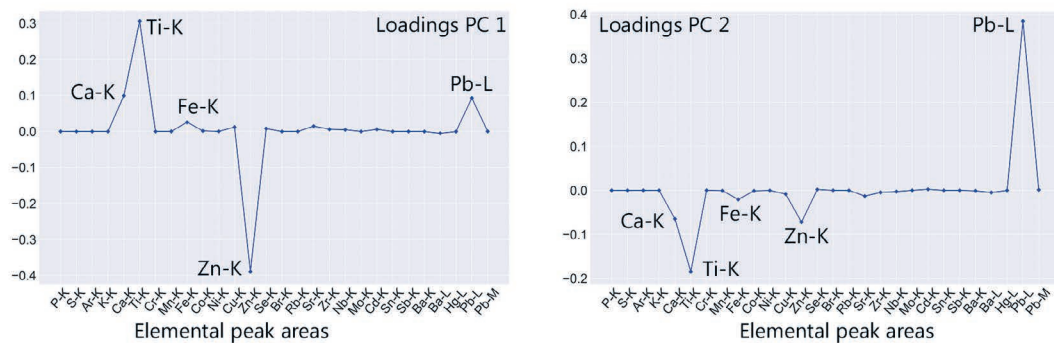
Figure 1.4 presents the same trend as previously depicted in Figure 1.2, namely of the gradual development from lead white to titanium white via the extensive use of zinc white. It shows interesting cross-connections between artist, time and paint compositions. One

Figure 1.4 PCA scoreplot of all artwork averaged for spectra taken from white areas and normalized to maximum. The scores in the plot are boxed by type of paint, colored using a red gradient by decade and labeled by artist. The origin lines are indicated in black. This figure can be interpreted as a reference roadmap of how different white pigments have been used throughout the 20th century. The time arrow represents the identified trend, despite several exceptions in the lead cluster.



White spectra (only yellow filter) from all artworks, averaged per artwork and normalized to the maximum peak. Data was time and threshold corrected

Figure 1.5 Loadingplots for PC1 and PC2 corresponding to Figure 1.4.



important finding is the strong representation of CoBrA artist (Appel, Constant, Corneille, Jörn and others) in the 'Zn paints' section. Zn paints are susceptible to problematic soap formation [19] which may become an even larger problem than already expected.

PCA of the complete dataset shows interesting general chronological trends. However, a closer look at data subsets can be equally interesting. Investigation of the subset of artworks with titanium as the main peak shows an anti-correlation of barium and calcium {SI Figure 22}. This indicates that in most cases one type of filler or composite pigment base was used. Furthermore, investigating the subset of artworks with zinc as the main peak yield an anti-correlation of titanium and lead {SI figure 22}. This observation supports once more that zinc white would either be combined with lead white or with titanium white but not with both.

1.3.3. Looking into the artist studio...

Another aim of this study was to investigate how the general trends in pigment use relate to individual artists. To this end, we selected three painters/artistic movements represented by a sufficient number of paintings in the dataset. This resulted in three examples: 11 paintings by J.C.J. van der Heyden, 7 paintings by K. van Bohemen and 30 paintings by CoBrA artists Appel, Constant, Corneille, Rooskens and Nieuwenhuis.

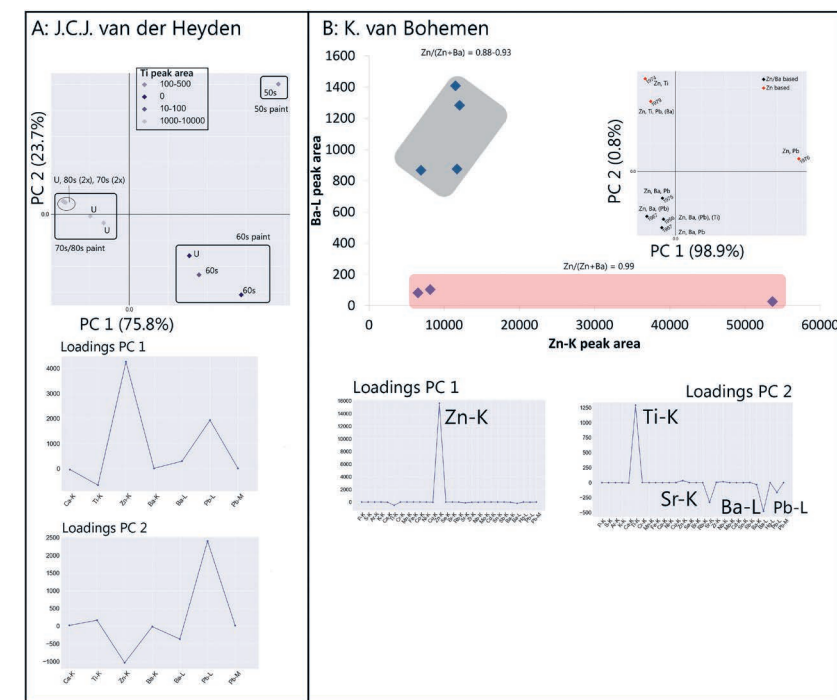


Figure 1.6 A: PCA scoreplot and loadingplots (PC1 and PC2) of 11 paintings by J.C.J. van der Heyden, averaged over the spectra of the white areas. PCA was done taking only the white elements (Ca, Ti, Ba, Zn, Pb) into account. **B:** Bivariate Ba-L vs Zn-K analysis and PCA scoreplot of 7 paintings by van K. van Bohemen, averaged over the spectra of white areas.

1.3.3.1 J.C.J. van der Heyden

The paints used by J.C.J. van der Heyden can be clustered in three different categories, Figure 1.6A. J.C.J. van der Heyden appears to undergo an identical development in his use of white pigments as the general development in the Netherlands discussed previously. In the 1950s he used lead white and zinc white (either mixed or superimposed), in the 1960s he moves on to use a zinc and barium containing paint (either a mixture of zinc white with barium sulfate or lithopone). Finally, in the 1970s and 1980s, he uses titanium based paints, four of which are in acrylic binders. XRD analysis shows that ‘Hellende Horizon’, a painting in acrylic from the 1970s, contains rutile, the more stable form of titanium white, and calcium carbonate. This could suggest that the other acrylic paints from that time may have been produced with similar pigments and could be less vulnerable to degradation. The results from this case study coincide with the general trends observed in the full dataset and thus support this method of analysis and data processing.

1.3.3.2 K. van Bohemen

In the case study of the K. van Bohemen paintings (by bivariate or PC analysis) two main types of paints can be identified: the zinc oxide based paints (post 1974) and the Zn/Ba based paints (up to 1975), Figure 1.6B. The Zn-based paints split into two groups indicating the mixtures of zinc white and titanium white (PCA scoreplot top left) and the mixture of zinc white and lead white (PCA scoreplot right). For this subset, the general trend of TiO_2 appearing in the 1970s is confirmed (paintings from 1974 and 1979). The Zn/Ba correlation, in the four black labeled points (Figure 1.6B), suggests the association of zinc and barium either as a mixture or as lithopone (co-precipitate of BaSO_4 and ZnS). Until 1945, lithopone was a strong competitor for the still developing titanium white pigments in the United States [5]. While the present data cannot differentiate between a mixture of zinc white and barium sulfate or the pigment lithopone, XRD of another sample from a different van Bohemen painting from 1966 indicates the presence of lithopone, placing the pigment on the artist’s pallet. Interestingly, investigating a subset, not necessarily requiring PCA, provides information about a paint composition ($\text{ZnO}+\text{BaSO}_4$ or lithopone) not noticeable in the full dataset (Figure 1.4). This highlights the possible benefit of doing further investigation of the data in the future.

1.3.3.3 CoBrA artists Appel, Constant, Corneille, Rooskens and Nieuwenhuis

As previously indicated, in this study it was found that CoBrA artists often used zinc white. To investigate this further, PCA was applied on a subset of 30 paintings by five CoBrA artists. The results indicated that the main difference between the paints was the zinc to lead ratio. While most paintings contain mainly zinc white, there is a selection of paintings containing zinc white and lead white. In this dataset, neither the date nor the artist coincides with the type of paint used therefore the visualization is omitted. This suggests random pigment choice in the CoBrA group. However, this did not compromise the detection of general trends in the full dataset.

1.3.4. Trace element indicators

The exploration of the data also resulted in the identification of two possibly indicative and characteristic trace elements: niobium and zirconium.

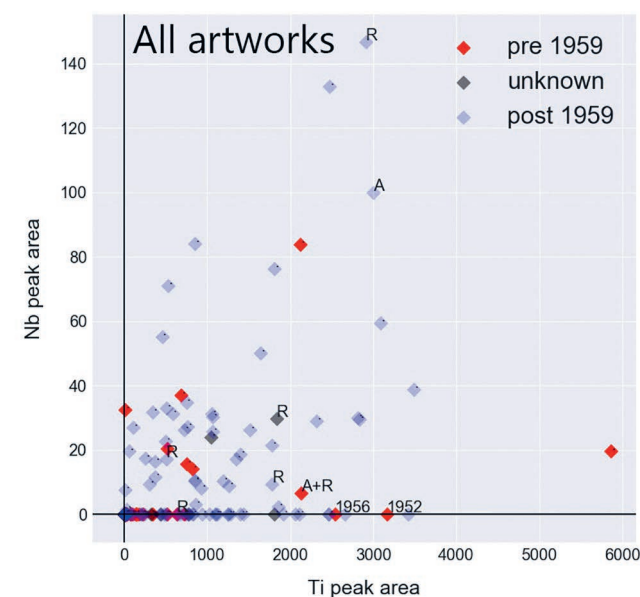


Figure 1.7 Scatter plots of niobium K vs titanium K peak areas of all artworks (average value of the spectra taken from white areas) colored by date, related to the date of introduction of the chloride process (1959) and labelled for unexpected dates or, if known, the pigment crystal structure.

The determination of the crystal structure of titanium white in paintings is the first step towards a possible risk assessment. However, XRF cannot determine the difference between rutile and anatase and less available techniques such as Raman and XRD are required. Our dataset indicates an association between titanium and niobium, Figure 1.7. With one exception, niobium is only present if titanium is also present. Niobium is a char-

1.6 The association of titanium and niobium has also been confirmed in the scope of another study (manuscript in preparation) by ICP-OES analysis.

acteristic element associated with ore impurities and is impossible to remove via the sulfate process [15], the earliest production process of titanium white pigments.

STEM-EDX confirms that indeed niobium and titanium are associated^{1,6}, Figure 1.8. The chloride process, started to be developed in 1948 (pilot plant) and a full-scale production facility was opened in 1959 by E.I du Pont de Nemours and Co., Tennessee. In Europe a production facility producing chloride processed rutile opened in 1965 (British Titan Products – one of the suppliers for Winsor&Newton paints) [1, 5]. While both processes can theoretically produce both crystal structures, generally the chloride process is used to produce the more stable rutile (developed in the 1940s). Hence the absence of niobium and thus the use of the chloride process can be an indication of the presence of rutile and dates the pigment to post 1959 (or post 1965 in Europe). The presence of niobium is related to the sulfate process which is still in use today. Therefore this can indicate both types of titanium dioxide pigment and any production date. Comparing the crystal structure analyzed by XRD from micro-samples, with the scatter plot (Figure 1.7) confirms this.

It should be noted that implementing the dating, colored as ‘pre’ or ‘post’ 1959 in Figure 1.7, presents some challenges. Several paintings, painted before 1959, show the absence of niobium. The amount of niobium left in the pigments is dependent on the ilmenite ore. For instance Norwegian ilmenite (containing 0.007% Nb) results in pigments with 0.012% Nb, while Australian ilmenite (containing 0.10% Nb) results in pigments with 0.22% Nb [1]. While the low niobium contents in titanium white derived from the Australian ilmenite should still be detectable by pXRF [38], some factors may inhibit the detection of niobium with XRF in sulfate processed titanium dioxide. This likely due to the paint composition, detection limit, set threshold (15 cnt/s), the measurement settings and subsequent signal-to-noise ratio. When the titanium counts are low, inherently the niobium counts will be low and possibly undetected. Similarly, when titanium is not the main peak but zinc or lead are strongly emitting the Nb signal may get lost in the noise (this is the case for the two red dots labelled 1956 and 1952). The latter was confirmed by investigating the reference material {SI figures 23 and 24}. In the scatter plot of the small dataset of all impasto’s the correlation is clearer and dating is consistent, which supports the idea that in some cases Nb is not detected, even though it is present. To confirm the absence or presence of niobium, and thus get an indication of crystal structure and dating, analytical improvement is required. In the case of the Bruker III-SD, this can be reached using the Cu/Ti/Al (green)

filter with a voltage of 40 kV, a current of 15µA and a measurement time of at least 120 s [39].

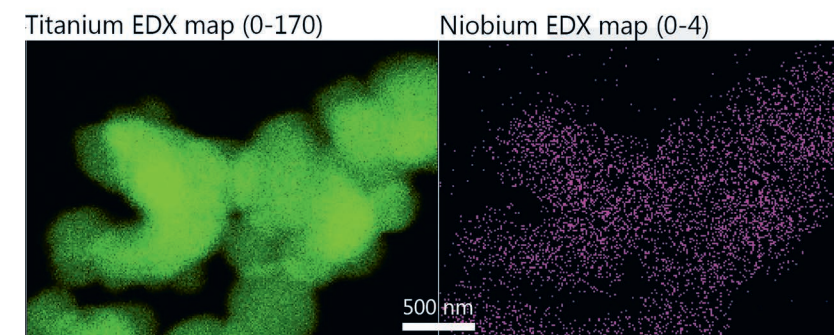


Figure 1.8 TEM-EDX map of Titanium dioxide pigment containing niobium impurity (powder: RCE9649 from RCE reference collection). The intensity range of EDX detection for Ti and Nb respectively are provided between brackets in the figure header.

Similar to niobium, zirconium is almost never present without titanium. Zirconium can originate, among others, from the paint drier or from a pigment coating on the titanium white that decreases its photocatalytic activity [40]. The simultaneous absence of zirconium and titanium suggest that if present, this indicates either an increased amount of drier (due to slow drying properties of titanium whites) or the detection of the inorganic coating. With the present dataset, using pXRF, the origin of the zirconium cannot be unambiguously determined. Nevertheless, if zirconium can be related to the presence of a pigment coating, which results in reduced photocatalytic activity, this is of interest from a risk management perspective. Further research should be performed, which notably entails optimizing pXRF settings as well as using a specifically designed set of reference material.

1.4. Conclusions & Outlook

This explorative study has provided new insights into the use of white pigments in the 20th century in the Netherlands. While pXRF is a widely used technique, it was not previously used to record and compare spectra of a large and diverse paintings dataset collected over a substantial amount of time.

Interestingly, our data has shown that the use of white pigments in the Netherlands is clearly different from the general assumption of the international use which seems to have a geographical bias toward the United States. It has been demonstrated that, instead of an immediate popularization of titanium white, the pigment entered the market rather slowly and initially predominantly in non-oil binders. The rather late rise of titanium white pigments in the Netherlands, starting from the fifties and stabilizing a secure position in the seventies, reduces the risk of photocatalytic binder degradation

for Dutch modern art collections. At the time, improved pigments were on the market, thus increasing the odds that they were used in artists' paints. Nevertheless, anatase was used by some Dutch manufacturers until the nineties and surface treatments were not always applied and still under development. Therefore, surveying and monitoring modern art collection for the use of potentially photocatalytically active pigments remains of high importance.

Zinc white was very popular in the mid-20th century, especially used by CoBrA artists and even lead white remained a popular artist pigment despite its known toxicity well into the 20th century. Both these pigments are not without risks either and have been reported in relation to problematic soap formation.

What is more, investigating subsets of one or more artists can provide insight into personal artist development, in terms of materials' use. This is clear for J.C.J. van der Heyden who follows the broader trend of using lead and zinc white in the fifties, zinc base paints in the sixties and titanium white based (acrylic) paints in the seventies and eighties.

Additionally, this study reveals that niobium, detectable by pXRF, may be a very useful marker to determine the production process and its absence can point to a post 1959 dating as well as to the rutile crystal structure. Rutile is considered to be more stable and is often found with a stabilizing inorganic coating. In other words, this provides an accessible, cheap and easy to use technique to make an initial classification of vulnerability to photocatalysis of a painting.

The trends brought about in the present study are in line with information from archives as well as the single-artist case-studies. In other words, despite the use of two instruments, the slightly different experimental conditions, the minimally restricted selection of objects and the experimental noise, this explorative study was useful and provided new insight. For the identification of more detailed developments in the use of white pigments, the dataset should be extended, focused on impasto areas and preferably art historically balanced. Involving more museums to gather a larger dataset of XRF spectra and metadata of white paints (or any color for that matter) would make this study more robust as a potential tool for risk analysis of the (white) paints in (Dutch) collections. Furthermore, multivariate data analysis via PCA in this study was mostly used for a visualization purpose. The dataset likely contains more information than was extracted in this study. Therefore, to answer other questions, outside the scope of this work, the dataset may be further analyzed in the future. Several options to explore are: analysis on the raw spectra rather than peak areas; analysis on

each separate paint area rather than on the averaged peak areas; and other types of data analysis such as t-Distributed Stochastic Neighbor Embedding (T-SNE), independent component analysis (ICA) or non-negative matrix factorization (NMF).

Acknowledgements

This work has been financially and experimentally supported by AkzoNobel and hosted by the Rijksmuseum Amsterdam. Additionally Prof. P.J. Kooyman is acknowledged for the involvement in van Driels Ph.D. research.

The Cultural Heritage Agency of the Netherlands (RCE) and Dennis Breakmans, formally at Delft University of Technology, are acknowledged for the use of the XRF instrumentation.

The Dutch association for company art collections (VBCN, Vereniging bedrijfscollecties Nederland) is acknowledged for forwarding my analysis request to the Dutch company collections associated with them. The following collections and people are acknowledged for providing access and support during data acquisition: Sabrina Kamstra at the AMC Kunstcollectie, Hilde de Bruijn at the Cobra Museum Amstelveen, Ruth Hoppe at the Gemeentemuseum, Annelies Koldewey at the ING Art Collection, Anita Jansen, Ron Stokhof and Mark Boers at Museum Prinsenhof Delft, Caroline Coffrie at the Bouwfonds kunstcollectie, Zeph Benders and Yuri van der Linden at the RCE collection, Colin Huizing and Marco Steketee at the Stedelijk museum Schiedam, Femke van der Knaap at Boeijink, Boekel & vander Knaap Schilderijen restauratie; Lise Steyn at the university of Amsterdam (UvA) and at the RCE; Maranthe Lamers formally at the UvA (PI student), freelancers Marya Albrecht, Jorinde Koenen, Annelies van Hoesel and Lydia Beerkens.

Furthermore we thank the RCE interns Rose Heaton, Rika Pause and Nathalie de Vries for their help during data acquisition and RCE scientist Luc Megens for his training on the XRD and many discussions about the topic of XRF. Similarly, we thank Ana Martins at the MoMA for the discussions we had about XRF and multivariate data analysis. At AkzoNobel Brenda Rossenaar and Wilma Ravesloot are acknowledged for STEM-EDX sample preparation and analysis. Arie Pappot and Rob Erdmann at the Rijksmuseum respectively helped me with the PyMCA deconvolution and the use of Python for data analysis.

References for chapter 1

- Laver M. Titanium White. In: West FitzHugh E, editor. *Artists' Pigments: A Handbook of their History and Characteristics*, Vol. 3. National gallery of Art, Washington. London:Archetype Publications. 1997. 3: 295-355.
- Markowitz G, Rosner D. History and Perspective on Lead. <http://www.toxipedia.org/display/toxipedia/History+and+Perspectives+on+Lead>. Accessed November 2014.
- Bacci M, Picollo M, Trumpy G, Tsukada M, Kunzelman D. Non-Invasive Identification of White Pigments on 20th-Century Oil Paintings by Using Fiber Optic Reflectance Spectroscopy. *JAIC*. 2007; 46(1): 27-37.
- Brunner H. Pitture. In: Singer C, Holmyard AJ, Hall AR and Williams T, editors. *Storia della tecnologia* Vol. 6. Turin: Bollati Boringhieri. 1982; 617-31.
- Stieg FB. Opaque White Pigments in Coatings. *ACS Appl Polym Sc*. 1985; 285: 1249-1269.
- Kuhn H. Zinc oxide. In: Feller RL, Roy A, editors. *Artists' Pigments: A Handbook of Their History and Characteristics*, Cambridge University Press London. 1986. p. 169-186.
- Phenix A, van den Berg KJ, Soldano A, van Driel BA. The Might of White: formulations of titanium dioxide-based oil paints as evidenced in archives of two artists' colourmen mid-twentieth century. In: ICOM-CC Triennial conference 2017, Copenhagen. 2017.
- van den Berg KJ, Miliani C, Aldrovandi A, Brunetti BG, de Groot S, Kahrim K, et al. The chemistry of Mondrian's paints in Victory Boogie Woogie. In: van Bommel MR, Janssen H, Spronk R, editors. *Inside Out Victory Boogie Woogie*. Haags Gemeentemuseum, Amsterdam University Press.
- Martins A, Albertson C, McGlinchey C, Dik J. Piet Mondrian's Broadway Boogie Woogie: non-invasive analysis using macro X-Ray fluorescence mapping (MA-XRF) and multivariate curve resolution-alternating least square (MCR-ALS). *Herit Sci*. 2016; 4.
- van Bommel MR, Janssen H, Sponk R. *Victory Boogie Woogie uitgepakt*. 1st edition. Haags Gemeentemuseum and Amsterdam University press. 2012.
- Linton J. The white test... 5 years in the making. <http://blog.jonathanlinton.com/2010/05/white-test-5-years-in-making.html>. Accessed November 2014.
- Sims E. White is white, right? <https://heymaryemma.wordpress.com/>. Accessed November 2014.
- Mancine-Hresko L. White test. <http://leomancinihresko.com/white-test-2013/>. 2013. Accessed November 2014.
- DuPont Magazine. 1935. <http://digital.hagley.org/islandora/object/islandora%3A1979489>. Accessed November
- Braun JH, Baidins A, Marganski RE. TiO₂ pigment technology: a review. *Prog Org Coat*. 1992; 20(2): 105-138.
- van Driel BA, Wezendonk TA, van den Berg KJ, Kooyman PJ, Gascon J and Dik J. Determination of early warning signs for photocatalytic degradation of titanium white oil paints by means of surface analysis. *Spectrochim Acta A*. 2017; 172: 100-108.
- Völz HG, Kaempf G, Fitzky HG, Klaeren A. The Chemical Nature of Chalking in the Presence of Titanium Dioxide Pigments. *ACS Photodegrad Photostabil Coat*. 1981; 151: 163-182.
- Morsch S, van Driel BA, van den Berg KJ and Dik J. Investigating the Photocatalytic Degradation of Oil Paint using ATR-IR and AFM-IR. *ACS Appl Mater Interfaces*. 2017; 9(11): 10169-10179.
- Hermans JJ. Metal Soaps in oil paint, structure mechanisms and dynamics. PhD thesis at Van 't Hoff Institute for Molecular Sciences, Universiteit van Amsterdam. 2017. ISBN: 978-94-629-5578-3 <http://hdl.handle.net/11245.1/53663926-183c-40aa-b7b3-e6027979cb7d> Accessed September 2017
- McGlinchey C. Handheld XRF for the examination of paintings: proper use and limitations. In: Shugar AN, Mass JL, editoris. *Handheld XRF for art and archaeology (studies in archeological sciences)*, 1st edn, vol. 4 Leuven University Press. 2013
- Namowicz C, Trentelman K, McGlinchey C. Erratum: XRF of cultural heritage materials: Round- Robin IV --- Paint on Canvas. *Powder diffrac*. 2009; 24: 124-129.
- Stulik DC, Kaplan A. Application of a handheld XRF spectrometer in research and identification of photographs. In: *Handheld XRF for Art and Archaeology*. Leuven University Press. 2012; 3: 75-130.
- Alfeld M, Pedroso JV, Eikema M, Hommes G, van der Snickt G, Tauber G, et al. A mobile instrument for in situ scanning macro-XRF investigation of historical paintings. *J Anal At Spectrom*. 2013; 28.
- Szőkefalvi-Nagy Z, Demeter I, Kocsonya A, Kovacs I Non-destructive XRF analysis of paintings." *Nucl Instrum Methods Phys Res B*. 2014; 226(1-2): 53-59.
- Solé VA, Papillon E, Cotte M, Walter P, Susini J. A multiplatform code for the analysis of energy-dispersive X-ray fluorescence spectra." *Spectrochim Acta B*. 2007. 62(1): 63-68.
- Rosi F, Burnstock A, van den berg KJ, Miliani C, Brunetti BG, Sgamellotti A. A non-invasive XRF study supported by multivariate statistical analysis and reflectance FTIR to assess the composition of modern painting materials." *Spectrochim Acta A*. 2009; 71(5): 1655-1662.
- Appoloni CR, Melquiades FL. Portable XRF and principal component analysis for bill characterization in forensic science. *Appl Radiat Isotopes*. 2014; 85: 92-95.
- Martins A, Coddington J, van der Snickt G, van Driel BA, McGlinchey C, Dahlberg D, Janssens J, Dik J. Jackson Pollock's Number 1A, 1948: a non-invasive study using macro-x-ray fluorescence mapping (MA-XRF) and multivariate curve resolution-alternating least squares (MCR-ALS) analysis." *Her Sci*. 2016; 4(1): 33.
- Capobianco G, Pelosi C, Agresti G, Bonifazi G, Santamaria U, Serranti S. X-ray fluorescence investigation on yellow pigments based on lead, tin and antimony through the comparison between laboratory and portable instruments. *J Cult Her*. 2017. In press.
- van der Snickt G, Janssens K, Schalm O, Aibeo C, Kloust H, Alfeld M. James Ensor's pigment use: artistic and material evolution studied by means of portable X-ray fluorescence spectrometry. *X-Ray Spectrom*. 2010; 39(2): 103-111.
- Burnstock A, van den Berg KJ, van der Gorp F, Bayliss S, Klein-Ovink B. Making paint in the 20th Century: the Talens Archive. In: Eyb-Green S, Townshend JH, Pilz K, Kroustallis S, van Leeuwen I, editors. *Sources in Art Technology, Back to Basics*. Pp. 43-50. Archetype. 2016
- de Keijzer M. The history of modern synthetic inorganic and organic artists' pigments. In: *Contributions to conservation at the Netherlands Institute for Cultural Heritage*, James & James (Science Publishers) Ltd. 2002
- Doerner M, Hoppe T. *Malmaterial und seine Verwendung im Bilde*. ISBN 13: 9783432017174. 1928
- Fischer M. *The permanent palette*. Mountain Lake Park, Md., and New York: National Publishing Society. 1930.
- de Keijzer M. *Apropos of Titanium white*. *Restauro*. 1989; 95(3): 214-217
- Dodelijk mooi. Cultural Heritage Agency of the Netherlands. http://www.kleurenvisie.nl/db/upload/documents/kleur_in_de_media/Dodelijk_mooi_RCE_1_2012.pdf. Accessed September 2017.
- Loodwit symposium - Geen witte onschuld, een blik op internationale loodwit regelgeving. <http://www.collectiewijzer.nl/2012/01/12/loodwitsymposium-geen-witte-onschuld-eeen-blik-op-internationale-loodwit-regelgeving-2/>. Accessed September 2017.
- Williams-Thorpe O. The Application of Portable X-Ray Fluorescence Analysis to Archaeological Lithic Provenancing. In: Potts PJ, West M, editors. *Portable X-ray Fluorescence Spectrometry: Capabilities for In Situ Analysis*, The Royal Society of Chemistry. 2008; Chapter 8 174-205.
- Speakman SA. Using the Bruker Tracer III-SD Handheld X-ray Fluorescence Spectrometer using PC software for data collection. <http://prism.mit.edu/xray/oldsite/Bruker%20XRF%20SOP.pdf>. Accessed 2015.
- Zirconium compounds in paint. *Pigment & Resin Technol*. 1978; 7(9): 15-17.

Chapter 2

Investigating the complex photoluminescence behaviour of titanium white pigments.

This work reports the analysis of the time-resolved photoluminescence behaviour on the nanosecond and microsecond time scale of fourteen historical and contemporary titanium white pigments. The pigments were produced with different production methods and post-production treatments, giving rise to a remarkable variety of titanium dioxide powders and, in some cases, to the formation of a complex surface of the crystal agglomerates. The pigments have been further characterized by Raman spectroscopy, scanning transmission electron microscopy coupled with energy dispersive X-ray spectroscopy and inductively coupled plasma atomic emission spectrometry. Our study provides a clear view of the main features of the photoluminescence (PL) emission of anatase- and rutile-based pigments. For both the polymorphs of titanium dioxide the room-temperature photoluminescence emission is complex and involves different relaxation paths, related to shallow levels close to the conduction bands and mid-gap trap states. The PL behaviour appears to be little affected by post-production treatments such as organic and inorganic coatings. Instead, the presence of niobium impurities in the TiO₂ crystal lattice, as residues of the sulphate synthesis process, induce a remarkable quenching of the visible emission of anatase-based pigments. We confirm that rutile-based and anatase-based pigments are significantly different in terms of photoluminescence behaviour. This clear distinction is a valuable point for non-invasive pigment identification by in-situ photoluminescence spectroscopy. In particular, while many organic binding media emit in the visible region, the near-infrared emission of rutile is specific and can likely be used to identify the pigment in more complex materials as paints. This research paves the way to future studies of the photo-physical properties of titanium white pigments, which is imperative to understand the risk of degradation induced by the well-known photocatalytic activity of this widely used 20th century pigment.

Based on the published paper: B.A. van Driel, A. Artesani, K.J. van den Berg, J. Dik, S. Mosca, B.D. Rossenaar, J.U. Hoekstra, A.N. Davies, A. Nevin, G. Valentini and D. Comelli (2018), *Dyes & Pigments* 155: 14-22.

Note This manuscript includes a document with supplementary material (in the text referred to as SI) which can be downloaded (link is provided in the back matter).

2.1. Introduction

Titanium white is a collective term for over 580 grades (in 1985) [1] of titanium dioxide-based pigments, respectively made of the anatase and rutile polymorphs of titanium(IV)oxide (TiO_2) [2]. The semiconductor pigment was introduced onto the market at the beginning of the 20th century and was extensively used by artists, including Picasso, Pollock, and Mondriaan [1, 3, 4]. It is still the most widely used white pigment in a broad range of applications (from artist materials to cosmetics), thanks to its high brightness and hiding power. Moreover, titanium dioxide, mainly in its anatase form, has a strong photocatalytic activity, which can be exploited for air/water purification, self-cleaning and antibacterial action applications [5-7]. Conversely, in artist' paintings, the photocatalytic activity of titanium white can cause severe degradation problems, such as paint colour change or chalking [8-10]. Despite this issue, it is important to note that only a limited number of degraded works of art containing titanium white have been documented thusfar, possibly as a consequence of the low speed of the degradation process combined with the relatively short existence of the paintings in question [1, 11, 12].

This research aims to study the distinct photoluminescence (PL) behaviour of anatase- and rutile-based polymorphs of TiO_2 pigments. Furthermore, it aims to investigate the possible correlations between the PL properties and pigment features - such as coatings, the presence of impurities, crystal structure and crystal size, - related to the pigment ore, the production process and post-process treatments.

The earliest titanium white pigments, produced at the beginning of the 20th century, were composite pigments composed of barium sulphate and TiO_2 in the anatase form. Later, pure anatase pigments came onto the market followed by rutile pigments in the 1940s [1, 13]. The production of titanium white pigments can follow two main processes: the sulphate process, developed in the 1920s, and the chloride process, stemming from the 1950s and mostly used for the production of rutile [1, 14, 15]. In the first step of the production, the titanium feedstock is converted to a purified intermediate: TiOSO_4 or TiCl_4 . Subsequently, TiO_2 is formed by heating the obtained intermediate. The crystal structure and particulate size of the final product are determined during the latter process and depends mostly on the calcination temperature [16, 17], with the synthesized product being completely transformed into the rutile phase at high temperatures [17-19]. The chloride process can reduce all impurities to below 10-20

ppm. The only compound usually present in the final material is AlCl_3 , since it is added as a co-oxidant and cannot be completely removed. In the sulphate process, the use of acids helps to remove all impurities except niobium, which incorporates itself in the crystal structure during calcination, and phosphorus, that remains on the particle surface. The niobium impurity, present as Nb_2O_5 , causes a slight colour change. Hence trivalent aluminium is added during calcination to compensate for the fifth electron of niobium [1, 16, 17, 20].

A range of post-production treatments, such as organic and inorganic surface coatings are further available to control the pigment behaviour [1, 14, 21-24]. The most common inorganic coating materials are silica and alumina [17, 20]. Depending on the application, a wide variety of organic treatments, including polyhydric alcohols (or polyols), alkanol amines, modified silicone oil or others, can be added at the final production stage [1, 17, 25]. The surface of TiO_2 pigments is thus highly complex [20, 25, 26]. Even for uncoated pigments, impurities or additives accumulate on the pigment surface while the pigments crystallize and grow [17]. All these industrial developments give rise to significant variability of titanium dioxide powders available in the past and on the current market, in terms of crystal structure, surface treatments, and impurities.

The two main (tetragonal) crystal structures of TiO_2 , anatase and rutile, are characterized by a band gap of 3.18 eV (390 nm) and 3.02 eV (410 nm), respectively [27, 28], with an indirect bandgap for anatase and a quasi-direct bandgap character for rutile [29, 30]. Indeed, extensive research on the photoluminescence properties of TiO_2 as single crystals, thin films and pure or mixed phase nanopowders has been published to indirectly study TiO_2 photocatalytic activity and surface properties [31-38]. The two stable TiO_2 crystalline forms are characterized by well-separated PL bands, with anatase showing a broad visible PL emission (VIS-PL) and rutile a narrower emission in the near-infrared (NIR-PL) [33, 36]. However, in the literature, there is no clear consensus on the nature of the recombination mechanism processes, and, only recently, researchers have proposed new possible schemes of TiO_2 recombination pathways following above and below bandgap excitation [24]. Conversely, fewer works deal explicitly with the PL properties of titanium white as a pigment [39-41]. As PL spectroscopy is a contactless and non-invasive method to investigate the electronic structure of materials, it is particularly attractive for pictorial material characterization such as pigments [42]. The technique is applied as a sensitive method to detect the presence of luminescent materials in artworks and as a research-

based tool, to achieve the photo-physical characterization of a variety of inorganic [43-46] and organic artists materials [47, 48].

In this study, by employing time-resolved photoluminescence spectroscopy (TRPL), we investigate the spectral and lifetime PL properties of fourteen samples of titanium white pigments from different historical and contemporary manufactures, produce by the two different processes and with several post-processing treatments. This is supported by an investigation of the material structure and composition with Raman spectroscopy, Scanning Transmission Electron Microscopy coupled with Energy Dispersive X-ray spectroscopy (STEM-EDX) and Inductively Coupled Plasma Atomic Emission Spectrometry (ICP-OES). Raman spectroscopy was used to determine the pigments polymorph structure. The STEM-EDX analysis was aimed to investigate the main elemental composition of pigments and possible inorganic coatings, while ICP-OES was employed to assess impurities present in the bulk samples with a higher level of sensitivity than possible with EDX analysis.

2.2. Experimental

2.2.1. Description of the pigment set

The pigments selected for the present study are described in Table 2.1 and are a selection of available modern and historical pigments for several applications. The pigments were gathered from contemporary manufacturers (Tronox, Kronos, and Huntsman), archival collections from Winsor&Newton and at the Cultural Heritage Agency of the Netherlands (RCE), as well as from a paint mill in the Netherlands (verfmolen de Kat). The powders from archival collections are historical pigments from several different, sometimes unknown, dates. The anatase reference powder was purchased from Sigma-Aldrich. The rutile reference originated from the former Engelhard Corporation (now part of BASF) and was available from a previous study.^{2.1}

The pigment powders were analysed as received for TRPL and Raman spectroscopy, while ICP-OES and STEM-EDX required preliminary sample preparation, described in the materials characterization section.

In the following, the pigments will be referred to by their code listed in Table 2.1.

2.1 It is noted that the rutile powder purchased at Sigma-Aldrich could not be used as the reference rutile sample since it contains detectable amounts of the anatase polymorph, too.

Table 2.1 Selection of pigments and their characteristics.
*RCE=Cultural Heritage Agency of the Netherlands
**Unpublished work

2.2 The Rotterdam Tiofine factory (now called Tronox) was founded in 1960. In 1989 the factory switched from the sulphate process to the chloride process. 'TiofineA20' is mentioned in Talens recipe 1971.

2.3 Sikkens is now an AkzoNobel paint brand, but it used to be a separate paint company (until 1962). At the Sassenheim plant of AkzoNobel a Sikkens museum was formed. The pigment collection from this museum was later transferred to the RCE, which is where this powder comes from.

2.4 Finding a pure, uncoated rutile reference (outside the nano-size range) proved challenging. Several powders were purchased at Sigma but characterization showed they were not appropriate in terms of purity. While 'Engelhard' rutile is unclear in terms of manufacturer or provenance, it is a powder of around 100 nm and without coating (inorg).

Code	Name	Description <i>Based on previous studies or other available information.</i>	Year/period of synthesis	Employed synthesis method (manufacturer)
A1	Hombitan LW	Uncoated anatase [8, 9, 24, 49]	Contemporary	n/a
A2	Huntsman A-HRF	Organically treated to promote dispersion.	Contemporary	Sulphate process
A3	Huntsman A-PP2	Treated with 2% Al ₂ O ₃ and 1% SiO ₂ + Polyol.	Contemporary	Sulphate process
A4	Tiofine	Pigment from Tiofine ²² .	Pigment likely post-1989 (based on results in Table 2.2).	n/a
A5	Winsor&Newton 3557	From the Winsor&Newton archive. Likely used in their paints.	The jar was labelled 1941.	Likely sulphate process (chloride process was not in use in 1941)
A6	RCE9649, "Sikkens kist 9"	Pigment from the Sikkens company ²³ .	Unknown date, likely pre-1962.	n/a
A _{ref}	Sigma-Aldrich 232033	Chemical grade: pure anatase reference.	Contemporary	n/a
R1	Tronox CR-826	SiO ₂ [10-20%], Al(OH) ₃ [0-10%], ZrO ₂ [0-2%] [8, 9, 24, 49].	Contemporary	n/a
R2	Huntsman HDCCD	Organically treated to promote dispersion	Contemporary	Sulphate process.
R3	De kat	Purchased at Dutch 'vermolen de kat' in 2011.	Contemporary	n/a
R4	Kronos 2310	Received from AkzoNobel in 2011.	Contemporary	n/a
R5	Kronos CL300	From RCE* reference collection. CL could stand for chloride process. After 1965 (chloride process in Europe), around 1996 (pigment reported in a patent [50]).	n/a	Possibly chloride process due to annotation 'CL'
R6	RCE2766	From RCE* reference collection.	n/a	n/a
R _{ref} ²⁴	Engelhard Rutile	From a previous study conducted by M.Zandbergen at RCE* and Delft University**. Uncoated rutile reference.	Contemporary	n/a

2.2.2. Material Characterization

2.2.2.1. Raman spectroscopy

Raman measurements were performed with a homemade device, based on a 785 nm CW laser source and a spectrometer (Acton SpectraPro2150 Princeton Instruments) coupled to a cooled CCD camera (iDUS DV401A, Andor Technology Ltd.) [51]. The grating (600 grooves/mm) allowed the detection of Raman peaks in the spectral range 130–3000 cm⁻¹, with a spectral resolution close to 10 cm⁻¹. Following data acquisition, spectral calibration was performed with the aid of standards samples. Raman spectra of samples were taken with a micro-probe, based on a 20× objective that allows analysis of a circular spot of 50 μm in diameter at a working distance of ~3 mm. The acquisition time is set at 5 s, and the irradiance on the sample is evaluated at 3200 W/cm².

2.2.2.2. Scanning Transmission Electron Microscopy - Energy Dispersive Spectroscopy (STEM-EDX)

The powders were prepared for STEM-EDX by dipping a lacey C coated Cu TEM grid in the powder. After removing excess of powder, the particles were imaged in a JEOL 2010F FEG-TEM equipped with a STEM unit and ThermoNoran EDX detector for elemental mapping. Data analysis using phase deconvolution (based on a multivariate approach locating the areas likely to consist out of the same material) was performed using the NSS software. The spatial resolution of the STEM-EDX is 2 nm. The elemental limit of detection, while dependent of overlapping peaks, matrix and absorption effects, is set at 0.1 at%. Measured values are local and do not relate to the bulk of the material.

2.2.2.3. Inductively coupled plasma atomic emission spectrometry (ICP-OES)

The samples were digested in duplicate with concentrated nitric acid and hydrofluoric acid in a medium pressure microwave digestion system (Anton Paar Go). The elemental composition of the diluted and undiluted samples was measured by ICP-OES using an Agilent 510-vdv in radial and axial mode. To determine the aluminium and silicon concentration the samples were fused in duplicate with lithium metaborate in an automated fluxer (Claisse TheOx) at 1050°C. The hot flux was poured into 1.6M nitric acid, and the element concentrations were analysed with ICP-OES in radial mode. The elemental limit of detection is element specific {Table 5 of the supplementary information}. It was calculated based on three times the standard deviation from ten blank samples with the same matrix as the measured sample

solution. The detection limit values are subsequently rounded up towards and corrected for dilution and sample preparation.

2.2.3. Time-resolved photoluminescence spectroscopy

The time-resolved photoluminescence system is based on a pulsed laser and on a fast-gated intensified camera coupled to a spectrometer. The camera is capable of high-speed gating to capture the decay kinetic of photoluminescence emission spectra. Excitation of PL from samples is provided by the third harmonic of a Q-switching Nd:YAG laser, emitting sub-ns pulses at 355 nm (CryLas FTSS 355-50, Crylas GmbH, Berlin, Germany) at a repetition rate of 100 Hz. The laser light is delivered onto the sample (powder were pressed into a sample holder of 2 mm diameter). An optical probe allows the excitation of the PL signal from sample surface in a circular spot of 1 mm in diameter with an average power of 2 mW. PL emission from samples is collected in a back-scattering geometry and focused into the entrance slit of an imaging spectrometer. The spectrometer (Acton Research 2300i, focal length = 300 mm, f/4 aperture) mounts two gratings with 150 l/mm with different blazing. The first grating is blazed at 300 nm and is used for PL acquisition in the spectral range 380–700 nm (UV grating, in the following). The second grating is blazed 800 nm and is used for PL acquisition in the spectral range 600–900 nm (NIR grating, in the following). The kinetics of the emission is detected by a gated intensified camera (C9546-03, Hamamatsu Photonics, Japan), mounted at the exit port of the spectrometer. The detector features an acquisition gate adjustable from 3 ns to continuous mode. A custom-built trigger unit and a precision delay generator complete the system, which has a temporal jitter close to 200 ps.

The measurement procedure is based on the detection of a sequence of PL gated spectra at different delays with respect to laser pulses. In this work, fast and long emissions were detected by employing different gate widths.

- Fast recombination emission was detected using a gate width of 10 ns and recording the emission decay kinetic for the first 100 ns following excitation and exposition time of 1 s.
- Long-lived emission at the microsecond scale was detected with a gate width of 1 μ s and recording the decay kinetic for 50 μ s following excitation and exposition time of 30 s.

TRPL results are shown in terms of gated emission spectra - displayed following correction for the instrumental efficiency and normalization at emission maximum - and emission decay kinetic

profiles. Decay kinetic profiles were further fitted to a multi-exponential decay model (with a maximum of three components) using a nonlinear least square method [44]. The effective lifetime was then calculated as the average of the lifetimes weighted over the amplitude of each component, as stated by equation 1, where A_i and τ_i refer to the amplitude and the lifetime of each component of the multi-exponential decay model.

$$\tau_{EFF} = \frac{\sum_{i=1}^3 A_i \tau_i}{\sum_{i=1}^3 A_i} \quad (1)$$

2.3. Results

2.3.1 Pigment characterization

Raman measurements confirm the expected crystalline structure of powders {SI part 1}, with all powders appearing to be made of one specific crystal structure.

STEM-EDX analysis indicates whether an inorganic coating is present on the pigments and provides information about pigment impurities (Figure 2.1, Table 2) {part 2 of SI}. Al or Si based coatings are easily recognized in the images as a 'fuzzy' material surrounding the pigment (lighter in colour). Furthermore, if a thick coating is present, it is common to find loose coating material as well (R1, R3, R6). The coating tends to surround the aggregates rather than primary particles due to clustering. Pigment A3 has a very thin and irregular coating, not always detectable, but loose coating material has been identified (red circle in the photograph). Next to variability in the coating, some variability in size and shape are noted, with A3 and A5 having relatively small particle sizes while A4 has relatively big particle size. Nevertheless, no statistically accurate statement can be made on the average particle size due to the limited number of TEM micrographs. Considering that they are all pigments, we expect them to be between 100 nm (Hombitan LW) and 200–250 nm (Tronox CR). In fact, this is the optimal size to reach the high opacity of titanium white paints [52].

The identification of an organic coating is less straightforward than the detection of an inorganic coating. Phase deconvolution of STEM-EDX mappings of samples A1, A2, A3, and R2 identifies a second phase (yellow colour, circled in red). Examination of the spectra {SI part 2} suggests TiO_2 for both the yellow and the blue phase. The difference between the phases is the Ti/O ratio, which possibly indicates a coating. However, the second phase could also be due to the accumulation of impurities on the surface during crystal growth [17]. Furthermore, local EDX analysis does not detect the presence of carbon. This can be either because no

organic coating is present or because the coating is too thin to generate a signal above the detection limit. Even though the manufacturer of pigments A2, A3 and R2 indicates that an organic coating has been applied, which is assumed in the following, STEM-EDX is not suitable to detect it conclusively. For pigment A3, Huntsman reports that the pigment is polyol treated. As this is a very common organic treatment [17], it is assumed for the other Huntsman pigments as well. A pigment with an inorganic coating is generally also organically treated, and this is taken into account when assuming if an organic treatment is present. Similarly, the older pigments are assumed to be untreated [17]. Determining the organic treatment and distinguishing it from process additives such as grinding aids can be challenging.

In order to quantify the elements in the bulk of the material, ICP-OES was used (Table 2) {SI Part 3}. All the pigments that proved to have an inorganic coating (A3, A4, R1, R3, R4, R5 and R6) when analysed by STEM-EDX, also showed Al, Si or Zr (coating materials) in the weight percentage range (>0.1%). Thus, while not localized, ICP-OES can indicate the inorganic coating as well. One exception is A5, where silicon is present in the weight percentage range but is an ore impurity. Phosphorus and niobium are also commonly detected in the weight percentage range (P: A1, A2, A3, A4, A5, A_{ref}, R3, R6 Nb: A5, A6, R2). The presence of niobium can provide an indication of the production process (Table 2) as niobium cannot be removed during the sulphate synthesis route. Additionally, potassium was also detected in four pigments in this range. A multitude of elements originating from the ore or the production process were detected in trace concentration such as calcium, chromium, iron, vanadium, magnesium, and others {SI part 3}.

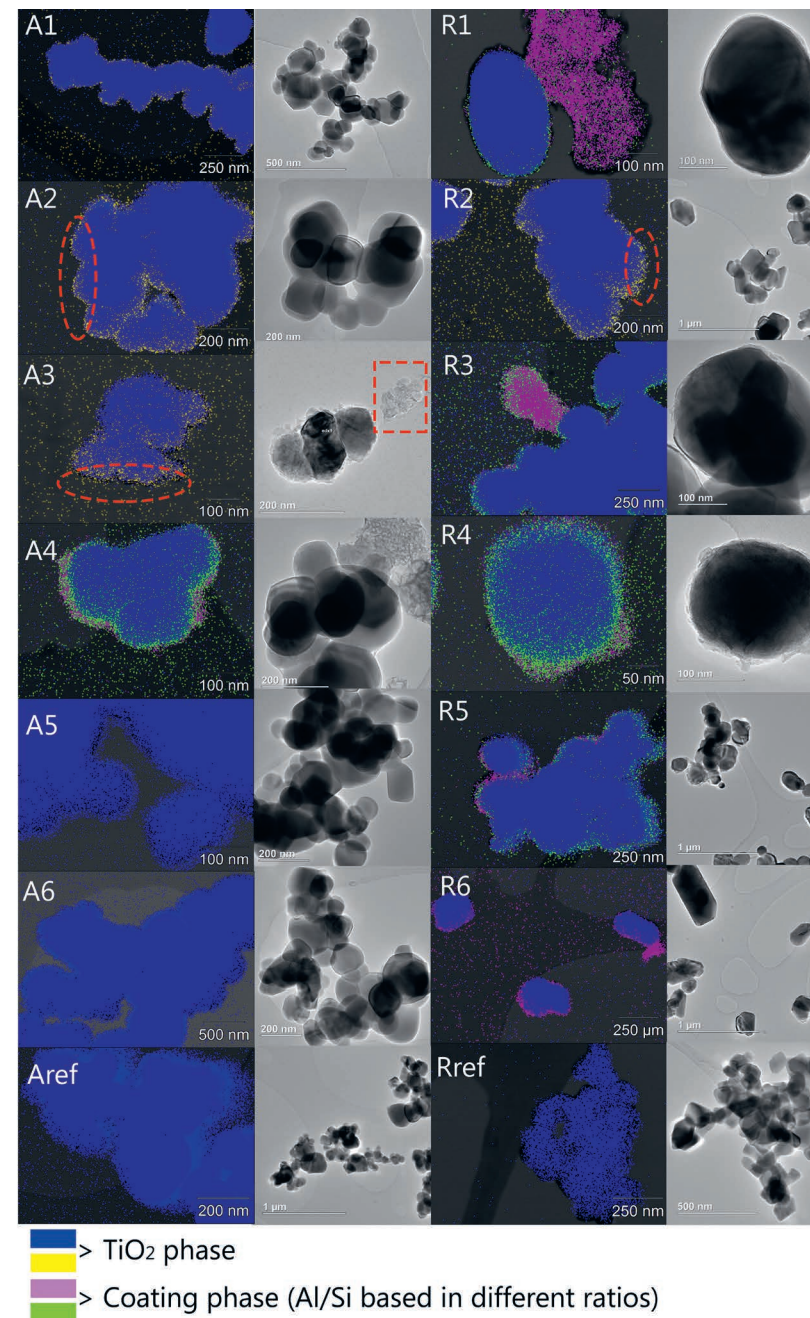


Figure 2.1 STEM-EDX phase maps and images of the pigments. The phase separation is performed automatically with the NSS software. EDX spectra of the different phases can be found in the supplementary information part 2.

Table 2.2 Results from ICP-OES (data as received by AkzoNobel presented in SI part 3) and interpretation of the organic, inorganic coating and production process.

2.5 The presence/absence of niobium is used as a marker for the production process since niobium cannot be removed in the sulphate process.

2.6 A4 is produced by Tiofine (now Tronox), a production facility that switched to the chloride process in 1989. Thus dating the pigment after 1989.

2.7 Rref is chosen as a reference because the Sigma-Aldrich rutile was not suitable (see footnote 1 and 4). Raman indicated only the rutile phase. Furthermore, ICP-OES indicated that no impurities are detected in major amounts (>0.1 wt%) and STEM-EDX confirms the absence of an inorganic coating thus confirming the powder is a suitable reference.

Code	Elements >0.1 wt%	Elements in ppm range > 100 mg/kg	Organic coating (based on manufacturer).	Inorganic coating based on STEM-EDX evaluation.	Suggested production process based on elemental composition ^{2,5} .
A1	K, P	Nb, S, Zr	Unlikely	None	Sulphate process
A2	K, P	Al, Nb, Zr	Likely polyol	None	Sulphate process (confirmation)
A3	Al, P, Si	K, Nb, S, Zr	Likely polyol	Inhomogeneous Al, Si	Sulphate process (confirmation)
A4	Al, P, Si	K, S, Zr	Likely	Inhomogeneous Al, Si	Chloride process ^{2,6}
A5	K, Nb, P, Si	Al, Ca, Mg, S, Zn, Zr	Unlikely	None	Sulphate process (confirmation)
A6	Nb	Ca, Fe, K, P, S, Si	Unlikely	None	Sulphate process
A _{ref}	K, P	Nb, Si, Zr	Unlikely	None	Sulphate process
R1	Al, Si	K, P, S, Zr	Likely polyol	Inhomogeneous 2 layers of coating (dense Si + Al)	Chloride process
R2	K, Nb	Al, Ca, P, S, Si, Zr	Likely polyol	No	Sulphate process (confirmation) Chloride process
R3	Al, P, Zr	Si	Likely	Inhomogeneous Al, Zr coating	Chloride process
R4	Al, Si, Zr	P, S	Likely	Inhomogeneous Al, Si, Zr coating	Chloride process
R5	Al	P, S, Si	Likely	Inhomogeneous Al, Si coating	(confirmation)
R6	Al, P, Si	Ca, Nb, S, Zr	Likely	Thick Al, Si coating	Sulphate process
R _{ref} ^{2,7}	-	Al, Si	Unlikely	Uncoated (some CuS particles)	Chloride process

2.3.2. TRPL

Since anatase and rutile-based pigments have different photoluminescence emissions, the TRPL results on the analysed pigments will be discussed separately in the following sections.

2.3.2.1. TRPL of anatase-based pigments

Figure 2.2 displays the photoluminescence emission of all the anatase pigments as gated spectra in three different temporal ranges following pulsed excitation. In the first 10 ns after excitation, PL spectra for all samples are characterized by an identical broad emission centred in the green at 500 nm (2.48 eV) (G-PL) with a

full width at half-maximum (FWHM) of about 150 nm (0.68 eV). The shape is asymmetric due to the presence of a shoulder in the red, in the following quoted R-PL. At longer delays (time space between 50 and 100 ns after excitation), the R-PL emission appears as the main emitting band in samples A5 and A6, giving rise to a red-shifted emission centered around 630 nm (1.97 eV). In all the other samples it still appears as a slight shoulder of the main G-PL emission. Finally, at microsecond delays (0.2-10.2 ms) in at least two samples (A3 and A_{ref}), it is possible to infer the presence of a faint, but detectable near-infrared emission (NIR-PL) centered in the spectral range 800-850 nm.

Figure 2.2 Gated spectrum of anatase pigments in the temporal intervals 0-10 ns(A), 50-100 ns (B) and (C) 0.2-10.2μs after pulsed excitation.

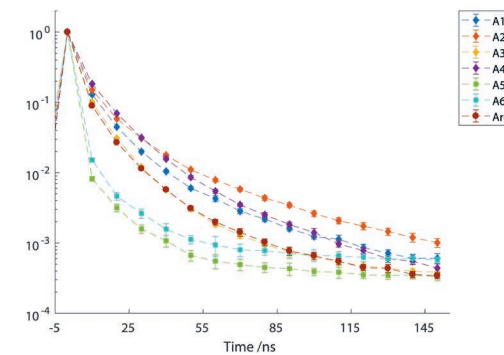
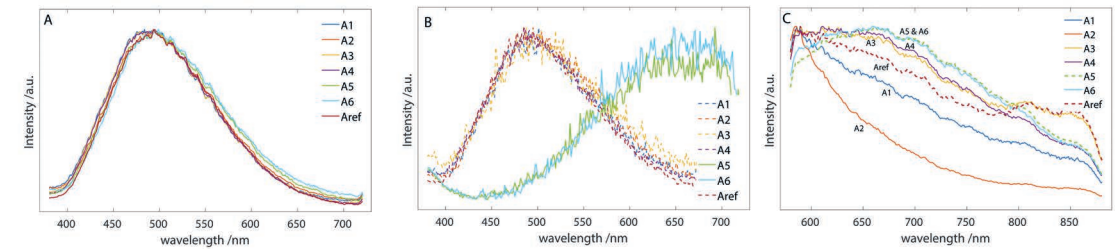


Figure 2.3 Emission decay kinetic of the G-PL emission (480-520 nm) of anatase pigments.

Sample	τ (ns) VIS-PL (450-550 nm)-> A
A1	4.3
A2	4.7
A3	3.8
A4	5.2
A5	1.6
A6	2.1
A _{ref}	3.6

Table 2.3 Results of decay kinetics analysis of the G-PL emission of anatase samples {full results presented in SI Part 4, table 6}.

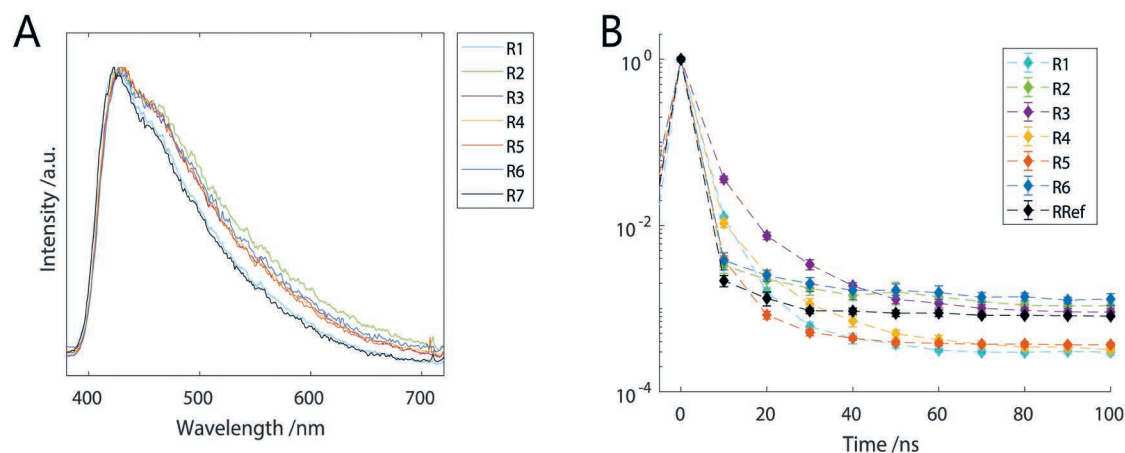
Analysis of the decay kinetics of the bright G-PL emission, Figure 2.3, indicates that the emission occurs at the nanosecond timescale. The effective lifetime is in the range 3.6- 5.2 ns ($m = 4.3$ ns, $1s = 0.6$ ns) for all anatase pigments except for samples A5 and A6, which have a more rapid decay and an effective lifetime around 1.8 ns (Table 2.3).

2.2.2.2. TRPL rutile-based pigments

All rutile-based samples show a well-detectable emission at both the nanosecond and microsecond timescales.

In Figure 2.4A, we report the spectral shape of the signal detected for all samples considering photons emitted in the first 10 ns after pulsed excitation. The gated spectrum appears as the left part of an emission centered at wavelengths minor than 420 nm (or equivalently at energies higher than 2.95 eV), in the following quoted as B-PL. Considering the spectral shape of the emission, it is possible to suggest the presence of two main bands; one peaked at 430 nm (2.88 eV) and the other at 470 nm (2.64 eV). The emission shape in rutile samples is differentiated by the relative intensity between these two components: the more intense is the second component, the broader is the PL band. Here, we report that samples R1 and R_{ref} are the ones characterized by the narrower PL spectral shape. Analysis of the emission decay kinetic of the B-PL band (Figure 2.4B) reveals that five pigments are characterized by an effective lifetime in the range 1.8 – 2.8 ns ($m = 2.3$ ns, $1s = 0.4$ ns). On the other hand, in samples R2, R6 and Rref the decay kinetic is dominated by a single subnanosecond component with a lifetime close to 0.5 ns (Table 2.4).

Figure 2.4 (A) 0-10 ns gated spectrum (normalize) and (B) nanosecond emission decay kinetic in the spectral band (400-550 nm) of rutile pigments.

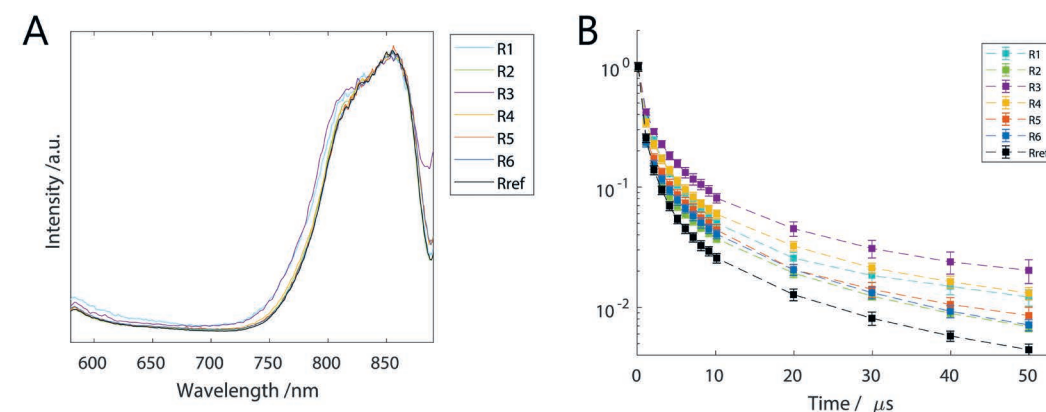


Sample	τ (ns) VIS-PL (420-440 nm)	τ (μ s) NIR-PL (800-820 nm)
R1	2.2	1.9
R2	0.5	1.0
R3	2.8	2.4
R4	2.3	1.7
R5	1.8	1.0
R6	0.5	0.9
R _{ref}	0.5	1.0

Table 2.4 Results of decay kinetics analysis of the two main emissions detected in rutile samples {full results presented in SI Part 4, Table 7 and 8}.

Figure 2.5A displays the gated spectra detected in the temporal interval between 0.2 and 10.2 μ s. In this timespace, all samples have a pretty similar emission shape consisting of a well-defined emission centred around 850 nm (1.45 eV), in the following quoted as NIR-PL. The emission occurs on the microsecond timescale. Following the analysis of the decay kinetic in the spectral band 800-850 nm, Figure 2.5B, we observe that all rutile-based samples are characterized by an effective lifetime in the range 1.0 -2.4 ms ($m = 1.4$ ms, $1s = 0.6$ ms).

Figure 2.5 (A) 0.2-10.2 ms gated spectrum (normalize) and (B) microsecond emission decay kinetic in the spectral band (800-850 nm) of rutile pigments.



2.4. Discussion

Material characterization of the available titanium white pigments, made through STEM-EDX, ICP-OES, and Raman, provided a clear distinction regarding crystal structure, inorganic coating and impurities. The organic coating identification instead was less precise and, to better understand it, additional methods should be employed, such as Py-GC-MS. Our selection of pigments is well balanced for an explorative study, with pigments of both crystal types, both production processes and with different types of coatings.

Firstly, TRPL results indicate significant differences between rutile and anatase pigments. This clear distinction is a valuable point for non-invasive pigment identification. In particular, while many organic binding media emit in the visible region [47], the emission for rutile is quite specific and can thus likely be used to identify the pigment in more complex materials such as paints.

Secondly, despite the high variety of available anatase samples, characterized by different inorganic and organic coatings and levels of impurities, the main features of the PL emission vary little among samples. Anatase-based pigments are all characterized by a broad visible photoluminescence emission, centred in the green region (Figure 2.2). This is in very good agreement with literature data [36, 38, 53, 54], where a PL emission centred between 2.3-2.5 eV (495-540 nm) with a FWHM of 0.9 eV (about 140 nm) is reported. The mechanism behind this radiative recombination is attributed to different kinds of species, without general consensus, such as self-trapped excitons, oxygen vacancies, and defect sites, impurities or reduced metal ions [33]. It is also reported that two distinct components contribute to this visible emission: one centred in the green (G-PL) and the other in the red (R-PL) [36], as we have detected in all our samples. The most recent research suggests that these two emissions are caused by different recombination mechanisms and are differently influenced by the interaction with molecular oxygen. The G-PL is proposed as the result of radiative recombination of excited electrons in the conduction band with trapped holes. In an O₂ environment, these hot excited carriers are scavenged by chemisorbed O₂, giving rise to the formation of superoxide species and a net decrease of the G-PL emission. On the other hand, the R-PL emission, less sensitive to electrons scavenging, is suggested to be correlated with the recombination of trapped electrons with valence band holes [36, 53]. In our study, we have observed that in the two oldest pigments (A5 and A6), produced by the sulphate process and with no inorganic coating, the relative intensity of the R-PL emission with respect to the G-PL emission, is more relevant than in the other anatase pigments. The shorter emission lifetime of the G-PL band detected in these two samples suggests that light quenching is the main mechanism ruling this intensity variation. Both uncoated, historical samples contain high levels of niobium, and we speculate that these impurities could be responsible for the observed G-PL quenching, but other impurities, like Fe, could be involved as well {SI, Tables 1, 2 and 5}. Indeed, it is recognised that impurities may affect the PL emission behaviour of titanium dioxide [55]. Moreover, considering that samples A5 and A6 are historical, we may expect that the surface of these early synthesized titanium dioxide pigments have not been treated, whereas the

opposite is expected for contemporary pigments even when manufacturers do not report it. The non-treated surface of these uncoated pigments could render them more interactive with environmental molecular oxygen, hence promoting the quenching of G-PL emission [36].

Further, in at least two of the analysed samples produced with modern synthesis processes, we detect a NIR-PL emission with spectral and lifetime features that closely resembles the typical PL emission of rutile, as will be further detailed in the next paragraphs. This occurrence suggests that trace amount of the rutile phase can be present in anatase pigments as a consequence of non-perfectly controlled synthesis processes. Here, the use of photoluminescence spectroscopy appears to be ideally suited to detect trace rutile present in concentrations below the detection limit of Raman spectroscopy.

All the rutile pigments analysed in this study are characterized by two distinct emissions. The first is a broad emission in the blue region (B-PL), rarely reported in the literature [56, 57]. The second is a NIR-PL band with a maximum at 850 nm commonly reported for rutile titanium dioxide [1, 36]. The energy position of the NIR-PL emission (about 1.45 eV) with respect to rutile bandgap (3.02 eV) suggest that a deep mid-gap state of unknown chemical origin is necessarily involved. Nowadays, the most reasonable theory for explaining the mechanisms for the NIR emission, as well as its intensity enhancement in an O₂ environment involves the recombination between a mid-gap trapped electron and a free (valence band) hole [38]. Interestingly, Allen et al. reported the detection of two NIR emissions for rutile pigments, one at 830 nm and one at 1015 nm, which, according to the author, should be characteristic for chloride or sulphate processed pigments [39]. As our detector is not sensitive at wavelengths higher than 900 nm, this could not be evaluated in the present research.

Concerning the detected B-PL emission of rutile, whereas the comprehension of the mechanisms behind its de-excitation process is still far to be understood, it is interesting to note that its nanosecond decay kinetic is severely shortened in three of the seven rutile-based samples giving rise to a sub-nanosecond mono-exponential temporal profile. Two of these samples (R2 and R6) are the only pigments being produced with the sulphate process, and hence containing detectable amounts of niobium, which could act as quenchers of the B-PL emission in rutile samples, too. Instead, no clear explanation can be retrieved for the sub-nanosecond lifetime detected in the Rref sample. Interestingly, the presence of niobium does not affect the spectral shape or the

emission lifetime of rutile NIR-PL emission, which is instead affected by other features of the analysed pigment particles with no clear trends on the basis of the present experiments.

In general, it is clear that, whereas the spectral PL features of anatase- and rutile- based pigments are little affected by the complexity and high variety of the selected pigments (mainly with reference to the presence of impurities and coatings), the use of a time-resolved approach allows to probe the sensitivity of the emission lifetime to the micro-environment of excited carriers. This sensitivity gives rise to the detection of different emission decay profiles, which are influenced by many competing factors. On the basis of this research, it is not possible to derive a clear correlation between the emission lifetime and specific properties of titanium white pigment particles – apart for the reported emission quenching induced by niobium impurities.

Similarly, while it is tempting to try to find a correlation between PL properties and the pigment photocatalytic activity, this relation is ambiguous and from our findings, there is no apparent correlation between the luminescence behaviour of the pigments and the presence of inorganic pigment coatings, which are known to strongly influence photocatalytic activity [24]. While others have attempted to correlate chemical properties such as photocatalytic activity with PL intensity [34-36], it is recognised that the intensity of the emission may be a poor parameter in the analysis of these white pigments, as intensity may depend on many factors including particle size, coating, milling, and heating.

2.5. Conclusion

This study provides a first clear step in illustrating and understanding the PL properties of TiO₂ pigments ranging from historical to contemporary and used in different end applications. The most important findings are first that rutile and anatase pigment have a very distinct and different emission, which could be useful for pigment identification. Secondly, the PL spectral and decay kinetic properties can be influenced by the presence of specific impurities, niobium in particular which is a trace impurity of sulphate processed pigments. Thirdly, rutile pigments present a blue emission that has rarely been reported in the literature and that, at present, is not clearly attributed.

Our results mostly agree with the previous studies regarding general emission shape, but the increased complexity for pigments compared to nanoparticles and single crystals is evident, which makes the study of luminescence intensity particularly challenging.

Further in-depth investigations are worthwhile on well-controlled materials stemming from an identical parent powder. Cryogenic temperatures could allow potentially allow the assessment of luminescence and the influence of processing on luminescence lifetimes at different wavelengths, including those in the IR. In addition to being an explorative step for in depth photoluminescence studies on complex titanium-based pigments, the study also marks the starting point for photoluminescence studies towards titanium white containing paints.

Acknowledgements

This work has received funding from the European Union Horizon 2020 research and innovation programme under grant agreement No. 654148 Laserlab-Europe. Furthermore, the Rijksmuseum is acknowledged for hosting and organizing van Driel's Ph.D. research. AkzoNobel is acknowledged for funding van Driel's Ph.D., as well as for their analytical support. AkzoNobel, Winsor & Newton, the RCE reference collection, Huntsman, Tronox and Sachtleben chemie are acknowledged for providing pigments.

- Laver M. Titanium White. In: West FitzHugh E, editor. *Artists' Pigments: A Handbook of their History and Characteristics*, Vol. 3. National gallery of Art, Washington. London:Archetype Publications. 1997. 3: 295-355.
- Eastaugh N, Walsh V, Chaplin T and Sidall R. *Pigment compendium, a dictionary and optical microscopy historical pigments*, Butterworth-Heinemann. 2004, Burlington: Elsevier.
- Martins A, Albertson C, McGlinchey C, Dik J. Piet Mondrian's Broadway Boogie Woogie: non-invasive analysis using macro X-Ray fluorescence mapping (MA-XRF) and multivariate curve resolution-alternating least square (MCR-ALS). *Herit Sci*. 2016; 4.
- van den Berg KJ, Miliani C, Aldrovandi A, Brunetti BG, de Groot S, Kahrim K, et al. The chemistry of Mondrian's paints in Vicotory Boogie Woogie. In: van Bommel MR, Janssen H, Spronk R, editors. *Inside Out Victory Boogie Woogie*. Haags Gemeentemuseum, Amsterdam University Press.
- Benedix R, Dehn F, Quaas J and Orgass M. Application of titanium dioxide photocatalysis to create self-cleaning building materials. 2000; p.157-168
- Gunnarsson SG. *Self-Cleaning Paint: Introduction of photocatalytic particles into a paint system*. PhD thesis DTU. 2011.
- Muneer M, Philip R and Das S. Photocatalytic degradation of waste water pollutants. Titanium dioxidemediated oxidation of a textile dye, Acid Blue 40. *Res Chem Intermediat*. 1997; 23(3): p. 233-246.
- van Driel BA, Wezendonk TA, van den Berg KJ, Kooyman PJ, Gascon J and Dik J. Determination of early warning signs for photocatalytic degradation of titanium white oil paints by means of surface analysis. *Spectrochim Acta A*. 2017; 172: 100-108.
- Morsch S, van Driel BA, van den Berg KJ and Dik J. Investigating the Photocatalytic Degradation of Oil Paint using ATR-IR and AFM-IR. *ACS Appl Mater Interfaces*. 2017; 9(11): 10169-10179.
- Völz HG, Kaempf G, Fitzky HG, Klaeren A. The Chemical Nature of Chalking in the Presence of Titanium Dioxide Pigments. *ACS Photodegrad Photostabil Coat*. 1981; 151: 163-182.
- Lauridsen CB, Sanyova J, Simonsen KP. "Analytical study of modern paint layers on metal knight shields: The use and effect of Titanium white. *Spectrochim Acta A*. 2014; 124: 638-645.
- Thorn A. Titanium dioxide: a catalyst for deterioration mechanisms in the third millennium." *Stud. Conserv*. 2000; 45(Supplement-1): 195-199.
- Stieg FB. Opaque White Pigments in Coatings. *ACS Appl Polym Sc*. 1985; 285: 1249-1269.
- de Keijzer M. The history of modern synthetic inorganic and organic artists' pigments. In: *Contributions to conservation at the Netherlands Institute for Cultural Heritage*, James & James (Science Publishers) Ltd. 2002
- Phenix A, van den Berg KJ, Soldano A, van Driel BA. The Might of White: formulations of titanium dioxide-based oil paints as evidenced in archives of two artists' colourmen mid-twentieth century. In: *ICOM-CC Triennial conference 2017, Copenhagen*. 2017.
- Gazquez MJ, Bolivar JP, Garcia-Tenorio, R and Vaca Federico. A review of the production cycle of titanium dioxide pigment. *Mater Sci Appl*. 2014.
- Braun JH, Baidins A, Marganski RE. TiO₂ pigment technology: a review. *Prog Org Coat*. 1992; 20(2): 105-138.
- Chen YF, Lee CY, Yeng MY and Chiu HT. The effect of calcination temperature on the crystallinity of TiO₂ nanopowders. *J Cryst Growth*. 2003; 247(3): 363-370.
- Tian C. Calcination intensity on rutile white pigment production via short sulfate process. *Dyes pigments*. 2016; 133(Supplement C): 60-64.
- Johansson LS. "Analysing coated powders with XPS." *Surf Interface Anal*. 1991; 17(9): 663-668.1991
- Werner AJ. Titanium dioxide pigment coated with silica and alumina. Google Patents. 1969
- Jacobson HW. Light-stable titanium dioxide pigment composition. Google Patents. 1980
- Albert D, et al. Titanium dioxide of improved chalk resistance. Google Patents. 1972
- van Driel BA, Kooyman PJ, van den Berg KJ, Schmidt-Ott A, Dik J. A quick assessment of the photocatalytic activity of TiO₂ pigments — From lab to conservation studio! *Microchem J*. 2016; 126: 162-171.
- Day RE and Egerton TA. Surface studies of TiO₂ pigment with especial reference to the role of coatings. *Colloid Surface*. 1971; 23(1-2): 137-155.
- Farrokhpay S. A review of polymeric dispersant stabilisation of titania pigment. *Adv Colloid and Interfac*. 2009; 151(1-2): 24-32.
- Valencia S, Marin JM and Restrepo G. Study of the bandgap of synthesized titanium dioxide nanoparticles using the sol-gel method and a hydrothermal treatment. *Open Mater Sci J*. 2010; 4(1): 9-14.
- Chinedu EE and Diola B. Ab-initio Electronic and Structural Properties of Rutile Titanium Dioxide." *Jpn J Appl Phys*. 2011; 50(10R): 101103.
- Zhu T and Gao SP. The Stability, Electronic Structure, and Optical Property of TiO₂ Polymorphs." *J Phys Chem C*. 2014; 118(21): 11385-11396.
- Landmann M, Rauls E and Schmidt WG. The electronic structure and optical response of rutile, anatase and brookite TiO₂." *J Phys- Condens Mat*. 2012; 24(19): 195503.
- Yamada Y and Kanemitsu Y. Determination of electron and hole lifetimes of rutile and anatase TiO₂ single crystals." *Appl Phys Lett*. 2012; 101(13): 133907.
- Dozzi MV, D'Andrea C, Ohtani B, Valentini G and Selli E. Fluorine-Doped TiO₂ Materials: Photocatalytic Activity vs Time-Resolved Photoluminescence. *J Phys Chem C* 2013; 117(48): 25586-25595.
- Shi J, Wang X, Feng Z, Chen T, Chen J and Li C. Photoluminescence Spectroscopic Studies on TiO₂ photocatalyst. In: Anpo M and Kamat PV, editor. *Environmentally Benign Photocatalysts: Applications of Titanium Oxide-based Materials*. Springer New York. 2010; p. 185-203.
- Stevanovic A, Buttner M, Zhang Z and Yates JT. Photoluminescence of TiO₂: Effect of UV Light and Adsorbed Molecules on Surface Band Structure. *J Am Chem Soc*. 2012; 134(1): 324-332.
- Stevanovic A and Yates JT. Electron Hopping through TiO₂ Powder: A Study by Photoluminescence Spectroscopy. *J Phys Chem C*. 2013; 117(46): 24189-24195.
- Pallotti DK, Passoni L, Maddalena P, Di Fonzo F and Lettieri S. Photoluminescence Mechanisms in Anatase and Rutile TiO₂. *J Phys Chem C*. 2017; 121(16): 9011-9021.
- Knorr FJ, Zhang D and McHale JL. Influence of TiCl₄ Treatment on Surface Defect Photoluminescence in Pure and Mixed-Phase Nanocrystalline TiO₂. *Langmuir*. 2007; 23(17): 8686-8690.
- Mercado CC, Knorr FJ, McHale JL, Usmani SM, Ichimura AS and Saraf LV. Location of Hole and Electron Traps on Nanocrystalline Anatase TiO₂. *J Phys Chem C*. 2012; 116(19): 10796-10804.
- Allen NS, Bullen DJ and McKellar JF. Luminescence properties and photo-activity of sulphate-processed rutile (titanium dioxide) pigments in commercial polyethylene. *J Mater Sci*. 1979; 14(8): 1941-1944.
- Allen NS, Edge M, Sandoval G, Ortega A, Lieauw CM, Stratton J and McIntyre RB. Interrelationship of spectroscopic properties with the thermal and photochemical behaviour of titanium dioxide pigments in metallocene polyethylene and alkyd based paint films: micron versus nanoparticles." *Polym Degrad Stabil*. 2002; 76(2): 305-319.

41. Janes R, Edge M, Rigby J, Mourelatou D and Allen NS. The effect of sample treatment and composition on the photoluminescence of anatase pigments." *Dyes Pigments*. 2001; 48(1): 29-34.
42. Nevin A, Cesaratto A, Bellei S, D'Andrea C, Toniolo L, Valentini G and Comelli D. Time-resolved photoluminescence spectroscopy and imaging: new approaches to the analysis of cultural heritage and its degradation. *Sensors*. 2014; 14.
43. Gonzalez V, Gourier D, Calligaro T, Toussaint K, Wallez G and Menu M. Revealing the Origin and History of Lead-White Pigments by Their Photoluminescence Properties. *Anal Chem*. 2017; 89(5): 2909-2918.
44. Artesani A, Gherardi F, Nevin A, Valentini G and Comelli D. A Photoluminescence Study of the Changes Induced in the Zinc White Pigment by Formation of Zinc Complexes. *Materials*. 2017; 10(4): 340.
45. Artesani A, Bellei S, Capogrosso V, Cesaratto A, Mosca S, Nevin A, Valentini G, Comelli D. Photoluminescence properties of zinc white: an insight into its emission mechanisms through the study of historical artist materials. *Appl Phys A* 2016; 122(12): 1053.
46. Cesaratto A, D'Andrea C, Nevin A, Valentini G, Tassone F, Alberti R, Frizzi R, Comelli D. Analysis of cadmium-based pigments with time-resolved photoluminescence. *Anal Method*. 2014; 6(1): 130-138.
47. Borgia I, Fantoni R, Flamini C, Di Palma TM, Giardini GA and Mele A. Luminescence from pigments and resins for oil paintings induced by laser excitation. *Appl Surf Sci*. 1998; 127: 95-100.
48. Comelli D, Capogrosso V, Orsenigo C and Nevin A. Dual wavelength excitation for the time-resolved photoluminescence imaging of painted ancient Egyptian objects. *Her Sci*. 2016; 4(1): 21.
49. Van Driel BA, van den Berg KJ, Smout M, Dekker N, Kooyman PJ and Dik J. Investigating the effects of artists' paint formulation on degradation rates of TiO₂-based oil paints. Unpublished Research.
50. Rinno H, Hessel F, Alberti K. Process for reducing the microbe count in aqueous multi-phase compositions that contain synthetic resin. 1996. Google Patents.
51. Mosca S, Frizzi T, Pontone M, Alberti R, Bombelli L, Capogrosso V, et al. Identification of pigments in different layers of illuminated manuscripts by X-ray fluorescence mapping and Raman spectroscopy." *Microchem*. 2016; 124(Supplement C): 775-784.
52. Dupont. Ti-pure titanium dioxide, titanium dioxide for coatings. In: Commercial information booklet Dupont. Accessed from https://www.chemours.com/Titanium_Technologies/es_US/tech_info/literature/Coatings/CO_B_H_65969_Coatings_Brochure.pdf. 20-12-2017.
53. Mercado C, Seeley Z, Bandyopadhyay A, Bose S, McHale JL. Photoluminescence of Dense Nanocrystalline Titanium Dioxide Thin Films: Effect of Doping and Thickness and Relation to Gas Sensing. *ACS Appl Mater Interface*. 2011; 3(7): 2281-2288.
54. Pallotti DK, Orabona E, Amoruso S, Aruta C, Bruzzese R, Chiarella F, et al. Multi-band photoluminescence in TiO₂ nanoparticles-assembled films produced by femtosecond pulsed laser deposition. *J Appl Phys*. 2013; 114(4): 043503.
55. Janes R, Edge M, Robinson J, Allen NS and Thompson F. Microwave photodielectric and photoconductivity studies of commercial titanium dioxide pigments: the influence of transition metal dopants." *J Mater Sci*. 1998; 33(12): 3031-3036.
56. Harada N, Masako G, Koji I, Hiroshi S, Noriya I, Hideyuki K and Kazuhiro E. Time-Resolved Luminescence of TiO₂ Powders with Different Crystal Structures. *JPN J Appl Phys*. 2007; 46(7R): 4170.
57. Fujihara K, Izumi S, Ohno T and Matsumara M. Time-resolved photoluminescence of particulate TiO₂ photocatalysts suspended in aqueous solutions. *J Photochem Photobiol A: Chem*. 2000; 132(1): 99-104.

PART 2



van Driel preparing titanium white oil paint. Photo credit: Maranthe Lammers

Understanding and monitoring the degradation process of titanium white containing oil paints

'The noblest pleasure is the joy of understanding'.²⁸

'When you want to know how things really work, study them when they're coming apart'.²⁹

²⁸ Leonardo da Vinci, https://www.brainyquote.com/quotes/leonardo_da_vinci_154285?src=t_understanding, Accessed 09-01-2018.

²⁹ William Gibson <https://www.goodreads.com/quotes/312004-when-you-want-to-know-how-things-really-work-study>

APPROACH PART 2

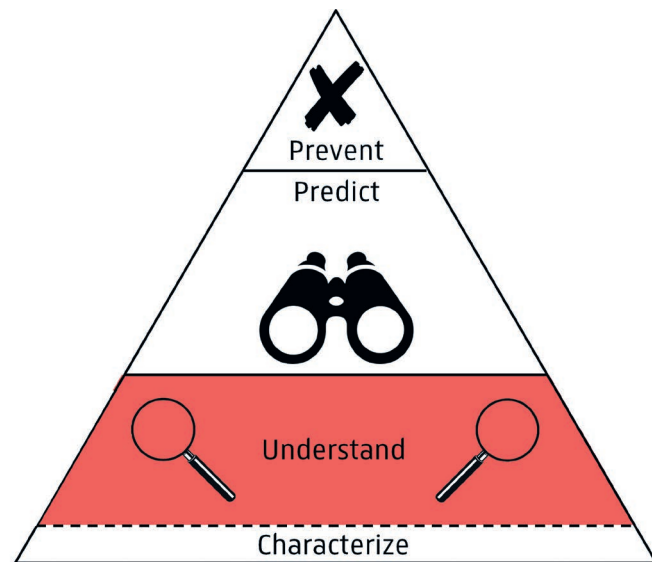
In this part of the thesis, the main goal is to find early warning signs for photocatalytic degradation and to understand the role of paint formulation on the degradation rate. These studies are important to get an idea of where we are on the degradation timeline (how fast is the clock ticking?).

30 Program within the RCE focussing on cultural heritage from modern times, <https://cultureelerfgoed.nl/dossiers/erfgoed-van-de-moderne-tijd/programma-erfgoed-van-de-moderne-tijd>, accessed 11-12-2017.

I decided to focus on titanium white in oil paints rather than other binding media. This choice has several reasons, starting with the most practical one: investigating the effect of titanium white in all binding media would simply take too much time. This would entail documenting the different degradation phenomenologies and investigating the effect of a vast amount of, often secret, additives used. Oil was chosen as the binding medium of interest given the large number of studies already conducted on the topic of oil degradation as well as on oil-pigment interaction. Furthermore, within the Cultural Heritage Agency of the Netherlands 'Modern oil paints' is one of the pillars of the research program 'Erfgoed van de moderne tijd'³⁰. Nevertheless, other binding media are known to contain titanium white and also require research attention {H}. In some cases, results from this part may be extrapolated and validated for other binding media.

The investigation of slow degradation processes is inherently sentenced to the use of accelerated/artificial aging methods {D.6}, in order to get results within four years. However, there are some intrinsic drawbacks to artificial aging studies that are discussed here. First of all, the intensity during artificial aging is much higher than in a regular environment. While the reciprocity principle {D.2} often applies, it does not always hold up. Some processes may only occur at a certain intensity threshold, or intensity may relate non-linearly to the degradation rate. Furthermore, in this study, the aging experiments are performed with UV-irradiation rather than full day light irradiation. Again, this may trigger different processes. Nevertheless, as the process under investigation specifically requires UV initiation, and research has been published on the influence of intensity on degradation rates {D.2}, it is assumed that the artificial aging process is suitable to research the specific degradation phenomenon of chalking further. However, care must be taken when using the irradiation dose to make predictions {I}.

Furthermore, as everyone who ever did reconstruction studies knows, the number of samples that are required increases drastically with each added parameter. This is a problem related to the 'one factor at a time' approach {chapter 5B}, which was partly



resolved by exploring and using the Design of Experiments (DoE) approach (under supervision of AkzoNobel experts). Nevertheless, artificial aging experiments remain time consuming. Thus choices regarding formulation had to be made. Two studies, that aim at the determination of early warning signs are carried out on simple TiO₂-oil paints. These paints are made with the two reference pigments (stable and photocatalytic) and only have an added drier to reduce the drying time. Additionally, one study is carried out to investigate the effect of different formulations on degradation rate. Here a broader range of parameters is investigated thanks to the use of DoE. I decided to keep the drier constant and to choose one additive of interest (aluminum stearate) as well as the two most common extenders (BaSO₄ and CaCO₃). Furthermore, mixtures of white pigments (stable, photocatalytic and ZnO) are investigated because this is a common combination described in archival sources {C.1} and detected in the collection survey {chapter 1}.

Since the process of photocatalytic activity is relatively well described and understood, the focus of the first two studies {chapter 3 and 4} is on the specific changes that occur upon UV-aging of an oil paint film containing TiO₂. To achieve this, visible/morphological (gloss), as well as chemical changes, are monitored. In chapter 3, the change in gloss, its relation to the surface characteristics (monitored by AFM), as well as the detection of 'TiO₂ surfacing' (by XPS) are presented. The choice for XPS is based on successful results in other binding media and the availability of the method in the labs of my research partners. In chapter 4, the organic part of the material is under investigation, which is monitored by two different modalities of infrared spectroscopy: ATR-FTIR and AFM-IR. ATR-FTIR is commonly used for the study of oil paints {D.6}. However, preliminary analysis with this method showed only minimal changes until degradation was already visible. Through AkzoNobel, access was obtained to an AFM-IR apparatus (Manchester University) which provided the possibility to compare both modalities (characterized by different resolutions and penetration depths) and to distinguish the characteristic markers for degradation.

In chapter 5, change in gloss is used to look into the different degradation rate of different paint formulations. Gloss change was validated in chapter 3 as a reliable method to monitor degradation, and was chosen because it is available, cheap, and easy/fast to use on a large number of samples continuously (aging – analysis – continue aging). In chapter 3, since we are monitoring degradation phenomenology, 85° gloss was used, which is sensitive to low gloss and thus provides information on a longer time scale. On the other hand, in chapter 5, 60° gloss is used, which covers low and high

gloss and is thus more useful considering the range of different paint formulations.

All chapters in this section serve the secondary goal to explore techniques and approaches not commonly used in cultural heritage research and show their applicability. In chapter 3, I introduce AFM and XPS, not unknown to the field but used in a novel manner. In chapter 4, the benefit of AFM-IR over conventional IR methods is illustrated. Finally, in chapter 5B, the benefit of the Design of Experiments methodology is discussed.

Chapter 3

Determination of early warning signs for photocatalytic degradation of titanium white oil paints by means of surface analysis.

Titanium white (TiO_2) has been widely used as a pigment in the 20th century. However, its most photocatalytic form (anatase) can cause severe degradation of the oil paint in which it is contained. UV light initiates TiO_2 -photocatalyzed processes in the paint film, degrading the oil binder into volatile components resulting in chalking of the paint. This will eventually lead to severe changes in the appearance of a painting. To date, limited examples of degraded works of art containing titanium white are known due to the relatively short existence of the paintings in question and the slow progress of the degradation process. However, UV light will inevitably cause degradation of paint in works of art containing photocatalytic titanium white.

In this work, a method to detect early warning signs of photocatalytic degradation of unvarnished oil paint is proposed, using atomic force microscopy (AFM) and X-ray photoelectron spectroscopy (XPS). Consequently, a four-stage degradation model was developed through in-depth study of TiO_2 -containing paint films in various stages of degradation. The XPS surface analysis proved very valuable for detecting early warning signs of paint degradation, whereas the AFM results provide additional confirmation and are in good agreement with bulk gloss reduction.

Based on the published cover paper: B.A. van Driel, T.A. Wezendonk, K.J. van den Berg, P.J. Kooyman, J. Gascon and J. Dik (2017), *Spectrochimica Acta Part A: Molecular and Biomolecular Spectroscopy* 172:100-108.

Note 1 This paper includes a document with supplementary material (in the text referred to as 'S') which can be downloaded (link is provided in the back matter).

Note 2 A list of symbols is included at the end of this chapter.

3.1. Introduction

Works of art degrade over time. Society in general, and collection curators specifically, perceive these changes as unwanted. As a result, museums take elaborate precautions to prevent damage to their collection [1]. Unvarnished paintings containing photocatalytic titanium white form a distinct risk group for degradation, since the pigment has the ability to break down the binder through UV light-initiated photocatalysis [2]. Titanium white was first introduced in the 1920s and rapidly became the most widespread pigment of the 20th century. Many famous artists such as Pablo Picasso, Jackson Pollock and Piet Mondriaan have used this pigment [2-4]. Until now, limited examples of degraded works of art containing titanium white have been documented [2, 5-7]. The limited documentation can be the consequence of the slow progress of the degradation process combined with the relatively short existence of the paintings in question. Nonetheless, degradation will inevitably take place if a painting containing photocatalytic titanium white is exposed to UV light [6]. Proper understanding of the degradation process and the development of methods to monitor degradation can provide fundamental information for preventive measures.

The two most commonly used forms of titanium dioxide are rutile and anatase; it is the anatase polymorph that is most photocatalytically active [8-10]. On the other hand, the rutile type is less photocatalytic by nature and additionally, often coated with an inorganic surface layer to further reduce photocatalytic activity [11]. This inorganic coating can consist of different layers of material such as alumina, silica and zirconia [2, 11-13]. In the course of the pigment development in the 20th century, various types of pigments with different properties have reached the market [12]. For instance, production of the rutile type pigment was discovered and implemented since the 1940s [2, 12], and surface coatings were patented from the 1960s onward [13]. Different qualities of surface coatings can be present resulting in different pigment qualities [14]. Properly coated pigments have low to non-existent photocatalytic activity, while still absorbing UV light. Therefore, these pigments can function as UV protectors rather than photocatalysts [15, 16]. Furthermore, uncoated anatase pigments were produced and used in oil paints until far into the 20th century [17]. In this work, we distinguish between two general types of titanium white pigments: photocatalytic pigment (uncoated anatase, UA) and photostable pigment (coated rutile, CR). The photocatalytic pigment is the pigment of interest, while the photostable pigment is used for comparison and to determine if the observed changes can be attributed to photocatalysis or to other degradation events.

Photocatalytic degradation can occur in different forms, depending on the material surrounding the photocatalytic pigment. In general, the degradation reactions are caused by radicals formed on the TiO₂ surface [18-20]. Photocatalytic reactions can cause alteration of surrounding pigments, such as the fading of Prussian blue or alizarin lake (Scheme 3.1, process 1) [21-23]. On the other hand, degradation of the paint binder can occur by extensive cross-linking, causing embrittlement [16, 24] mainly visible in the form of cracks, or by degradation into volatile components (Scheme 3.1, process 2 and 3). The current chapter focuses on the latter process, more specifically on the degradation of the oil binder (Scheme 3.1, process 3). This degradation process causes roughening of the surface and eventually leads to chalking: the top layer of the paint has degraded and the pigment is now located freely on the surface [18, 25-27].

Scheme 3.1 TiO₂ catalyzed degradation processes, process #3, indicated in bold, is the process of interest in this chapter.

- 1 TiO₂ + hv + binder formed by a radical addition polymerization → Further cross-linking leading to embrittlement
- 2 TiO₂ + hv + colored pigments → change of color due to modification of the chemical structure or oxidation/reduction of inorganic pigments
- 3 **TiO₂ + hv + oil binder → Volatile organic components**

Chalking of titanium white alkyd paints was demonstrated by Voltz et al. in 1981 [18]. Scanning electron microscopy (SEM) images showed the morphological differences between a chalked surface caused by photocatalysis and a chalked surface caused by ordinary photo-oxidative degradation. Monitoring the aging of titanium white paints has been performed using several other techniques as well such as weight loss, change of gloss, Gel Permeation Chromatography (GPC), Fourier Transform Infrared spectroscopy (FTIR), XPS and AFM [16, 28-33]. Most of this work has been done on modern paint binders and polymeric systems such as alkyds, acrylics and polyalkenes. The aging of oil paint has also been studied widely, but not many papers concerning the effect of titanium white on oil paint aging have been published [34-38].

The main purpose of monitoring the aging of paint films is to gain understanding of the degradation processes, but also to be able to determine whether degradation is taking place before this is visible to the human eye. Investigating the aging of paint films can be performed by monitoring bulk and surface changes. These changes can be classified as optical changes (in the case of chalking, caused by changes in surface morphology of the paint film), chemical changes (in the case of chalking, related to the degradation of oil and the appearance of unbound titanium dioxide), and mechanical

changes (in the case of chalking, the loss of coherence of the paint film by oil degradation).

The methods currently used and widely available in the field of conservation science, such as FTIR, are challenging to use as early detection methods due to the unknown ‘initial state’. The term ‘initial state’ in this chapter refers to the non-degraded state of the painting, as if it were analyzed immediately after production. When monitoring changes using the current methods, these can be detected but only in relation to a previous state that was analyzed. Furthermore, in the case of FTIR, unambiguous proof of degradation is detectable only when this is also visible by eye^{3.1}.

Until today, there is no straightforward analytical method to determine any early warning signs for photocatalytic degradation of unvarnished oil paints containing titanium white, and the methods currently used in the field of conservation are not sufficient to detect this specific process. Therefore, for this chapter, new analytical approaches have been explored. In the 20th century, paintings were often unvarnished and unframed [39]. This leads to a lack of protection from the environment as well as a lack of reference material (‘initial state’), such as the area protected by the frame. An unknown initial state of the material makes determination of degradation challenging. Once it is clear that photocatalytic degradation is taking place, the object can be completely removed from UV light to stop the degradation. However, it is not feasible, with the exception of some museum collections, to preventively remove UV light everywhere, such as in company art collections that contain large numbers of 20th century works of art [40, 41]. It is therefore important to know which works of art should be protected. For curators and conservators, assessment of paintings is based on visual inspection [42]. A connection between analytical results and a parameter that is related to a common visual observation, is therefore required for good communication with the field of conservation.

In the current chapter, we follow the aging of unvarnished titanium white oil paints on the nano-scale with AFM and XPS and we relate this to the macro-scale phenomena of gloss change and chalking. Even though SEM can provide sharper images, AFM offers, as advantage, information about the height profile of the paint sample. On the other hand, XPS is a surface sensitive technique, therefore small changes in elemental composition at the surface of the paint film can be determined. In practice, an oil paint film has a so-called medium skin {see Figure S1^{3.2}}, which is a thin layer of unpigmented oil at the surface of the paint film formed during the drying process. The thickness of this layer (t_{ms})

3.1 Personal experience of the authors during preliminary studies.

3.2 Figures labelled ‘S’ can be found in the supplementary information.

depends on, among others, pigment volume concentration (PVC) and manner of application [39]. If this organic layer, composed mainly of carbon, hydrogen and oxygen, is thicker than the penetration depth (d_{xps}) of XPS analysis ($t_{\text{ms}} > d_{\text{xps}}$), an unaged paint film should show only carbon and oxygen signals in XPS analysis. In this case, the initial situation ($x_{\text{Ti}}=0$) is known and fixed which offers a benefit over methods described previously. During aging, the binder is broken down and a titanium signal should appear in the XP Spectra ($x_{\text{Ti}}>0$). If this process can be verified for several types of paint, XPS could serve as an early warning detection method for degradation. In this study, the focus is on linseed oil-based paint that serves as a model binder for all types of drying oils.

Combining morphological and elemental information of the paint surface and at the same time connecting this to the macro phenomena of gloss change and chalking will offer insight into the degradation process of oil paints containing photocatalytic titanium dioxide. The insight gained is used to propose a four-step degradation model. Even though XPS and AFM are not common and accessible methods in the field of conservation yet, these techniques may prove their value in the coming years and are therefore put in perspective using a step-by-step method to determine early warning signs for photocatalytic degradation. In the field of conservation, a micro-destructive technique will only be performed if the presence of titanium dioxide in the paint film is confirmed. This can be determined by a non-invasive method such as portable X-ray fluorescence spectrometry {chapter 1} or Raman spectroscopy [2, 43]. Furthermore, the crystal structure of the titanium white could be characterized prior to XPS/AFM investigation. This can be done non- or micro-invasively, depending on the available equipment with X-ray diffraction or Raman spectroscopy [2].

3.2. Materials & Methods

3.2.1. Sample preparation

Paint films were prepared by mixing titanium dioxide with linseed oil. Two types of titanium dioxide were used: Hombitan LW, an uncoated anatase (UA) from Sachtleben Chemie, and CR-826, a coated rutile (CR) pigment of the highest durability grade from Tronox. The powders were used as received^{3,3}. The used oil is commercial bleached linseed oil of the brand van Beek. In view of the long drying time of oil paint, a drying agent was used to speed up oil polymerization. The drying agent, a mixture of cobalt and zirconium carboxylates, was obtained from Pieter Keune and used as received. 0.1% v/v was added to 1 L of oil, and the resulting oil

was sealed and kept in the dark to prevent polymerization [44]. Paints with a PVC of 15% were prepared by mixing pigment with oil. The mixture was mixed three times for 25 rotations on a glass plated paint mill, an automatic Muller, with a weight of 5 kg. In between mixing, the mixture was scraped together with a palette knife. The paints were spread out on melinex supports with a draw down bar, applying a fixed layer thickness of 100 μm , and left to dry for 14 days in the lab environment ($T=20^\circ\text{C}$, cyclic lighting). The paint with photocatalytic pigment was prepared in duplo (UA-1 and UA-2), since it was expected to show severe degradation. As comparison to the degrading paints, the paint with photostable pigment (CR) was exposed to the same conditions and analyzed using the same techniques.

After drying, the paints were cut into seven fragments of 1 by 2 cm and one larger fragment of 7.5 by 2.5 cm {Figure S2}. The larger fragment was used to monitor gloss during the aging process. After the gloss measurement, the large sample was returned to the aging chamber. The small fragments were taken out of the UV chamber at different irradiation dose and were analyzed using XPS and AFM on multiple spots. Previous experience with aging experiments indicated this would be necessary, because aging is an inhomogeneous process. The samples were aged in an Opsytec Dr. Gröbel BS-02 UV chamber with UV-MAT dose control. The chamber was equipped with UVA lamps. The UV distribution of the UV chamber, provided by the company, is taken into account to calculate the amount of UV received by each sample, as summarized in Table 3.1.

After removal from the UV-chamber, samples were kept in the dark until analysis. Dark storage causes yellowing of the oil, which is a property of linseed oil unrelated to the presence of TiO_2 and will therefore not be discussed in this chapter [47]. To confirm that the analyzed change is related to UV exposure, paint samples of UA-2 and CR have been kept in the lab environment, parallel to the aging in the UV chamber, for 970 hours ($T=20^\circ\text{C}$, cyclic lighting).

AFM&XPS samples	I_0 [J/cm ²]	I_1 [J/cm ²]	I_2 [J/cm ²]	I_3 [J/cm ²]	I_4 [J/cm ²]	I_5 [J/cm ²]	I_6 [J/cm ²]	I_7 [J/cm ²]	LAB t [h]
UA-1	0	2115	4231	5261	6346	7267	10883	12704	-
UA-2	0	1662	3324	4134	4845	5548	8309	9698	970
CR	0	1899	3799	4724	6278	7189	10766	12567	970
Gloss samples	I_0 [J/cm ²]	I_1 [J/cm ²]	I_2 [J/cm ²]	I_3 [J/cm ²]	I_4 [J/cm ²]	I_5 [J/cm ²]	I_6 [J/cm ²]	I_7 [J/cm ²]	LAB t [h]
UA-1	0	1705	3411	4241	5391	6173	9245	10791	-
UA-2	0	2115	4231	5261	6687	7658	11468	13387	0-970
CR	0	1985	3972	4939	6278	7189	10766	12567	0-970

Table 3.1 Irradiation dose received by each sample. Maximum irradiation [13387 J/cm²] is equivalent to 7 years of outdoor exposure. Calculation based on 1.35 W/m² UV content on earth [45] and an average of 12 hours of light a day [46].

3.2.2. Analysis

Gloss was measured using a Sheen Instruments Ltd Tri-GLOSSmaster. The gloss number is measured at three different angles: 20°, 60° and 85°. Low angles of measurement are commonly used for high gloss, while high angles are more suitable for low gloss measurements. High angle gloss will therefore be discussed in this chapter but all angles have been monitored. The gloss was measured three times per measuring point, with the equipment being repositioned in between the analyses.

AFM analysis was performed using an NT-MDT Ntegra instrument equipped with a silicon Etalon tip. Samples were analyzed at three to five different locations of either 10*10 µm or 20*20 µm. In case of visible sample heterogeneity {Figure S3 and S4}, clearly distinct areas (white and yellow) were both analyzed in three to five locations. All samples of UA-1 were imaged, while only the beginning and end stages as well as the sample kept in the lab were selected for imaging for UA-2 and CR. Imaging parameters (force and scan speed) were optimized per image. From the AFM images, the Nova software provides the minimum and maximum recorded height value which was used to calculate the largest height difference in the image, Δz_{max} . For each sample these values were averaged over the three to five recorded images.

XP Spectra were recorded on a K-alpha Thermo Fisher Scientific spectrometer using monochromated Al Ka X-ray source. The UA-1 measurements were carried out by using a line scan of four points to account for possible sample heterogeneity, with each point having a spot size of 300 µm at ambient temperature. The chamber pressure was about 10^{-7} mbar. UA-2 and CR measurements were performed with a line scan of three points. UA-1 line scan locations were oriented on white or yellow areas by using the built-in sample microscope, whereas for the UA-2 and CR samples random locations on the overall yellow paint film were studied {Figure S3}. A flood gun was used during data acquisition for charge compensation. All spectra were corrected by setting the reference binding energy of carbon (1s) to 284.8 ± 0.1 eV. The electron energy analyzer was operated with a pass energy of 50 eV, and every location was scanned ten times. The spectra were analyzed and processed using Thermo Avantage v5.913 software (Thermo Fisher Scientific). The peaks were fitted using Lorentzian–Gaussian product functions. Smart background subtraction (derived from the Shirley background) was used over the peak width. Relative atomic compositions were calculated using atomic sensitivity factors of 1.000, 2.881 and 6.471 for C1s (element), O1s (element) and Ti2p (titania), respectively. Atomic

composition values reported are averages over at least 2 line scans for titanium and at least 3 line scans for carbon and oxygen.

XPS is a highly surface sensitive technique. The penetration depth is approximated by the inelastic mean free path of crystalline graphite which has a lattice spacing of 3.4 Angstrom and therefore a penetration depth that ranges between 3 to 6 monolayers of graphite or 1-2 nm [48]. Since dried linseed oil is not a well-defined crystal lattice but an amorphous matrix, the penetration depth cannot be determined accurately and is estimated to be between 1 and 5 nm which is the range and slightly larger than the penetration depth for crystalline graphite.

3.3. Results

3.3.1 General observations during aging

As expected, inhomogeneity of aging was observed. Intermediate samples of UA-1 (I4-I6) had clearly visible yellow and white areas, {Figure S3a and Figure S4}. In this case, the white and yellow areas were analyzed separately labeled 'via yellow' and 'via white' respectively. In gloss measurements, the inhomogeneity is averaged out due to the large measuring area. The difference in color is a result of the various stages in the degradation process. In white areas, the oil binder had decomposed, and consequently it did not produce a yellow color. In the white areas, degradation is visible by eye. Yellow areas were still visibly in an earlier degradation stage and had not started chalking [43]. In yellow areas, degradation is not visible by eye yet. Therefore 'via yellow' is of more interest for the determination of early warning signs.

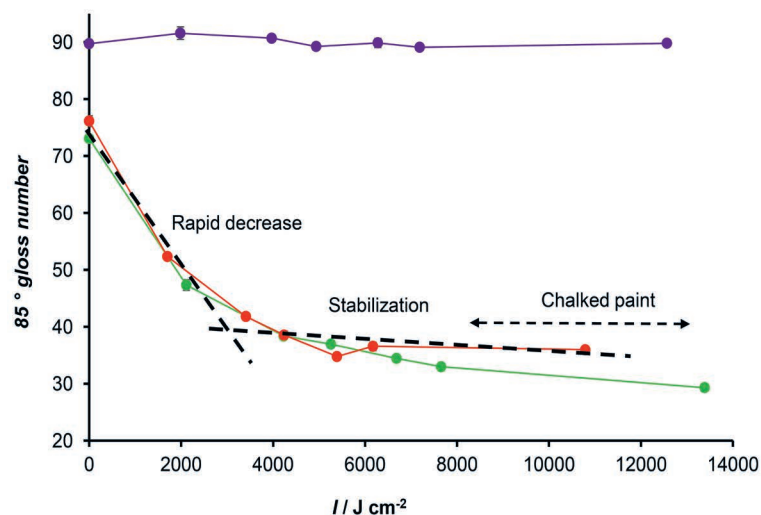
The inhomogeneity of the UA-2 samples was far less pronounced {Figure S3c}. The paint film seemed to degrade more gradually and remained yellow until it had reached the point of severe chalking. Therefore, results of UA-2 are not differentiated in yellow and white. As anticipated, the CR samples showed no signs of degradation {Figure S3b}, and are treated similarly to UA-2.

3.3.2 Gloss

Figure 3.1 shows the gloss results of uncoated anatase and coated rutile aged under UV. A large gloss drop of roughly 50% for the uncoated anatase samples can be observed upon initial exposure to 3000 J/cm² UV light. The gloss number quickly stabilizes to a value of around 40 gloss units, showing very slight decrease in gloss for the following 8000 J/cm². Partial paint chalking is confirmed after 8000 J/cm², however complete chalking of the paint film occurs after 10.000 J/cm², indicating that the stabilization

stage gradually turns into a degraded stage. Both stages have similar gloss. Both UA paints follow the same trend confirming inter-sample reproducibility. The low standard deviation of 0.1 to 1.1 gloss units confirms reproducibility of the analysis. The paint containing the photostable pigment (CR) does not show any change in gloss during UV exposure (Figure 3.1). The same holds for the paints exposed to the lab environment.

Figure 3.1 85° gloss during UV exposure. Error bars are included in the plot, however the error is small and therefore not visible.



3.3.3. AFM

Figure 3.2 shows a selection of the AFM images of sample UA-1. A z-scale development from 100 to 2000 nm can be seen upon UV exposure in the uncoated anatase samples. In the initial stage, the z-scale varies between 25 and 250 nm in relatively continuous patterns. Upon UV light irradiation, the paint films quickly become rougher and the patterns become increasingly discontinuous. After 2000 J/cm² of UV light, the z-scale has risen 5-fold, and after 5000 J/cm² the z-scale reads 1600 nm, nearly reaching the maximum obtained value of 2000 nm at 12.000 J/cm². The same trend is demonstrated in Figure 3.3, where the maximum height difference is plotted (Δz_{\max}). Again, the largest change is detected at the beginning of the aging process until roughly 6500 J/cm². The stabilized stage merges into the chalking stage beyond values of 10.000 J/cm². The via white curve stabilized earlier, confirming the general observation that white areas have reached the chalking stage at the end of the degradation process. The photostable reference (CR), illustrated in Figure 3.3 {and Figure S5}, shows high stability in the height difference during irradiation. The same holds for the sample kept in the lab environment {Figure S6}.

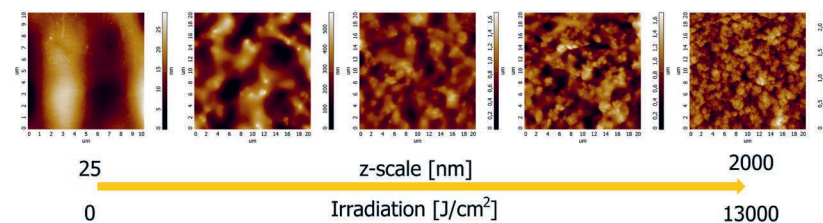


Figure 3.2 2D AFM images of UA-1 during aging.

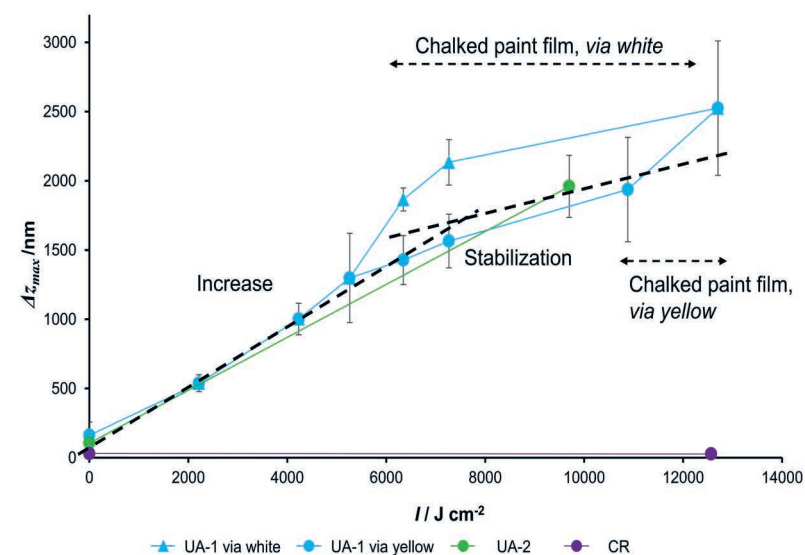


Figure 3.3 Δz_{\max} during aging, averaged over 3 to 5 AFM scanning areas.

3.3.4. XPS

XPS survey spectra of UA-1 are shown in Figure 3.4a {the total survey spectrum is shown in Figure S7a}. The observed signals in the survey spectra are identified as C1s (284.8 eV), Ti2p (485.8 eV) and O1s (532.4 eV). In the initial I₀ sample, only carbon and oxygen signals are present. This remains the case in samples I₂ and I₃: after more than 5200 J/cm² of irradiation, there is no clear signal for titanium. The spectra for I₄ differ from the previous ones: a clear Ti contribution can be distinguished around 458.8 eV. The specific binding energies of the Ti2p_{3/2} (458.8 eV) and Ti2p_{1/2} (464.5 eV) signals confirm the oxidized nature of the titanium species. The Ti peak intensity is further enhanced for samples I₅ to I₇, indicating that increasing amounts of TiO₂ are located on the surface of the paint. The Ti3s (59 eV) and Ti3p (33 eV) peaks now become visible as well. The relative atomic concentration of Ti on the surface was quantitatively assessed and plotted together with the relative atomic concentrations of C and O in Figure 3.4b. The error bars (similar to Figure 3.6b) are due to the sample heterogeneity and the averaging of multiple analysis

spots. Two lines are plotted for the Ti content, differentiating between yellow and white areas. These differences for the oxygen and carbon signals are incorporated in the error of the measurements of the intermediate samples. The results show that Ti is not detected on the surface unless the paint is exposed to over 6000 J/cm² of UV irradiation (I₄). A steep rise in the Ti signal is observed, reaching a value of around 10 at% for the white area. The value for the yellow areas remains lower for the entire range until the sample has chalked completely.

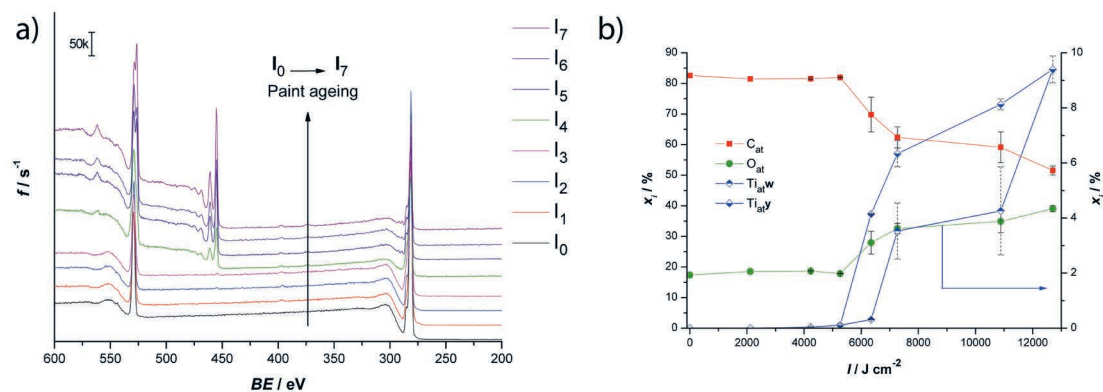


Figure 3.4 a) Survey spectra of UA-1 paint film samples in various stages of degradation. b) Atomic composition of UA-1 paint film during aging, differentiating between white and yellow areas.

The relative atomic content of carbon decreases (figure 3.4b), while the relative amount of titanium is increasing as more binder decomposes to reveal the white pigment. Core-level spectra of titanium (Figure 3.5a) show the evolution of the Ti signal with irradiation in more detail. Where the survey spectra could not reveal the minor amount of Ti on the surface, the core-level spectra display the onset of Ti surfacing in samples I₂ and I₃. These subtle, but significant changes may prove valuable as early warning signs. From sample I₄ onwards, the full Ti signal is well defined and it confirms a huge increase in Ti surface concentration. As a consequence, the oxygen content increases as well, since for every atom of titanium, two atoms of oxygen will reach the surface. This increase is clearly displayed in Figure 3.5b, allowing differentiation between the oxygen originating from the organic matrix and the oxygen from the metal oxide source. The binding energy for the metal oxide is shifted roughly 3 eV to lower binding energy, confirming unambiguously the presence of titanium white on the paint surface. {Core-level spectra of carbon are displayed in Figure S7b}.

To investigate the degradation of the paint in more detail, UA-2 paint films were analyzed with XPS, since the overall yellow paint film seemed to degrade more gradually and homogeneously. Survey

spectra of UA-2 samples are displayed in Figure 3.6a {total survey in Figure S8} with the relative atomic composition in Figure 3.6b. Certainly, from both the spectra and atomic content it can be seen that the onset period is far better defined. The results suggest that only after more than 5500 J/cm² (I₅) Ti is starting to surface on the entire paint film. The value of the Ti atomic content then quickly rises to above 9 at%.

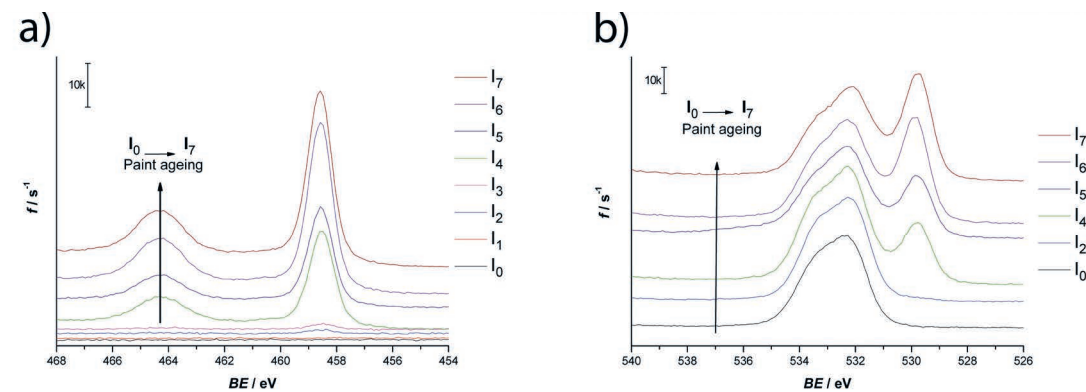


Figure 3.5 Core-level XPS spectra of titanium a) and oxygen b) in UA-1 paint film in various stages of degradation.

XPS analysis of CR shows high stability of the survey spectrum during irradiation {Figure S9}. The characteristic Ti contribution is not detected in any of the spectra. The same is true for samples aged under lab conditions.

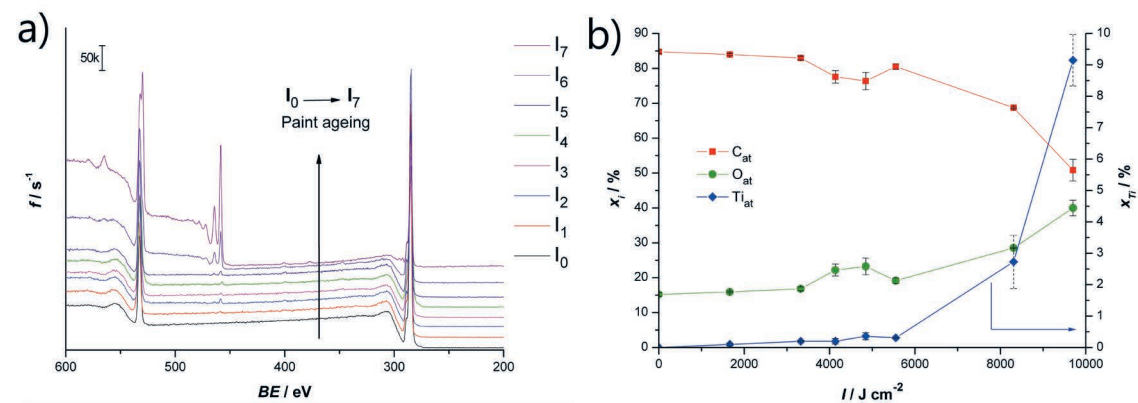


Figure 3.6 a) Survey spectra of UA-2 paint film samples in various stages of degradation. b) Atomic composition of UA-2 paint film during aging.

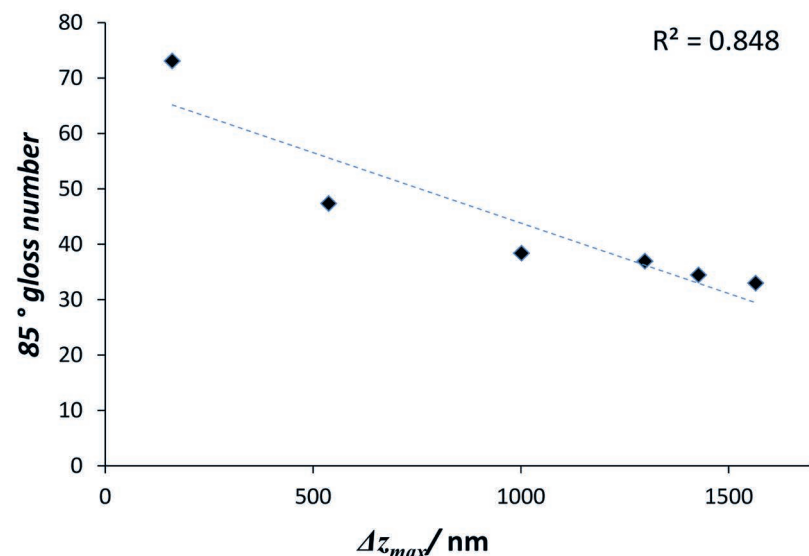
3.4. Discussion

3.4.1 Gloss, AFM and XPS

Both gloss and AFM analysis show a steep change in the initial stages of degradation for paints containing uncoated anatase. The gloss results stabilize around 3000 J/cm², the AFM stabilization occurs somewhat later around 6000 J/cm² due to the higher level

of detail that can be measured by this technique. The similar trend observed in both techniques can be explained by the changes taking place at the surface of the paint film: they are of morphological nature. The close relation between gloss and AFM results is confirmed by correlating gloss versus Δz_{max} obtaining a linear fit with an R2 of 0.84 (Figure 3.7).

Figure 3.7 Correlation plot 85 degree gloss and Δz_{max} (AFM). Values of degradation 'via-yellow' of sample UA-1 are used.



In the XPS results of uncoated anatase, Ti only significantly surfaces after 6000 J/cm² for both UA-1 and UA-2 samples. Below 6000 J/cm², there is hardly any change in the XPS spectra (<0.5 At% Ti), in contrast to AFM and gloss results. The shift in analysis difference is closely related to the elemental nature of the XPS technique and its penetration depth. To demonstrate that the elemental changes are not random, but related to absolute differences in the paint films, the fully-averaged Ti content for UA-1 and UA-2 samples are compared in Figure 3.8. The large errors indicated by the error bars are the result of averaging the heterogeneity of paint samples. Nevertheless, the two very similar samples show a near-equal behavior for the entire range of irradiation. These results confirm that XPS is capable of determining the onset in elemental change when paint degradation is imminent. Core-level spectra of high resolution more clearly show the signals of these early warning signs. The Ti2p spectra provide valuable information regarding the onset of Ti surfacing, and O1s spectra allow for unambiguous identification of TiO₂ species due to the rising shoulder around 529 eV [44].

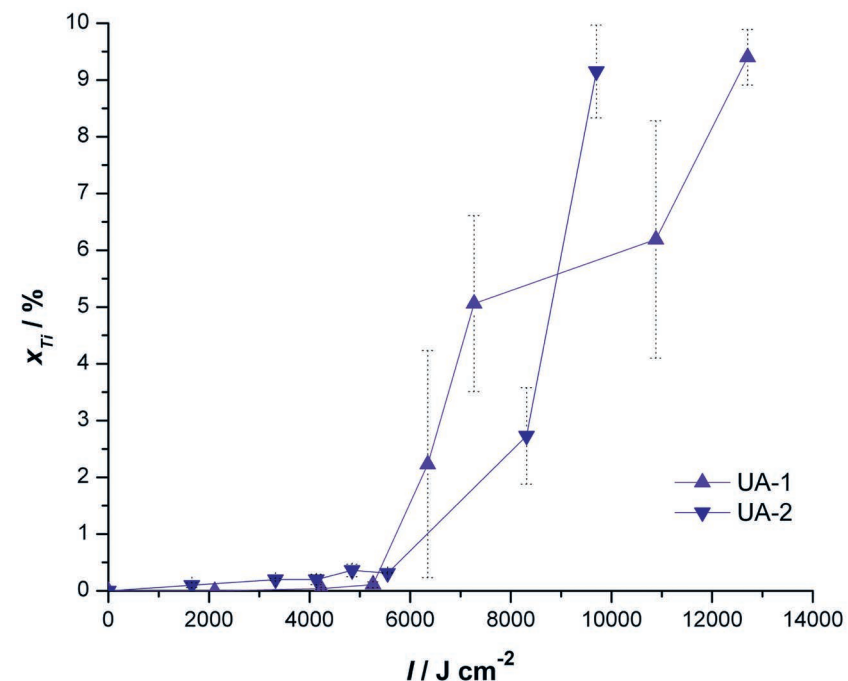


Figure 3.8 Ti content on paint film during aging, as determined by XPS for UA-1 and UA-2 samples. Large error is due to heterogeneity of paint films.

The results indicate that the various stages of degradation possess certain resemblances and contrasts. The first stages of degradation cause a large morphological change (surface roughness), which is followed by a large change in elemental composition (Ti surfacing), finally resulting in a dramatic mechanical change (chalking). Both the morphological change and the elemental stage follow a rather steep trend. The different changes require analysis by different surface analysis techniques.

In general, AFM is less sensitive to disturbances such as dust/paint strokes than gloss measurement. Furthermore, on a real object it is hard to find a large enough area to measure gloss. Finally, the gloss measurement is mostly valuable as comparative data over time, therefore knowing the initial situation is necessary. For this reason, we propose to use AFM imaging as confirmation of the situation as assessed by XPS and as an indication of the stage before TiO₂ surfacing. Nevertheless, the relation to real gloss change will be an important factor in the communication with conservators.

Paints containing the photostable pigment show high stability in all analytical techniques. This is an indication that no other effects apart from photocatalytic degradation cause the change observed in the paints containing photocatalytic pigments. It confirms that an inorganic coating is a very effective way to reduce the photocatalytic activity of titanium white pigments [2, 11-13].

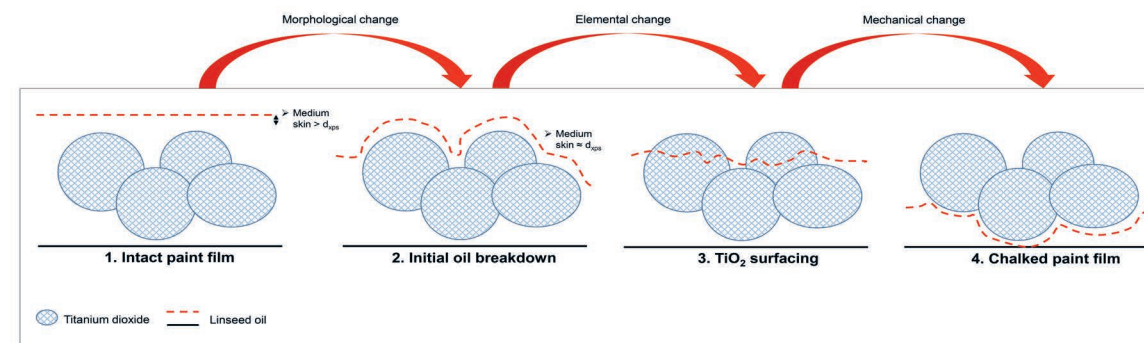
Paints that were not exposed to such high doses of UV light (being kept in the lab environment) also showed high stability during the employed timeframe (970 h of cyclic low intensity light) in all analytical techniques. The results of these lab references confirm the process of UV-initiated photocatalysis, which is caused by the size of the bandgap of titanium dioxide [2]. It has been shown that the photocatalytic degradation rate scales with the square root of the intensity [49]. This suggests that degradation will inevitably take place but that the monitored 970 h with very low exposure compared to high-powered UV light of the lamps correspond to only a very small irradiation dose in the UV chamber.

Other (white) pigments may show degradation processes based on soap formation and pigment migration [50-51], but it is unlikely that this is the case here for several reasons. Boundary conditions for pigment migration include the reaction of the pigment with the binding medium or free fatty acids, the dissolution of the pigment in the binding medium or in free fatty acids, and a driving force causing the movement (such as a concentration gradient). There is no reason to assume UV light could be a driving force for migration. If migration would play a role, both lab-aged and UV-aged samples should show similar effects and this is not the case. Furthermore, it is well known no solvents for titanium dioxide are available [52]. If dissolution would occur, both anatase and rutile samples would be expected to show changes and this is not the case.

3.4.2. Proposed model for photocatalytic degradation of titanium dioxide oil paints

Based on the different results and previous knowledge of photocatalytic degradation, we propose the model illustrated in Figure 3.9 for photocatalytic degradation of oil paint. It is known that photocatalytic degradation proceeds via the absorption of UV light by the titanium white pigments. This leads to the production of highly reactive radicals that can break down the oil binding medium into small volatile components such as CO₂ and H₂O [53,54]. This type of severe binder degradation leads to an effect called chalking, when the pigment is no longer bound by the binding medium [18]. We propose that this process happens in four stages: the intact paint film (stage 1), the initial oil breakdown (stage 2), the TiO₂ surfacing (stage 3) and the chalked paint film (stage 4). Between stage 1 and 2 the largest morphological change occurs at the surface, causing optical changes such as a strong decrease of gloss. This decrease in gloss, even though it is strong, can sometimes be difficult to assess because the initial gloss is not known. After the morphological change stabilizes, between stage 2 and 3, and the medium skin is thinner than the XPS penetration

depth, titanium dioxide starts to be detected by XPS. This is the early warning sign that degradation is taking place. Depending on the location of the measurement this sign can be detected in stage 2 or it can be determined unambiguously in stage 3. Finally, between stage 3 and 4 the real damage occurs: dramatic mechanical change leading to a completely chalked paint film.



3.4.3. Method for detection of early degradation signs for photocatalytic degradation

A first step in the investigation of possible photocatalytic degradation of unvarnished oil paint is confirming the presence of titanium dioxide. Without this knowledge, no micro-destructive method would be considered. There are several ways to confirm the presence of titanium dioxide by none-invasive techniques, the most straightforward being to use a portable XRF instrument (e.g. Bruker Tracer) [55]. In the field of conservation, this technique is often used as a 'point and shoot' method [56]. The presence of the element titanium is mostly related to titanium dioxide. However, care should be taken for instance with respect to the overlap of Ti-K lines with Ba-L lines in XRF analysis. Also the use of filters, adjusting the X-ray source for background reduction and speciation to a specific element need to be taken into account when performing XRF analysis. Furthermore, interpretation of the results is always complex due to the unknown layer structure of a painting, especially because grounds also often consist of white pigments [43] {chapter 1}.

When the presence of titanium dioxide is confirmed, the crystal structure should be determined either non-invasively by portable Raman spectroscopy or micro-invasively by XRD of a micro sample. If the high risk anatase crystal structure is found, a sample for XPS and AFM analysis should be taken. The presence of the rutile crystal structure indicates a lower risk of degradation. However this risk is not zero: it has been shown that several rutile

Figure 3.9 Proposed model of the TiO₂-photocatalyzed degradation mechanism of linseed oil in relation to gloss, AFM and XPS analysis.

pigments have lower but not negligible photocatalytic activity [14]. A sample for XPS and AFM preferably has the largest possible size acceptable to conservators with a minimum XPS spot size of 50 μm . With a larger spot size XPS resolution is increased. Taking a surface sample and transporting it without damaging the surface is a practical challenge that still needs to be faced. Since AFM may disturb the sample surface, XPS analysis should be performed first. It is important to use both AFM and XPS since AFM may detect roughening before XPS detects titanium dioxide. AFM has a less clear initial state than XPS analysis ($x_{\text{Ti}} = 0$), nevertheless, a height difference of more than 250 nm ($\Delta z_{\text{max}} > 250 \text{ nm}$) is a clear indication of initial degradation. All paints containing coated rutile or paints aged in the lab environment had Δz_{max} distances varying between 20 and 250 nm depending on variations during paint application and drying. This is considered to be the unaged reference and therefore an indication of the range of the initial state for AFM. If it is found that photocatalytic degradation is occurring, the object should be removed from UV light to stop the degradation process and prevent severe mechanical damage.

3.5. Conclusions

A combined study of loss of gloss, AFM and XPS analysis was performed on the surface of model paints containing titanium white. The photocatalytic degradation of the oil paint was successfully mapped using these techniques, and reference material confirmed that photocatalysis initiated by titanium white is responsible for paint degradation. It was found that AFM and XPS are suitable techniques to monitor paint aging at the surface and that new and valuable information can be gained about changes occurring during the aging process. Combined XPS and AFM analysis is a strong method to detect early degradation in these types of paint. Both techniques offer a fixed initial state ($x_{\text{Ti}} = 0$, $\Delta z_{\text{max}} < 250 \text{ nm}$, respectively) making them particularly useful for the field of conservation science. For investigation of real works of art and the application of the proposed step-by-step method of determining early warning signs of degradation, the sampling technique needs to be optimized. Surface samples of a minimum spot size of 50 μm and preferably a larger spot size, for enhanced resolutions, are required.

Based on the analysis, a four-stage model of the degradation process was proposed. Initial degradation (stage 2) of the intact paint film (stage 1) causes the biggest morphological change. This can be monitored by AFM analysis. After the initial breakdown, extensive titanium white surfacing occurs as a result of bulk oil

binder degradation (stage 3). At this point, the dramatic mechanical changes leading to chalking (stage 4) have not yet taken place, and the method can therefore be used as an early warning sign for degradation.

The work presented here shows that, provided proper micro sampling can be performed, combined application of AFM and XPS analysis is a promising approach to detect early photocatalytic degradation in titanium white containing oil paints. Furthermore, the combination of methods offers valuable insight and a better understanding of the steps in the degradation process.

Symbols

t_{ms} = thickness medium skin
 d_{xps} = penetration depth of XPS analysis
 x_{Ti} = atomic composition Titanium
 PVC = Pigment volume concentration = $(V_{\text{pigment}}/V_{\text{total}}) \cdot 100$
 Δz_{max} = maximum height difference per AFM image
 d_{min} = minimal diameter of a paint sample usable for AFM and XPS investigation
 d_{pref} = preferred diameter of a paint sample usable for AFM and XPS investigation
 T = lab temperature

Acknowledgements

This work is supported by AkzoNobel and accommodated by the Rijksmuseum. The authors would like to thank Ing. Marcel Bus, ChemE, Delft University of Technology, for his assistance with the AFM analysis. The Automatic Muller is on permanent loan from Old Holland to the Cultural Heritage Institute of the Netherlands.

- Michalski, S. (1997). The lighting decision.
- M. Laver (1997). Chapter 10: Titanium white. In E.W. Fitzhugh (Ed.), *Artists' Pigments: Volume 3: A Handbook of their History and Characteristics* (pp. 295-355). National Gallery of Art. DOI: 10.2307/1506685
- van den Berg, K.J., Miliani, C., Aldrovandi, A., Brunetti, B. G., de Groot, S., Kahrim, K., . . . van Bommel, M. R. (2012). Chapter 7: The Chemistry of Mondrian's paints in Victory Boogie Woogie. In M. R. van Bommel, H. Janssen, R. Spronk & Het Gemeentemuseum (Eds.), *Inside Out Victory Boogie Woogie*. Amsterdam: Amsterdam University Press. ISBN: 9789089643735
- Cooper, H., Spronk, R., Museums, Harvard University Art Museums and Dalles Museum of Art. (2001). *Mondrian: the Transatlantic Paintings*: Yale University Press. ISBN: 9780300089288
- Thorn, A. (2000). Titanium dioxide: a catalyst for deterioration mechanisms in the third millennium. *Stud Conserv*, 45(Supplement-1), 195-199. doi: doi:10.1179/sic.2000.45
- Lauridsen, C. B., Sanyova, J., & Simonsen, K. P. (2014). Analytical study of modern paint layers on metal knight shields: The use and effect of Titanium white. *Spectrochim Acta A*, 124, 638-645. doi: http://dx.doi.org/10.1016/j.saa.2014.01.077
- de Keijzer, M., de Groot, S., Megens, L., & Van Keulen, H. (2008). *Schildertechnisch onderzoek aan Mondriaans Compositie met rood, zwart, geel en grijs uit 1920*. Instituut collectie Nederland.
- Sclafani, A., & Herrmann, J. M. (1996). Comparison of the Photoelectronic and Photocatalytic Activities of Various Anatase and Rutile Forms of Titania in Pure Liquid Organic Phases and in Aqueous Solutions. *J. Phys. Chem.*, 100(32), 13655-13661. doi: 10.1021/jp9533584
- Zhang, J., Zhou, P., Liu, J., & Yu, J. (2014). New understanding of the difference of photocatalytic activity among anatase, rutile and brookite TiO₂. *Phys. Chem. Chem Phys.*, 16(38), 20382-20386. doi: 10.1039/C4CP02201G
- Kim, W., Tachikawa, T., Moon, G.-h., Majima, T., & Choi, W. (2014). Molecular-Level Understanding of the Photocatalytic Activity Difference between Anatase and Rutile Nanoparticles. *Angew. Chem. Int. Ed.*, 53(51), 14036-14041. doi: 10.1002/anie.201406625
- Day, R. E., & Egerton, T. A. (1987). Surface studies of TiO₂ pigment with especial reference to the role of coatings. *Colloids Surf.*, 23(1-2), 137-155. doi: http://dx.doi.org/10.1016/0166-6622(87)80255-X
- de Keijzer, M. (2002). The history of modern synthetic inorganic and organic artists' pigments: James & James (Science Publishers) Ltd.
- Allen, A. (1979). TiO₂ pigment coated with dense silica and porous alumina/silica. Patent US4075031 A.
- van Driel, B.A., et al. (2016), A quick assessment of the photocatalytic activity of TiO₂ pigments — From lab to conservation studio! *Microchem J*, 126, 162-171.
- Blakey, R.R. (1980). The role of Titanium dioxide in the protection of Paint Media. Technical Service Report Tioxide
- Spathis, P., Karagiannidou, E., & Magoula, A.-E. (2003). Influence of Titanium Dioxide Pigments on the Photodegradation of Paraloid Acrylic Resin. *Stud Conserv*, 48(1), 57-64. doi: 10.2307/1506823
- [Personal communication Bert Klein-Ovink from Royal Talens.] (2014).
- Völz Hans, G., Kaempf, G., Fitzky Hans, G., & Klaeren, A. (1981). The Chemical Nature of Chalking in the Presence of Titanium Dioxide Pigments. In F.H. Winslow (Ed.) *Photodegradation and Photostabilization of Coatings*, Acs symposium series (Vol. 151, pp. 163-182). American Chemical Society.
- Linsebigler, A. L., Lu, G., & Yates, J. T. (1995). Photocatalysis on TiO₂ Surfaces: Principles, Mechanisms, and Selected Results. *Chem. Rev.*, 95(3), 735-758. doi: 10.1021/cr00035a013
- Fujishima, A., Rao, T. N., & Tryk, D. A. (2000). Titanium dioxide photocatalysis. *J. Photochem. Photobiol. C*, 1(1), 1-21. doi: 10.1016/S1389-5567(00)00002-2
- Johnston-Feller, R., Feller, R. L., Bailie, C. W., & Curran, M. (1984). The Kinetics of Fading: Opaque Paint Films Pigmented with Alizarin Lake and Titanium Dioxide. *JAIC*, 23(2), 114-129. doi: doi:10.1179/019713684806028269
- Samain, L., Silversmit, G., Sanyova, J., Vekemans, B., Salomon, H., Gilbert, B., . . . Strivay, D. (2011). Fading of modern Prussian blue pigments in linseed oil medium. *J. Anal. At. Spectrom.*, 26(5), 930-941. doi: 10.1039/C0JA00234H
- Zhang, A. (2013). Photocatalytic Effect of TiO₂ pigments on the surface of Paint films. Master thesis Materials Science and Engineering, Delft university of Technology. Retrieved from <http://repository.tudelft.nl/view/ir/uuid%3A940a74cf-2f11-45af-a4d5-d66218632535/>
- Yousif, E., & Haddad, R. (2013). Photodegradation and photostabilization of polymers, especially polystyrene: review. *SpringerPlus*, 2(1), 398.
- Kampf, G., Papenroth, W., Voltz, G., & Weber (1982), G. Time-lapse observation of Chalking under the electron microscope. 16th FATIPEC Congress Proceedings, 3, 167-174
- Pappas, S. P., & Fischer, R. M. (1975). Photo-chemistry of pigments. Studies on the mechanism of chalking. *Pigm. Resin Technol.*, 4(1), 3-10. doi: 10.1108/eb041057
- Colling, J. H., & Dunderdale, J. (1981). The durability of paint films containing titanium dioxide — Contraction, erosion and clear layer theories. *Prog. Org. Coat.*, 9(1), 47-84. doi: http://dx.doi.org/10.1016/0033-0655(81)80015-5
- Shang, J., Chai, M., & Zhu, Y. (2003). Solid-phase photocatalytic degradation of polystyrene plastic with TiO₂ as photocatalyst. *J. Solid State Chem.*, 174(1), 104-110. doi: http://dx.doi.org/10.1016/S0022-4596(03)00183-X
- Zhao, X. u., Li, Z., Chen, Y., Shi, L., & Zhu, Y. (2007). Solid-phase photocatalytic degradation of polyethylene plastic under UV and solar light irradiation. *J. Catal. A*, 268(1-2), 101-106. doi: http://dx.doi.org/10.1016/j.molcata.2006.12.012
- Allen, N. S., Edge, M., Ortega, A., Sandoval, G., Liauw, C. M., Verran, J., . . . McIntyre, R. B. (2004). Degradation and stabilisation of polymers and coatings: nano versus pigmentary titania particles. *Polym. Degrad. and Stab.*, 85(3), 927-946.
- Gaumont, S., Siampiringue, N., Lemaire, J., & Pacaud, B. (1997). Influence of titanium dioxide pigment characteristics on durability of four paints (acrylic isocyanate, polyester melamine, polyester isocyanate, alkyd). *Surf. Coat. Int.*, 80(8), 367-372. doi: 10.1007/BF02692692
- de Sá, M. H., Eaton, P., Ferreira, J. L., Melo, M. J., & Ramos, A. M. (2011). Ageing of vinyl emulsion paints—an atomic force microscopy study. *Surf. Interface Anal.*, 43(8), 1160-1164. doi: 10.1002/sia.3664
- Gesenhues, U. (2000). Influence of titanium dioxide pigments on the photodegradation of poly(vinyl chloride). *Polym. Degrad. Stab.*, 68(2), 185-196. doi: http://dx.doi.org/10.1016/S0141-3910(99)00184-6
- Izzo, F. C., Zendri, E., Biscontin, G., & Balliana, E. (2011). TG-DSC analysis applied to contemporary oil paints. *J. Therm. Anal. Calorim.*, 104(2), 541-546. doi: 10.1007/s10973-011-1468-y
- Lazzari, M., & Chiantore, O. (1999). Drying and oxidative degradation of linseed oil. *Polym. Degrad. Stab.*, 65(2), 303-313. doi: http://dx.doi.org/10.1016/S0141-3910(99)00020-8

36. Spyros, A., & Anglos, D. (2004). Study of Aging in Oil Paintings by 1D and 2D NMR Spectroscopy. *Anal. Chem*, 76(17), 4929-4936. doi: 10.1021/ac049350k
37. van den Berg, J. D. J., van den Berg, K.J., & Boon, J. J. (1999). Chemical changes in curing and ageing oil paints. Paper presented at the ICOM Committee for Conservation.
38. Bonaduce, I., Carlyle, L., Colombini, M. P., Duce, C., Ferrari, C., Ribechini, E., . . . Tine, M. R. (2012). New Insight into the ageing of linseed oil paint binder: A Qualitative and Quantitative analytical study. *Plos ONE*, 7(11). doi: 10.1371/journal.pone.0049333
39. Burnstock, A., de Keijzer, M., Krueger, J., Learner, T., de Tagle, A., Heydenreich, G., & van den Berg, K. J. (2014). *Issues in Contemporary Oil Paint* (pp. 11). Springer International Publishing.
40. Vereniging Bedrijfscollecties Nederland. Retrieved 25-09-2015, 2015, from <http://www.vbcn.nl/>
41. [Personal communications with representatives of several Dutch company art collections] (2015).
42. [Personal experience during contact with conservators] (2014-2015).
43. Namowicz, C., Trentelman, K., & McGlinchey, C. (2009). Erratum: XRF of cultural heritage materials: Round- Robin IV --- Paint on Canvas. *Powder diff.*, 24, 124-129. doi: DOI: 10.1154/1.3132591
44. Boyatzis, S., Ioakimoglou, E., & Argitis, P. (2002). UV exposure and temperature effects on curing mechanisms in thin linseed oil films: Spectroscopic and chromatographic studies. *JAPS*, 84(5), 936-949. doi: 10.1002/app.10117
45. Wikipedia, Sunlight Retrieved 28-08-2015, from <https://en.wikipedia.org/wiki/Sunlight>
46. Amsterdam climate. Retrieved 28-8-2015, from <http://www.amsterdam.climateemps.com/sunlight.php>
47. Mallégol, J., Lemaire, J., & Gardette, J.-L. (2001). Yellowing of Oil-Based Paints. *Stud. Conserv.*, 46(2), 121-131. doi: 10.2307/1506842
48. Lüth, H. (1993), *Surfaces and interfaces of solids*. Springer-Verlag.
49. Egerton, T. A., & King, C. J. (1979). The influence of light intensity on photoactivity in TiO₂ pigmented systems. *J. Oil Col. Chem. Assoc*, 62, 386-391.
50. Osmond, G. (2012), Zinc white: a review of zinc oxide pigment properties and implications for stability in oil-based paintings. *AICCM Bulletin*, 33(1), 20-29.
51. Higgitt, C., M. Spring, and D. Saunders (2003), *Pigment-medium Interactions in Oil Paint Films containing Red Lead or Lead-tin Yellow*. National Gallery Technical Bulletin, 24, 75-95
52. Diebold, M.P., et al. (2004), Rapid assessment of TiO₂ pigment durability via the acid solubility test. *JCT Research*, 1(3), 239-241.
53. Jin, C., et al. (2006). Rapid measurement of polymer photo-degradation by FTIR spectrometry of evolved carbon dioxide. *Polym. Degrad. Stab.* 91(5): 1086-1096. DOI: <http://dx.doi.org/10.1016/j.polymdegradstab.2005.07.011>
54. Christensen, P. A., et al. (1999). Infrared spectroscopic evaluation of the photodegradation of paint Part I The UV degradation of acrylic films pigmented with titanium dioxide. *J. Mater. Sci.* 34(23): 5689-5700. DOI: 10.1023/A:1004737630399
55. Palmer, D. P. Introduction to energy-dispersive x-ray fluorescence (XRF) - an analytical chemistry perspective Presentation. Department of chemistry & biochemistry San Francisco state university Retrieved from <http://www.google.nl/url?sa=t&rct=j&q=&esrc=s&source=web&cd=1&ved=0CDIQFjA-A&url=http%3A%2F%2Fwww.asdlib.org%2FonlineArticles%2Fecourseware%2FPalmer%2FASDL%2520Intro%2520to%2520XRF.pdf&ei=5XHsU5fSMsTZPI72gMAO&usq=AFQjCNGOh7qSMPZIWk-7GbuldddRg620K0Q>
56. SRAL. (2015). Portable X-Ray Fluorescence Spectroscopy Conference and Workshop. Retrieved 24-09-2015, 2015, from <http://www.sral.nl/nl/nieuws/portable-x-ray-fluorescence-spectroscopy-conference-and-workshop/>

Chapter 4

Investigating the photocatalytic degradation of oil paint using ATR-IR and AFM-IR.

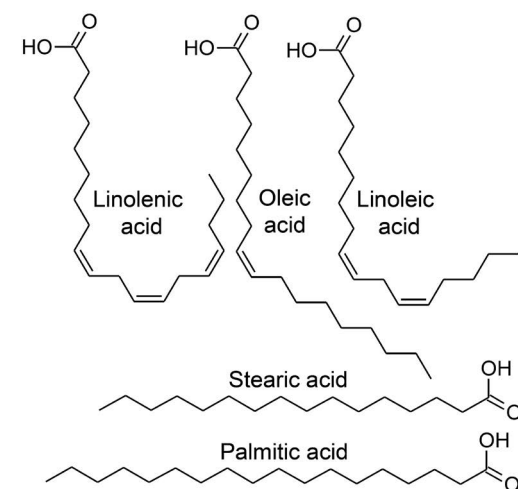
As linseed oil has a longstanding and continuing history of use as a binder in artistic paints, developing an understanding of its degradation mechanism is critical to conservation efforts. At present, little can be done to detect the early stages of oil paint deterioration due to the complex chemical composition of degrading paints. In this work, we use advanced infrared analysis techniques to investigate the UV-induced deterioration of model linseed oil paints in detail. Sub-diffraction limit infrared analysis (AFM-IR) is applied to identify and map accelerated degradation in the presence of two different grades of titanium white pigment particles (rutile or anatase TiO_2). Differentiation between the degradation of these two formulations demonstrates the sensitivity of this approach. The identification of characteristic peaks and transient species residing at the paint surface allows infrared absorbance peaks related to degradation deeper in the film to be extricated from conventional ATR-FTIR spectra, potentially opening up a new approach to degradation monitoring.

Based on the published paper: S. Morsch, B.A. van Driel, K.J. van den Berg and J. Dik (2017), ACS Applied Materials and Interfaces 9(11): 10169-10179.

4.1. Introduction

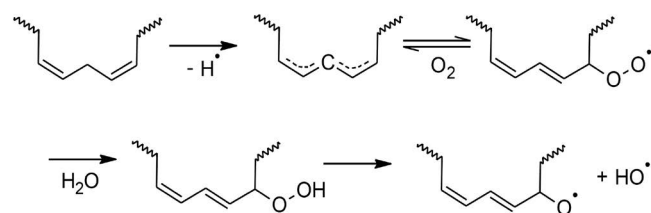
Linseed oils have been used as a medium for oil paintings since medieval times, owing to their capacity to form reasonably stable, continuous films with good optical and mechanical properties. Nonetheless, paints made from these and other drying oils are susceptible to long-term degradation, leading to e.g. undesirable changes in optical appearance [1,2]. For conservation purposes, an in-depth understanding of these degradation mechanisms is necessary to design effective detection and prevention strategies. However, in common with other drying oils, defining the degradation process is notoriously problematic, since linseed oils are complex mixtures of naturally-derived triglyceride molecules based on fatty acids (primarily linolenic, linoleic, oleic, stearic and palmitic acids, with concentrations dependent on the source), Scheme 4.1. Numerous competing radical reactions drive cross-linking and chain scission, and furthermore, these processes can occur simultaneously. Therefore, no clear distinction can be made between drying and aging [3-6].

A general mechanism for linseed oil hardening has nonetheless been established; it is widely accepted that oxidative curing is initiated by hydrogen abstraction from methylene groups adjacent to fatty acid *cis* alkenes (since the unsaturated bonds stabilise generated radicals by conjugation), Schemes 4.1 and 4.2.



Scheme 4.1 Chemical structures of major fatty acid components of triglyceride molecules in linseed oil.

Scheme 4.2 Proposed mechanism of hydroperoxidation of linoleic acid.



Oxygen sorption then results in the formation of highly reactive peroxy radicals, followed by a variety of radical coupling reactions that ultimately lead to cross-linking [7]. At the same time, chain-scission reactions are initiated by further radical formation (via e.g., β -scission reactions). Furthermore, in artists' paint the complexity of this process is compounded by interaction with the inorganic pigments, which can affect both the drying process and the degradation kinetics. For example, pigments behaving as Lewis acids or bases locally induce metal salt or soap formation and may accelerate hydrolysis [8-14], whereas photocatalytic pigments, such as titanium white, can induce additional radical formation [15-16].

Titanium white pigments were introduced in the beginning of the 20th century, and paints containing these pigments have been used in many renowned artworks produced since (e.g., paintings by Picasso, Mondrian, and Pollock). These prevalent pigments occur in numerous forms, including the pure anatase and rutile polymorphs, with or without surface coatings. As a result, photocatalytic activity varies drastically. Generally, pure anatase exhibits the highest photocatalytic activity while rutile is considered more benign, and surface coatings further reduce activity [17-18]. Upon UV absorption, photocatalytic pigments provide reactive electrons at the surface of particles, resulting in the formation of organic radical and reactive oxygen species. For binders that cure by radical polymerization (e.g., linseed oil), the presence of photocatalytic pigments is therefore expected to accelerate cross-linking, and this may result in embrittlement. Concurrent degradation processes are also expected to initiate, and these ultimately manifest as chalking, where pigment powders are exposed at the paint surface after the binder has been broken down into volatile low molecular weight species [16, 19]. Valuable works of art containing titanium dioxide are relatively recent and often stored under controlled conditions, therefore these long-

term degradation effects are rarely observed [20]. Nonetheless, understanding the degradation mechanism is key to the development of prophylactic conservation strategies. It has recently been reported that uncoated anatase pigments dramatically accelerate UV-induced degradation of linseed oil when compared to coated rutile pigments. Surface sensitive techniques (AFM, XPS) [chapter 3] were used to prove that the pigments were rapidly exposed at the paint surface, and that this was followed by visible chalking. However, little information about the binder degradation mechanism is provided by these techniques [16].

One approach to polymeric analysis, infrared spectroscopy, can provide detailed information about the presence and chemical environment of functional groups, and has previously been used to investigate the drying and aging mechanisms of oil paints [7, 11, 21]. However, conventional FTIR analysis is ordinarily confined to bulk measurements, where lateral resolution is restricted by the beam spot size and the penetration depth is dependent on the collection mode. Bulk spectra therefore represent an average of all chemical changes occurring within this sampling space. In contrast, the early stages of pigment-induced degradation are expected to be heterogeneous, involving highly localised chemical changes. To overcome this, FTIR microspectroscopy has previously been used to map aged paint samples. For example, Boon et al have mapped lead soap aggregate in cross-sections of aged paints [22-24], and Mazzeo et al applied the same technique to map metal soap formation in reconstructed paint films [12]. Whilst this methodology allows the chemical differences between layers of paint to be resolved post-degradation, infrared microspectroscopy techniques conventionally suffer diffraction-limited resolution associated with the wavelength of light in the mid-IR spectral range, and are typically restricted to several microns per pixel [25]. In contrast, the recently developed AFM-IR technique circumvents these limitations by using an AFM probe to detect local photothermal expansion in response to infrared excitation, routinely providing local spectra and infrared mapping with lateral resolution <50 nm [26]. AFM-IR has previously been applied to map chemical heterogeneity and water transport within an unpigmented epoxy-phenolic lacquer [27-29]. In this study, we extend this approach to a model linseed oil paint containing titanium dioxide pigments, and apply ATR-FTIR alongside AFM-IR to identify and map the infrared peaks associated with photocatalytic degradation.

4.2. Experimental

4.2.1. Sample Preparation

Model paints with a pigment volume concentration (PVC) of 15% were prepared by mixing commercially available titanium dioxide (either Hombitan LW uncoated anatase by Sachtleben Chemie or Tronox CR-826 coated rutile by Tronox), bleached commercial linseed oil (van Beek, NL, used without further treatment), and 0.1% v/v drying agent (cobalt and zirconium carboxylates, Pieter Keune, NL) {chapter 3}. All reagents were used as received. After milling, paint was applied onto melinex supports using a draw down bar coater, (nominal thickness of 100 μm), and left to dry for 14 days under ambient conditions ($T = 20\text{ }^\circ\text{C}$, cyclic lighting). Samples were aged in an Opsytec Dr. Gröbel BS-02 UV chamber equipped with UVA lamps (i.e., broad irradiation at wavelengths between 300 nm - 400 nm) and removed periodically. The received UV dose was continuously monitored by a UVA sensor inside the chamber, and then the sample location was corrected for in accordance with the manufacturer's specifications, Table 4.1. After removal from the UV-chamber, samples were stored under ambient conditions in the dark prior to analysis.

Table 4.1 UV doses received by uncoated anatase and coated rutile pigmented linseed oil paint samples.

Irradiation Step	UV Dose / J cm^{-2}	
	Anatase	Rutile
Dried&stored	0	0
1	2.1×10^3	1.9×10^3
2	4.2×10^3	3.8×10^3
3	5.4×10^3	4.7×10^3
4*	6.3×10^3	6.3×10^3
5*	7.3×10^3	7.2×10^3

*local chalking is observed by eye for anatase paint samples

4.2.2. ATR-FTIR

Bulk infrared spectra were obtained from the paint surface from 16 co-averaged scans collected in ATR mode using an FTIR spectrometer (Perkin Elmer Spectrum 1000 FT-IR) operating at 1 cm^{-1} resolution across the 450– 4000 cm^{-1} range, with a Graseby

Specac Golden Gate Single Reflection Diamond ATR. The penetration depth of the evanescent wave generated at a diamond internal reflection element is estimated to be $\sim 2\text{ }\mu\text{m}$ in the mid-IR range. Spectra were collected from five different locations on each sample.

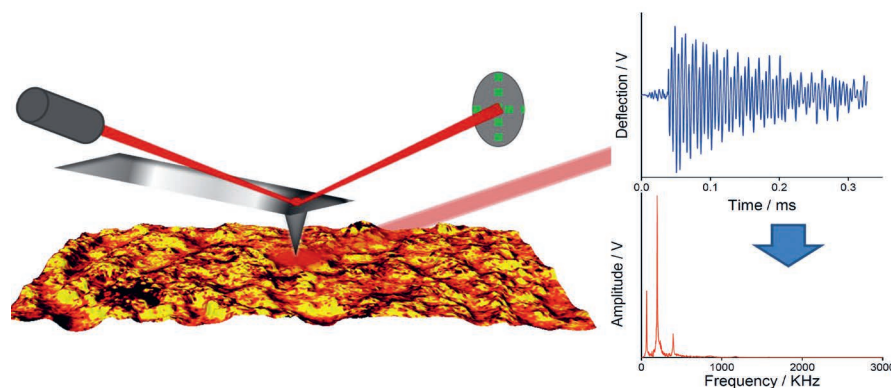
4.2.3. AFM-IR

Nanoscale infrared analysis (AFM-IR) was performed on a NanoIR2 system (Anasys Instruments) operating with top-down illumination. During AFM-IR analysis, specimens were illuminated by a pulsed, tuneable infrared source (optical parametric oscillator, 10 ns pulses at a repetition rate of 1 kHz, approximate beam spot size 30 μm). Sub-diffraction limit resolution is achieved by monitoring the deflection of an AFM probe, which responds to rapid infrared-induced thermal expansions of the sample in contact with the probe tip, Scheme 4.3. The recorded AFM-IR signal is the amplitude of induced AFM probe oscillation, obtained after fast Fourier transform. This has previously been shown to correlate to infrared absorbance measured using conventional macroscopic FTIR [30]. Furthermore, since the IR pulse (10 ns duration), thermal expansion, and damping down of the induced oscillation occur on a shorter timescale than the feedback electronics of the AFM, simultaneous contact-mode topographical measurement and infrared mapping can be performed at a given wavelength [31-34]. For the present study, AFM-IR images were collected in contact mode at a scan rate of 0.1 Hz using a gold-coated silicon nitride probe (0.07 – 0.4 N/m spring constant, 13 ± 4 kHz resonant frequency, Anasys Instruments). The amplitude of infrared induced oscillations were recorded at a given wavelength using 16 co-averages for 600 points per 150 scan lines. Spectra were obtained at a single position using 1024 co-averages for each data point. Infrared ratio images were generated using AnalysisStudio software (v3.8, Anasys Instruments) by division of the overlapping regions of IR amplitude maps, cross-correlated using the corresponding height images. For cross-section analysis, samples were cut using a scalpel and then immediately mounted at 90° in a sample holder (model SD-103, Bruker) and imaged.

4.2.4. SEM

Scanning electron microscopy images were obtained using an FEI Quanta 650 field emission gun scanning electron microscope operating in low vacuum mode using an accelerating voltage of 10kV.

Scheme 4.3 The AFM-IR experiment with top-down illumination. The IR source is pulsed, inducing rapid thermal expansion of the sample, which is detected by deflection of the AFM probe cantilever. The recorded AFM-IR signal is the amplitude following a fast Fourier transform of the deflection signal.



4.3. Results

4.3.1. ATR-FTIR

Before AFM-IR analysis, specimens were investigated using bulk ATR-FTIR, Figure 4.1. All samples displayed absorbance peaks characteristic of linseed oil, summarised in Table 4.2. Prior to UV aging, the absence of a characteristic *cis* =C-H stretch absorbance at 3010 cm^{-1} indicated that oxidation of the *cis* unsaturated groups had taken place during drying and storage under ambient conditions. This is in keeping with findings detailed by Lazzari et al, who found that for unpigmented linseed oil, absorption associated with the fatty acid *cis* alkene groups disappeared within 8 hours drying time [7]. The dried linseed oil spectra show typically broad carbonyl and hydroxyl absorbance peaks; this is because the alkoxy and peroxy radicals formed by oxidation of the *cis* unsaturated groups (Scheme 4.2) react further during drying, generating a variety of functional groups including ethers, esters, acids, alcohols, aldehyde and ketone species. Natural maturing/degradation then occurs as a result of further oxygen sorption and (less favourable) organic radical formation in a continuation of the same process. The resulting complex mixture of functional groups yields characteristically broad and overlapping infrared absorbance peaks, where peak assignment is necessarily approximate. Nonetheless, the spectral changes which correspond to aging can readily be identified.

In the case of anatase pigmented samples, UV irradiation resulted in spectra comparable to those reported for degradation of unpigmented linseed oil (aged thermally, under natural conditions, or by UV acceleration [4, 7, 11, 35]). The intensity of the broad carbonyl peak (C=O stretch, centred on 1736 cm^{-1}) and hydroxyl region (OH stretch, 2500-3300 cm^{-1}) increased relative to that of

characteristic CH absorbance peaks; at 2930 cm^{-1} and 2880 cm^{-1} (CH stretches), 1464 cm^{-1} (CH₂ scissoring) and 1378 cm^{-1} (CH₂ wag) [11], Figure 4.1. This has been attributed to the release of volatile short chain alkanes during degradation, in keeping with the literature [7, 21, 36]. Furthermore, both the carbonyl and hydroxyl peaks broaden significantly, indicating that an increased range of oxygen functional groups are formed.

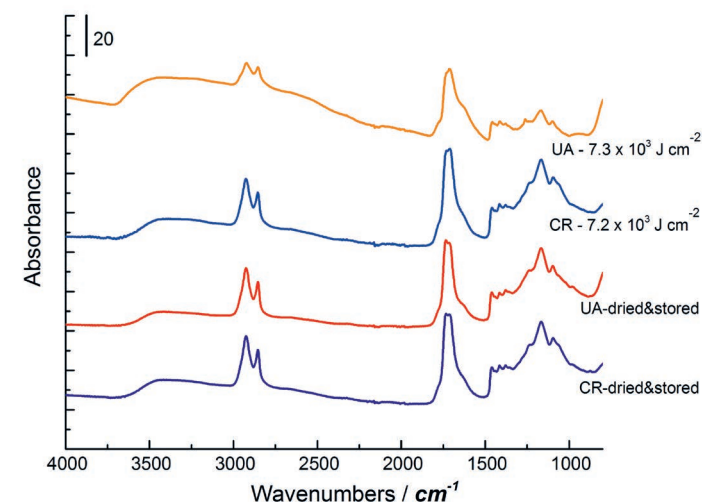


Figure 4.1 ATR mode FTIR spectra of linseed oil samples pigmented with uncoated anatase (UA) or coated rutile (CR) after drying under ambient conditions for 14 days and storage, and after drying under ambient conditions for 14 days followed by exposure to $7.3 \times 10^3 \text{ J cm}^{-2}$ UV or $7.2 \times 10^3 \text{ J cm}^{-2}$ UV respectively.

In order to assess the effect of UV irradiation in more detail, carbonyl regions were averaged, baseline corrected and normalised relative to the ester peak (at 1736 cm^{-1}), Figure 4.2. It can be seen that upon initial UV exposure, similar features are observed for both the samples containing uncoated anatase pigments (highly photocatalytic) and coated rutile pigments (considered inactive). For example, the broad absorbance around 1640 cm^{-1} , related to the presence of carboxylic acids and aldehydes, and at 1717 cm^{-1} , attributed to free acids and ketones, increase in intensity relative to the ester peak. Acid and aldehyde end groups are formed following cleavage around ester groups, β -scission and oxidation reactions, Scheme 4.4a [7, 35]. Whilst the broad absorbance centred at 1640 cm^{-1} is potentially also associated with conjugated C=C functionalities (Table 4.2), we ascribe this absorbance to low molecular weight carboxylic acids and aldehydes, since these are known products of linseed oil oxidation [8-9, 36-38]. Following the initial UV exposure, the chemical state of the rutile containing samples appears to stabilise, whereas this absorbance peak continues to grow for anatase-containing samples, confirming that the presence of photocatalytic anatase leads to increased oxidative degradation. In addition, it is notable that the intensity of

absorbance at higher wavenumbers (around 1780 cm^{-1}) increased upon UV irradiation. This has previously been proposed as a diagnostic peak for linseed oil aging [11]. Whilst this peak is consistent with the presence of peracids, peresters, lactones or anhydrides, absorbance in this region is widely attributed to lactone formation during the oxidative degradation of ester-containing polymers (e.g., during thermal and UV accelerated aging of acrylic resins [39–44], via various proposed mechanisms, e.g., Scheme 4.4b). However, in contrast to the progressively increasing absorbance noted at lower wavenumbers, the intensity of this peak stabilised after the initial UV dose for both rutile and anatase samples.

Scheme 4.4 Suggested mechanistic pathways for the degradation of linseed oil paint: (a) the formation of aldehydes and carboxylic acids by β -scission and oxidation; and (b) the formation of γ -lactones.

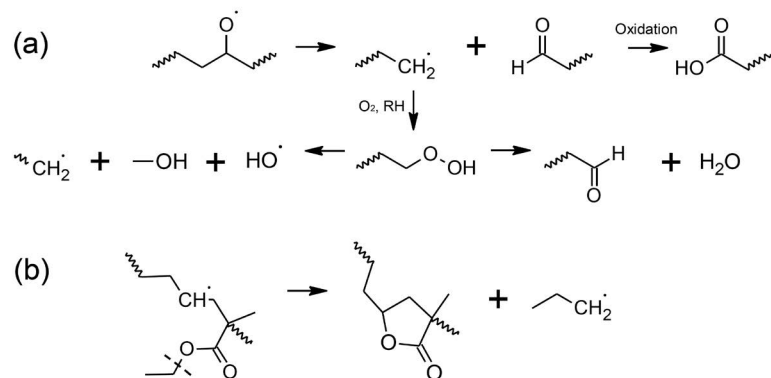
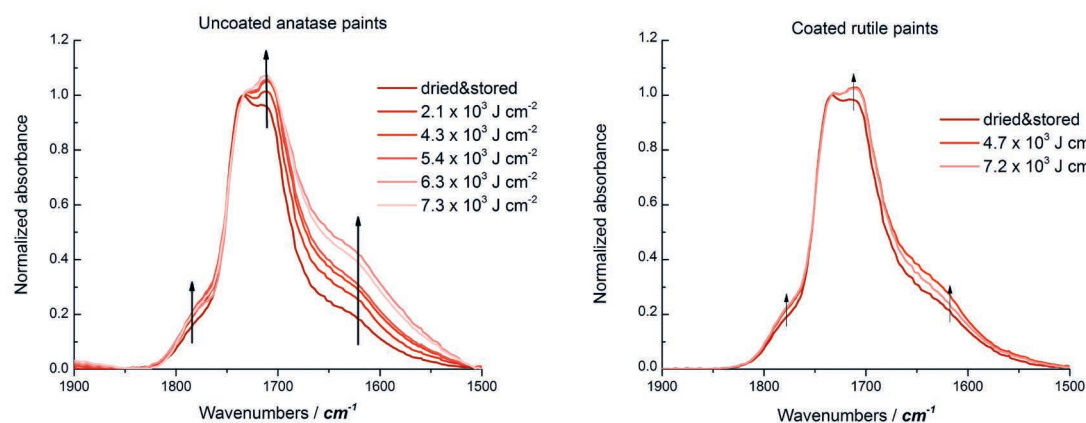


Figure 4.2 Baseline corrected infrared spectra for linseed oil samples pigmented with 15 % PVC anatase or rutile forms of TiO_2 before and after increasing levels of exposure to UV. Spectra are normalised to the 1736 cm^{-1} ester peak, and each spectrum is the mean of 5 individual spectra gathered from various positions.



Wavenumber	Peak assignment
$\sim 3393\text{ cm}^{-1}$	hydroperoxide, alcohol and acid O-H stretch
2919 cm^{-1}	alkyl CH-CH_2 C-H stretch
2852 cm^{-1}	alkyl CH-CH_2 and CH_3 C-H stretch
$\sim 2650\text{ cm}^{-1}$	O-H from $(\text{-OH})\text{COOH}$, broadening of O-H due to carboxylic acids.
1780 cm^{-1}	peracids, peresters, γ -lactones and anhydrides C=O stretch.
1736 cm^{-1}	ester C=O stretch.
1717 cm^{-1}	saturated ketones and free fatty acid C=O stretch.
$\sim 1640\text{ cm}^{-1}$	Conjugated C=C stretch, acid or aldehyde C=O stretch
$\sim 1613\text{ cm}^{-1}$	Aldehyde, carboxylic acids and α/β unsaturated ketone C=O stretch.
1463 cm^{-1}	Alkyl $\text{CH-CH}_2, \text{CH}_3$ C-H bending
1410 cm^{-1}	Acid C-O bend, $-\text{CH}_2\text{-CO-O}$ C-H bending
1377 cm^{-1}	Alkyl CH_2 C-H bending
1054 cm^{-1}	Alcohol C-O stretch.

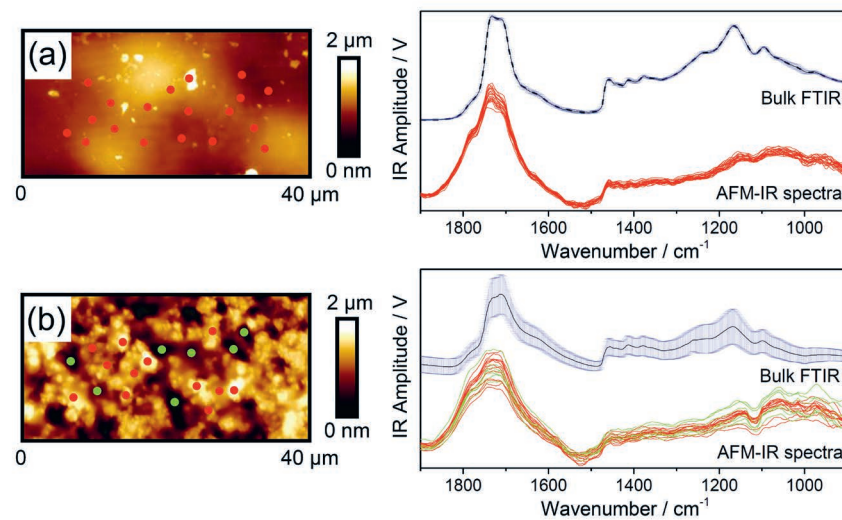
Table 4.2 Linseed oil infrared peak assignments.

4.3.2. AFM-IR

Localised infrared spectra were initially obtained for the anatase paints before and after extensive UV irradiation (step 5). This was achieved by positioning the AFM-IR probe in contact with the sample surface, and stepping pulsed radiation incident on the probe tip through the mid-IR fingerprint range (900 cm^{-1} – 1900 cm^{-1}). The amplitude of probe oscillations induced by thermal expansion of the sample (IR amplitude) was then monitored and plotted to produce spectra, where peak positions were found to be in broad agreement with those produced using bulk ATR-FTIR, Figure 4.3.

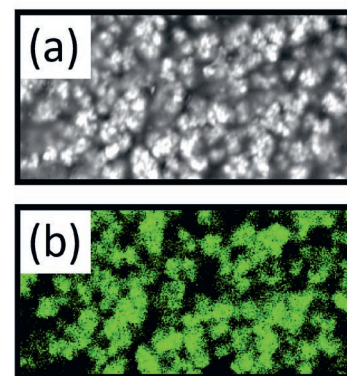
Contact mode AFM height profiles revealed increasing surface roughness of the paints pigmented with anatase during UV irradiation, in keeping with previously reported tapping mode AFM images and gloss measurements [16], Figure 4.3. XPS analysis has previously shown that titanium is detected in association with this roughening, indicating that pigments become gradually exposed [16]. To verify this, SEM analysis and EDX mapping was performed, which demonstrated that raised areas indeed correspond to locally increased concentrations of titanium at the surface, Figure 4.4.

Figure 4.3 AFM-IR contact mode height images (left) alongside ATR-FTIR spectra and AFM-IR spectra (right) corresponding to tip locations indicated by markers for samples of linseed oil pigmented with uncoated anatase after (a) drying under ambient conditions for 14 days and dark storage; (b) drying under ambient conditions for 14 days followed by exposure to $7.3 \times 10^5 \text{ J cm}^{-2}$ UV (irradiation step 5). ATR-IR spectra correspond to the mean of 5 individual measurements, and error bars correspond to 1 standard deviation.



For the rougher, aged specimens, local AFM-IR spectral intensity was found to vary more across the sample, Figure 4.3. A similar effect was observed for bulk infrared spectra, where variations were found to increase dramatically after UV doses of $5.4 \times 10^3 \text{ J cm}^{-2}$ or more. The intensity of local AFM-IR spectra did not however specifically correlate to ‘high’ or ‘low’ areas of the surface profile, Figure 4.3b. The relative signal intensity is instead proposed to change as a result of both chemical heterogeneity and local variations in the effective sampling volume caused by the presence of underlying pigment particles. This is because during AFM-IR, the sampling volume is not limited by the penetration of infrared radiation, but by the volume of material under the AFM-IR probe tip that contributes to the thermal expansion ‘felt’ by the probe.

Figure 4.4 $20 \mu\text{m} \times 10 \mu\text{m}$ scanning electron microscopy images of the model anatase pigmented linseed oil paint surface following drying under ambient conditions for 14 days and exposure to $7.3 \times 10^5 \text{ J cm}^{-2}$ UV (irradiation step 5): (a) secondary electron image and (b) energy dispersive x-ray spectroscopy map for titanium.



Both the thermal expansion co-efficient and infrared absorbance of titanium dioxide are negligible in comparison to the organic binder, so the effective sampling depth is considered to be limited to material between the probe and nearest underlying pigment. In light of this, direct comparison of the UV irradiated anatase samples was achieved using averaged AFM-IR spectra normalized to the ester C=O absorbance at 1736 cm^{-1} , similar to the bulk FTIR analysis presented in Figure 4.2. Inspection of the carbonyl region after UV exposure revealed a relative increase in absorbance associated with degradation products, namely carboxylic acids and aldehydes at 1640 cm^{-1} , free acids and ketones at 1710 cm^{-1} and lactones at 1780 cm^{-1} , Figure 4.5 [45]. Note that whilst these spectral changes appear minor, this analysis was repeated in three different regions for each sample, and the relative changes in absorbance were found to be consistent within each data set. It was, however, noted that the absorption at 1780 cm^{-1} appears far more pronounced in the AFM-IR spectra than in ATR-FTIR, whereas the increases in absorbance at lower wavenumbers (1710 and 1640 cm^{-1}) are less prominent. This can be potentially be explained by the difference in detection techniques (i.e., a difference in the thermal expansion coefficients for various chemical species) or a concentration gradient at the paint surface, since AFM-IR is expected to be more surface sensitive. In reality, both effects appear to contribute; the presence of a concentration gradient through samples was verified by AFM-IR analysis on the reverse of paint specimens, removed from the melinex support using a scalpel, Figure 4.6.

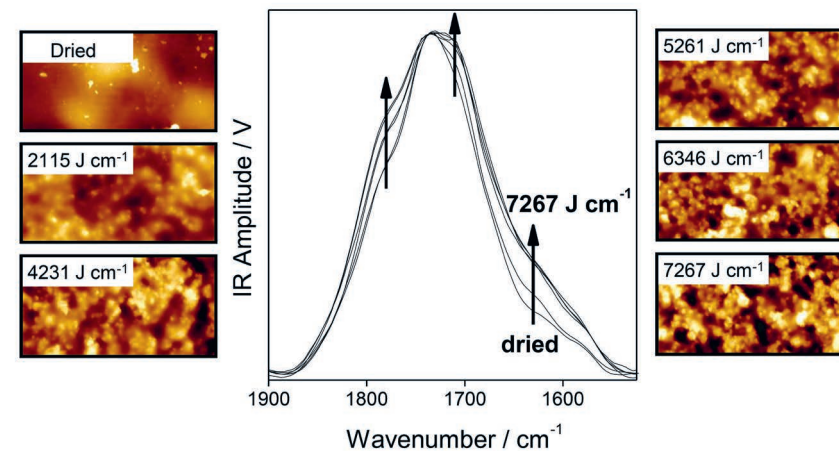


Figure 4.5 $40 \mu\text{m} \times 20 \mu\text{m}$ contact mode AFM images of linseed oil samples pigmented with uncoated anatase after drying under ambient conditions for 14 days, and after exposure to increasing UV doses (irradiation steps 1 to 5), alongside the carbonyl region of AFM-IR spectra produced by averaging 20 AFM-IR spectra gathered from random positions within each of these regions. For comparison, spectra are normalised to the 1736 cm^{-1} ester band. Z scale for AFM images is $2 \mu\text{m}$.

Due to the imprecise detachment method, direct comparison between the spectra gathered from reverse side of different samples is not possible (the apparent roughness of the reverse of aged rutile pigmented samples is a sampling artefact). Nonetheless, carbonyl peaks detected at the back of detached paint films were consistently

found to be more defined than those gathered from the front, i.e., the shoulder peaks associated with degradation were comparatively attenuated, Figure 4.6. Interestingly, this was also found to be the case for anatase pigmented samples examined before UV aging, and control samples prepared using the less active coated rutile form of titanium white. This can be explained by consideration of the linseed oil curing and aging mechanisms: whilst the precise penetration depth of UV, moisture and oxygen are not known, the outer surface of the paints is more exposed. Indeed, Zumbühl et al. recently demonstrated gradients of oxidation in oil paint cross sections using ATR-FTIR spectroscopy [37], finding high concentrations of polar chemical groups toward paint surfaces, and this is in line with the reported preferential formation of azeleic acids at the surface [9]. In the present case, natural aging and photocatalytic aging can be seen to induce similar spectral changes but at a significantly different rate, which is in keeping with the titanium white acting as a radical initiator (a direct comparison between spectra gathered from the surface of UV aged anatase and rutile spectra is given in Figure 4.7). In the case of rutile control samples however, the UV-induced process is sufficiently retarded that spectra obtained from the front of samples change little as a consequence of UV irradiation, and no increases in roughness are observed.

Figure 4.6 AFM-IR contact mode height images (z scale is 2 μm) and the carbonyl region of spectra produced by averaging 20 AFM-IR spectra taken from random positions within the imaged region. Spectra were gathered from the front (red dashed line) and reverse (black solid line) side of linseed oil samples pigmented with the uncoated anatase and coated rutile forms of titanium dioxide before and after extensive UV aging (irradiation step 5).

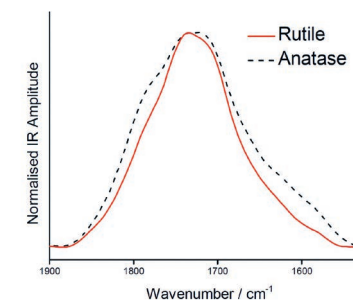
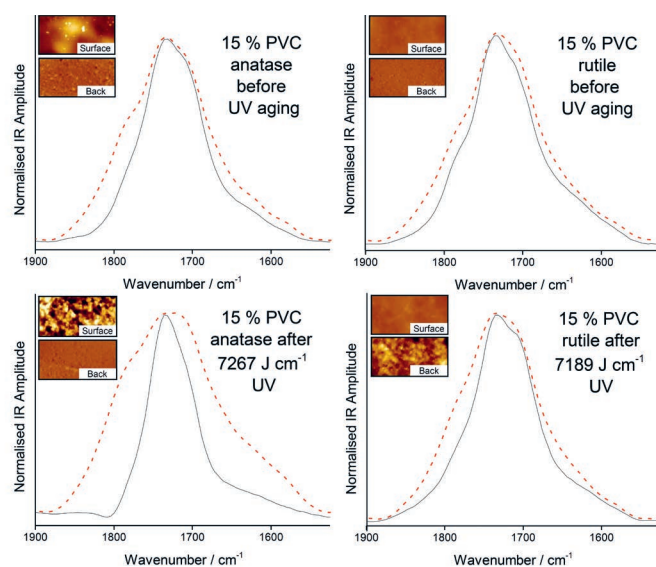
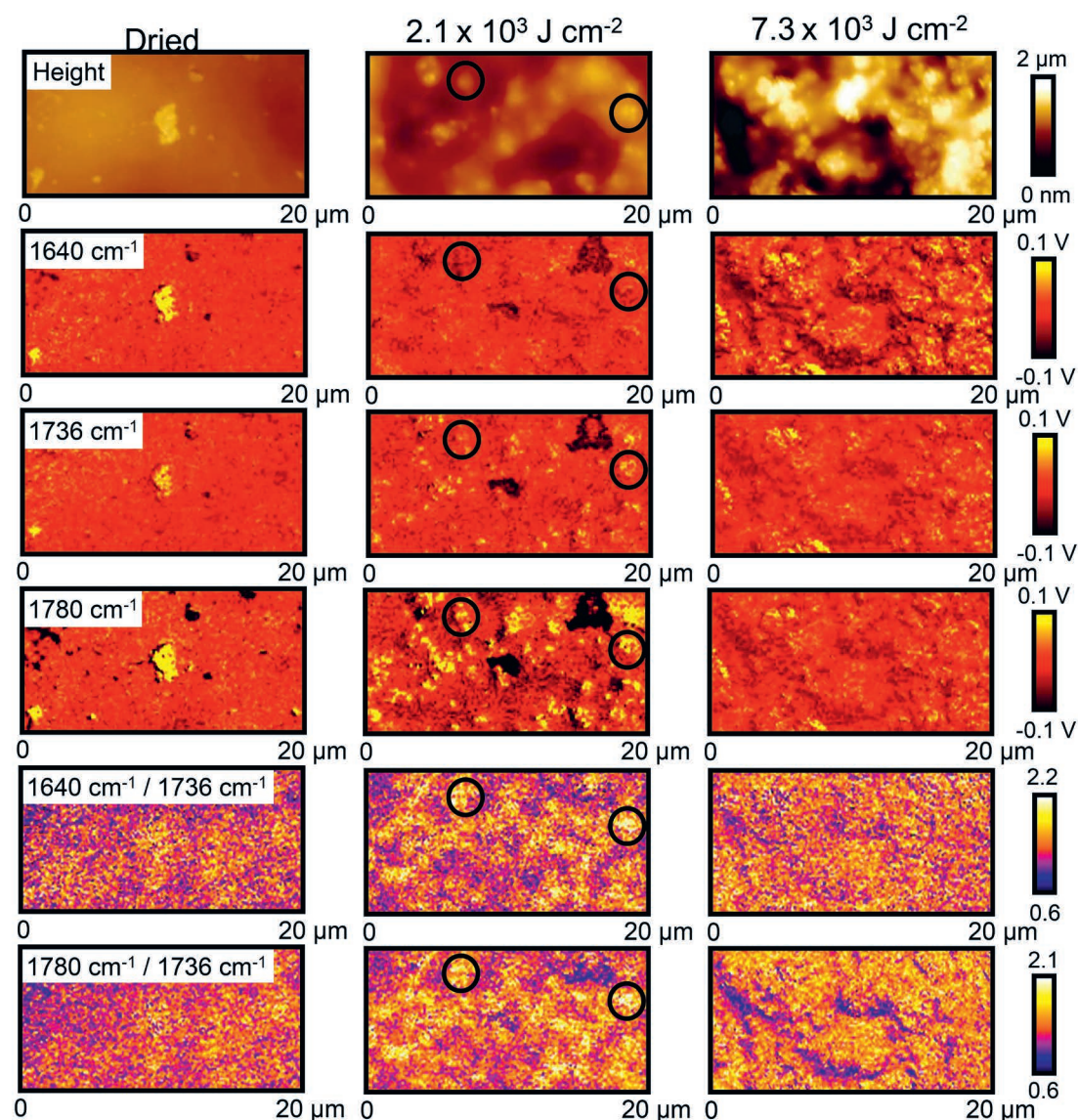


Figure 4.7 Comparison of the carbonyl region of spectra produced by averaging 20 AFM-IR spectra taken from the surface of linseed oil samples pigmented with the uncoated anatase (black dashed line) and coated rutile (red line) forms of titanium dioxide after drying under ambient conditions for 14 days and exposure to $7.3 \times 10^3 \text{ J cm}^{-2}$ and $7.2 \times 10^3 \text{ J cm}^{-2}$ doses of UV respectively (irradiation step 5).

The generation of degradation products at the surface of the anatase-pigmented paints was further investigated by AFM-IR mapping, Figure 4.8. Infrared amplitude maps were gathered at 1640 cm^{-1} (corresponding to carboxylic acid and aldehyde groups produced during aging), 1736 cm^{-1} (corresponding to ester groups) and 1780 cm^{-1} (corresponding to lactone groups produced during aging), and these varied in line with height images. This confirms that the local amplitude signal corresponds to the effective sampling volume between the probe tip and underlying pigment particles [46]. In order to overcome this and isolate chemical differences, ratio images were generated by division of the infrared amplitude data gathered at different wavenumbers, Figure 4.8. In the case of dried and stored samples which had not been exposed to UV aging, ratio images generated from $1640 \text{ cm}^{-1} / 1736 \text{ cm}^{-1}$ (showing the location of carboxylic acid and aldehyde degradation products in relation to esters) and $1780 \text{ cm}^{-1} / 1736 \text{ cm}^{-1}$ (corresponding to the location of lactones in relation to esters) were relatively homogeneous, confirming that differences in the amplitude signal due to sampling volume effectively cancel out. In contrast, immediately after exposure to UV ($2.1 \times 10^3 \text{ J cm}^{-2}$ dose), ratio images revealed a heterogeneous distribution of degradation products around raised areas (e.g., circled regions, central column of Figure 4.8) which are attributed to anatase pigment clusters. Further UV exposure yielded more homogeneous ratio images, (obtained under identical imaging conditions), indicating increased coverage of the surface with degradation products.



4.4. Discussion

Numerous investigators have previously reported FTIR analysis of linseed oil paint degradation, describing the appearance of characteristic absorbance peaks which may be of use in a diagnostic device [7, 11, 21]. In the present case, infrared spectra revealed that the breakdown of linseed oil containing anatase pigments generally involves increased absorbance at wavenumbers consistent with lactone, carboxylic acid and aldehyde species, alongside the

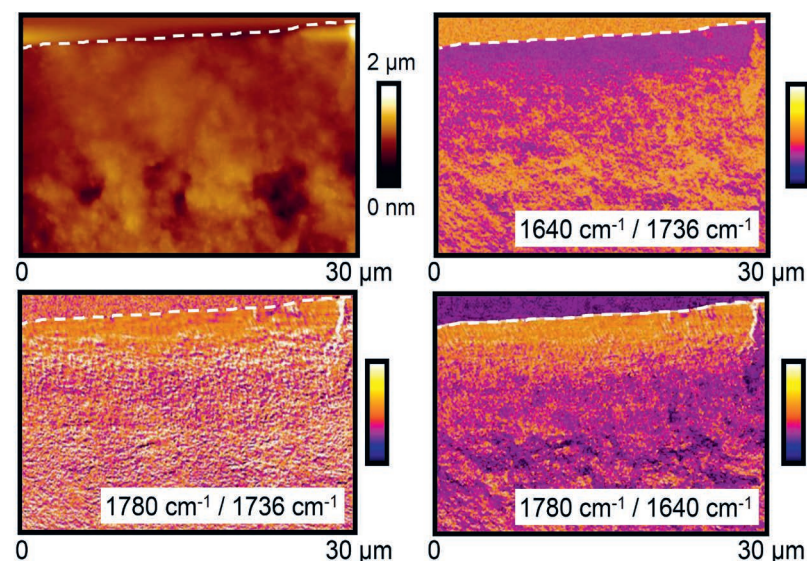
release of short chain volatiles. However, the concentration of lactones stabilised rapidly, and its role in degradation is unclear. In the case of carboxylic acids, it has been documented that hydrolytic attack may lead to the preferential formation of short chain dicarboxylic acids near the surface of oil paint samples [8-9,37-38]. The origin of detected carboxylic acid species within a given sample (i.e., hydrolysis or photocatalytic radical attack), cannot be gauged directly using infrared techniques, precluding the use of this absorbance as a direct measure of catalytic activity. Nonetheless, comparison of AFM-IR and ATR-IR analysis of rutile and anatase pigmented paint performed here gives some insights into the degradation mechanism, pointing towards a predominately photocatalytic radical-induced mechanism for the formation of carboxylic acids and aldehydes in the presence of anatase pigments.

Oxidation and hydrolysis during drying is supported by the fact that the surface of both anatase and rutile pigmented samples were found to differ substantially from the bulk prior to UV aging. The formation of carboxylic acids and aldehydes concentrated towards the surface is expected, since the outer surface of the paint sample is directly exposed to ambient oxygen, humidity and light. Whilst ATR-FTIR spectra indicate that this process continues on initial illumination with UV, in the case of rutile pigmented samples the chemical state then stabilised. This may be because the relatively inactive rutile pigments provide a protective effect by absorbing UV without producing further radicals, preventing degradation deeper in the film (i.e., UV-initiated oxidation is limited to the exposed surface, and the reactions producing lactone, aldehyde and acid species are therefore slowed in comparison to the anatase samples). In contrast, chemical change continued for anatase paints, and this is characteristic of a photocatalytic process, where UV illumination of the semi-conductor pigment provides reactive electrons at the surface of particles to initiate further degradation. In the case of lactones, ATR-FTIR analysis indicated that their formation occurs immediately upon UV illumination, but then rapidly stabilised, even as degradation visibly continued. This indicates that lactones are a transient species formed during linseed oil degradation. Indeed, AFM-IR analysis confirmed that lactones are concentrated towards the sample surface, where the greatest degree of oxidation is expected to occur. In contrast, the measured absorbance of other degradation products (acids, aldehydes and ketones) was found to stabilise when measured using AFM-IR, whilst continuing to increase in the less surface sensitive bulk FTIR spectra. Given that AFM-IR mapping also showed a relatively homogeneous concentration of degradation products is ultimately established across the paint surface, we propose that within the sampling depth of AFM-IR, a dynamic

Figure 4.8 20 μm x 10 μm AFM-IR height images and corresponding infrared maps of linseed oil paint pigmented with anatase after drying under ambient conditions for 14 days, after exposure to 2.1 x 10³ J cm⁻² UV (irradiation step 1), and after exposure 7.3 x 10³ J cm⁻² UV (irradiation step 5). To identify local variations in signal, IR amplitude images gathered at 1640 cm⁻¹, 1736 cm⁻¹ and 1780 cm⁻¹ are flattened by centring each scan line around zero. Ratio images generated from raw data are also presented for 1640 cm⁻¹ / 1736 cm⁻¹ (showing the location of carboxylic acid functional groups) and 1780 cm⁻¹ / 1736 cm⁻¹ (corresponding to the location of lactone functional groups).

surface layer is formed where the generation of degradation products is matched by their further breakdown and release as volatile species. It is suggested that lactones are predominately produced within this region, leading to increasing absorbance in the AFM-IR spectra until full surface coverage is achieved. Upon further UV exposure, acids, aldehydes and ketones are generated deeper inside the paint and their increasing absorbance can be detected using ATR-FTIR (but not AFM-IR). Support for this proposed mechanism was found by cross-sectional AFM-IR analysis of an anatase pigmented sample cut after UV aging (irradiation step 5). Lactone absorbance was found to be concentrated towards the paint film surface, whereas absorbance associated with acids and aldehydes was found to be more intense deeper inside the coating, Figure 4.9. Note, however, that this cross-section was prepared using a scalpel under ambient conditions and this places limitations on any further interpretation of the data (due to an imprecise cutting angle, potential smearing of degradation products etc.).

Figure 4.9 30 μm x 20 μm AFM-IR height and ratio images corresponding to an uncoated anatase pigmented linseed oil paint cross-section exposed to a $7.3 \times 10^3 \text{ J cm}^{-2}$ dose of UV (irradiation step 5), held at 90° immediately after cutting through with a scalpel (no embedding). White dashed lines correspond to the outer surface of the paint, ratio images correlate to the location of carboxylic acids and aldehydes relative to esters ($1640 \text{ cm}^{-1} / 1736 \text{ cm}^{-1}$); lactones relative to esters ($1780 \text{ cm}^{-1} / 1736 \text{ cm}^{-1}$) and lactones relative to carboxylic acids and aldehydes ($1780 \text{ cm}^{-1} / 1640 \text{ cm}^{-1}$).



A previously suggested disadvantage of infrared spectroscopy in conservation science is that significant changes in the detected peak positions and intensities coincide with visible paint degradation [16]. In the present case, visible degradation was only evident in the case of anatase samples exposed to UV doses of $6.3 \times 10^3 \text{ J cm}^{-2}$ or more, whereas normalised FTIR spectra showed significant changes for the degrading paint well in advance of this exposure, Figure 4.3. From the discussion above it is however

evident that infrared absorbance at a given wavelength cannot be used to directly ascertain the level of degradation. Instead, a better approach would be to monitor the carboxylic acid/aldehyde absorbance relative to that of esters. Despite the overlapping, broad nature of these peaks, the relative changes described were consistently detected for degraded paint specimens using both infrared spectroscopy techniques. Nonetheless, this alone cannot provide a direct measure of the level of degradation, since both species are formed during drying and aging, and furthermore, initial concentrations will depend on the source of linseed oil. Monitoring the changes in this ratio over time will, however, give an indication of the degradation kinetics. This opens up the tantalising possibility that the emerging field of handheld infrared technologies could provide a convenient non-destructive diagnostic device in the field of cultural heritage [47]. This would require a systematic and long term approach for preventive condition monitoring within art collections, taking spectra at fixed locations on a painting at specific time intervals (3, 5, 10 years) and is of potential interest not only for photocatalytic degradation in the presence of titanium white, but also to monitor natural aging and other degradation phenomena such as soap formation below the surface. Finally, it is noteworthy that the results presented in this chapter represent the first application of sub-diffraction limit infrared mapping to pigmented coatings, demonstrating the potential of the recently developed AFM-IR technique in this field. This approach could be used to generate further insights in cultural heritage research, where envisioned examples include the spatially resolved characterization of local drying and aging effects, the study of metal soap formation, detailed pigment-binder interactions [12, 23], and cleaning studies on reconstructed paint samples (e.g., mapping the residues of the cleaning agent on the paint surface) [10, 48].

4.5. Conclusions

Sub-diffraction limit AFM-IR imaging has provided direct evidence for locally induced photocatalytic degradation in the vicinity of anatase titanium white pigments at the surface of linseed oil paints. A spectral signature associated with the products of radical oxygenation reactions has been identified, and this can also be detected using bulk FTIR methods prior to visible degradation. Moreover, the combination of these varyingly surface sensitive techniques has been used to differentiate between the relative concentrations of degradation products through the depth of paint films.

Acknowledgments

The authors are grateful to AkzoNobel for financial support, materials, and S. Gibbon and B. Rossenaar specifically for their expertise. Suzan de Groot is acknowledged for training on the ATR-FTIR. The authors also thank J. Hermans and K. Keune for fruitful discussions and help with interpretation. Finally P.Kooyman is acknowledged for her involvement in Van Driel's Ph.D. research.

References for chapter 4

1. Rasti, F.; Scott, G. The Effects of Some Common Pigments on the Photo-Oxidation of Linseed Oil-Based Paint Media. *Stud. Conserv.* 1980, 25, 145–156.
2. Privett, O. S.; Blank, M. L.; Lundberg, W. O. An Accelerated Test of the Yellowing Tendency of Drying Oils. *J. Am. Oil Chem. Soc.* 1961, 38, 27–30.
3. Mills, J. S. The Gas Chromatographic Examination of Paint Media. Part I. Fatty Acid Composition and Identification of Dried Oil Films. *Stud. Conserv.* 1966, 11, 92–107.
4. Mallégo, J.; Gardette, J. L.; Lemaire, J. Long-Term Behaviour of Oil-Based Varnishes and Paints I. Spectroscopic Analysis of Curing Drying Oils. *J. Am. Oil Chem. Soc.* 1999, 76, 967–976.
5. Mallégo, J.; Gardette, J. L.; Lemaire, J. Long-Term Behaviour of Oil-Based Varnishes and Paints II. Fate of Hydroperoxides in Drying Oils. *J. Am. Oil Chem. Soc.* 2000, 77, 249–255.
6. Mallégo, J.; Gardette, J. L.; Lemaire, J. Long-Term Behaviour of Oil-Based Varnishes and Paints III. Photo- and Thermooxidation of Cured Linseed Oil. *J. Am. Oil Chem. Soc.* 2000, 77, 257–263.
7. Lazzari, M.; Chiantore, O. Drying and Oxidative Degradation of Linseed Oil. *Polym. Degrad. Stab.* 1999, 65, 303–313.
8. Van den Berg, J. D. J.; Van den Berg, K. J.; Boon, J. J. Determination of the Degree of Hydrolysis of Oil Paint Samples Using a Two-Step Derivatisation Method and on-Column GC/MS. *Prog. Org. Coat.* 2001, 41, 143–155.
9. Van Dam, E. P.; Van den Berg, K. J.; Proaño Gaibor, A. N.; Van Bommel, M. Analysis of Triglyceride Degradation Products in Drying Oils and Oil Paints Using LC–ESI-MS. *Int. J. Mass Spectrom.* 2016, 1–10.
10. Osmond, G.; Boon, J. J.; Puskar, L.; Drennan, J. Metal Stearate Distributions in Modern Artists' Oil Paints: Surface and Cross-Sectional Investigation of Reference Paint Films Using Conventional and Synchrotron Infrared Microspectroscopy. *Appl. Spectrosc.* 2012, 66, 1136–1144.
11. Ioakimoglou, E.; Boyatzis, S.; Argitis, P.; Fostiridou, A.; Papapanagiotou, K.; Yannovits, N. Thin-Film Study on the Oxidation of Linseed Oil in the Presence of Selected Copper Pigments. *Chem. Mater.* 1999, 11, 2013–2022.
12. Mazzeo, R.; Prati, S.; Quaranta, M.; Joseph, E.; Kendix, E.; Galeotti, M. Attenuated Total Reflection Micro FTIR Characterisation of Pigment-Binder Interaction in Reconstructed Paint Films. *Anal. Bioanal. Chem.* 2008, 392, 65–76.
13. Hermans, J.; Keune, K.; Van Loon, A.; Corkery, R. W.; Iedema, P. Ionomer-like Structure in Mature Oil Paint Binding Media. *RSC Adv.* 2016, 6, 93363–93369.
14. MacDonald, M. G.; Palmer, M. R.; Suchomel, M. R.; Berrie, B. H. Reaction of Pb(II) and Zn(II) with Ethyl Linoleate To Form Structured Hybrid Inorganic–Organic Complexes: A Model for Degradation in Historic Paint Films. *ACS Omega* 2016, 1, 344–350.
15. Rogge, C. E.; Arslanoglu, J. Distinguishing Manufacturing Practices for Titanium White Pigments: New Raman Markers for Dating Commercial Oil-Based Paints. *Stud. Conserv.* 2016, 61, 324–326.
16. Van Driel, B. A.; Wezendonk, T. A.; Van den Berg, K. J.; Kooyman, P. J.; Gascon, J.; Dik, J. Determination of Early Warning Signs for Photocatalytic Degradation of Titanium White Oil Paints by Means of Surface Analysis. *Spectrochim. Acta, Part A* 2016, 172, 100–108.
17. Luttrell, T.; Halpegamage, S.; Tao, J.; Kramer, A.; Sutter, E.; Batzill, M. Why Is Anatase a Better Photocatalyst than Rutile? Model Studies on Epitaxial TiO₂ Films. *Sci. Rep.* 2014, 4, 4043.

18. Van Driel, B. A.; Kooyman, P. J.; Van den Berg, K. J.; Schmidt-Ott, A.; Dik, J. A Quick Assessment of the Photocatalytic Activity of TiO₂ Pigments - From Lab to Conservation Studio! *Microchem. J.* 2016, 126, 162–171.
19. Pappas, S. P.; Fischer, R. M. Photochemistry of Pigments. Studies on the Mechanism of Chalking. *Pigm. Resin Technol.* 1975, 4, 3–10.
20. Lauridsen, C. B.; Sanyova, J.; Simonsen, K. P. Analytical Study of Modern Paint Layers on Metal Knight Shields: The Use and Effect of Titanium White. *Spectrochim. Acta, Part A* 2014, 124, 638–645.
21. Dlugogorski, B. Z.; Kennedy, E. M.; Mackie, J. C. Low Temperature Oxidation of Linseed Oil: A Review. *Fire Sci. Rev.* 2012, 1, 3.
22. Boon, J. J.; Keune, K.; Van der Weerd, J.; Geldof, M.; Van Asperen de Boer, J. R. J. Imaging Microspectroscopic, Secondary Ion Mass Spectrometric and Electron Microscopic Studies on Discoloured and Partially Discoloured Smalt in Cross- Sections of 16th Century Paintings. *Chimica* 2001, 55, 952–960.
23. Keune, K.; Boon, J. J. Analytical Imaging Studies of Cross-Sections of Paintings Affected by Lead Soap Aggregate Formation. *Stud. Conserv.* 2007, 52, 161–176.
24. Van Loon, A.; Boon, J. J. Characterization of the Deterioration of Bone Black in the 17th Century Oranjezaal Paintings Using Electron-Microscopic and Micro-Spectroscopic Imaging Techniques. *Spectrochim. Acta, Part B* 2004, 59, 1601–1609.
25. Bhargava, R. Infrared Spectroscopic Imaging: The next Generation. *Appl. Spectrosc.* 2012, 66, 1091–1120.
26. Dazzi, A.; Prater, C. B. AFM-IR: Technology and Applications in Nanoscale Infrared Spectroscopy and Chemical Imaging. *Chem. Rev.* 2016, DOI: acs.chemrev.6b00448.
27. Morsch, S.; Lyon, S.; Smith, S. D.; Gibbon, S. R. Mapping Water Uptake in an Epoxy-Phenolic Coating. *Prog. Org. Coat.* 2015, 86, 173–180.
28. Morsch, S.; Lyon, S.; Greensmith, P.; Smith, S. D.; Gibbon, S. R. Mapping Water Uptake in Organic Coatings Using AFM-IR. *Faraday Discuss.* 2015, 180, 527–542.
29. Morsch, S.; Liu, Y.; Lyon, S. B.; Gibbon, S. R. Insights into Epoxy Network Nanostructural Heterogeneity Using AFM-IR. *ACS Appl. Mater. Interfaces* 2016, 8, 959–966.
30. Lahiri, B.; Holland, G.; Centrone, A. Chemical Imaging Beyond the Diffraction Limit: Experimental Validation of the PTIR Technique. *Small* 2013, 9, 439–445.
31. Dazzi, A.; Glotin, F.; Carminati, R. Theory of Infrared Nanospectroscopy by Photothermal Induced Resonance. *J. Appl. Phys.* 2010, 107, 124519.
32. Kjoller, K.; Felts, J. R.; Cook, D.; Prater, C. B.; King, W. P. High-Sensitivity Nanometer-Scale Infrared Spectroscopy Using a Contact Mode Microcantilever with an Internal Resonator Paddle. *Nanotechnology* 2010, 21, 185705.
33. Deniset-Besseau, A.; Prater, C. B.; Virolle, M.-J.; Dazzi, A. Monitoring TriAcylGlycerols Accumulation by Atomic Force Microscopy Based Infrared Spectroscopy in Streptomyces Species for Biodiesel Applications. *J. Phys. Chem. Lett.* 2014, 5, 654–658.
34. Mayet, C.; Dazzi, A.; Prazeres, R.; Ortega, J.-M.; Jaillard, D. In Situ Identification and Imaging of Bacterial Polymer Nanogranules by Infrared Nanospectroscopy. *Analyst* 2010, 135, 2540–2545.
35. De Viguierie, L.; Payard, P. A.; Portero, E.; Walter, Ph.; Cotte, M. The Drying of Linseed Oil Investigated by Fourier Transform Infrared Spectroscopy: Historical Recipes and Influence of Lead Compounds. *Prog. Org. Coat.* 2016, 93, 46–60.
36. Fjällström, P.; Andersson, B.; Nilsson, C.; Andersson, K. Drying of Linseed Oil Paints: A Laboratory Study of Aldehyde Emissions. *Ind. Crops Prod.* 2002, 16, 173–184.
37. Zumbühl, S.; Scherrer, N. C.; Eggenberger, U. Derivatization Technique to Increase the Spectral Selectivity of Two-Dimensional Fourier Transform Infrared Focal Plane Array Imaging: Analysis of Binder Composition in Aged Oil and Tempera Paint. *Appl. Spectrosc.* 2014, 68, 458–465.
38. Bonaduce, I.; Carlyle, L.; Colombini, M. P.; Duce, C.; Ferrari, C.; Ribechini, E.; Selleri, P.; Tiné, M. R. New Insights into the Ageing of Linseed Oil Paint Binder: A Qualitative and Quantitative Analytical Study. *PLoS One* 2012, 7, e49333.
39. Gesenhues, U. Influence of Titanium Dioxide Pigments on the Photodegradation of Poly(vinyl Chloride). *Polym. Degrad. Stab.* 2000, 68, 185–196.
40. Spathis, P.; Karagiannidou, E.; Magoula, A. Influence of Titanium Dioxide Pigments on the Photodegradation of Paraloid Acrylic Resin. *Stud. Conserv.* 2003, 48, 57–64.
41. Allen, N. S.; Parker, M. J.; Regan, C. J.; McIntyre, R. B.; Dunk, W. A. E. The Durability of Water-Borne Acrylic Coatings. *Polym. Degrad. Stab.* 1995, 47, 117–127.
42. Melo, M. J.; Bracci, S.; Camaiti, M.; Chiantore, O.; Piacenti, F. Photodegradation of Acrylic Resins Used in the Conservation of Stone. *Polym. Degrad. Stab.* 1999, 66, 23–30.
43. Liang, R. H.; Tsay, F.-D.; Gupta, A. Photodegradation of Poly (n-Butyl Acrylate). *Photochemical Processes in Polymeric Systems. Macromolecules* 1982, 15, 974–980.
44. Grassie, N.; Speakman, J. G.; Davis, T. I. Thermal Degradation of Poly(alkyl Acrylates). II. Primary Esters: Ethyl, n-Propyl, n-Butyl, and 2-Ethylhexyl. *J. Polym. Sci., Part A-1: Polym. Chem.* 1971, 9, 931–948.
45. Lin-Vien, D.; Colthup, N. B.; Fateley, W. G.; Grasselli, J. G. *The Handbook of Infrared and Raman Characteristic Frequencies of Organic Molecules*; Academic Press Ltd: London, 1991.
46. Hill, G. A.; Rice, J. H.; Meech, S. R.; Craig, D. Q. M.; Kuo, P.; Vodopyanov, K.; Reading, M. Submicrometer Infrared Surface Imaging Using a Scanning-Probe Microscope and an Optical Parametric Oscillator Laser. *Opt. Lett.* 2009, 34, 431–433.
47. Hoffmann, U.; Pfeifer, F.; Hsuing, C.; Siesler, H. W. Spectra Transfer Between a Fourier Transform Near-Infrared Laboratory and a Miniaturized Handheld Near-Infrared Spectrometer. *Appl. Spectrosc.* 2016, 70, 852–860.
48. Ormsby, B.; Learner, T.; Schilling, M.; Druzik, J.; Khanjian, H.; Carson, D.; Foster, G.; Sloan, M. The Effects of Surface Cleaning on Acrylic Emulsion Paintings: A Preliminary Investigation. *Tate Papers* 2006, 6, 1–14.

Chapter 5

Investigating the effect of artists' paint formulation on degradation rates of TiO₂ based oil paints.

This study reports on the effect of artists' paint formulation on degradation rates of TiO₂-based oil paints. Titanium white oil paint exists in a multitude of different recipes, and the effect of the formulation on the photocatalytic binder degradation rate is unknown. These formulations contain, among others, one or both titanium dioxide polymorphs, zinc oxide, the extenders barium sulfate or calcium carbonate and various additives. Most research performed on the photocatalytic degradation process focusses on pure titanium white-binder mixtures and thus does not take into account the complete paint system. Since photocatalytic oil degradation is a process initiated by the absorption of UV light, any ingredient or combination of ingredients influencing the light scattering and absorption properties of the paint films may affect the degradation rate.

In this study three sets of experiments are conducted, two of which were designed using the Design of Experiments (DoE) approach, to screen for the most important formulation factors influencing degradation rate. These three sets of experiments investigate 1) the influence of the TiO₂ type, 2) the impact of different mixtures of two types of TiO₂, ZnO and the additive aluminum stearate and 3) the influence of extenders in combination with photocatalytic TiO₂, on the photocatalytic degradation of the oil binder.

The impact of the formulation on the degradation rate became apparent, indicating the shortcoming of oversimplified studies. The protective effect of photostable TiO₂ pigments, even in a mixture with photocatalytic TiO₂ pigments, as well as the negative effect of extenders was demonstrated. Furthermore, the ambiguous role of ZnO (photocatalytic or not) and aluminum stearate is highlighted. Neither can be ignored in a study of degradation behavior of modern oil paints and require further investigation.

Based on the published paper: B.A. van Driel, K.J. van den Berg, M. Smout, N. Dekker, P.J. Kooyman and J.Dik (2018), *Heritage Science* 6:21.

Note A list of terminology is included at the end of the chapter.

5.1. Introduction

The degradation of titanium white artists' oil paints has been under investigation in recent years [1, 2]. This degradation is of interest because, while it is expected to occur, it is not yet commonly observed. Until now, only one clear example of indoor titanium-white initiated photocatalytic degradation was described in the literature [3]. One possible hypothesis for this lack of reported degradation problems is the possible inhibiting effects of other components in the paint on the degradation rate, investigated in this chapter.

Titanium white pigments were introduced to the market around 1920. Especially the early pigments exhibited undesirably high photocatalytic activity [4, 5]. The photocatalytic activity of titanium white pigments can lead to several degradation phenomena, such as the breakdown of the binding medium leading to chalking, or the degradation of colored pigments [1, 6, 7]. Photocatalytic degradation occurs when UV excitation of an electron leads to radical formation at the pigment surface. These radicals can attack their surroundings and thus cause degradation [4, 8]. In the case of oil paint, the binder is broken down into volatile components until the pigment is left unbound at the paint surface (chalking). UV absorption is the first step in photocatalytic degradation [9,10]. The penetration of light into a paint film is dependent on absorption and scattering of light by the binding medium and particles within it [11], which in turn are dependent on their intrinsic properties (e.g. refractive index and photocatalytic properties), composition and particle size, as well as on the quality of dispersion [9]. The combination of short penetration depths of short wavelengths and the presence of UV absorbing pigments will confine the degradation to the top surface of the paint [12, 13] {chapter 3 and 4}.

The decrease of gloss was shown to be an accurate measure of photocatalytic oil degradation for home-made paint samples in previous research by the authors [1] {chapter 3}. Therefore, the changing gloss during UV aging, forms the basis of this investigation. Gloss is a measure of smoothness, thus, an agglomerate present at the surface, the so-called 'tip of the iceberg effect,' results in an increased roughness, observed as a decrease in gloss [14, 15]. Another aspect relating to the gloss of paint is the pigment-volume-concentration, PVC. The gloss decreases with increasing PVC, most notably when it surpasses the critical-pigment-volume-concentration, cPVC [16]. PVC has another effect on degradation, in the sense that a higher TiO₂ content results in higher UV absorption. Depending on the photocatalytic activity of the TiO₂, this leads to higher radical formation or UV scavenging capabilities [14].

In this study, we aim to achieve a realistic dispersion and UV absorption for the different home-made paints using an identical preparation method. Thus, it is taken into account that differences in degradation rates are partly due to differences in dispersion quality or UV absorption. However, it is assumed that this relates back to the mixture composition or pigment type and is thus characteristic for a specific recipe {section 5.4}.

Titanium white exists in many different qualities, with different photocatalytic activities, which differ among others in the crystal structure, surface treatment, and production process. When titanium white was first used as a pigment, the anatase crystal structure was used. More recently, the rutile structure is being used, as it is known to have much lower photocatalytic activity than anatase [4]. Both organic and inorganic surface treatments have been applied to adjust pigment properties such as wettability (which affects dispersion) or photocatalytic activity [4, 17-20]. In case of photocatalytic TiO₂ (nano)powders, powder characteristics such as particle size, surface area, or doping differently influence the photocatalytic activity of the different polymorphs [21, 22]. However, for pigments, the crystal structure and the inorganic coating are the most important characteristics influencing photocatalytic activity [5] {chapter 6}. Uncoated anatase pigments have the highest photocatalytic activity, while inorganically coated rutile pigments are relatively photostable and even photoprotective [1, 4, 5, 23-25]. This classification is also used in this paper, since the same pigments are used that were described in our previous studies, in which photocatalytic activity and photostability were confirmed [1, 2] {chapter 3, 4 and 6}.

Titanium white oil paints exist in a wide range of formulations. They can contain a combination of: titanium white (one or more types), zinc white, extenders such as CaCO₃ or BaSO₄, additives (e.g. metal stearates or drying agents) and the binder (in this study linseed oil) [26]. Most earlier investigations have focused on pure titanium white - binder mixtures to elucidate degradation phenomenology [1, 2, 23, 25, 27]. However, for the investigation of degradation rates, this constitutes an oversimplified formulation. In order to predict degradation rates (and thus risk) in real paintings, understanding the effect of the formulation on the degradation rate is important. To that end, three screening phase sets of experiments are conducted, two of which are based on the Design of Experiments (DoE) methodology, to determine the significant formulation factors and factor interactions which affect the photocatalytic oil degradation rate. DoE is a well-known methodology often used in industry to establish factor-response relationships in a robust and sample efficient way [28-31] {chapter 5B}.

5.2. Experimental

5.2.1. Aging chamber

The paints were aged in an Opsytec Dr. Gröbel BS-02 UV chamber (46 by 32 cm) with dose control. Dose control was performed using the 'UV-MAT' controller connected to a UV sensor from the same company. The chamber is equipped with UVA lamps. The light distribution of the chamber was determined by measuring UV intensity at each sample spot. Thus at every irradiation interval, each sample had its own irradiation value, based on the sample location in the chamber. Samples were aged during two months reaching a total irradiation of approximately 10.000 J/cm². The amount of paint samples that can be aged at the same time is restricted to 30 samples for practical reasons: the gloss meter requires a specific area for analysis (2.5 by 7.5 cm) and the size of the aging chamber is about 30 times that area (46 by 32 cm). Thus, the designed experiment sets (referred to as experiments) were purposely limited to this number of samples (referred to as runs). Blocking was considered a too time-consuming option considering the time per aging cycle. Optimal use, based on theory, of the Design of Experiments methodology, can sometimes be compromised by practical restrictions. In this study which describes the experimental phase of screening, the driver to use DoE was to conduct an informative and time-efficient investigation to identify the factors and factor interaction that significantly affect the degradation behavior.

5.2.2. Paint preparation

The paint compositions of each run within experiments I, II and III respectively are reported in Table 5.2, Table 5.3 and Table 5.5. All powders, Table 5.1, were used as received and added by weight. The binder is a bleached linseed oil (Van Beek, Amsterdam) and was added to the powder mixture using a micropipette. A Co/Zr drying agent (0.1% v/v in oil, donated by Pieter Keune), was used to accelerate oil polymerization. The paint mixture was pre-mixed with a palette knife and subsequently mixed on a glass-plated paint mill (automatic muller from an unknown brand) twice for 25 rotations, with a weight of 5 kg. Between mixing, the paint mixture was scraped together and centered on the mill. The paints were spread out on a Melinex support with a drawdown bar applying a fixed layer thickness of 100 μm and left to dry in a lab environment (T=20°C, cyclic lighting) until they were touch dry. Linseed oil dries via a chemical drying process based on cross-linking of the triglyceride components [32]. Previous studies indicated the required drying time to be approximately two weeks for paints of this thickness and composition [1, 2]. The daily

5.1 20° and 85° were also measured.

production of paint samples is 10 to 15. Thus, it took two to three days to produce a set of 30 samples. All samples in one set of experiments start the aging process simultaneously. Therefore, drying time varies between 14 and 16 days. A preliminary experiment verified that a two day difference in drying time does not significantly influence the degradation rate [33]. For each paint sample three drawdowns were produced, and after drying the most pristine of these three was chosen for the aging process and cut to the required size with household scissors. Care was taken to produce all paint samples in an identical and randomized manner.

Table 5.1 Pigments, extenders, and additives for paint preparation.

*The bulk density was used to convert volume fraction to the added weight of pigment. While this introduces unknown variations due to differences in particle shape, size, and packing, the pigment-volume-concentration is a commonly used descriptor for paint films and was thus chosen in this study.

Name	Description	Brand & product specification	Bulk density used to convert volume fraction to added weight*
UA, TiO ₂	Uncoated Anatase	Hombitan LW, Sachtleben Chemie	4.0
CA(org), TiO ₂	Organically coated Anatase	A-HRF Huntsman	4.0
CA(inorg), TiO ₂	Inorganically coated Anatase	A-PP2 Huntsman	4.0
CR(org), TiO ₂	Organically coated Rutile	HCDC Huntsman	4.0
CR(inorg), TiO ₂	Inorganically coated Rutile	Tronox CR-826	4.0
AlSt	Aluminum stearate	Kremer 58960	1.07
BaSO ₄	Barium sulfate	Kremer 58700	4.5
CaCO ₃	Calcium carbonate	Kremer 58720	2.9
ZnO	Zinc oxide	Kremer 46300	5.6

5.2.3. Gloss analysis

At irradiation intervals during the aging cycle, gloss at an angle of 60° was measured using a Sheen Instruments Ltd Tri-GLOSSmaster^{5.1}. The gloss was determined in triplicate per time point, and the apparatus was repositioned in between each analysis. The three gloss measurements were subsequently averaged. Plotting the averaged gloss value against irradiation yields gloss decay curves which can be fitted with an exponential decay function:

$$G(I) = A \exp(-k \cdot I) + G(0) \quad (1)$$

where 'k' can be considered the reaction rate coefficient.

This equation was subsequently used to calculate the gloss value at fixed irradiation doses. For very slow degradation and stable paints, the gloss curve remains in the linear regime and thus cannot be fitted with an exponential decay curve. This is the case for many paints containing CR(inorg). For these samples, a linear fit was used to calculate the gloss value at fixed irradiation doses.

To compensate for the variable initial gloss, relative gloss decay after a certain amount of irradiation (500 J/cm² for experiment I and III and 750 J/cm² for experiment II), equation 2, was used to compare reaction rates (Table 5.2, Table 5.3 and Table 5.5). It was confirmed that investigating the reaction rate coefficient 'k' as the response yields equivalent results as using the relative gloss decay as the response.

$$\Delta_{gloss} I_{rel} = \left(\frac{|G(I) - G(0)|}{G(0)} \right) * 100 \quad (2)$$

5.2.4. State of chalking

Chalking, the final stage of photocatalytic binder degradation, can present itself in different ways. In some cases, e.g. for well-dispersed paints, chalking starts evenly, but the layer of loose pigment on the surface remains very thin. In other cases, the chalking starts in 'patches' on the surface. This can be in one or multiple spots, before reaching an even chalking stage. Assessment of the state of chalking was carried out by swiping a black cotton swab (brand: Malian) across the paint surface. The contrast between the white pigment and the black cotton swab enhances chalk visibility.

In this study, chalking was determined visually and assessed on a three or a five level scale. The three level scale, used for experiment II, has the following levels: 'no chalking'=0, 'slight chalking or patched chalking' = 0.5 and 'complete and even chalking'=1.

The five level scale was introduced for experiment III because the paints displayed a larger variety of chalking effects. It has the following levels: 'no chalking'=0, 'chalk spots covering <50% of surface'=0.25, 'chalk spots covering >50% of surface'=0.5, 'even but thin chalking' =0.75, 'complete and even chalking'= 1. In experiment III, all runs contain the photocatalytic pigment and will thus eventually chalk. Therefore in this experiment the state of chalking was assessed during the aging process at two different levels of irradiation: I6 (2355-3381 J/cm²) and I8 (3633 -5214 J/cm²).

The use of a non-continuous scale is common in the paint industry for application testing. It is based on practical considerations and should not be used in a DoE optimization study.

5.2.5. Experiments

In the scope of this work three experiments were designed each containing a specific number of runs (paint samples). These experiments addressed the following research questions:

1. What is the effect of TiO₂ pigment type on degradation rate?
2. How do mixtures of two TiO₂ types (photocatalytic + photostable), zinc oxide and aluminum stearate affect the degradation rate?
3. What is the effect of extenders, introduced to a formulation containing photocatalytic TiO₂, on the degradation rate?

The software DesignExpert® version 10 by Stat-Ease, was used to design and analyze the experiments.

5.2.5.1. Experiment I: The effect of different TiO₂ pigments

Experiment I is a univariate factorial experiment in which only the TiO₂ type is varied. The 22 runs prepared for this experiment are reported in Table 5.2. In all runs, the same pigment content (15% v/v) was added to linseed oil as described in section 5.2.2. Prior knowledge of the pigments characteristics, specifically their crystal structure and the presence of a coating, as well as previous results from photocatalytic activity experiments [4, 5], were used to code the pigment type {chapter 6}. From A to E the pigments are ranked in the following order from photostable to highly photocatalytic: CR(inorg), CA(inorg), CR(org), CA(org), UA. Within the scope of the research of TiO₂ pigments, the authors had already prepared and aged identical samples before this study [2] {chapter 3 and 4}. Hence, data on additional samples containing the photocatalytic and photostable TiO₂ standards were available and were included as additional replicates.

5.2.5.2. Experiment II: Rutile, Anatase, ZnO and Aluminum stearate mixtures

Experiment III is a D-optimal randomized mixture design containing 30 runs, built to evaluate a special cubic model. It is built up by 25 runs to estimate the model terms, three replicate runs and two runs to conduct the lack of fit test. In a mixture design, the sum of all components is required to sum up to 1. The components in this experiment are CR(inorg), UA, ZnO, AlSt and linseed oil (table 1). These components were chosen because they represent a photostable TiO₂ reference, a photocatalytic TiO₂ reference, a common admixed pigment and a common oil paint additive respectively. The compositions of the 30 runs are summarised in Table 5.3.

The boundary conditions (factor ranges and constraints) for this mixture design are:

- A: TiO₂ [UA], range: 0-0.2 v/v
- B: TiO₂ [CR(inorg)], range: 0-0.2 v/v
- C: [ZnO], range: 0-0.2 v/v
- D: [Binder] (linseed oil), range: 0.78-0.9 v/v
- E: Aluminum stearate [AlSt], range: 0-0.035 v/v at 3 levels (0, 0.02, 0.035)
- Constraint: A+B+C > 0.1 (in other words, the pigment-volume-concentration of all pigments combined is minimally 10%).

5.2.5.3. Experiment III: Anatase, calcium carbonate and barium sulfate mixtures

Experiment III is a D-optimal randomized mixture design, built to evaluate a special cubic model (seven runs to estimate the model terms), containing three replicates and eleven samples to conduct the lack of fit test. The number of samples to estimate the lack of fit was increased due to additional space in the aging chamber and to function as back-up samples. The components in this experiment are UA, CaCO₃, BaSO₄ and linseed oil. These components were chosen as the photocatalytic TiO₂ reference (fixed volume), to ensure photocatalytic degradation, filled with the two most common extenders found in recipes from important 20th century paint manufacturers [26]. The compositions of the 21 paint samples are summarised in Table 5.5. The boundary conditions for this mixture design are:

- A: TiO₂ [UA], fixed at v/v=0.14
- B: CaCO₃, range: 0-0.14 v/v
- C: BaSO₄, range: 0-0.14 v/v
- D: Oil (linseed oil binder), range: 0.72-0.86 v/v

5.2.6. Design analysis

Analysis of variance (ANOVA) was performed on the initial gloss, the relative gloss decay after a specific irradiation dose, and on the state of chalking to determine factors and factor interactions with a significant effect on those responses. No mathematical transformations were performed before analysis of variance except for the analysis of the state of chalking. For that response a logit transformation was used to force the response to stay between 0 and 1, because this has physical meaning {described in 5.2.4} [34]. Model reduction was performed based on hierarchical backward p-value selection (p<0.05) [34, 37]. The resulting models were

significant and have a non-significant lack of fit. The reduced models were evaluated on robustness using numerical and graphical diagnostics such as adjusted and predicted R², Cooks distance, leverage and residuals analysis [35-37]. Contour plots were produced to visualize the reduced models and to interpret the system. In this (screening) experimental phase the models are not validated for prediction.

5.3. Results

5.3.1. Experiment I: The effect of different TiO₂ pigments

Table 5.2 presents the initial gloss and relative gloss decay on which ANOVA was performed. The initial gloss is not significantly affected by the TiO₂ type ($p=0.0725$). On the other hand, the gloss decay after 500 J/cm², Figure 5.1, is significantly affected by the TiO₂ type ($p<0.0001$).

Table 5.2 Initial gloss and calculated relative gloss decay of paints with different types of titanium white (Experiment I). All mixtures contain a fixed volume fraction (0.15) of TiO₂.

Code, TiO ₂ type	Initial gloss	Δ gloss 500 rel
A, CR(inorg)	88.5	0.0273
A, CR(inorg)	87.9	1.5
A, CR(inorg)	87.2	0.1
A, CR(inorg)	89	1
A, CR(inorg)	85.2	1.4
A, CR(inorg)	81.9	0
B, CA(inorg)	83.4	2.4
C, CR(org)	76.7	3.2
C, CR(org)	78.5	10.3
D, CA(org)	84.5	24.9
E, UA	80.9	41.8
E, UA	85.5	52.3
E, UA	82.1	61.6
E, UA	83.7	52
E, UA	83.5	56.2
E, UA	83.5	52.8
E, UA	83.7	61.9
E, UA	76.8	72.4
E, UA	73.8	71.4
E, UA	85.2	55.7
E, UA	49.4	49.8
E, UA	41.7	55.2

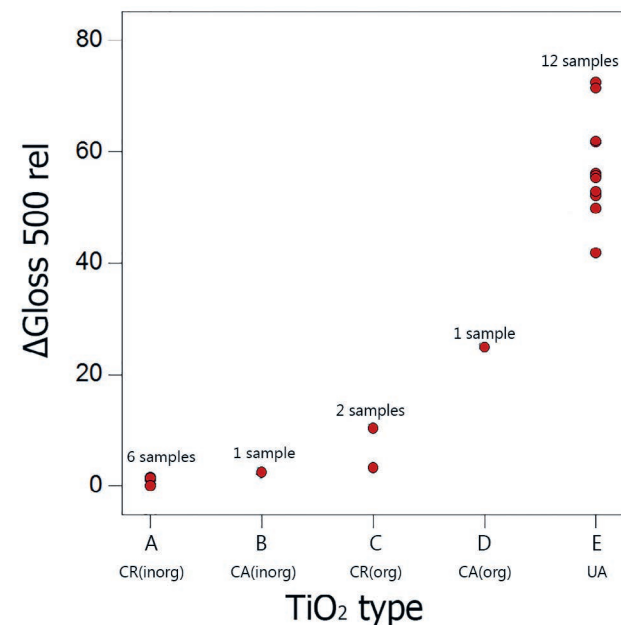


Figure 5.1 The calculated relative gloss decay after 500 J/cm² for each titanium white type. All mixtures contain a fixed volume fraction (0.15) of TiO₂.

5.3.2. Experiment II: Rutile, Anatase, ZnO and Aluminum stearate mixtures

Table 5.3 presents the composition, initial gloss, gloss decay, and state of chalking of the runs. ANOVA was performed on the three responses.

The initial gloss of mixtures containing UA, CR(inorg), ZnO, AlSt, and linseed oil can be described by a reduced model containing the linear mixture ($p<0.0001$), the interaction between UA and CR(inorg) ('A-B', $p=0.0492$), and the interaction between UA and ZnO ('A-C', $p=0.0014$), illustrated in Figure 5.2.

The reduced model for the gloss decay of those mixtures contains the linear mixture ($p<0.0001$) and the interaction between the binder and the AlSt ('D-E', $p=0.0359$), represented in Figure 5.3. The interaction 'D-E' is significant for $I<1500$ J/cm² and insignificant for $I\geq 1500$ J/cm², Table 5.4.

Chalking (the end stage of degradation) can be described by a reduced model containing the linear mixture ($p<0.0001$) and the interactions between UA and CR(inorg) ('A-B', $p=0.0042$) and ZnO and CR(inorg) ('B-C', $p=0.0044$), Figure 5.4. At the end of the exposure, the samples have been subjected to an extreme dose of UV (unrealistic for a regular indoor environment). Thus 'no chalking' ('0') is assumed to represent a paint type that would not chalk on a realistic timescale, in a regular indoor environment.

Table 5.3 Composition, Initial gloss, calculated relative gloss decay and state of chalking for experiment II.

Composition					Responses		
A: Φ UA	B: Φ CR (inorg)	C: Φ ZnO	D: Φ Oil	E: Φ AlSt	Initial Gloss	Δ gloss 750 rel	State of chalking at I_{end}
0.00	0.10	0.09	0.81	0	57.03	25.59	0
0.14	0.03	0.03	0.80	0	44.27	36.90	1
0.07	0.07	0.00	0.84	0.02	77.87	7.46	0
0.10	0.09	0.00	0.81	0	78.37	9.49	0
0.19	0.00	0.00	0.79	0.02	717	60.33	1
0.00	0.00	0.20	0.80	0	42.60	52.76	1
0.00	0.20	0.00	0.80	0	82.27	2.94	0
0.12	0.00	0.00	0.88	0	83.23	49.03	0.5
0.13	0.02	0.00	0.82	0.02	74.30	34.95	0.5
0.00	0.05	0.09	0.86	0	78.53	15.60	0.5
0.10	0.00	0.00	0.90	0	82.30	21.98	0.5
0.00	0.07	0.07	0.84	0.02	54.83	22.10	0
0.07	0.00	0.07	0.84	0.02	40.63	33.59	1
0.06	0.07	0.06	0.80	0	56.50	22.03	0
0.07	0.00	0.07	0.84	0.02	35.33	43.27	1
0.10	0.08	0.01	0.78	0.02	23.17	60.72	0
0.03	0.04	0.04	0.90	0	83.80	19.21	0
0.00	0.00	0.13	0.87	0	75.20	29.85	0.5
0.11	0.01	0.08	0.78	0.02	33.27	34.98	1
0.01	0.09	0.10	0.78	0.02	41.97	21.02	0
0.00	0.13	0.00	0.87	0	87.87	1.07	0
0.00	0.17	0.01	0.79	0.035	48.43	48.14	0
0.00	0.00	0.19	0.79	0.02	15.60	59.40	1
0.00	0.00	0.18	0.79	0.035	16.50	59.58	1
0.05	0.05	0.05	0.85	0	45.93	31.99	0
0.00	0.07	0.07	0.84	0.02	43.27	24.75	0
0.00	0.20	0.00	0.78	0.02	71.8	2.89	0
0.09	0.00	0.10	0.81	0	36.63	41.72	1
0.05	0.05	0.05	0.85	0	50.77	29.12	1
0.20	0.00	0.00	0.78	0.02	64.83	56.31	1

Table 5.4 p-value of the 'D-E' interaction in the reduced models for gloss decay after specific irradiation doses (Experiment II).

Irradiation [J/cm^2]	p-value of 'D-E' interaction
750	0.0359
1000	0.0441
1500	0.1714
2500	0.6736

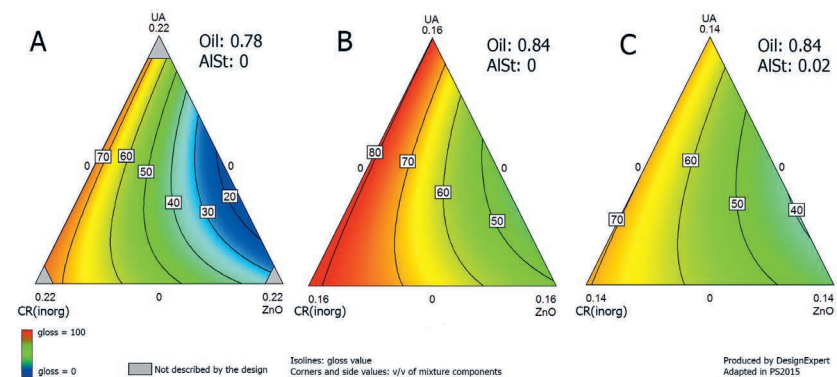


Figure 5.2 Contour plots for the initial gloss in relation to the formulation in Experiment II. A: Contour plot for low oil content and no aluminum stearate. B: Contour plot for high oil content and no aluminum stearate. C: Contour plot for high oil content and added aluminum stearate. All numbers are volume fractions (summing up to 1).

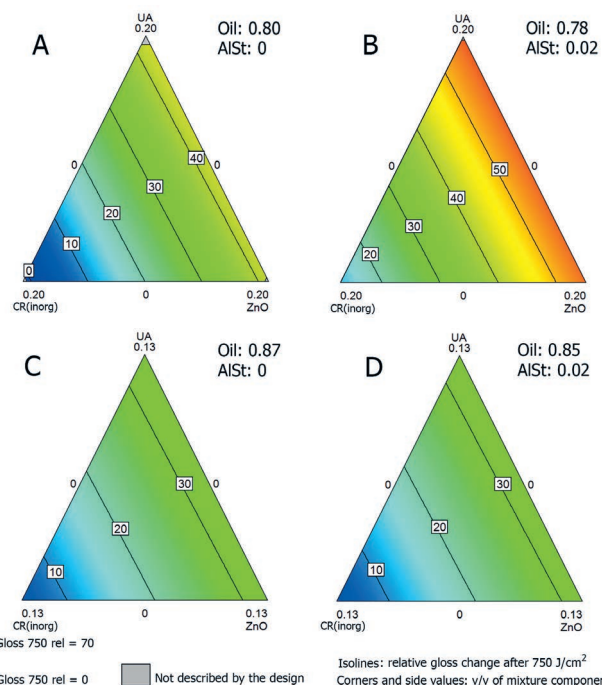


Figure 5.3 Contour plots for different oil and aluminum stearate contents, for the calculated relative gloss decay after 750 J/cm² in relation to formulation for Experiment II. A: low oil content and no AlSt; B: low oil content and AlSt; C: high oil content and no AlSt and D: high oil content and AlSt.

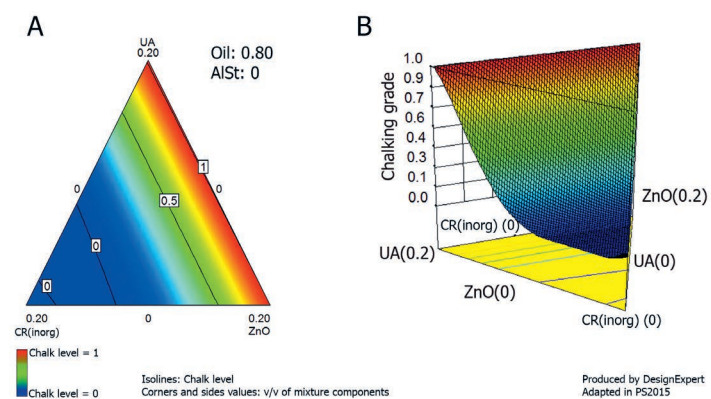


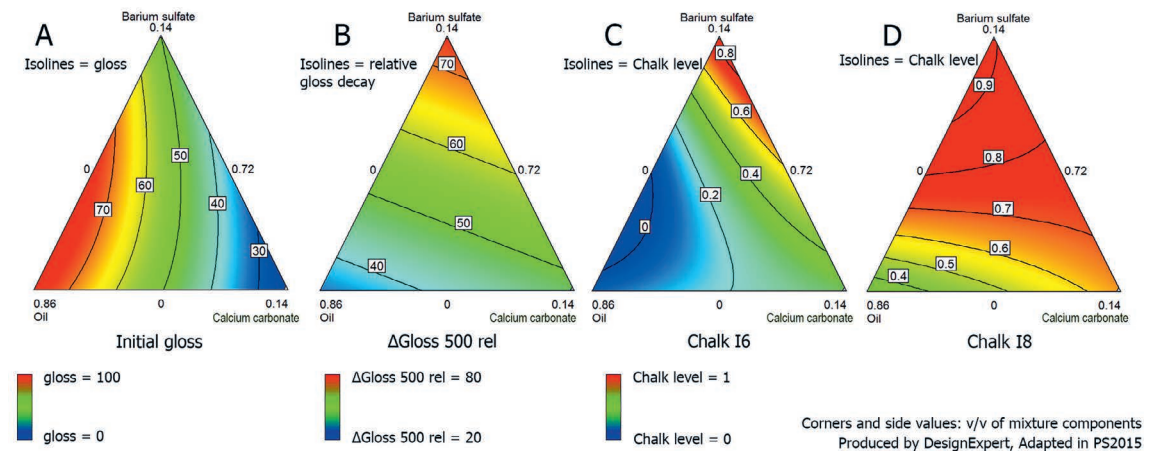
Figure 5.4 A Contour plot for the state of chalking at the end of the full aging procedure (around 10.000 J/cm²) in relation to the formulations of Experiment II. B: 3D projection of figure A showing the completely flat CR(Inorg) corner. All numbers represent volume fractions. The analysis was performed applying a logit transformation, forcing the response to stay between 0 and 1.

Table 5.5 Composition, Initial gloss, calculated relative gloss decay and state of chalking for experiment III.

Composition				Responses			
A: Φ_{UA}	B: Φ_{CaCO_3}	C: Φ_{BaSO_4}	D: Φ_{Oil}	Initial Gloss	Δ gloss 500 rel	Chalk I6	Chalk I8
0.14	0.05	0.04	0.77	58.13	43.59	0.5	0.25
0.14	0.05	0.04	0.77	52.67	51.97	0.5	0.25
0.14	0.05	0.05	0.76	51.07	52.91	0.75	0.25
0.14	0.00	0.07	0.79	65.53	56.32	1	0.25
0.14	0.00	0.00	0.86	73.8	33.09	0.25	0
0.14	0.00	0.13	0.73	55.93	69.06	1	0.75
0.14	0.13	0.00	0.73	27.13	42.75	0.5	0.25
0.14	0.07	0.00	0.79	49.5	44.38	0.5	0.25
0.14	0.03	0.01	0.82	63.4	50.38	0.5	0.25
0.14	0.02	0.05	0.79	63.33	62.81	0.75	0
0.14	0.07	0.00	0.79	44.57	44.24	0.75	0
0.14	0.06	0.08	0.72	39.7	69.42	0.75	1
0.14	0.00	0.13	0.73	42.7	84.74	1	1
0.14	0.05	0.04	0.77	50.93	47.14	0.75	0
0.14	0.00	0.00	0.86	85.37	28.81	0.25	0
0.14	0.00	0.04	0.82	79.6	48.71	1	0
0.14	0.09	0.04	0.73	33.23	52.11	0.75	0.75
0.14	0.03	0.08	0.75	59.97	53.72	0.75	0
0.14	0.00	0.04	0.82	81.67	46.07	0.5	0.25
0.14	0.13	0.00	0.73	26.43	51.14	0.75	0.25
0.14	0.00	0.10	0.76	71.83	57.35	0.75	0

5.3.3. Experiment III: Anatase, calcium carbonate and barium sulfate mixtures

Table 5.5 represents the composition, initial gloss, gloss decay and state of chalking of runs in experiment III. ANOVA was performed on the four responses. Figure 5.5 presents the contour plots for the initial gloss, the gloss decay, and the state of chalking at two different irradiation levels of mixtures of photocatalytic TiO_2 with extenders $CaCO_3$ and $BaSO_4$. The reduced model for the initial gloss contains significant effects from the linear mixture ($p < 0.0001$) and the interaction between the $BaSO_4$ and the binder ('C-D', $p = 0.0086$). The gloss decay after $500 J/cm^2$, is described by a reduced model containing only a significant effect from the linear mixture, ($p < 0.0001$). In this case, interactions do not play a role. The reduced model for chalking at I6 again contains the linear mixture ($p = 0.0009$) and the interaction between the $BaSO_4$ and the binder ('C-D', $p = 0.0142$). Finally the reduced model for chalking at I8 only contains the linear mixture ($p = 0.0010$). For each figure, the bottom left corner of the contour plot (only UA+oil) is used to compare to the rest of the plot (replacing part of the oil by $CaCO_3$, $BaSO_4$, or both).



5.4. Discussion

The experiments are interpreted taking the parameters presented in Figure 5.6 under consideration. In this study the formulation (paint recipe) is directly connected to the degradation rate. The steps in between, which can be challenging to quantify, are not under investigation here. These steps relate to quality of dispersion, powder properties, light absorption and scattering, photocatalytic activity and so on. Since information about these steps is lacking, exact underlying causes for differences in degradation rate, at this stage, can only be speculated upon. Nevertheless, the components in the formulation playing a role can be identified, which is the aim of this screening phase.

Figure 5.5 Contour plots for A: initial gloss, B: calculated relative gloss decay at $500 J/cm^2$, C: state of chalking at I₆ and D: state of chalking at I₈ in relation to the formulations of Experiment III. All mixtures contain a fixed volume fraction (0.14) of UA. Mind that in figure A red indicates a high gloss while in figure B-C red indicates high degradation and thus a low gloss.

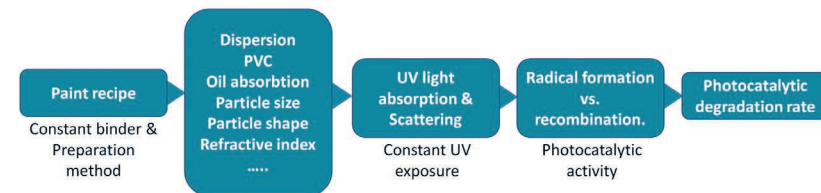


Figure 5.6 The parameters playing a role in the degradation rate of TiO_2 based oil paints.

5.4.1. Experiment I: The effect of different TiO_2 pigments

Experiment I, Figure 5.1, confirms that uncoated anatase (photocatalytic) and inorganically coated rutile (photostable), behave completely differently regarding gloss decay under UV irradiation [1, 2, 4, 5, 23-25], which validates their use as photocatalytic and photostable references. Furthermore, we previously showed the order of the photocatalytic activity of the TiO_2 powders to be $UA > CA(org) > CR(org) > CR(inorg)$ [5] {chapter 6}. This is also found in experiment I, underlining the predictive value of the previously published photocatalytic activity test [5]. It is interesting to note the similarity between $CR(inorg)$, $CA(inorg)$ and $CR(org)$,

demonstrating the anti-photocatalytic properties of rutile titanium white and of inorganic coatings. Finally, experiment I illustrates the reproducibility obtained for a stable paint, originating from a retained gloss, compared to the wide spread in results obtained from a degrading paint.

Interestingly, the initial gloss of the paints with different TiO₂ types is not significantly affected by the type of pigment. This indicates that, below the critical PVC, the influence of particle size (ranging from 100 to 250 nm for the different TiO₂ pigments), crystal structure and coating is of minor influence (or compensate each other) on the quality of dispersion and thus the gloss.

5.4.2. Experiment II: Rutile, Anatase, ZnO and Aluminum stearate mixtures.

When components other than TiO₂ are added to the paint, experiment II, the initial gloss becomes affected by the composition, Figure 5.2. The initial gloss decreases, as expected, with higher pigment volume concentration. However, at the same total pigment volume concentration, paints containing ZnO have a lower initial gloss. This could be due to the significantly different average size [38, 39] of the pigment compared to TiO₂ pigments or to a difference in dispersion quality which in turn affect the interaction of the paint film with light. This effect is stronger in interaction with UA than in interaction with CR(inorg). AlSt further decreases the initial gloss, which is unexpected as it is used as a wetting agent [40], which should improve dispersion. Several hypotheses could be explored. Firstly, AlSt is known to gellify [41]. It is a possibility that the critical concentration is reached, causing a 'gel haze' on the paint surface which reduces the gloss. Secondly, technical stearates often contain considerable amounts of free fatty acids, which may be responsible for a matting behavior. The variation in initial gloss is accounted for by comparing relative gloss decay.

Comparison between Figure 5.3 and Figure 5.4 shows that samples in the CR(inorg) corner do lose gloss (around 20 gloss units), but do not end up chalking. In fact, half the samples (14 out of 30) do not end up chalking, illustrating the protective effect of CR(inorg). The other half (16 samples) do reach a degree of chalking, but five of them are not completely chalked at the end of the extreme aging cycle. These five samples are expected to reach the fully chalked state if they would be subjected to continued exposure. The ratio at which chalking is still prevented by CR(inorg) in this design space is: 40% CR(inorg) to 60% UA+ZnO. We propose that, in the protected mixtures, the initial photocatalytic breakdown caused by UA or ZnO leads to a small

initial gloss decay and thus a rougher surface, which subsequently enhances the UV scavenging properties of CR(inorg) at the surface.

At the chalking stage (Figure 5.4), two interactions, 'A-B' ('UA-CR(inorg)') and 'B-C' ('CR(inorg)-ZnO'), are significant that were insignificant for the relative gloss decay in the early stage of degradation. These interactions are of the same order of magnitude in terms of their effect on the response. The interactions indicate that there is an inhibiting effect caused by CR(inorg) on both UA and ZnO, which is likely related to the UV scavenging behavior of rutile that prevents chalking. It shows that coated rutile equally protects anatase- and zinc oxide-photocatalyzed chalking. Communication with Talens, a Dutch artists' paint manufacturer, indicates that while paint manufacturers commonly order one type of TiO₂, the delivered powders sometimes consist of mixtures. Such mixtures have been found in a Talens paint tube from the 1970s [26]. Not known by the paint manufacturer, the presence of coated rutile within a batch of uncoated anatase pigment may protect the artwork from degradation.

At low irradiation dose, the interaction 'D-E' is found to be significant. At low binder content (0.78-0.80), adding aluminum stearate enhances the gloss decay (Figure 5.3A and 5.3B). On the other hand, at high binder content (0.85-0.87) aluminum stearate has no effect on the gloss decay (Figure 5.3C and 5.3D). Additionally, an increased amount of binder (automatically decreasing the amount of pigment and thus of photocatalytic material), as expected, slows down the degradation (Figure 5.3B and 5.3D). Technical stearates can contain free fatty acids (stearic acid) that can be degraded via TiO₂ photocatalysis [42, 43]. As these are smaller molecules than the oil network, decomposition into volatile components occurs faster. This effect is minor, due to the very small amount of aluminum stearate added to the paint. We propose that the effect is negligible at high oil content and noticeable at low oil content. Consequently, when all free acids from the technical stearate have been degraded, at higher irradiation doses, the interaction becomes insignificant. Furthermore, this hypothesis requires the stearates to be in proximity to the pigments, which is to be expected from a wetting agent [44].

Finally, the symmetry of the contour plot in Figures 5.3 and 5.4, indicates that UA, chosen for its extreme photocatalytic activity [5], has the same effect on the gloss decay as ZnO. Even though it is known that zinc oxide can behave as a photocatalyst, this similar behavior was unexpected as the photocatalytic activity of ZnO is considered to be lower [45]. The similarity may alternatively stem

from a dispersion effect, as mixtures containing ZnO, based on the initial gloss, may have a lower quality of dispersion. Thus less oil needs to be degraded for a similar relative loss of gloss. Nevertheless, ZnO-containing paint also reaches the chalking stage. Thus ZnO definitely contributes to the degradation. It would be interesting to investigate different qualities of ZnO pigments and their effect on oil degradation rates. Furthermore, the relation between ZnO photocatalytic activity and other ZnO-related degradation problems such as soap formation [46, 47] may be an interesting avenue to pursue further. While ZnO is known for its reactivity towards stearates, the interaction between ZnO and AlSt does not play a role in the gloss decay, either indicating that soap formation does not influence the gloss of a painting (at this time scale) or indicating that photocatalytic degradation is preferred over soap formation under the conditions used. While both degradation phenomena may be competitive in natural aging, soap formation is not enhanced by UV light.

5.4.3 Experiment III: Anatase, calcium carbonate and barium sulfate mixtures

Figure 5.5A indicates that the extenders have a lowering effect on the initial gloss, which is partly due to the increased solid content (PVC) of the paint. This negative effect is larger for CaCO₃ than for BaSO₄, which is suggested to be due to the differences in particle sizes and oil absorption properties and thus the quality of dispersion of the extenders. Barium sulfate and calcium carbonate both consist of much larger and non-spherical particles in comparison to titanium white (Manufacturer information: CaCO₃≈20μm, BaSO₄≈1.7 μm, TiO₂≈0.1 μm). In the case of barium sulfate, a substantial part of the oil can be replaced by the filler without influencing the initial gloss ('Oil-BaSO₄' axis), which is described in the model by the significance of the 'C-D' interaction. This could be related to the statement by Kremer Pigmente that BaSO₄ 'lowers oil absorption'. Again, the variable initial gloss is accounted for by comparing relative gloss decay rather than absolute gloss decay.

Experiment III has a fixed amount of uncoated anatase (photocatalytic material) in the mixtures. This results in a variable 'UA:oil' ratio (active material vs. degradable material) due to the addition of extenders, which replace part of the oil. An increase of active material vs. degradable material ('catalyst loading') should, as illustrated in Figure 5.3, increase gloss decay/degradation [48]. However, if this were the only effect at play, the graphs would be symmetrical. In other words, the same enhancement would be expected for BaSO₄ as for CaCO₃. Since this is not the case, the

results can be used to investigate the effect of the different types of extenders on the degradation rate. However, care must be taken during interpretation because the extent of the effect based on the change in 'UA-oil' ratio was not verified. Both extenders transmit light in the UV region [39, 49], which results in a deeper penetration depth of the UV light and a larger volume of paint in which radicals can be formed. Both extender types have a larger particle size than the anatase pigments by a factor 20 and 200 respectively for BaSO₄ and CaCO₃, which will affect the distribution of the active particles within the paint film. These aspects all contribute to the observed enhanced degradation rates. The substantially increased gloss decay when BaSO₄ is added, shown in Figure 5.5, is problematic as many titanium white oil paints contain BaSO₄ extenders, such as those by Weber (Permalba) [26].

Figure 5.5C and 5.5D illustrate the chalking of the samples. All samples contain photocatalytic uncoated anatase; thus, eventually, all samples will chalk. Similar to the gloss decay, a higher chalking rate is observed for the paints that contain extenders, with a larger negative effect for the barium sulfate containing paints. As CaCO₃ has a much larger particle size, a thicker layer of binder needs to be degraded before the particles are unbound and complete chalking is observed. This could account for the lower state of chalking for CaCO₃ containing paints.

5.5. Conclusion

The results presented in this screening study indicate that photocatalytic degradation rate is complex and influenced by common paint components and by the TiO₂ quality, which in turn influences quality of dispersion, critical PVC, and interaction with light. Despite the differences in degradation rates that are indeed caused by differences in formulation, it seems that the photocatalytic activity of the titanium white remains the most important factor governing photocatalytic degradation. The only inhibiting factor that was confirmed in this study is the presence of photostable TiO₂ pigments, such as inorganically coated rutile pigments. This effect is substantial and very beneficial for mixtures of both pigments in paintings. The presence of extenders, often added to bring the price of paints down, as well as, in specific cases, the presence of aluminum stearate, enhance rather than decrease degradation rate. Additionally, factors that ambiguously influence the degradation behavior were identified. These include the role of ZnO (photocatalytic or not) and aluminum stearate. Neither can be ignored in a study of degradation behavior of modern oil paints and both deserve further investigations.

Paint formulation is often a tradeoff between cost reduction and paint quality. However, quality is often not intended for hundreds of years, as we would like it to be for artworks. Thus, time will tell how titanium white containing oil paints will behave in the long term. Here, a start has been made to understand their behavior in relation to paint composition in a sample efficient and robust manner using DoE. This methods allows us to study complex paint formulations, and can potentially be very useful in the field of heritage science to study the effect of material formulation on object behavior {chapter 5B}. Follow-up studies can further validate the findings of these screening phase experiments so that degradation can be predicted and possibly prevented.

Terminology

Analysis of Variance (ANOVA): A statistical method that splits the variability in the response by the selected factors in the analysis and supplies information about the significance of these factors on the response.

Blocking: To account for certain uncontrollable factors by splitting and grouping the design (e.g. day 1 / day 2). Blocking results in an additional run.

Constraints: Applied boundary conditions that have to be met in the design space.

Contour plot: Visualization of the component effect on the response. Mixture designs are always represented as a (subset) of a triangle.

Design: Combination of factor settings, model order and constraints used to build the experimental set.

Design of Experiments (DoE): A statistical research approach, often applied in several industries with the aim of designing a set of runs in order to explain/ model variation in the response (also known as Experimental Design).

Design space: Multidimensional space characterized by the factor ranges and levels.

Diagnostics: Graphs or numerical values to evaluate outliers and model robustness.

Experiment: Selection of runs produced based on design criteria.

Factor: Variable tested for its influence on the response (this can be a component or a process condition, such as temperature).

Factor interaction: When the effect of two factors is different than the effect of the sum of both (linear mixture). An 'A-B' interaction is a second order interaction; these are common in mixtures. An 'A-B-C' interaction is a third order interaction – DoE experience shows that 3rd order interactions are uncommon in mixtures.

Factor range: Boundary conditions set for a specific factor/component.

Formulation: Term used to denote the recipe of a mixture, in this manuscript a paint.

Inhibition: When a factor or factor interaction causes a preventive effect.

Lack of Fit sample: Run(s) included in the experimental design to check if the polynomial model order is correct.

Lack of Fit test: test to check if the model order is correct.

Levels: Chosen settings for discrete/categorical factors. For instance, when studying five different TiO₂ types, these are five levels for the factor 'TiO₂ type'.

Linear mixture: When only the pure components contribute to the model.

Logit transformation: A mathematical transformation that forces the predicted response to be between two set values (in this case 0 and 1). Used in this study for the state of chalking to ensure physical meaning in the contour plot.

Mathematical transformation: A mathematical transformation of the response can be performed before ANOVA to obtain a constant error in the response range. This is one of the assumptions of ANOVA.

Mixture design: Design used specifically for determining the effect of formulations (*vide infra*) on certain properties. It has the characteristic that all factors are interdependent due to the convention that the total sum of the mixture components has to sum to 100% or 1.

Model reduction: Process of model analysis and evaluation to reach a reduced model that describes the significant effects on the response. Process used in this study is described in the experimental section.

Optimized design: Optimization following a specific algorithm (I-Optimal, D-Optimal, A-Optimal). This algorithm chooses runs that minimize the integral of the prediction variance across the factor space. In this study, we use D-optimal designs. D-optimal designs are used to best estimate the factor effect and are optimized by minimizing the matrix determinant of the squared design matrix.

Pigment-Volume-Concentration (PVC): Volume ratio of solid material vs. binder material: $V_{\text{pigment}} / (V_{\text{pigment}} + V_{\text{binder}})$.

cPVC: The stage where there is just sufficient binder to wet the pigments.

p-value: Value used to determine significance of model terms against a predetermined value: α .

Randomization: To carry out the runs in the experiment in completely random order to spread the contribution of uncontrolled factors across all the modeled factors and interactions.

Reduced model: Model that includes only the significant model terms based on the selected design order.

Replication: Runs included in the design used to estimate the pure error. These runs have to be produced and treated completely separately and thus cannot be produced from the same paint batch or measured from the same paint sample as their replicate. The whole process has to be reproduced to properly assess the pure error.

Run: Sample in the experiments. In this study run refers to a specific home-made paint sample produced by following a predetermined recipe.

Significance: In any statistical analysis, significance is evaluated based on a chosen cut off value ($p < \alpha$). Here we use the common cut-off $\alpha < 0.05$.

Special cubic: Third order interaction model specifically for mixtures.

Univariate: An experiment in which only one variable is changed.

Acknowledgements

This work has been financially supported and co-authored by AkzoNobel and organized and hosted by the Rijksmuseum Amsterdam. AkzoNobel is further acknowledged for providing access to an in-house Design of Experiments course. Old Holland (Driebergen) is acknowledged for the paint muller on loan at the RCE and Pieter Keune for providing the paint drier. Furthermore, the authors acknowledge Bill Wei at the Cultural Heritage Agency of the Netherlands (RCE) for the availability of the Sheen Instruments Ltd Tri-GLOSSmaster. Finally, Dr. M.J.M. Stols-Witlox (UvA) and Dr. L. Megens (RCE) are acknowledged for their feedback on the initial manuscript during the writing stage.

- van Driel BA, Wezendonk TA, van den Berg KJ, Kooyman PJ, Gascon J and Dik J. Determination of early warning signs for photocatalytic degradation of titanium white oil paints by means of surface analysis. *Spectrochim Acta A*. 2017; 172: 100-108.
- Morsch S, van Driel BA, van den Berg KJ and Dik J. Investigating the Photocatalytic Degradation of Oil Paint using ATR-IR and AFM-IR. *ACS Appl Mater Interfaces*. 2017; 9(11): 10169-10179.
- Lauridsen CB, Sanyova J, Simonsen KP. "Analytical study of modern paint layers on metal knight shields: The use and effect of Titanium white. *Spectrochim Acta A*. 2014; 124: 638-645.
- Laver M. Titanium White. In: West FitzHugh E, editor. *Artists' Pigments: A Handbook of their History and Characteristics*, Vol. 3. National gallery of Art, Washington. London:Archetype Publications. 1997. 3: 295-355.
- van Driel BA, Kooyman PJ, van den Berg KJ, Schmidt-Ott A, Dik J. A quick assessment of the photocatalytic activity of TiO₂ pigments — From lab to conservation studio! *Microchem J*. 2016; 126: 162-171.
- Johnston-Feller R, Feller RL, Bailie CW, Curran M. The Kinetics of Fading: Opaque Paint Films Pigmented with Alizarin Lake and Titanium Dioxide. *JAIC*. 1984; 23(2): 114-129.
- Samain L, Silversmit G, Sanyova J, Vekemans B, Salomon H, Gilbert B, et al. Fading of modern Prussian blue pigments in linseed oil medium. *J Anal Atom Spectrom*. 2011; 26(5): 930-941.
- Völz H, Kaempf G, Fitzky H and Klaeren A. The Chemical Nature of Chalking in the Presence of Titanium Dioxide Pigments. In: Winslow, editor. *Photodegradation Photostabilization of Coatings ACS symposium series*. 1981; vol. 151: 163-184
- Egerton T. UV-Absorption—The Primary Process in Photocatalysis and Some Practical Consequences. *Molecules*. 2014; 19(11): p. 18192.
- Egerton TA and Tooley IR. Effect of Changes in TiO₂ Dispersion on Its Measured Photocatalytic Activity. *J Phys Chem B*. 2004; 108(16): p. 5066-5072.
- Thomson G. Penetration of Radiation into Old Paint Films. In *National Gallery Technical Bulletin*. 1979; Vol 3, pp 25–33. Accessed at: <http://www.nationalgallery.org.uk/technical-bulletin/thomson1979>. 15-12-2017.
- Creagh DC and Bradley D. *Physical Techniques in the Study of Art, Archaeology and Cultural Heritage*. Elsevier Science, editor. 2007; Vol 2: p 203.
- Pfaff G. *Inorganic Pigments*. De Gruyter, editor. 2017. ISBN: 978-3-11-048451-9
- Colling JH and Dunderdale J. The durability of paint films containing titanium dioxide — Contraction, erosion and clear layer theories. *Prog Org Coat*. 1981; 9(1): p. 47-84.
- Paints & coatings Industry. *A Comprehensive Understanding of TiO₂ Pigment Durability*. 2005; Available from: <http://www.pcimag.com/articles/a-comprehensive-understanding-of-tio2-pigment-durability> 15-12-2017.
- Zorll U. New aspects of gloss of paint film and its measurement. *Prog Org Coat*. 1972; 1(2): p. 113-155.
- Rogge CE, Arslanoglu J. Distinguishing manufacturing practices for titanium white pigments: New Raman markers for dating commercial oil-based paints. *Stud Conserv*. 2016 61(sup2): 324-326.
- Werner AJ. Titanium dioxide pigment coated with silica and alumina. *Google Patents*. 1969
- Nelson WK. Chalk-resistant titanium dioxide pigment and method for preparing the same. *Google Patents*. 1944
- Jacobson HW. Light-stable titanium dioxide pigment composition. *Google Patents*. 1980
- Linsebigler AL, Lu G and Yates JT. Yates, Photocatalysis on TiO₂ Surfaces: Principles, Mechanisms, and Selected Results. *Chem Rev*. 1995. 95(3): p. 735-758.
- Fujishima A, Rao TN and Tryk DA. Titanium dioxide photocatalysis. *J Photochem Photobiol C*. 2000. 1(1): p. 1-21.
- Gaumont S, Siampiringue N, Lemaire J, Pacaud B. Influence of titanium dioxide pigment characteristics on durability of four paints (acrylic isocyanate, polyester melamine, polyester isocyanate, alkyd). *Surf. Coat. Int*. 1997; 80(8): 367-372.
- de Keijzer M. The history of modern synthetic inorganic and organic artists' pigments. In: Mosk JA, editor. *Contributions to conservation: research in conservation at the Netherlands Institute for Cultural Heritage (ICN Instituut Collectie Nederland)*. James & James. 2002. p 42-54.
- Gesenhues, U. Influence of titanium dioxide pigments on the photodegradation of poly(vinyl chloride). *Polym Degrad Stabil*. 2000; 68(2): 185-196.
- Phenix A, van den Berg KJ, Soldano A, van Driel BA. The Might of White: formulations of titanium dioxide-based oil paints as evidenced in archives of two artists' colourmen mid-twentieth century. In: *ICOM-CC Triennial conference 2017, Copenhagen*. 2017.
- Spathis P, Karagiannidou E, Magoula A-E. Influence of Titanium Dioxide Pigments on the Photodegradation of Paraloid Acrylic Resin. *Stud Conserv*. 2003; 48(1): 57-64.
- Cornell JA. *Experiments with Mixtures: Designs, Models, and the Analysis of Mixture Data*. Wiley, publisher.
- Goos P and Jones B. *Optimal Design of Experiments: A Case Study Approach*. Wiley, publisher. 2011.
- Brereton RG, Jansen J, Lopes J, Marini F, Pomerantsev A, Rodionova O, Roger JM Walczak B and Tauler R. Chemometrics in analytical chemistry—part I: history, experimental design and data analysis tools. *Anal Bioanal Chem*. 2017; 409(25): p. 5891-5899.
- Brereton RG. Statistical experimental design. *J Chemometr*. 2017; 31(7).
- Tumosa CS and Mecklenburg MF. The influence of lead ions on the drying of oils. *Stud Conserv*. 2005; 50(Supplement-1): p. 39-47.
- van Driel BA. Unpublished data. 2017.
- Stat-Ease. *Handbook for Experimenters*. Accessible at: http://www.statease.com/pubs/handbk_for_exp_sv.pdf. 15-12-2017
- Weisberg S. *Applied Linear Regression*, 2nd edition. John Wiley & Sons, Inc. 1985
- Raymond M. *Classical and Modern regression with applications*. Duxbury Press. 1986.
- McCullagh PM and Nelder JA. *Generalized Linear Models*. 2nd edition ed. Chapman and Hall. 1990
- Lohmander S. The influence of particle shape of coating pigments on their packing ability and on the flow properties of coating colours. *Trita-PMT, Institutionen för pappers- och massateknologi*. 2000; 5: 71.
- Feller RL and Roy A. Barium sulfate. In: *Artists' Pigments: A Handbook of their History and Characteristics*, Vol. 1. National gallery of Art, Washington. London:Archetype Publications. 1986; p. 47.
- Lower ES. The properties of aluminium stearate and its uses in the coating and allied industries. *Pigm resin technol*. 1982; 11(2): 13-18.
- Wang X, Rackaitis M. Gelling nature of aluminum soaps in oils. *J Colloid Interf Sci*. 2009; 331(2): 335-342.
- Vicente JP, Gascoin T, Barboux P, Boilot JP, Rondet M and Gueneau L. Photocatalytic decomposition of fatty stains by TiO₂ thin films. *Int J Photoenergy*. 2003; 5(2).
- Mills A, Hill C and Robertson PKJ. Overview of the current ISO tests for photocatalytic materials. *J Photochem Photobiol A*. 2012; 237: p. 7-23

44. van den Berg KJ. Issues in Contemporary oil paint. Springer International Publishing. 2014.
45. Kobayashi M, Kalriess W. Photocatalytic Activity of Titanium Dioxide and Zinc Oxide. *Cosmetics & Toiletries magazine*. 1997; 112: 83-85.
46. Osmond G. Zinc white: a review of zinc oxide pigment properties and implications for stability in oil-based paintings. *AICCM Bulletin*. 2012; 33(1): 20-29.
47. Hermans JJ. Metal Soaps in oil paint, structure mechanisms and dynamics. PhD thesis at Van 't Hoff Institute for Molecular Sciences, Universiteit van Amsterdam. 2017. ISBN: 978-94-629-5578-3 <http://hdl.handle.net/11245.1/53663926-183c-40aa-b7b3-e6027979cb7d> Accessed September 2017.
48. Akpan UG and Hameed BH. Parameters affecting the photocatalytic degradation of dyes using TiO₂-based photocatalysts: A review. *J Hazard Mat*. 2009; 170(2-3): p. 520-529.
49. Kuhn H. Zinc oxide. In: Feller RL, Roy A, editors. *Artists' Pigments: A Handbook of Their History and Characteristics*, Cambridge University Press London. 1986. p. 169-186.

Chapter 5B

The applicability of Design of Experiments (DoE) for heritage science.

Chapter 5 investigates the influence of paint formulation on the degradation rate. This is done by making mock-up paint samples and monitoring the gloss change during aging. In two of the presented experiments, the formulations to test were chosen based on a Design of Experiments methodology. In this addendum I will briefly discuss the benefit that DoE could have for cultural heritage research.

Unpublished work.

5B.1. Introduction to Design of Experiments (DoE)

In the field of Cultural Heritage research, understanding the long-term behavior of materials is one of the key goals. For this type of research, ‘reconstructions’ or ‘model paints’ are often used to answer questions about the behavior of paints [1-18], inks [19, 20], dyed textiles [21] and others materials, such as cleaning solutions [22]. Traditionally, (degradation) studies are performed on paint samples specifically prepared for these studies. These samples are often oversimplified, or attempts are undertaken to produce more or less historically accurate materials. Artificial aging of those reconstructed materials and subsequent analysis is commonly performed. Most studies follow some form of the one-factor-at-a-time (OFAT) methodology, where a single parameter is changed, while all others are held constant. This approach, while systematic if performed accurately, is not predictive, efficient, or robust, nor does it take factor interactions into account [23]. With an increasing number of variables involved, this approach becomes time consuming and can compromise the representative nature of the study. In other words, the traditional methodology is too rigid when investigating the complexity of degradation behavior involving a multitude of components, ageing conditions and other variables.

To overcome these difficulties, Design of Experiments (DoE) can be used. DoE is a statistics-based methodology that allows the design of small but robust and representative sample sets by varying multiple factors simultaneously. The method is known for its high sample efficiency, the estimation of factor interactions and thus the modelling of the behavior of complex mixed materials. The method is commonly accepted, validated and used in industrial optimization as well as in other fields of science, and could be of great benefit for Cultural Heritage research.

Design of experiments (DoE) was originally developed for agricultural studies [24] in the early 1900s, by Sir Ronald Aylmer Fisher [25, 26]. The method rapidly spread to other industrial and scientific applications such as the development of fuel cells [27], the investigation of photocatalytic reactions [28], the improvement of properties of fly ash cement [29] and the optimization of coating performance [30-32].

In industry, DoE is often used to find cost-effective formulations with all the required product and process specifications [33, 34]. DoE is increasingly mentioned in scientific publications as well, among others in the field of paints and coatings. It’s use was reported for research into solvent-borne coatings [33], emulsified

paints [35], UV-curable polyurethanes [30], acrylates [36] and water-based [32] and thermoplastic road marking paints [31].

The goal of DoE is to model factor-response relationships in a robust and efficient way, while using a manageable number of samples. The samples are determined using optimization algorithms, thus the same design input (design type, factors, factor ranges) can yield different sample sets. Building the factor response model is done by calculating polynomial equations to relate factors and factor interactions to the variability of the response with ANOVA (Analysis of variance). The polynomials are intended to approximate the relation between factor and response within the design space and not to estimate the real physical or chemical models behind the observed behavior [23, 24, 37, 38].

DoE is considered more efficient than other approaches, such as the OFAT approach or the random walk approach (trying randomly chosen combinations of factors), in terms of number of samples. When the number of factors under investigation increases, the sample efficiency of DoE compared to OFAT also increases [39]. Furthermore, DoE has the ability to model interactions between several factors on the response, while this is not possible with the other approaches. Many multicomponent systems, among which paints and coatings, can have synergetic or inhibiting effects and not taking those interactions into account leads to incomplete results [33]. Furthermore, DoE can be used for prediction within the design space while the other experimental approaches cannot. With this in mind, the field of Cultural Heritage research could use DoE to design more efficient sample sets with a higher information content, which answer the research questions with more certainty, precision and speed.

In order to perform a proper analysis of variance it is important to consider several things such as [23, 38]: (A) choosing and building a suitable design for the research questions; (B) developing and analyzing the measurement system; (C) randomization of runs; (D) replications and (E) blocking.

Several different design types are available depending on the research questions [32]. The type of design is always directed by the research question and the nature of the factors studied. Generally, we can identify: controllable factors that are varied, controllable factors that are kept constant and uncontrollable factors. Another way to classify factors is: components in the formulation and (operational) parameters affecting the process [23, 24, 37-39].

5B.2. Previous studies that could have benefited from DoE

By evaluating reconstruction studies performed in the past, we will demonstrate that, while very valuable, these studies could have been performed more efficiently and could have provided more information if DoE had been used.

An often referred-to approach when it comes to reconstructions of historical paint materials, is the approach developed by Carlyle, who introduced the term historically 'accurate' paint reconstructions in the HART project [8]. Following this approach, Stols-Witlox et al. [7] produced systematic sets of reconstructions based on historical recipes to investigate the effects of water washing, vinegar grinding and decanting on the visual characteristics and composition of lead white particles. While such studies are very valuable, they currently lead to what can best be described as screening: a selection of the most influential factors. By approaching this type of research with a systematic DoE approach, researchers could elucidate how factors interact.

Pellegrini et al. [1], like many other researchers, limit themselves by only testing one factor (pigment type) at multiple (in this case 6) levels. Therefore, in this case both DoE and OFAT result in the same sample set. However, DoE could have been used to investigate additional factors. For instance, the paper reports adding enough binder to produce a workable paint. This introduces an uncontrolled variability, while the effect of liquid/solid content could have been introduced in a DoE. Studies are often limited to one factor. While this approach may be useful in studies focusing on a particular mechanism [17, 18], such systems are often not representative for the whole paint system under investigation. Therefore they cannot be used for predictive or comparative studies [11, 12].

DoE is often chosen for its high sample efficiency. However, for factorial designs this is not always the case [10, 12, 13, 19, 20]. In a study investigating the influence of lead compounds on oil drying by DeViguerie et al. [5], nine samples are reported while the DoE approach for this same question requires twenty samples. In this case, a DoE approach is beneficial because it yields all information about the interactions and the effect of $PbCO_3$ at all levels in a continuous range (rather than at one level). What is compromised in terms of number of samples, is gained in information.

More often, DoE can show significant benefits in terms of numbers of samples. Poli et al. [2] investigated seven pigments, in four binders, on two supports, aged at four aging conditions. This is a typical example of a sample set that rapidly expands. When using

the OFAT approach, this would result in a sample set of 224 samples – without any replicate samples (and thus information about the experimental error). On the other hand, an optimal factorial DoE design, which has the additional benefit of taking into account all second order factor interactions, lack of fit samples and replicates, requires only 79 samples. The challenge here, and in many of the examples, is to convert spectral data into a numerical response for straightforward analysis of the data (such as peak areas, peak intensities or peak ratios).

Also investigations into the effect of cleaning treatment in the Cultural Heritage field could benefit from a DoE approach. Dillon et al. [22] investigated the effect of solvent parameters (pH, conductivity and ionic strength) on cleaning (responses: swelling and surfactant removal). In order to do so, 192 cleaning solutions were prepared and tested. Using a DoE with 3 factors: ionic strength (3 levels), pH (range: 2.5-9.5) and conductivity (range: 0.5-48), this investigation would have required only 22 solutions.

5B.3. Guidelines for a successful DoE

This addendum demonstrated the possible benefit of DoE for Cultural Heritage research. It also allows us to share some advice on the application of DoE in this field:

- You get what you design for - Building the design is the main step that determines the success DoE. Especially if executing the design is a time consuming activity, which is often the case for aging experiments.
- Take time to think about the question you want to answer - Many of the papers discussed in the previous section are not easily translated directly to a DoE, since these are factorial designs with many factor levels. However, rethinking the question may result in a much more efficient and information-dense sample set based on a mixture design or response-surface design.
- Prepare: Gather information about the system and the responses - It is absolutely vital to think carefully about how you will perform the experiments, what the weaknesses of the measurement systems are and how you will process the responses. In many of the papers from the previous section, the behavior was analyzed using spectroscopic methods. In this case it is important to think about translating this response to a numerical value representative for the investigated system, such as a changing peak intensity or peak ratio. Furthermore, DoE should be a practical tool. Sometimes optimal use of DoE is not

possible simply because it is not practical (e.g. aging each sample in a separate oven run). In these cases, DoE is still very useful but it is important to be aware of the (mathematical) consequences.

- Stay critical - Everything can be modeled but it has to physically make sense. While DoE has predictive power, it is important not to extrapolate outside the sample range and not to use the model equations as descriptions of the real behavior. They are merely polynomial estimations of the behavior within the sample range.
- Successful use of DoE requires statistical insight as well as material/system specific knowledge - This makes the use of DoE for cultural heritage highly multidisciplinary which is characteristic for this field of research.

1. Pellegrini D, Duce C, Bonaduce I, Biagi S, Ghezzi L, Colombini MP. Fourier transform infrared spectroscopic study of rabbit glue/inorganic pigments mixtures in fresh and aged reference paint reconstructions. *Microchim J.* 2016; 124: 31-35.
2. Poli T, Piccirillo A, Nervo M, Chiantore O. Interactions of natural resins and pigments in works of art. *J Colloid Interf Sci.* 2017; 503: 1-9.
3. La Nasa J, Degano I, Modugno F, Colombini MP. Effects of acetic acid vapour on the ageing of alkyd paint layers: Multi-analytical approach for the evaluation of the degradation processes. *Polym Degrad Stabil.* 2014 105: 257-264.
4. Sanches D, Ramos AM, Coelho JFJ, Costa CSMF, Vilarigues M, Melo MJ. Correlating thermophysical properties with the molecular composition of 19th century chrome yellow oil paints. *Polym Degrad and Stabil.* 2017; 138: 201-211.
5. de Viguierie L, Payard PA, Portero E, Walter P, Cotte M. The drying of linseed oil investigated by Fourier transform infrared spectroscopy: Historical recipes and influence of lead compounds. *Prog Org Coat.* 2016; 93: 46-60.
6. Baudys M, Krysta J, Zlamal M, Mills A. Weathering tests of photocatalytic facade paints containing ZnO and TiO₂. *Chem Eng J.* 2015; 261: 83-87.
7. Stols-Witlox M, Megens L, Carlyle L.: 'To prepare white excellent...': reconstructions investigating the influence of washing, grinding and decanting of stack-process lead white on pigment composition and particle size. In: Eyb-Green S, Townsend JH, Clarke M, Nadolny J, Kroustallis S, editors. *The artist's process: technology and interpretation.* Londen: Archetype; 2013. p. 112-129
8. Carlyle L.: *Historically Accurate Reconstructions of Oil Painters' Materials: An overview of the Hart Project 2002-2005.* In: Boon JJ, Ferreira SB, editors. *Reporting Highlights of the De Mayerne Programme.* Netherlands Organisation for Scientific Research. 2006. p. 63-76. http://assets.kennislink.nl/upload/181089_391_1193921849265-HighlightsMayerne.pdf. Accessed September 2017.
9. Monico L, van der Snickt G, Janssens K, de Nolf W, Miliani C, Verbeeck J, et al. Degradation Process of Lead Chromate in Paintings by Vincent van Gogh Studied by Means of Synchrotron X-ray Spectromicroscopy and Related Methods. 1. Artificially Aged Model Samples. *Anal Chem.* 2011; 83(4): 1214-1223.
10. Samain L, Silversmit G, Sanyova J, Vekemans B, Salomon H, Gilbert B, et al. Fading of modern Prussian blue pigments in linseed oil medium. *J Anal Atom Spectrom.* 2011; 26(5): 930-941.
11. Spathis P, Karagiannidou E, Magoula A-E. Influence of Titanium Dioxide Pigments on the Photodegradation of Paraloid Acrylic Resin. *Stud Conserv.* 2003; 48(1): 57-64.
12. Gaumet S, Siampiringue N, Lemaire J, Pacaud B. Influence of titanium dioxide pigment characteristics on durability of four paints (acrylic isocyanate, polyester melamine, polyester isocyanate, alkyd). *Surf. Coat. Int.* 1997; 80(8): 367-372.
13. Ropret P, Zoubek R, Skapin AS, Bukovec P. Effects of ageing on different binders for retouching and on some binder-pigment combinations used for restoration of wall paintings. *Mater Charact.* 2007; 58(11-12): 1148-1159.
14. Johnston-Feller R, Feller RL, Bailie CW, Curran M. The Kinetics of Fading: Opaque Paint Films Pigmented with Alizarin Lake and Titanium Dioxide. *JAIC.* 1984; 23(2): 114-129.
15. Mallégol J, Lemaire J, Gardette JL. Drier influence on the curing of linseed oil." *Prog Org Coat.* 2000; 39(2-4): 107-113.
16. Burnstock A, Lanfeer I, van den Berg KJ, Carlyle L, Clarke M, Hendriks E, Kirby J. Comparison of the fading and surface deterioration of red lake pigments in six paintings by Vincent Van Gogh with artificially aged paint reconstruction. In: Verger I, editor. *ICOM-CC fourteenth triennial meeting, The Hague, 12-16 September 2005, Committee for Conservation: preprints.* Londen: James and James. 2005. p. 459-466
17. van Driel BA, Wezendonk TA, van den Berg KJ, Kooyman PJ, Gascon J and Dik J. Determination of early warning signs for photocatalytic degradation of titanium white oil paints by means of surface analysis. *Spectrochim Acta A.* 2017; 172: 100-108.
18. Morsch S, van Driel BA, van den Berg KJ and Dik J. Investigating the Photocatalytic Degradation of Oil Paint using ATR-IR and AFM-IR. *ACS Appl Mater Interfaces.* 2017; 9(11): 10169-10179.
19. Reháková M, Ceppan M, Vizarova K, Peller A, Stojkovičová D, Hricková M. Study of stability of brown-gray inks on paper support. *Heritage Science.* 2015; 3(1): 8.
20. Boyatzis SC, Velivasaki G, Malea E. A study of the deterioration of aged parchment marked with laboratory iron gall inks using FTIR-ATR spectroscopy and micro hot table. *Heritage Science.* 2016; 4(1): 13.
21. Gervais C, Languille MA, Reguer S, Garnier C, Gillet M. Light and anoxia fading of Prussian blue dyed textiles. *Heritage Science.* 2014; 2(1): 26
22. Dillon CE, Lagalante AF, Wolbers RC. Acrylic emulsion paint films: The effect of solution pH, conductivity, and ionic strength on film swelling and surfactant removal." *Stud Conserv.* 2014; 59(1): 52-62.
23. Dekker, N., *Design of Experiments course AkzoNobel.* 2016.
24. Steven G. *Design of Experiments.* In: Loper ML, editor. *Modeling and Simulation in the Systems Engineering Life Cycle: Core Concepts and Accompanying Lectures.* Springer Londen. 2015. p.187-200.
24. Fisher RA. *Statistical Methods for Research Workers.* Cosmo Publications; 1925.
25. Fisher RA. *The design of experiments.* Hafner Pub.Co. 1966.
26. Wahdame B, Candusso D, Fancois X, Harel F, Kauffmann JM, Coquery G. Design of experiment techniques for fuel cell characterisation and development. *Int J Hydrogen Energ.* 2009; 34(2): 967-980.
27. Sakkas VA, Islam A, Stalikas C, Albanis TA. Photocatalytic degradation using design of experiments: A review and example of the Congo red degradation. *J Hazard Mater.* 2010; 175(1-3): 33-44.
28. Nardi JV, Acchar W, Hotza D. Enhancing the properties of ceramic products through mixture design and response surface analysis. *J Eur Ceram Soc.* 2004; 24(2): 375-379.
29. Mashouf G, Ebrahimi M, Bastani S. UV curable urethane acrylate coatings formulation: experimental design approach. *Pigm Resin Technol.* 2014; 43(2): 61-68.
30. Mirabedini SM, Jamali SS, Haghayegh M, Sharifi M, Mirabedini AS, Hashemi-Nasab R. Application of mixture experimental design to optimize formulation and performance of thermoplastic road markings. *Prog Org Coat.* 2012; 75(4): 549-559.
32. Fatemi S, Varkani MK, Ranjbar Z, Bastani S. Optimization of the water-based road-marking paint by experimental design, mixture method. *Prog Org Coat.* 2006; 55(4): 337-344.
32. Webster DC, Chrisholm BJ, Stafslie SJ. Mini-review: Combinatorial approaches for the design of novel coating systems. *Biofouling.* 2007; 23(3): 179-192.
33. Cost optimisation by using DoE. In: *European Coatings Journal.* 2003. <http://www.european-coatings.com/content/download/61481/709701/version/1/file/46842>. Accessed September 2017.

34. Carmen A, Papa J, Gladys R, Blanco B. High quality emulsified paints formulations by mean of a software for the statistical design of experiments. In: Proc. VIII International Conference on Computational plasticity, Barcelona, Spain. 2005
35. Pichavant L, Coqueret X. Optimization of a UV-curable acrylate-based protective coating by experimental design. *Prog Org Coat.* 2008; 63(1): 55-62.
36. Kraber S, Whitcomb PJ, Anderson MJ. Handbook for Experimenters: A Concise Collection of Handy Tips and Statistical Tables to Help You Set Up and Analyze Your Designed Experiments. Stat-Ease. 2007. http://www.statease.com/pubs/handbk_for_exp_v06.8.pdf. Accessed September 2017.
38. Gatti C. Design of Experiments for Reinforcement Learning. Springer International Publishing: 53-66. 2015.
38. Anderson MJ, Whitcomb PJ. Design of Experiments for coatings. Stat-Ease. 2006 https://www.researchgate.net/publication/253843410_Design_of_Experiments_for_Coatings. Accessed September 2017.

PART 3



van Driël carrying out Pall experiments. Photo credit: Art Ness Proano Galbor

Predicting degradation by titanium white pigments

‘Prediction is certainly a valuable goal in science, but not the only one. Explanation is also important, and there are plenty of sciences that do a lot of explaining and not much predicting.’³¹

‘It is better to risk saving a guilty man than to condemn an innocent one.’³²

‘Simplicity is the ultimate sophistication’³³

31 Eric Maskin Read more at: <https://www.brainyquote.com/quotes/quotes/e/ericmaskin726471.html>

32 Voltaire https://www.brainyquote.com/search_results.html?q=risk

33 Leonardo Da Vinci https://www.brainyquote.com/quotes/leonardo_da_vinci_107812

All URL's accessed on 11-12-2017

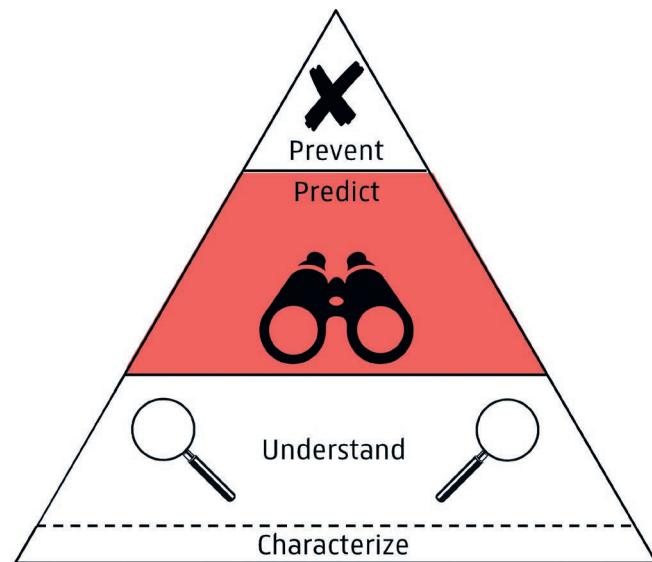
APPROACH PART 3

In chapter 1, pXRF, allows us to determine the presence of titanium white in a non-invasive manner. However, the drawback is that pXRF does not provide information on the photocatalytic activity of the pigment. To overcome this, the aim of part 3 is to develop easy-to-use photocatalytic activity tests. As the bridge between theory and practice, such tests should be developed and implemented in conservation studios as soon as possible.

Given the information about tests already described in the literature and available as ISO standards, the approach is to adjust existing methods {E} to make them applicable for pigments powders and embedded paint fragments.

The envisioned test should predict the likelihood of degradation of a painting by evaluation of the pigment's photocatalytic activity. This is achieved by the development of two test methods that are easy-to-use and accessible. A logical consequence of this requirement is that both tests are based on color change which is observable without analytical equipment.

The first test, in chapter 6, is an adaptation of the dye degradation test {E.2.1}, optimized for pigment powders. The second test, in chapter 7, is the application of photocatalytic activity indicator inks {E.2.2, chapter 7 theory} on paint fragments of cross-sections in analogy with staining tests. The second test in particular can be easily implemented into conservation studios and may have an immediate impact.



Chapter 6

A quick assessment of the photocatalytic activity of TiO₂ pigments – From lab to conservation studio!

Titanium dioxide is the most abundantly used white pigment of the 20th century. The pigment is still in use, both in the production of contemporary art and for the conservation of older artwork as a retouching pigment. Unfortunately, next to its positive characteristics, the pigment has one major potential drawback: its photocatalytic activity that can cause degradation of artworks in which it is used. In this chapter, we report on a new method to test the photocatalytic activity of different quality grades of titanium dioxide white pigments. This can be done quantitatively in a chemical lab or qualitatively in a quick and easy way, in a museum or artists' studio, with limited use of lab equipment. The photocatalytic degradation of an organic dye, acid blue 9, in an aqueous solution containing titanium dioxide, is followed over time by means of UV-Vis spectrophotometry. Dye solutions containing pigments with high photocatalytic activity lose their color within several hours of UVA exposure. On the other hand, dye solutions containing UV-stable titanium dioxide do not degrade within 24 hours of UVA exposure. Insight in the photocatalytic activity of titanium white pigments, which can be obtained with this novel test, is of great importance for preventive conservation of modern art.

Based on the published paper: B.A. van Driel, P.J. Kooyman, K.J. van den Berg, A. Schmidt-Ott and J. Dik (2016), *Microchemical Journal* 126: 162-171.

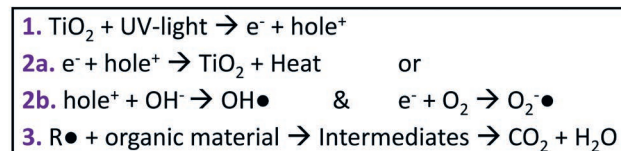
6.1. Introduction

In 1921, when Pablo Picasso was forty years old, a method to produce titanium white pigment on an industrial scale was developed and introduced soon after [1]. Since then he has been using titanium white in his work: a photocatalyst [2], which may cause major damage to his legacy. And he was not the only one ...[1]

Not only is titanium white used in paintings [3-6], it has also found its way into plastic art objects and photographic paper (resin coated prints), leading to degradation problems [7, 8].

6.1.1. Photocatalysis

Titanium dioxide is a known photocatalyst. The photocatalytic degradation cycle is shown in Scheme 6.1. When titanium dioxide absorbs UV light (step 1) a chain of events possibly leading to the production of radicals (step 2b) is initiated. These radicals can attack the surroundings of the pigment and that can cause a breakdown of the organic medium resulting in embrittlement, loss of gloss or chalking (step 3). When colorants, pigments or dyestuffs are involved, the color can also be affected (step 3) [9-11].



Scheme 6.1 Photocatalytic degradation cycle.

If one of the steps leading to radical formation is prevented, the catalytic degradation cycle is stopped. This happens, for instance, when a pigment with an inorganic surface coating is used. In this chapter the term coating or surface coating indicates a coating on the surface of the pigment grains. This treatment is performed during the production of the pigment, prior to the addition of the pigment to the paint. The coating on the pigment particles, often alumina and/or silica, functions as a barrier between charge carriers and surface adsorbents, and prevents radical formation (step 2a). In this case, the pigment has a protective effect on the organic matrix by acting as a UV absorber [12, 13].

The ratio between recombination (step 2a) and radical formation (step 2b) determines for a large part the photocatalytic activity of a titanium dioxide powder. This ratio is affected by a number of characteristics (one of which is the titanium dioxide crystal structure). Two crystal structures of titanium dioxide are used in

the pigment industry: anatase and rutile. In general, literature shows that anatase has the highest photocatalytic activity of the two polymorphs [14, 15]. Several explanations have been proposed for this phenomenon, such as differences in bandgap, recombination rate, charge carrier mobility and mobility of the hydroxyl radical. However, to date no consensus has been reached [14-17].

Several methods exist to assess photocatalytic activity of photocatalytic semiconductors such as titanium dioxide. Test reactions such as the conversion of isopropanol to acetone [18] and dye degradation reactions [19, 20] are commonly described to characterize catalyst powders. However, they require a certain level of expertise and equipment. The same limitation holds for other methods that have been proposed such as photoconductivity measurements [21], the evaluation of CO₂ from an enclosed paint film [22], ESR analysis [23] and full characterization of the pigment. Finally, accelerated aging tests are a valuable tool in the field of paint development. These tests can assess the stability of a paint over time, which, in a paint containing titanium dioxide, can be related to the photocatalytic activity of the pigment. However, these tests are time consuming and cannot be performed on original material [24]. Thus, there are currently no routine methodologies to determine the photocatalytic activity of TiO₂ pigments prior to their use by artists or conservators. The main goal of this chapter is the introduction, description and validation of such a method.

6.1.2. Pigments

Titanium white is a group name for titanium dioxide based white pigments, known in the pigment industry as pigment white 6 (PW6). During the development of titanium white, many pigments with different characteristics have been on the market. First, composite pigments were developed, followed by pure anatase pigments and pure rutile pigments, produced by either the chloride or the sulfate process. The different processes yield pigments with different characteristics and containing different trace elements [1, 6, 25]. A wide variety of inorganic and organic coatings have been employed to decrease the photocatalytic activity or to improve other properties, such as wettability of the pigment [1, 6, 26].

Titanium white pigments used in art before 1940 consist of either composite pigments or pure anatase [1]. After the discovery of rutile, the pigment industry continued the production and supply of anatase for some applications such as artist pigments. Artist paint manufacturer Talens, for instance, switched to rutile for oil paints only in the 1990s and still uses anatase for gouache today [27]. The motivation for the switch in oil paints was partly

based on artists complaining about discoloration of mixtures of titanium white and alizarin lake [28, 29].

Currently, pigments of a very high stability grade [30-32] are available. However, industrial pigments with high photocatalytic activity are also still readily available. Hombitan LW by Sachtleben Chemie GmbH, an anatase grade pigment, is among others recommended for 'road marking paints, lime paints and interior emulsion paints' [33]. Because anatase is the cheaper grade of TiO₂, there is an economic benefit to using it [34].

The above-mentioned facts demonstrate that photocatalytically active titanium dioxide pigments have been, and still are, widely present on the pigment market. It has thus been finding its way into artist paints, restoration materials and industrial paints (which are also used in works of art), posing a serious threat to 20th century restoration works and 20th century art objects.

6.1.3. Motivation and objective

In general, it is wise to do a quick screening of the photocatalytic activity of TiO₂ pigments before using them. When considering putting a work of art on display, one should investigate what type of pigment is present. Insight in the photocatalytic activity of different titanium dioxide pigments, and how this relates to their effect in artworks, is essential to protect our cultural heritage.

Currently, no method is available to do a screening of TiO₂ pigments in a quick and easy way. Therefore, the main objective of this study is to develop a quick test to distinguish the different grades of titanium white pigments based on their photocatalytic activity. The test should be simple, reliable, robust, fast, cheap, easy to use and it should provide quantitative or qualitative results depending on the users' objective.

6.2. Material and methods

6.2.1. Titanium dioxide powders

Ten titanium dioxide powders were collected to evaluate the photocatalytic activity test. The powders have different applications such as catalysts, industrial pigments and artist pigments, and cover a wide range of characteristics (Table 6.1). The TiO₂ powders were acquired from different sources and used without any treatment. Due to confidentiality issues the source of the powders cannot always be disclosed. Some titanium dioxide powders were accompanied by characterization data from the supplier (Table 6.1). Others were analyzed in our laboratories to determine the

most important properties that can influence the photocatalytic activity, such as crystal structure, specific surface area, particle size and surface coating (bold in Table 6.1).

Table 6.1 Titanium dioxide powder properties*. In the text, the titanium dioxide powders are indicated using the code listed in the first column. C indicates a catalyst, I indicates an industrial pigment, A indicates an artist pigment and O indicates an unknown type of pigment ('other').

Code	Structure	Particle Size [nm]	BET [m ² /g]	Coating	Type
C1	Rutile	100	12	Uncoated	Catalyst
C2	Anatase	10	250	Uncoated	Catalyst
I1	Rutile ^{6.1}	190	15	SiO ₂ [10-20%], Al(OH) ₃ [0-10%], ZrO ₂ [0-2%]	Industrial pigment
I2	Rutile	30	60	Al, Si, Zr, polyacohol	Industrial pigment
I3	Anatase ^{6.2}	100	11	Uncoated	Industrial pigment
I4	Rutile	40	40-60	Al(OH) ₃ [5-10%], ZrO ₂ [0-2%]	Industrial pigment
I5	Rutile	300	18	Al, Si, Zr	Industrial pigment
A1	Rutile	175	19	Al, Si	Artist pigment
O1	Anatase	140	8	Polyol coated	Reference collection RCE*
O2	Anatase	80	12	Polyol coated	Hobby pigment (meant to paint textile)

6.1 Coated Rutile, CR in other chapters.

6.2 Uncoated Anatase, UA in other chapters.

*Differences in precision are due to information obtained from the manufacturer vs. obtained by our own analysis. The latter are indicated in bold. *Cultural Heritage Agency of the Netherlands.

Titanium dioxide powders with an unknown crystal structure were characterized using X-ray diffraction (XRD). The diffractometer used during this study is a Bruker D8 Advance with a Cu-K α X-ray source. The crystal structure was determined using the search and match application of the Eva software. The specific surface area (BET area) was determined via nitrogen sorption isotherms at 77 K using a Quantachrome autosorb degasser and autosorb-6B or a Micromeritics TriStar II 3020. The powders were degassed for 16 hours at 200°C to prevent the structural transformation from anatase to rutile which has been reported to happen in a wide temperature range between 400 and 1200°C [35]. The BET area was calculated via the multipoint BET method over a linear range of relative pressures between 0.05 to 0.26 using 20 to 21 data points.

Transmission electron microscopy (TEM) images were obtained using an FEI Tecnai F20 electron microscope, equipped with a FEG and operated at 200 kV. Particle size distributions were determined by hand from the micrographs. Scanning electron microscopy and energy-dispersive X-ray spectroscopy (SEM-EDX) with a JSM5910LV SEM and a ThermoScientific SDD detector or TEM-EDX using the previously described TEM and an Oxford Instruments EDX system were used to investigate inorganic coatings. The copper signal in the TEM-EDX spectra is due to background radiation hitting the copper sample holder grid.

Organic coatings on the TiO₂ powders were investigated by pyrolysis-gas chromatography-mass spectroscopy (Py-GC-MS) using a ThermoScientific Focus GC coupled to a ISQ LT MS using the Xcalibur software and a multi-shot pyrolyzer EGA/Py-3030D. 1 μ l tetramethylammonium hydroxide (TMAH) is added to the samples before injection of the cup.

6.2.2. UV box

A UV box was constructed at Delft University of Technology [2] (Figure 6.1). The UV box has ten spots where beakers can be placed with a magnetic stir unit, of which the 6 central spots ensure similar UV exposure. The UV box was equipped with 8 UV lamps of 18W providing an intensity of 100 \pm 20 μ W/cm², with a wavelength maximum at 365 nm. The temperature in the UV box was kept below 40°C with a water-cooling system.

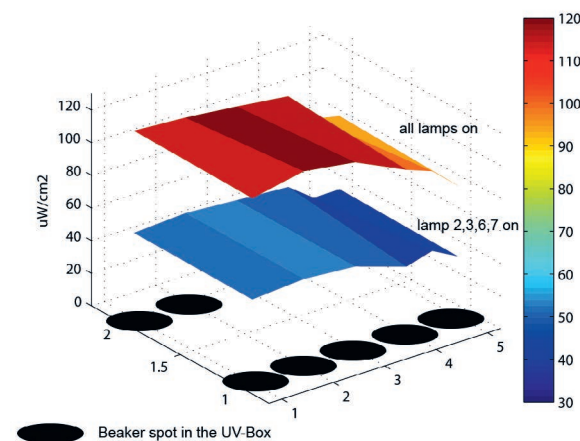


Figure 6.1 UV box with UV intensities measured with all lamps on and with lamps 2,3,6 and 7 on. The distance between the stirring plate and the lamps is approximately 25 cm.

At full intensity, the amount of UV radiation within the UV box is about 27 times as high as in an 'office environment' (Table 6.2), 200 times as high as in a 'low UV office environment', 270 times as high as in a 'high UV dimmed light environment' and 2000 as high as in a 'low UV dimmed light environment' [36]. It is assumed that the degradation time of the dye in the test scales accordingly.

	Illuminance [lumen/m ²] [36]	Illuminance [lumen/Beaker area]	UV-content [μ W/lumen][37]	UV- light per beaker [μ W]	Ratio
UV-box	-	-	-	3630	
Office environment	500	1.82	75	135	27
Low UV office environment	500	1.82	10	18	202
High UV dimmed light environment	50	0.18	75	13.5	269
Low UV dimmed light environment	50	0.18	10	1.8	2017

Table 6.2 Ratio of UV in the UV box to real indoor situations (beaker area = 36.3 cm², luv box=100 μ W/cm²).

6.2.3. Photocatalytic activity test

The test developed in this study, further referred to as the ‘developed test’ or the ‘standard test’, is a dye degradation test. Similar experimental setups have been reported in literature [19, 38-40]. Each test is optimized for a specific purpose but all these tests have a similar approach. An organic dye is dissolved in a liquid to which the active powder, in this case titanium dioxide, is added. The dispersion is properly mixed and irradiated by, in this case UVA, light. At time intervals samples are taken from the beaker and the dye solution is separated from the powder and subsequently analyzed by UV-Vis spectrophotometry.

The developed test is based on a method, further referred to as the ‘base test’, designed to determine the photocatalytic activity of titanium dioxide catalyst powders [2]. Several problems occurred with the base test, which required adjustments and thus the development of a new test for a new purpose: determining the photocatalytic activity of titanium dioxide pigment powders.

Table 6.3 describes the parameters that were adjusted during the development of the test and indicates the reason for the adjustment. This section further describes the developed test and the development process in detail.

Table 6.3 Adjustments made for test development.

Parameter	Base test [2]	Developed test	Reason for adjustment
Dye	Methylene blue	Acid Blue 9	Methylene blue adsorbs on surface coating of pigments
Volume dye solution	100 ml	10-100 ml	Scale down
Mass TiO ₂	50 mg	5-50 mg	Scale down
Separation for analysis	PTFE Millipore membrane filter	Sedimentation by centrifugal force	PTFE filter malfunctions with dispersion agent and clogs with large TiO ₂ particles
Dispersion aid	Ultrasonic bath	1% v/v Calgon	Pigments with a surface coating do not disperse properly

6.2.3.1. Adjustments during test development

The methylene blue used in the base test [2] adsorbs on the silica coating of some titanium white pigments which disturbs the result of the test [41]. It was substituted with acid blue 9 (Erioglaurine disodium salt, referred to as AB9, used as received from Sigma-Aldrich) [42].

Titanium dioxide pigment powders, when coated, are difficult to disperse in water and a dispersing agent needs to be added. The dispersion agent was chosen based on a tradeoff between quality

of dispersion and effect on the photocatalytic degradation process. The chosen dispersion agent is a sodium polyphosphate solution [100 g/L] (further referred to as Calgon) used as received from Tronox. Two batches were used; one received in 2012 and one received in 2015. When Calgon is used, the ultrasonic bath has a negligible benefit on the dispersion and therefore on the final AB9 degradation rate. However, it is important to employ constant stirring to avoid the titanium dioxide powder to settle on the bottom of the beaker.

When performing the test with the dispersion agent, the previously used filters [2] to separate the dye solution from the TiO₂ prior to UV-Vis analysis did not function. Furthermore, the filters clogged due to the larger particle size of the pigment powders. The new separation method is sedimentation of the titanium dioxide powder using an Eppendorf centrifuge for 2 runs of 5 min at 5000 rpm.

6.2.3.2. Developed/Standard test

50 mg of TiO₂ powder was dispersed in a 100 ml 0.03 mM acid blue 9, 1% v/v Calgon solution. The dispersion was stirred with a spatula for initial mixing. A magnetic stirrer was added to the dispersion and the beaker was covered with a watch glass. The beaker was put on a stirring plate in the UV box. At time intervals samples (4 ml) were taken from the beaker and centrifuged twice for 5 minutes at 5000 rpm in a Savant Speedfuge HSC10 AC. Between the two runs, the supernatant was transferred to a clean Eppendorf centrifuge tube to separate it from the titanium dioxide. The solution was analyzed with a UV-Vis spectrophotometer, Unicam UV 500, at 630 nm and the concentration of acid blue 9 was evaluated with Vision software according to a calibration line (Equation 1).

$$C(AB9)=0.012+0.0001; R^2=0.99 \quad (1)$$

Degradation curves were fitted by a first order exponential decay (Equation 2), which yields a value for the reaction rate coefficient. For the degradation curves that do not reach $C(t)=0$ mM, this fit has an error due to manual extrapolation.

$$C(t)=C_0E^{-kt} \text{ with } C(0)=0.03 \text{ mM} \quad (2)$$

6.2.3.2. Effect of operational parameters

Operational parameters such as temperature, stirring speed, UV intensity, initial concentration of dye and titanium dioxide loading can have an effect on the results [43]. If the test is performed in a

comparative manner and these parameters are kept constant, the categorizing of pigment grades is accurate. Nevertheless, these parameters were investigated in order to obtain insight into the order of magnitude of these variations and to investigate the feasibility of downscaling.

Effect of UV intensity, temperature and stirring speed

The effect of UV intensity on the degradation time is investigated by performing the test at full and half UV intensity. Experiments were performed with eight lamps on (standard) and with four lamps on. Turning four lamps off (positions 1,4,5,8) reduces the UV intensity by approximately 50% (Figure 6.1).

The effect of stirring speed was investigated by performing the experiments at different stirrer settings on the magnetic stirring plate (setting 2-5). The effect of temperature was investigated in the range between 29 and 39°C. The temperature was monitored using a thermometer connected to the UV box and adjusted with the water-cooling system.

Scale down

The possibility of scaling down the test is considered in case only small amounts of pigment powders are available. Two different downscaling strategies were considered. First, reducing the absolute amount of powder. This changes the TiO₂:AB9 solution ratio or pigment loading (category 1). Second, scaling down the total experiment while keeping the TiO₂:AB9 solution ratio constant (category 2). The experiments were carried out with titanium dioxide powders C2, I3 and O1 (Table 6.1). Because of the smaller volume of the experiments, smaller aliquots (1ml) were removed at time intervals. Consequently 1 ml cuvettes were used. Furthermore, influencing effects were investigated such as liquid surface to volume ratio (category 3), type of glassware (extension B) and Calgon age (extension N). Finally, fragments of the paint reconstructions of titanium dioxide powders I3 and O1 were scraped off their support and tested without further treatment. In this case the available amount of scraping was used. With knowledge of the pigment volume concentration, this amount is calculated back to an approximate mass of TiO₂ in the acid blue 9 solution, which is not necessarily equal to 50 mg. The specifications of the experiments are summarised in Table 6.4.

Experiment code	Volume of AB9 solution (0.03 mM) [ml]*	Mass of TiO ₂ [mg]	Category	Category	Remark	n
I3-25/50	50	25	2	2	Experiment in 250 ml beaker	6
I3-10/20	20	10	2	2	Experiment in 50 ml, small neck bottle	4
I3-10-20B	20	10	2	2	Experiment in 50 ml beaker	2
I3-5/10	10	5	2	2	Experiment in 50 ml, small neck bottle	2
I3-5/10B	10	5	2	2	Experiment in 50 ml beaker	1
I3-25/100	100	25	1	1	Experiment in 250 ml beaker	4
I3-10/100	100	10	1	1	Experiment in 250 ml beaker	2
I3-5/100	100	5	1	1	Experiment in 250 ml beaker	3
I3-50/100	100	50	Standard and 3	Standard and 3	Experiment in 250 ml beaker	3
I3-50/100N	100	50	Standard	Standard	Experiment in 250 ml beaker New batch of Calgon	1
O1-25/50	50	25	2	2	Experiment in 250 ml beaker	2
O1-10/20	20	10	2	2	Experiment in 50 ml, small neck bottle	2
O1-5/10	10	5	2	2	Experiment in 50 ml, small neck bottle	2
C2-50/100Z	100	50	Standard	Standard	Experiment in 250 ml beaker No Calgon added	1
C2-50/100N	100	50	Standard	Standard	Experiment in 250 ml beaker New batch of Calgon	1
I3-100/200	200	100	3	3	Experiment in 250 ml beaker	1
I3-75/150	150	75	3	3	Experiment in 250 ml beaker	1
I3-25/50	50	25	3	3	Experiment in 250 ml beaker	1
I3-12.5/25	25	12.5	3	3	Experiment in 250 ml beaker	1
I3-paint-1	100	53**	Paint	Paint	119 mg paint, dried approximately 2 months	1
I3-paint-2	100	65-100**	Paint	Paint	156 mg paint, dried approximately 6-8 months	1

Table 6.4 List of downscaling experiments. The code name consists of TiO₂ code-mass TiO₂/Volume AB9 solution*-extension explained in the remark column. n represents the number of times the test was performed.

*the AB9 solution contains 1 vol% of Calgon solution, except if stated otherwise in remark column.

** TiO₂ mass in paint fragments is an estimate based on mass of the paint film and initial pigment volume concentration.

6.2.3.3. Further test development

To use the test in conservation practice as a qualitative evaluation, the use of lab equipment should be limited. The UV box may be replaced by any UVA source available, as the degradation time scales directly with the UV intensity. The separation step, which is necessary to do UV-Vis spectrophotometry, can be skipped for qualitative evaluation because a visual evaluation of the dye degradation can be done with a color scale or with reference dispersions. For the production of this color scale, a range of TiO₂/AB9 dispersions with different acid blue 9 concentrations has been produced and photographed (Figure 6.7).

6.2.3. Paint reconstructions

Paint reconstructions were prepared as a preliminary assessment of the predictive character of this test. The reconstructions were evaluated with respect to chalking after UV exposure (qualitative visual assessment). Degradation of the binder material causes the pigment to appear unbound at the surface, this phenomenon is called chalking.

Paint reconstructions were prepared of all ten titanium dioxide powders (Table 6.5). All reconstructions, with the exception of samples I3 and O2, were prepared and investigated in 2012 at Tronox and Delft University respectively. The samples were prepared by mixing pigment with hot-pressed linseed oil with an added drier. The drier, provided by Tronox and used without any treatment, was a mix of industrial driers with 0.15% w/w calcium drier, 0.20% w/w zirconium drier and 0.05% w/w cobalt drier with respect to the oil. Reconstructions of I3 and O2 were prepared and investigated at the RCE in 2014. Again pigment was mixed with, in this case, bleached linseed oil obtained from van Beek. Talens Siccatief de Courtai was used as a drier, one drop was added to approximately three grams of paint.

The paints were mixed with a pigment-volume-concentration (PVC) ranging between 15 and 40% and ground on an automatic muller. At Tronox a Mimex type 2000 was used and at the RCE a similar model was used. The muller was operated 3 times 25 rotations employing a weight of 5 kg. A pallet knife was used to handle the paint during the grinding of pigments and the paint application. The paints were then spread on Leneta cards at Tronox or on a piece of melinex at RCE, using an applicator with a layer thickness of 200 µm.

The paint reconstructions were irradiated by UVA lamps in the UV box described previously or in a similar UV box at RCE and visually evaluated for chalking. Further investigation of the surface was done by imaging the surface using SEM. To this end, the paint reconstructions were gold coated for 15 seconds with a JEOL JFC-1200 fine coater using a vacuum of 45 Pa at a working distance of approximately 5 cm. The SEM was operated in high vacuum mode.

Table 6.5 Preparation of paint reconstructions.

*Unknown brand, purchased at a paint store.

Paints	Oil	Drier	Muller	Support	Layer thickness	Location	Year
C1, C2, A1, O1, I1, I2, I4, I5	Hot-pressed linseed oil*	Industrial drier provided by Tronox (Ca, Zr, Co)	Mimex type 2000	Leneta card	200 µm	Tronox & TU Delft	2012
I3, O2	Bleached linseed oil, van Beek	Siccatief de Courtai, Talens	Similar model	melinex	200 µm	RCE	2014

6.3. Results and discussion

6.3.1. Test evaluation

The developed test was evaluated with respect to feasibility, the effect of the dispersing agent and the reproducibility. Furthermore, we aim to relate the developed test to surface degradation of reconstructed paints, which is discussed in this section as well.

6.3.1.1. Feasibility

Figure 6.2A demonstrates that acid blue 9 without TiO₂ does not degrade under UV irradiation and that acid blue 9 with TiO₂ without UV irradiation also does not degrade. We can thus conclude photocatalysis is the degradation mechanism.

Figure 6.2 and Table 6.6 illustrate the initial results of the ten titanium dioxide powders measured with the developed test. Based on the results, the titanium dioxide powders were divided into four different categories: stable pigments (Figure 6.2A) and fast (Figure 6.2B), intermediate (Figure 6.2C) and slow (Figure 6.2D) degradation. We defined the categories in terms of reaction rate coefficients (Table 6.7).

Categories fast and intermediate degradation (Figure 6.2B and 6.2C) correspond to anatase and rutile without inorganic coating. All the anatase powders without inorganic coating (Figure 6.2B), with different characteristics, degrade the dye faster than the rutile powder without inorganic coating (Figure 6.2C). This confirms that rutile is less active than anatase. The ‘fast degradation’ category has two subsections (Table 6.7). The two less active anatase powders O1 and O2 (Figure 6.2B) correspond to the powders with a polyol coating. It seems that the organic surface treatment has an influence on the photocatalytic activity, possibly by occupying surface absorption sites. Within the group of anatase powders (see Figure 6.2B) powder I3 is interesting. This product, Hombitan LW from Sachtleben Chemie, is advised for use in interior paints as discussed in the introduction. Remarkably, it is illustrated here that it has a similar photocatalytic activity as Hombikat UV-100 (C2) from the same company, which is produced to be a highly active catalyst. The differences between the rutile powders with an inorganic coating (Figure 6.2A vs. 6.2D) are possibly due to the different qualities of the pigment coatings: an incomplete coating can offer active sites for photocatalysis.

These results would not have been obtained with the base test, thus the test proves its feasibility and worth.

Figure 6.2 Feasibility of the photocatalytic activity test – Degradation of acid blue 9 over time. The results are categorized in four categories: (A): Blanks and stable pigments, (B): Fast degradation which has two subcategories, (C): Intermediate degradation and (D): Slow degradation.

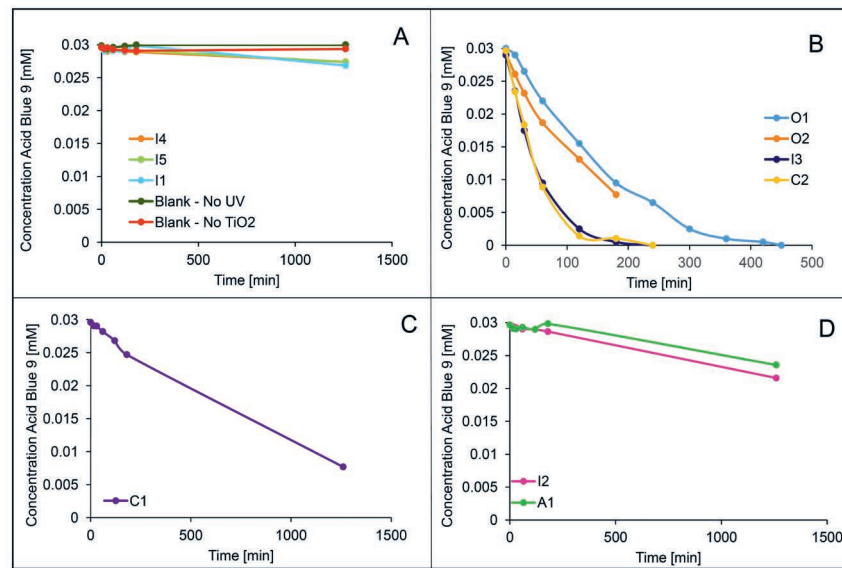


Table 6.6 Reaction rate coefficients calculated based on a first order exponential decay fit and evaluation of chalking of paint reconstruction after artificial UV aging two months.

Code	k [min ⁻¹]	Category	Chalking [yes/no]
C1	0.001	Intermediate	No
C2	0.018	Fast	Yes
I1	5.9E-5	Stable	No
I2	0.00025	Slow	No
I3	0.016	Fast	Yes
I4	3.2E-5	Stable	No
I5	3.8E-5	Stable	No
A1	0.00018	Slow	No
O1	0.005	Fast	Partially*
O2	0.007	Fast	Yes

*The edges of the paint film, which are thinner than the rest of the film, show chalking.

Table 6.7 Degradation categories in terms of reaction rate coefficients.

Category	k range [min ⁻¹]
Fast	k > 0.0025 Sub-categories: k > 0.015 0.0025 < k < 0.015
Intermediate	0.0005 < k < 0.0025
Slow	0.0001 < k < 0.0005
Stable	k < 0.0001

If the UV ratios described in from Table 6.2 are assumed, as well as the direct relation between degradation rate and UV intensity; extrapolation of the results yields a degradation time of the dye in a dispersion with stable titanium dioxide (I5) of 60 days (UV Box) to 300 years (dimmed light, low UV environment, 50 Lux@10 μW/lumen). In comparison, for the dye in a dispersion with an unstable pigment (C2) this range is 200 min (UV box) to 280 days (dimmed light, low UV environment). For the dye in a dispersion with an intermediate pigment (A1) this is 13 days (UV box) to 60 years (dimmed light, low UV environment). Since this test deals with a well-mixed system, these times will be much higher for real paints systems. Nevertheless, the time frame for anatase-mediated degradation is alarming!

Dispersion agent

The dispersion agent has an effect on the degradation rate (Figure 6.4): the reaction rate coefficient is 1.6 times smaller with the addition of the dispersion agent. This can have several reasons. Firstly, the Calgon acts on the surface of the pigment where it may block some of the radical formation by occupying surface sites. This is similar to the effect of an organic coating on the photocatalytic activity. Secondly, the addition of an excess of Calgon can change the pH of the solution and supply ions (sodium and phosphate) to the dispersion. A change in pH can alter the surface charge of titanium dioxide and therefore affect the dye adsorption to the surface [19]. Furthermore, ions present can interact with the radicals further influencing the degradation rate [19]. The effect of Calgon is assumed to be the same for each experiment, therefore the relative photocatalytic activities evaluated with the test are not affected. In fact, adding two or ten times more Calgon had no effect on the degradation rate. This suggests that it is in fact the Calgon surface monolayer which is rate-determining.

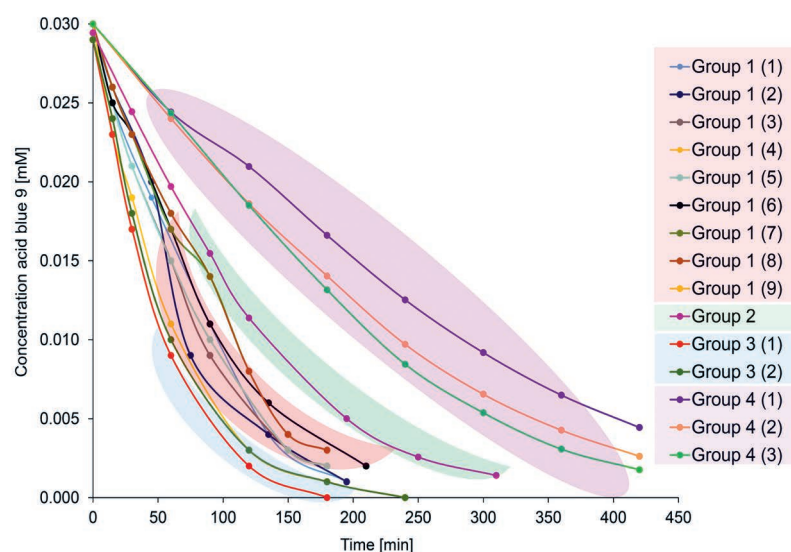
6.3.1.2. Reproducibility

For the envisioned application, the test should classify the pigments in terms of their photocatalytic activity (pigment grade). Since many parameters can influence the test results [43], the test should be performed in a comparative way by including a known stable and a known catalytic powder as references.

Figure 6.3 illustrates two types of variation of test results, first the variation per team of researchers (within a group) and second the variation between the different teams (between the groups). Each group, indicated by a different color, represents a different team of two researchers performing the experiments. To investigate reproducibility, the experiments with titanium dioxide I3 under

standard conditions (50mg TiO₂, 100 ml AB 9 dye solution, 1%vol/vol Calgon) are compared. In group 1 temperature (range 29-33 °C) and stirring speed (setting 2-5) were varied to investigate operational parameters. However, no clear trends were observed, therefore these experiments can be added to this comparison.

Figure 6.3 Degradation of acid blue 9 - Indication of reproducibility. Degradation curves of 13 experiments under standard conditions. The different groups indicate different researchers performing the test at different moments between 2012 and 2015.



The variation within each group is understandable and is attributed to the experimental error because the experiment consists of many steps, there is a slight variation of UV intensity per beaker spot, there is a warm-up time for the lamps to reach full intensity which is not always taken into account and the ambient temperature of the lab can fluctuate.

The variations between the different groups are not well understood. However, the effect on each TiO₂ powder is similar and therefore classification can still be done accurately. Some equipment change took place, however this does not explain the differences in the results. Figure 6.4 shows the variation of results within one group of experiments performed without the addition of the dispersion agent Calgon. This indicates that it is not the presence of Calgon which causes the variation in results.

It is clear from these results that it is important to perform the test in a comparative fashion (by one team of researchers) with a known catalytic and a known stable standard in order to perform proper classification.

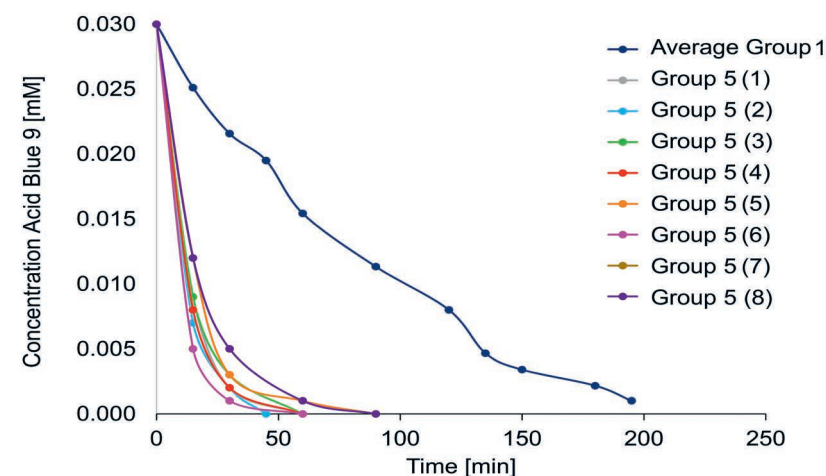


Figure 6.4 Influence of Calgon on the degradation of acid blue 9 – Group 5: Degradation curves of 13 experiments under standard conditions without Calgon. Average Group 1: Average of degradation curves (Group 1) shown in Figure 6.3, experiments with Calgon.

6.3.2. Paint degradation

Figure 6.5 shows the clear difference in morphology of the paint surface of a chalked (A) and a non-chalked (B) paint film after artificial UV aging. The chalked paint is clearly rough compared to the non-chalked paint, caused by the free pigment particles on the paint film surface.

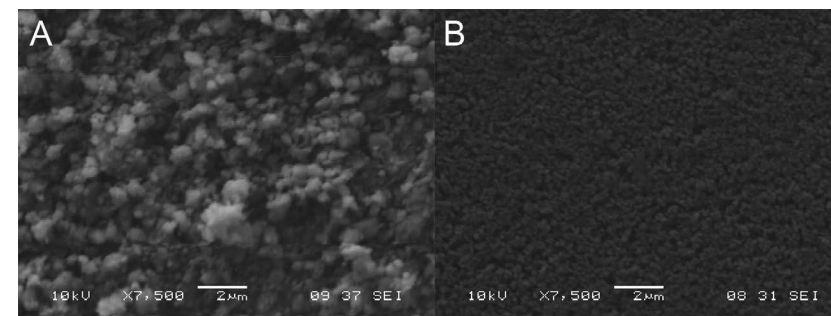


Figure 6.5 SEM picture of a chalked paint surface, C2 (A) and a non-chalked paint surface, I1 (B) after 2 months of accelerated aging.

Table 6.6 shows that all the paints with titanium dioxide powders from the category 'fast degradation' exhibited chalking within two months of artificial aging by UV radiation, whereas all the other paints did not. It is therefore concluded that the measured photocatalytic activity is a good indication for the stability of a simple (pigment+binder) paint system.

It is assumed, for simplicity, that the 200 minutes exposure that leads to dye degradation in the photocatalytic activity test of

powder I3 and C2 (Figure 6.2A) directly correlates to the two months exposure leading to chalking of the paint-out. Within this assumption, the degradation of a reconstructed paint film with pigment from the category ‘fast degradation’ would lead to damage in a dimmed light low UV environment (50 Lux@10 μ W/lumen) within 340 years. This time decreases in environments with higher light intensity and UV content to 32 years (500 lux@10 μ W/lumen) and 5 years (500 lux@75 μ W/lumen). On the other hand, a pigment of the category ‘stable’ will not affect its binder for thousands of years. It is therefore essential for risk assessment and preventive conservation to have an indication of the photocatalytic activity of the pigment.

6.3.3. Effect of operational parameters

The effect of temperature within the range of 29-39°C and stirring speed (setting 2-5) did not have a clear effect on degradation speed (Figure 6.3, group 1).

6.3.3.1. The effect of UV intensity

Table 6.8 shows the effect of UV intensity on the reaction rate coefficient. Reducing the UV intensity by approximately half caused a decrease in reaction rate coefficient of 1.6 times for powder I3 and of 2.3 times for powder O1. Taking into account the variation in the photocatalytic activity test shown in Figure 6.3 and the fact that 4 lamps yield approximately half the UV intensity including some slight variations inside the UV box (Figure 6.1), this suggests that the decrease in UV intensity is directly correlated to the decrease in reaction rate coefficient.

Table 6.8 Reaction rate coefficients for the developed test with powders I3 and O1 at different exposure conditions, calculated based on a first order exponential decay fit.

Code	k_4 lamps [min ⁻¹]	k_8 lamps [min ⁻¹]	k_8 / k_4
I3	0.010	0.016	1.6
O1	0.002	0.005	2.3

These results are in agreement with the review by Zangeneh et al. [43] who describe different relationships between degradation rate and UV intensity at low, intermediate and high UV intensities. The threshold intensity between low and intermediate intensity is a factor 200 higher than the intensities used in this experiment meaning that we operate at low intensity according to this scale. The results also corresponds to the results obtained by Egerton et al. [10] who observe a direct correlation of isopropanol to acetone conversion rate to UV intensity at low UV intensities. The threshold intensity between low and intermediate intensity is a factor 10 to 20 higher than the intensities used in this experiment.

6.3.3.2. Scale down

Figure 6.6 provides an overview of the downscaling results. The main experiments were performed with titanium dioxide powder I3. Figure 6.6A shows the effect of decreasing the total size of the experiment while keeping the TiO₂:AB9 solution ratio constant. The plot demonstrates that decreasing the scale in this fashion decreases the remaining acid blue 9 concentration after five hours of exposure, thus the degradation proceeds faster. No change in degradation rate was expected. This result is explained by the investigation of the effect of liquid surface to volume ratio in the beaker. The investigation shows that higher surface to volume ratio systems degrade faster. The 100 ml and 50 ml experiments were both carried out in a 250 ml beaker, and since the amount is fairly large, taking a sample does not influence the surface to volume ratio significantly. However, 20 ml and 10 ml experiments were carried out in a 50 ml beaker and taking out a 1 ml sample strongly influences the volume of the experiment, causing an increase of the surface to volume ratio and thus an increase of degradation rate.

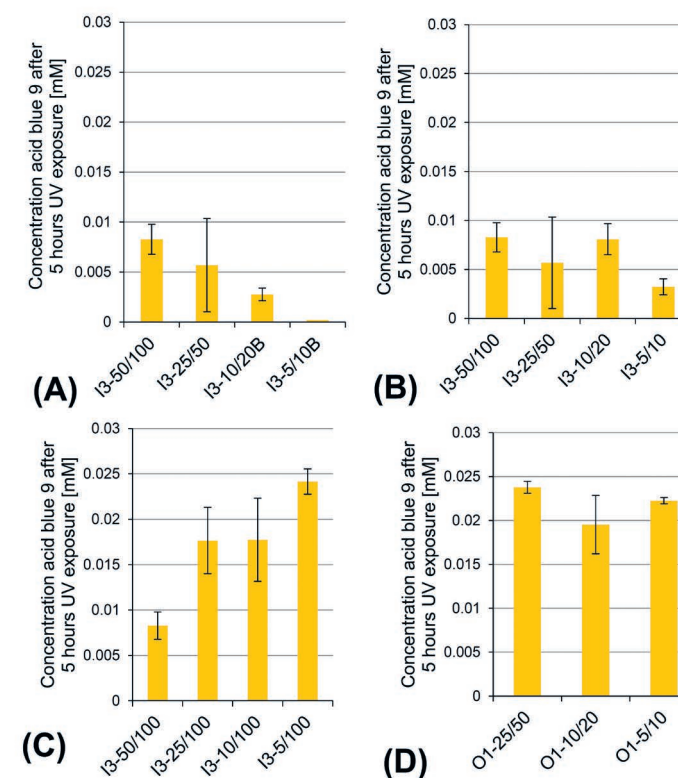


Figure 6.6 Results of downscaling. Concentration of acid blue 9 after 5 hours of UV exposure. A) Powder I3, category 2, B) Powder I3, category 2, using a 50 ml small neck bottle for the 20 ml and 10 ml experiments, C) Powder I3, category 1, D) Powder O1, category 2, using a 50 ml narrow-necked bottle for the 20 ml and 10 ml experiments. Experiments are summarized Table 6.4.

This is also confirmed by the degradation plots as a whole. The first data points of the experiments follow the same trend, however, when the surface to volume ratio starts to be significantly affected, these trends start to differentiate. A higher surface to volume ratio causing a higher degradation rate may be explained by a higher oxygen content per volume (entering the dispersion through the liquid surface) and a higher UV irradiation per volume (reaching the beaker mostly from above). Both effects are expected to increase the degradation rate.

Figure 6.6B and 6.6D illustrate the results of the same experiments that do not show the rate-increasing trend. This is due to the glassware. The small volume experiments illustrated in Figure 6.6B and 6.6D (10 and 20 ml) were carried out in a narrow-necked bottle instead of a beaker (Table 6.4). This influences the liquid surface and thus the surface to volume ratio with the above-described consequences. Furthermore, the glass was rather thick which could result in some UV filtering thereby decreasing the UV-intensity. The rate-increasing trend shown in Figure 6.6A is compensated by the rate-decreasing trends caused by doing the experiment in the bottle.

Finally, Figure 6.6C shows that decreasing only the absolute amount of titanium dioxide decreases the degradation rate as was expected.

In general, the results demonstrate that scaling down the test is feasible. However, going below 5 mg of TiO₂ leads to practical problems. Furthermore, new effects, such as surface to volume ratio, cannot be neglected.

6.4. Further development

6.4.1. Color scale

Figure 6.7 illustrates the color scale and the reference dispersions used to make the scale. The usability of the reference dispersions was assessed by asking researchers to estimate the acid blue 9 concentration. The concentration was subsequently evaluated by UV-Vis spectrophotometry. All researchers were successful in the estimation of the acid blue 9 concentration based on the reference dispersions attesting to the power of this visual method.

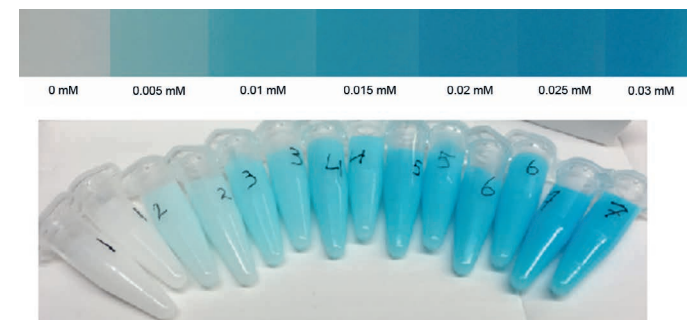


Figure 6.7 Color scale and reference dispersions. The reference dispersions contain TiO₂ powders and a known concentration of AB9 dye.

6.4.2. Testing reconstructed paint fragments

Figure 6.8 shows the results of the degradation test performed on paint fragments of reconstructed paints. This is a test for real object applicability and it gives an indication that separation of pigment and binding media is not necessarily required. Degradation of acid blue 9 happens five to ten times slower than for the same pigment as a loose powder. This is expected because the pigment surface, where radicals are formed, is not easily accessible for the organic dye. Some binder may need to be degraded before the radicals reach the dye and start the degradation mechanism. Nevertheless, this result is promising for further development in the applicability of this test for the field of conservation. Paint 1 degrades slower than paint 2 due to the lower pigment loading (Table 6.4).

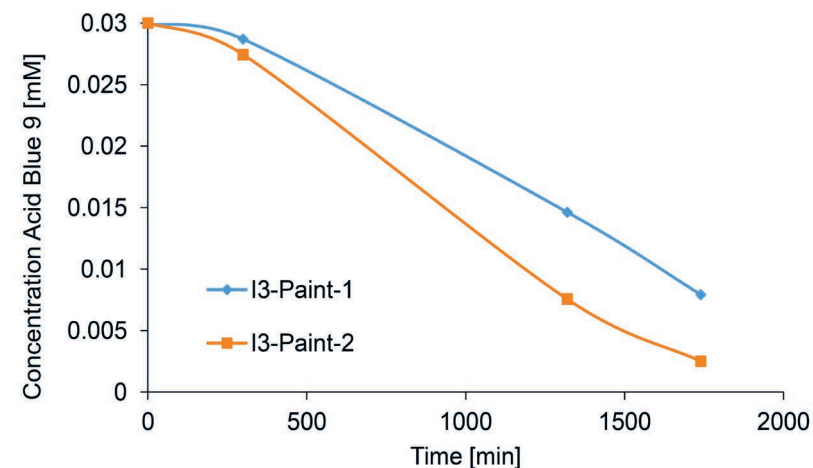


Figure 6.8 Acid blue 9 degradation of paint fragments in suspension.

6.5. Conclusions

A test was developed to assess the photocatalytic activity of titanium dioxide pigments in a comparative manner. Several parameters influencing the test have been investigated. The proposed test is based on existing dye degradation tests commonly used in the field of catalysis engineering. The base test proved to be inadequate for direct use in our application. The main problem of the existing methodology was the absorption of the methylene blue dye to the pigment surface and dispersion of the pigment powders into the dye solution. This prevents proper assessment of the photocatalytic activity of pigment powders. In this study, we have shown that these limitations can be overcome using acid blue 9 as an alternative for methylene blue and by adding a dispersion agent. The new test distinguishes between four categories of stability and relates well to chalking of artificially aged reconstructed paint-outs. Our main innovative contribution is therefore that a quick and easy test is now available for quantitative and qualitative assessment of titanium dioxide pigment photocatalytic activity. This was previously not possible without expertise, complex equipment or very time-consuming accelerated aging procedures. The test is especially suitable for powder material. We are currently considering the assembly of a toolkit which could be made available to potential users. Furthermore, the first steps have been taken to design a test suitable for real object samples. It has been demonstrated that the test is not chemically limited in sample size, which means that only the practical aspects need to be tackled for further developments of the test.

Acknowledgements

This work is facilitated by the Rijksmuseum Amsterdam and financially supported by AkzoNobel, who also provided some of the tested TiO₂ powders. Further materials were provided by Tronox (TiO₂, driers and dispersing agents), Sachtleben Chemie (TiO₂) the van Gogh museum (TiO₂) and the RCE reference collection (TiO₂). The automatic miller used at RCE is on permanent loan from Old Holland. The authors are thankful for these contributions. Several experiments have been carried out by students Molecular Science and Technology (D. van den Berg, I. du Fossé, R. Verheijen F. van Dockum, E. Remmelts and S. Pahud de Mortange) from Delft University of Technology and by high school students Max Koster and Michel Pan. Willy Rook and Ben Norder have contributed to BET and XRD analysis performed at Delft University of Technology. Bart van der Linden has been a great help during the laboratory work. Furthermore, the authors would like to acknowledge Henk van Keulen and Ineke Joosten at Cultural Heritage Agency of the Netherlands (RCE) for their help with Py-GC-MS and SEM-EDX analysis.

References for chapter 6

1. M. Laver (1997). Chapter 10: Titanium white. In: E.W. Fitzhugh (Ed.), *Artists' Pigments: Volume 3: A Handbook of their History and Characteristics* (pp. 295-355). National Gallery of Art. DOI: 10.2307/1506685
2. Du, P., Bueno-López, A., Verbaas, M., Almeida, A. R., Makkee, M., Moulijn, J. A., & Mul, G. (2008). The effect of surface OH-population on the photocatalytic activity of rare earth-doped P25-TiO₂ in methylene blue degradation. *J. Catal.*, 260, 75-80. doi: <http://dx.doi.org/10.1016/j.jcat.2008.09.005>
3. de Keijzer, M., de Groot, S., Megens, L., & Van Keulen, H. (2008). Schildertechnisch onderzoek aan Mondriaans Compositie met rood, zwart, geel en grijs uit 1920. *Unpublished results*. Instituut Collectie Nederland.
4. de Keijzer, M. (1989). The colourful twentieth century. In: S. Fairbrass & J. Hermans (Eds.), *Modern Art: the restoration and techniques of modern paper and paints* (pp. 13-20). United Kingdom institute of Conservation. ISBN: 1871656044
5. van den Berg, K.J., Miliani, C., Aldrovandi, A., Brunetti, B. G., de Groot, S., Kahrim, K., de Keijzer, M., van Keulen, H., Megens, L., Sgamellotti, A. and van Bommel, M. R. (2012). Chapter 7: The Chemistry of Mondrian's paints in Victory Boogie Woogie. In: M. R. van Bommel, H. Janssen, R. Spronk (Eds.), *Inside Out Victory Boogie Woogie*. Amsterdam: Amsterdam University Press. ISBN: 9789089643735
6. de Keijzer, M. (2002). The history of modern synthetic inorganic and organic artists' pigments. In: J.A. Mosk & N.H. Tennent (eds.) *Contributions to conservation: research in conservation at the Netherlands Institute for Cultural Heritage*. James & James (Science Publishers) Ltd. ISBN: 1-902916-09-3
7. van Oosten, T. B., Fundeanu, I., Bollard, C., Castro, C. d., & Lagana, A. (2008). Lights out! The conservation of polypropylene wall tapestries. In B. Keneghan & L. Egan (eds.) *Plastics. Looking to the future and learning from the past*. Archetype Books. ISBN: 1904982433
8. Parsons, T. F., Gray, G.G. & Crawford, I.H. (1979). To RC or not to RC. *J. Appl. Photogr. Eng.*, 5(2), 110-117.
9. Völz Hans, G., Kaempfer, G., Fitzky Hans, G., & Klaeren, A. (1981). The Chemical Nature of Chalking in the Presence of Titanium Dioxide Pigments. In: F.H. Winslow (Ed.) *Photodegradation and Photostabilization of Coatings, Acs symposium series* (Vol. 151, pp. 163-182). American Chemical Society.
10. Egerton, T. A., & King, C. J. (1979). The influence of light intensity on photoactivity in TiO₂ pigmented systems. *J. Oil Col. Chem. Assoc.*, 62, 386-391.
11. Allen, N. S., Edge, M., Ortega, A., Sandoval, G., Liauw, C. M., Verran, J., Stratton, J. and McIntyre, R. B. (2004). Degradation and stabilisation of polymers and coatings: nano versus pigmentary titania particles. *Polym. Degrad. and Stabil.*, 85(3), 927-946. doi:<http://dx.doi.org/10.1016/j.polymdegradstab.2003.09.024>
12. Blakey, R. R. (1980). The role of Titanium dioxide in the protection of Paint Media. In: *Tioxide technical service report D 9104 GC*.
13. Hare, C. H. (1992). The degradation of coatings by ultraviolet light and electromagnetic radiation. *JPCL*
14. Kim, W., Tachikawa, T., Moon, G.-h., Majima, T., & Choi, W. (2014). Molecular-Level Understanding of the Photocatalytic Activity Difference between Anatase and Rutile Nanoparticles. *Angew. Chem. Int. Ed.*, 53(51), 14036-14041. doi: 10.1002/anie.201406625
15. Scalfani, A., & Herrmann, J. M. (1996). Comparison of the Photoelectronic and Photocatalytic Activities of Various Anatase and Rutile Forms of Titania in Pure Liquid Organic Phases and in Aqueous Solutions. *J. Phys. Chem.*, 100(32), 13655-13661. doi: 10.1021/jp9533584

16. Linsebigler, A. L., Lu, G., & Yates, J. T. (1995). Photocatalysis on TiO₂ Surfaces: Principles, Mechanisms, and Selected Results. *Chem. Rev.*, 95(3), 735-758. doi: 10.1021/cr00035a013
17. Christensen, P. A., Dilks, A., Egerton, T. A., & Temperley, J. (2000). Infrared spectroscopic evaluation of the photodegradation of paint Part II: The effect of UV intensity & wavelength on the degradation of acrylic films pigmented with titanium dioxide. *J. Mater. Sci.*, 35(21), 5353-5358. doi: 10.1023/A:1004898913140
18. Irick, G. (1972). Determination of the photocatalytic activities of titanium dioxides and other white pigments. *J. Appl. Polym. Sci.*, 16(9), 2387-2395. doi: 10.1002/app.1972.070160917
19. Rauf, M. A., & Ashraf, S. S. (2009). Fundamental principles and application of heterogeneous photocatalytic degradation of dyes in solution. *Chem. Eng. J.*, 151(1-3), 10-18. doi: http://dx.doi.org/10.1016/j.cej.2009.02.026
20. Doushita, K., & Kawahara, T. (2001). Evaluation of Photocatalytic Activity by Dye Decomposition. *J. Sol-Gel Sci. Technol.*, 22(1-2), 91-98. doi: 10.1023/A:1011220505116
21. Chin, J., Scierka, S., Kim, T., & Forster, A. (2003). Photoconductivity Technique for the Assessment of Pigment Photoreactivity. In: *Proceedings of the 81st annual meeting of the FSCT, November 2003*
22. Jin, C., Christensen, P. A., Egerton, T. A., Lawson, E. J., & White, J. R. (2006). Rapid measurement of polymer photo-degradation by FTIR spectrometry of evolved carbon dioxide. *Polym. Degrad. Stab.*, 91(5), 1086-1096. doi: http://dx.doi.org/10.1016/j.polymdegradstab.2005.07.011
23. Ceresa, E., Burlamacchi, L., & Visca, M. (1983). An ESR study on the photoreactivity of TiO₂ pigments. *J. Mater. Sci.*, 18(1), 289-294. doi: 10.1007/BF00543837
24. Feller, R. L. (1994). Accelerated aging: Photochemical and thermal aspects (D. Berland Ed.). Getty conservation institute. ISBN: 0-89236-125-5. 1
25. Braun, J. H., Baidins, A., & Marganski, R. E. (1992). TiO₂ pigment technology: a review. *Prog. Org. Coat.*, 20(2), 105-138. doi: http://dx.doi.org/10.1016/0033-0655(92)80001-D
26. Furlong, D. N. (1994). Surface Chemistry of Silica Coatings of Titania. In H.E. Bergna (Ed.), *The Colloid Chemistry of Silica* (Vol. 234, pp. 535-559). American Chemical Society.
27. Klein-Ovink, B. (2014). Personal communication. Apeldoorn.
28. Keune, P. (2015). Personal communication. Amsterdam.
29. Johnston-Feller, R., Feller, R. L., Bailie, C. W., & Curran, M. (1984). The Kinetics of Fading: Opaque Paint Films Pigmented with Alizarin Lake and Titanium Dioxide. (1984). *JAI/C*, 23(2), 114-129. doi: 10.1179/019713684806028269
30. Kronos®. (2015). TiO₂ - Grades and Applications, Kronos information 2.1. Retrieved 26-05-2015, from http://kronostio2.com/data-sheets-and-literature/brochures/finish/7/81.
31. DuPont™. Titanium Dioxide for coatings, Ti-Pure® titanium dioxide. Retrieved 26-05-2015, from http://www2.dupont.com/Titanium_Technologies/en_US/tech_info/literature/Coatings/CO_B_H_65969_Coatings_Brochure.pdf.
32. de Bondt, R. TiO₂, the technical and the rational. Retrieved 26-05-2015, from http://sv.slf.cc/dokument/Robin%20De%20Bont,%20Tronox,%20TiO2,%20the%20technical%20and%20the%20rational..pdf.
33. Sachtleben Chemie GmbH. Product information 04.001.03.14.e. Retrieved 26-05-2015, from http://www.sachtleben.de/fileadmin/pdf_dateien/titandioxid/HOMBITAN_LW.pdf.
34. Sherman, L. M. (1999). Stretch TiO₂. Retrieved 18-11-2014, 2014, from http://www.ptonline.com/articles/stretch-tio2
35. Hanaor, D. H., & Sorrell, C. (2011). Review of the anatase to rutile phase transformation. *J. Mater. Sci.*, 46(4), 855-874. doi: 10.1007/s10853-010-5113-0
36. The engineering toolbox. Retrieved 10-03-2015, from http://www.engineeringtoolbox.com/light-level-rooms-d_708.html
37. Guire, K. P. M. SoLux Ultraviolet Radiation primer. Retrieved 19-11-2014, from http://www.solux.net/cgi-bin/tlistore/infopages/uv.html
38. Dias, M., & Azevedo, E. (2009). Photocatalytic Decolorization of Commercial Acid Dyes using Solar Irradiation. *Water Air Soil Poll.*, 204(1-4), 79-87. doi: 10.1007/s11270-009-0028-6
39. Bianco Prevot, A., Baiocchi, C., Brussino, M. C., Pramauro, E., Savarino, P., Augugliaro, V., Marci, G. and Palmisano, L. (2001). Photocatalytic Degradation of Acid Blue 80 in Aqueous Solutions Containing TiO₂ Suspensions. *Environ. Sci. Technol.*, 35(5), 971-976. doi: 10.1021/es000162v
40. Jank, M., Köser, H., Lücking, F., Martienssen, M., & Wittchen, S. (1998). Decolorization and Degradation of Erioglaucine (Acid Blue 9) Dye in Wastewater. *Environ. Technol.*, 19(7), 741-747.
41. Gude, K., Gun'ko, V. M., & Blitz, J. P. (2008). Adsorption and photocatalytic decomposition of methylene blue on surface modified silica and silica-titania. *Colloids Surf., A.*, 325(1-2), 17-20. doi: http://dx.doi.org/10.1016/j.colsurfa.2008.04.035
42. Daneshvar, N., Salari, D., Naei, A., & Khataee, A. R. (2006). Photocatalytic degradation of the herbicide erioglaucine in the presence of nanosized titanium dioxide: comparison and modeling of reaction kinetics. *J. Environ. Sci. Health., B.*, 41(8), 1273-1290. doi: 10.1080/03601230600962302
43. Zangeneh, H., Zinatizadeh, A. A. L., Habibi, M., Akia, M., & Hasnain Isa, M. (2015). Photocatalytic oxidation of organic dyes and pollutants in wastewater using different modified titanium dioxides: A comparative review. *J. Ind. Eng. Chem.*, 26(0), 1-36. doi: http://dx.doi.org/10.1016/j.jiec.2014.10.043

Chapter 7

Determining the presence of photocatalytic titanium white pigments via paint sample staining: a proof of principle.

Twentieth century white paints often contain titanium dioxide based white pigments, which can range from highly photostable to highly photocatalytic. Photocatalytic pigments can cause the degradation of paint upon UV exposure, whereas photostable pigments can protect paintings from degradation. Hence, knowing whether a pigment is photocatalytic or not, is of high importance for risk assessment and the subsequent decision making process concerning storage and exposure conditions of a painting.

Photocatalytic activity indicator inks are commercial inks that change color, upon UV exposure, in the presence of a photocatalytic pigment. While the speed of degradation in a well-controlled system can be used for precise assessment of photocatalytic activity (compliant with ISO standards), this is challenging for non-homogeneous paintings samples of unknown composition.

Here we present the successful and easy-to-use application of a photocatalytic activity indicator ink (PAII) on paint cross-sections, to determine, by a 'yes' or 'no' answer, if a photocatalytic pigment is present in a paint sample. The developed PAII staining application shows an obvious color change within 5 minutes of UV irradiation (visible by eye and by investigation of extracted RGB values), for paint samples containing photocatalytic pigments. The method requires taking a small paint sample to be embedded in a cross-section, which avoids application on the painting. A microscope with a camera and a UV source are the only necessary equipment for the application of this method.

This new application of a commercial ink offers a wide range of possibilities, not just for assessment of photocatalytic activity of titanium white pigments, but also potentially for the investigation of other semiconductor pigments.

Based on the submitted manuscript: B.A. van Driel, S. van der Meer, K.J. van den Berg and J.Dik (2018), *Studies in Conservation*.

Note This chapter contains a name-based reference style.

Titanium dioxide is a widely used, well known, semiconducting and possibly photocatalytic material (Laver 1997; T.G. and S. 2011; Baudys et al. 2015; Yang et al. 2010; Kobayashi and Kalriess 1997; van Driel et al. 2016, 2017; Morsch et al. 2017; Benedix et al. 2000; Gunnarsson 2011). In this study we present a practical method indicated as ‘PAII staining’ to identify if a paint contains harmful photocatalytic material or not.

Many pigments, commonly found in works of art, can be classified as semiconductors. These materials have a forbidden bandgap between the valence band and the conduction band, that can be bridged by photons of an energy exceeding the bandgap. Semiconductor pigments include vermillion, cadmium red and yellow, chrome green, zinc white and titanium white (Anaf et al. 2014). Several semiconductor pigments, such as zinc white and titanium white may also function as photocatalyst (Kobayashi and Kalriess 1997). When such a pigment is irradiated with larger than bandgap energy irradiation, an electron from the valence band is excited to the conduction band, forming a photogenerated electron and a positive hole. The electron and hole can migrate to the pigment surface, where they react with water and oxygen forming highly reactive radicals. The radicals can participate in several reactions such as the breakdown of surrounding organic material, like pollutants or the paints binding medium (Mills and Le Hunte 1997; van Driel et al. 2017a; Morsch et al. 2017; Umar and Aziz 2013; Zangeneh et al. 2015). Depending on the application, the photocatalytic activity of the pigment can be a benign or malignant characteristic. Photocatalytic activity can be adjusted among others by modification of the crystal structure (Sclafani and Herrmann 1996; Ohno, Sarukawa, and Matsumura 2002), the use of dopants (Dozzi et al. 2013; Luo and Gao 1992) or the application of (inorganic) surface coatings (Van Driel et al. 2016; Braun, Baidins, and Marganski 1992; Laver 1997; Johansson 1991; Werner 1969; Schiller, Müller, and Damm 2002).

Titanium white, the most abundantly used pigment of the 20th century, has occurred and still occurs in a range of photocatalytic activities ranging from highly photocatalytic to photostable. Presently, most artist pigments are photostable rutile pigments with inorganic surface coatings, classified as type IV pigments following D476-84 ASTM 1988^{7.1}. However, this was not always the case. Photocatalytic, uncoated anatase, pigments have been on the market and have been found in works of art (Driel et al. 2017b; Laver 1997). These pigments are potentially detrimental to works of art. Thus, knowledge about the photocatalytic activity of the

titanium white pigments in a painting, is of high importance. Specifically, for the decision making processes on display conditions, which are based on risk assessment.

Many methods have been proposed for the assessment of photocatalytic activity, some of which were developed into ISO guidelines (Mills, Hill, and Robertson 2012). Most methods monitor a catalysed ‘dummy’ process to categorize photocatalytic activity (Van Driel et al. 2016; Rauf and Ashraf 2009; Xu et al. 1999; Daneshvar et al. 2006; Irick 1972; Mills et al. 2005; Mills, Hill, and Robertson 2012). Other proposed approaches are photoconductivity measurements (Irick 1972), monitoring the radical formation by electron spin resonance spectroscopy (Ceresa, Burlamacchi, and Visca 1983) or artificial aging of paint films (van Driel et al. 2017a; Morsch et al. 2017), for instance by measuring the evolution of CO₂ from a confined paint film under irradiation (Christensen et al. 2000, 1999). All of these methods have limitations: they are time consuming, require professionals and specific equipment to carry out, cannot be performed on original material and some can only be performed on powdered material, while the pigment under investigation is often trapped in an organic matrix (the paint) (van Driel et al. 2016; Mills et al. 2013).

The most promising methods for use by conservators (without access to analytic equipment and used to visual assessments), are based on color change, such as monitoring the color change of a dye in an aqueous solution under UV-irradiation. This has been described in a previous paper by the authors and was the starting point of this study (van Driel et al. 2016). {chapter 6} The aim to develop a test usable on real object samples was initially envisioned to be an adaptation of the reported dye system by van Driel (2016). However, development of a new formulation was considered redundant when the authors got acquainted with the work of Mills and co-workers on indicator inks available as a commercial product^{7.2}. This product is called a photocatalytic activity indicator ink (PAII) and was developed and validated to determine photocatalytic activity of self-cleaning tiles and windows (Mills and Wells 2015a; Mills, Wells, and O’Rourke 2017, 2016, 2014; Mills, Hepburn, et al. 2014; Mills, O’Rourke, et al. 2014; Mills et al. 2005; Mills et al. 2016; Baudys, Krýsa, and Mills 2017; Mills and McGrady 2008; Mills et al. 2013).

Cross-section staining techniques have been employed since the mid-20th century for the characterization of organic components in paint samples. These techniques usually rely on dyes forming colored compounds in reaction with proteins, polysaccharides, resins and oils. The usability is highly dependent on the selectivity

7.2 <http://www.inkintelligent.com/>. The authors want to state, that they were not involved in the development of any PAII formulation or validation studies. We simply identified another interested field, validated the method when used on a microscale cross-sections and adapted the user protocol accordingly.

of the reaction and can be influenced by sample age and dye absorption properties (Sandu et al. 2012). The technique lost popularity with the introduction of new, non-invasive techniques. Nevertheless, cross-section and microscopy analysis is still the first step of micro-invasive analysis and staining remains a very useful and generally accessible method of investigation. Hence, it is in this scope that we propose the application of PAII, developed by Mills et al. (2005-2017), by staining on cross-sections from modern paintings.

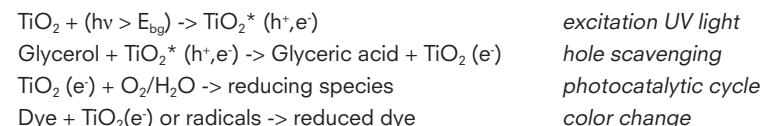
The goal of this study is to develop the application of a suitable commercially available PAII, as a cross-section staining method, for the assessment of the presence of photocatalytic material in paint samples. The application is investigated by testing well characterized reference paint samples and three real paint samples from modern artworks. With this method, we introduce a quick and easy method to determine, qualitatively, by a 'yes' or 'no' classification, if photocatalytic material is present in a painting and if so, in which layer. This information is critical for risk assessment and subsequent decisions about exposure conditions of 20th century art objects.

7.2. Theory

This section is fully based on the work of Mills and co-workers first documented in 2005 and described in a list of papers on the subject (Mills and Wells 2015a; Mills, Wells, and O'Rourke 2017, 2016, 2014; Mills, Hepburn, et al. 2014; Mills, O'Rourke, et al. 2014; Mills et al. 2005; Mills et al. 2016; Baudys, Krýsa, and Mills 2017; Mills and McGrady 2008; Mills et al. 2013).

Over the past decade, photocatalytic activity indicator inks have been developed as a fast and easy assessment tool for photocatalytic activities of macroscopic surfaces (tiles and windows). The concept of the inks is that they irreversibly change color, upon UV irradiation in the presence of a photocatalyst. The ink consists of a mixture of a dye, a polymer solution (hydroxyl ethyl cellulose, HEC), a surfactant and a sacrificial electron donor (commonly glycerol). The sacrificial electron donor reacts with the photogenerated hole, while the photogenerated electron reduces the dye. The reaction of the sacrificial electron donor (glycerol-> glyceric acid) prevents the recombination of electron and hole, thus facilitating the reaction of electrons with the ink inducing the color change. It has been demonstrated that the inks, in the absence of glycerol, show no color change.

The reactions involved are:



With the goal to provide an answers within ten minutes, inks were developed with different response times: Resazurin (Rz), basic blue 66 (BB66), acid orange 7 (AO7) and methylene blue (MB) are described. Basic blue 66 PAII is most suitable for low activity surfaces (6 times faster than Rz PAII) and offers the most intuitive color change (from blue to colorless). Methylene blue is converted to colourless leuco-methylene blue, which is O₂ sensitive. Hence, a PAII based on methylene blue will slowly regain their blue color when exposed to air.

If performed in a completely standardized way, the rate of change is directly related to the photocatalytic activity. If performed on inhomogeneous samples of unknown composition, the test is qualitative and will provide information on whether the surface is photocatalytic but not exactly to what extent. The reproducibility and repeatability studies have shown similar results to present ISO standards, indicating the validity of the test compared to other methods of assessment.

PAII color change curves have been demonstrated, on multiple occasions, to relate directly with the photocatalyzed oxidation of several pollutants, proving its reliability as a method to assess photocatalytic activity. Furthermore, several methods of monitoring color change such as: change of absorbance (UV-VIS), diffuse reflectance spectroscopy and digital photography (RGB (ΔR) or Lab (Δa) color space) have also shown to have good correlation.

As digital photography is the easiest to use, and good correlations have been established with other methods to assess color change, as well as with real pollutant degradation tests, Mills et al. suggest to use RGB values to monitor color change. For BB66 the largest change occurs in the 'R' value from blue (RGB \approx 0, 0, 255) to colorless (RGB \approx 255, 255, 255). The 'R' value is normalized by dividing by the sum of R+G+B to compensate for minor changes in photograph settings. This method of monitoring color change has even been successfully performed using a mobile phone and an 'app' (ColorMeter) (Mills and Wells 2015b).

Table 7.1 Investigated samples (powder is mixed into a paint with bleached linseed oil and applied on as support) and the used PAII staining set-up.

*PVC=pigment volume concentration.

Name	Description	Abbr.	Microscope	Aging magnification	Figure
Uncoated anatase (22%) on canvas	Hombitan LW, Sachtleben Chemie	UA	RMA	50	7.2, 7.5
Coated rutile (layer between canvas and tube paint)	Tronox CR-826 PVC*: 37%	CR	RMA	50	7.3, 7.5
Coated rutile (layer between canvas and tube paint)	Tronox CR-826 PVC: 37%	CR	RCE	External light source	7.3
Tube (A+ZnO) on coated rutile on canvas	Talens amsterdam oil colors, dated: between 1982 and 1986.	Tube(A+ZnO)	RMA	50	7.3, 7.4, 7.5
Tube (A+ZnO) on coated rutile on canvas	Talens amsterdam oil colors, dated: between 1982 and 1986.	Tube(A+ZnO)	RCE	External light source	7.3, 7.4
Uncoated anatase (25%) on melinex	Hombitan LW, Sachtleben Chemie	UA	RMA	50	7.3, 7.4, 7.5
Uncoated anatase (25%) on melinex	Hombitan LW, Sachtleben Chemie	UA	RCE	External light source	7.3, 7.4
BaSO₄ on melinex	Kremer Pigmente 58700	BaSO ₄	RMA	50	7.5
Uncoated anatase (15%) on melinex	Hombitan LW, Sachtleben Chemie	UA	RMA	50	7.5
Uncoated anatase+ZnO on melinex	1:1 (v/v), PVC: 10% UA+10% ZnO Hombitan LW, Sachtleben Chemie + Kremer Pigmente 46300	UA+ZnO	RMA	50	7.4
Uncoated anatase + BaSO₄ (1:1, v/v) on melinex	PVC: 14% UA + 14% BaSO ₄ Hombitan LW, Sachtleben Chemie + Kremer Pigmente 58700	UA+BaSO ₄	RMA	50	7.4, 7.5
Coated rutile on canvas	Tronox CR-826 PVC=37%	CR	RMA	25	7.2
BaSO₄ on canvas	Kremer Pigmente 58700 PVC: 44%	BaSO ₄	RMA	50	7.2, 7.5
Tube (A+ZnO) on canvas	Talens amsterdam oil colors, dated: between 1982 and 1986.	Tube(A+ZnO)	RMA	50	7.5
Coated rutile and aluminum stearate on melinex	Tronox CR-826+ Aluminium-di/tri-stearate, Kremer Pigmente 58960 PVC: 20%	CR+AlSt ZnO	RMA RMA	50 50	7.5 7.2, 7.5
ZnO on melinex	ZnO, Kremer Pigmente 46300 PVC: 13%	Ca(org)	RMA	50	7.5
Ca(org) on melinex	Huntsman A-HRF, Organically coated anatase PVC: 15%	n/a	RMA	50	7.5, 7.6
Untitled, Robert Ryman, paint sample	Date:1960 Stedelijk Museum Amsterdam Sample C (L.Steyn)	n/a	RMA	50	7.4, 7.5, 7.6
Alle schatten komen uit Afrika, Lucebert, paint sample	Date: 1985 Bouwfonds kunstcollectie Date: 1944	n/a	RMA	50	7.5, 7.6
Victory Boogie Woogie, Piet Mondriaan paint sample	Gemeentemuseum, Den Haag Sample 2207/05: Cultural Heritage Agency of the Netherlands (RCE)	n/a	RMA	50	7.5, 7.6

Table 7.2 Paint materials.

Material	Description
Oil	Van Beek bleached linseed oil
Drier	Co/Zr drier, donated by Pieter Keune (0.1% v/v in oil)
Canvas board	Lefranc & Bourgeois, The original studio canvas board CB1015, Canvas board for oil, acryl & alkyd.
Melinex	Labshop 250 um

Recent work (Mills and Wells 2015a) on PAII's deals with their limitation of only being applicable to horizontal and smooth solid surfaces. Among others, researchers are investigating the possibility of including MB PAII in a label that can be adhered to a surface in any direction. The labels are fabricated with (poly)vinyl alcohol (PVA) rather than HEC as a polymer offering the ability to adhere to a surface. Furthermore, the labels are reusable due to the re-oxidation of leuco methylene under atmospheric oxygen.

Furthermore, the analysis of powdered materials, pressed as pallets mixed with SiO₂ and PTFE is also reported (Mills, Wells, and O'Rourke 2017). This study includes other semiconductors such as CdS, WO₃ and C₃N₄. In ambient conditions only TiO₂ is suitable for photocatalytic activity testing. The other powders suffer from competition with O₂, which is resolved by using transparent tape and preventing the reaction with oxygen. Additionally, when irradiated with visible light (for smaller bandgap semiconductor), the dye can bleach due to a photolysis reaction, independent on the presence of a semiconductor. To avoid bleaching, the excitation light was chosen (based on absorption and diffuse reflectance spectra) to ascertain it is not absorbed by the ink.

7.3. Experimental

7.3.1. Paint samples

Table 7.1 describes the investigated paint samples presented in this chapter. All samples are analysed as embedded paint fragments. The powder samples are all prepared into a paint by mixing pigment, linseed oil and drier on a glass plate mill and subsequently cast on canvas or melinex (Table 7.2). The detailed process of paint making is described elsewhere (van Driel et al. 2017a; Driel; Morsch et al. 2017) {chapter 3-5}. The tube paint was painted

7.3 Sample from the CMOP project, from case study painting supplied by the Stedelijk Museum.

7.4 Sample acquired (from painting at the Bouwfonds Kunstcollectie) during the Ph.D. project of the author in the scope of "The white of the 20th century – An explorative survey into Dutch modern art collections." Chapter 1.

onto the support using a brush and the real paint samples were taken from the paintings with a scalpel in the scope of other research projects. After appropriate drying time, the samples were embedded using Technovit 2000LC (producer: Heraeus Kulzer, purchased at Deffner&Johann) and subsequently polished to create a flat and smooth surface. Between experiments on the same sample, the surface was re-polished to remove the blue ink.

The results of the full dataset are presented (figure 7.5). Different subsets are presented in figures 7.2, 7.3 and 7.4 to illustrate the proof of principle as well as for the evaluation of the measurement set-up. Sample 2207/05 was part of the investigation of the Victory Boogie Woogie performed by the Cultural Heritage Agency of the Netherlands and the Gemeentemuseum in The Hague (van den Berg et al. 2012) and was additionally analysed by Scanning Transmission Electron microscopy with Energy dispersive X-ray spectroscopy (STEM-EDX) at AkzoNobel. The samples from the Ryman^{7.3} and Lucebert^{7.4} paintings, as well as the Talens tube paint and the canvas board were additionally analysed by the authors with a variety of methods (prior and unrelated to this study) such as X-ray fluorescence spectrometry (XRF), X-ray diffraction (XRD) and STEM-EDX.

7.3.2. Characterization

XRF was performed using a Bruker tracer III-SD. The crystalline phases were analyzed by XRD using a Discover D8 micro-diffractometer with a general area detection diffraction system (GADDS) two dimensional detector (Bruker AXS, Karlsruhe, Germany). The samples were measured without preparation on a concave microscope slide. Diffractograms were acquired in reflection mode with CuK α radiation (40 kV, 30 mA). The GADDS software was used for integration and the Bruker AXS Eva software for phase identification using the ICDD PDF database.

Paint fragments were glued with a cyano acrylate glue to an Al pin, and after 30 minutes drying time sectioned with a Leica UC6 cryo-ultramicrotome using a diamond knife (cryo 35 degrees). Thin sections of ~100 nm thickness were collected dry on C coated Cu TEM grids. The prepared samples were analyzed in a Jeol 2010F FEG-TEM (200kV) equipped with a STEM unit. The STEM-EDX mappings were acquired using a ThermoFisher 30 mm² Ultradry SDD EDX detector.

7.3.3. PAII staining

All PAII staining experiments were carried out using the 'visualizer' pen, based on basic blue 66 (BB66), purchased from Ink Intelligent. The PAII pen was kept in the fridge. The experimental procedure is illustrated in Figure 7.1.

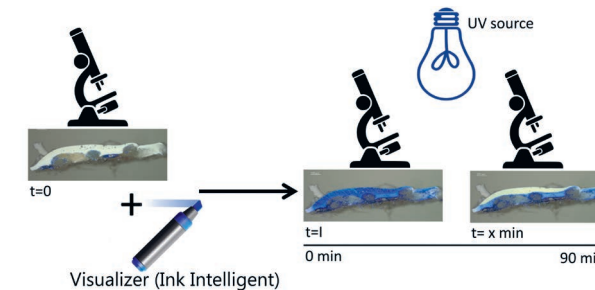


Figure 7.1 Overview of analysis method indicating the uncoloured cross-section (left), the application of the ink (middle) and the aging procedure (right).

The cross-section without ink is examined and photographed with a microscope under visible light (Dark field microscopy, DF) and UV light (no color correction equipped with filterset 02 EX G 365, BS FT 395, EM LP 420). After the $t=0$ examination, the ink (visualizer pen) is applied onto the cross-section until the entire sample is covered by the blue color. Subsequently, the sample is again examined and photographed under visible light (DF) with the microscope ($t=1$). In this study two different Zeiss microscopes were used ('RCE' and 'RMA', Table 7.1). Microscope 'RMA' is equipped with a LED light and an in-house color calibration software (Smelt and Erdmann, 2017), whereas microscope 'RCE' is equipped with a halogen lamp (100W) and does not have color calibration. After the examination of the blue color on the sample, the cross-section is exposed to a UV source. In the case of microscope 'RMA' this was done in situ using the Calibri UV LED (365 nm, equipped with filterset 02 EX G 365, BS FT 395, EM LP 420) on the microscope, set at 10% UV intensity and using a 50x magnification (UV intensity = 2.29 mW/cm²). If UV irradiation is performed through the microscope, it is important to keep the optics, including the magnification, constant. Varying the microscope setting can alter the UV-intensity reaching the sample. When using microscope 'RCE' irradiation was performed on an external UV source (Spectroline SB100/F, UV intensity = 1.4 mW/cm²).

At the following time points (5, 10, 15, 20, 25, 30, 60 and 90 min) the sample was examined and photographs under visible light (DF, fixed exposure time) were taken. Subsequently color correction was carried out for the photographs taken on the 'RMA' microscope. The photographs are evaluated as such, but they are also used to extract RGB changes of the region of interest, over

time. Mills, Wells and O'Rourke (2014) validated that the change in RGB value correlates to the change in absorbance (UV-VIS) and the destruction of stearic acid which is assumed to be equally valid in the microscopic case.

7.3.4. Data processing

ImageJ^{7.5} using the MBF imageJ for Microscopy plugin bundle (Collins 2007) was used to extract RGB values from the photographs but other image software such as Adobe Photoshop could be used. Using Image J the following steps can be followed:

- Convert a set of photographs to a stack (Image/Stacks/Image_to_stack)
- Split the single photograph or stack in separate color images for red, green and blue
Open ROI manager (Analyze/Tools/ROI manager)
Click Rectangular Tool and select the region to be measured
Add to ROI manager
Copy ROI to other photographs
(each photograph has its own ROI manager window)
Click RGB/Merge Split Tool
- Measure R: ROI manager -> Measure
- Measure G: ROI manager -> Measure
- Measure B: ROI manager -> Measure

Because the region of interest (ROI) is duplicated for each photograph, slight movement of the photograph can result in a slightly shifted region of interest, which may affect the extracted RGB values. This is particularly significant when analysing small regions (for example in thin paint layers). To account for this variability RGB values over several (large and small) regions of interest are averaged. In the future automated RGB extraction may address this variability.

The final value of interest is the change in normalized red value as described in equation 1.

$$\Delta RGB_r = (R/(R+G+B))_{t=I} - ((R/(R+G+B))_{t=t} \quad (1)$$

7.4. Results & Discussion

7.4.1. Proof of principle

Figure 7.2 shows the results of a set of three reference samples: photocatalytic (uncoated anatase), photostable (coated rutile) and inert (barium sulphate). Per sample, three pictures of the initial situation are presented: a UV photo, a dark field photo and a dark field photo after application of the ink. Additionally, two photographs after respectively 15 and 90 min of UV irradiation are shown. This sample set provides the proof of principle that color change is observed in the sample containing photocatalytic pigment. On the other hand, color change is not observed for the samples containing photostable or inert pigments. Additionally, the different behaviour of layers is visible. The uncoated anatase was painted on a canvas board containing rutile and calcium carbonate (XRD). In the photographs it is clear that the top layer changes color whilst the bottom layer remains blue. Thus, this serves as a proof of concept that the method is also spatially resolved and thus suitable to investigate layered structures.

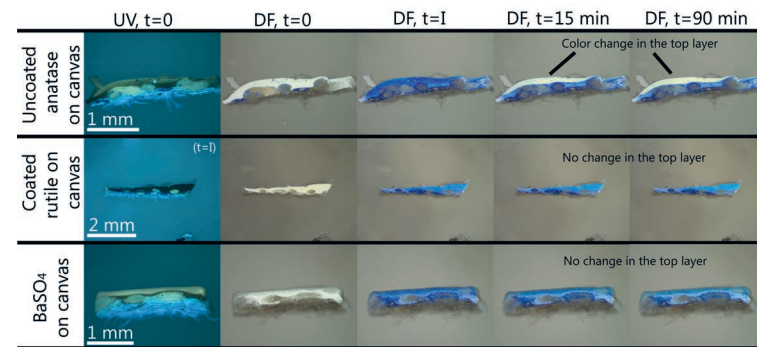


Figure 7.2 Photographs of a subset of reference samples (uncoated anatase, coated rutile and barium sulfate) at t=0 (UV and DF), when the ink is applied (t=I) and after 15 and 90 min of UV irradiation. Uncoated anatase shows color change in the top layers.

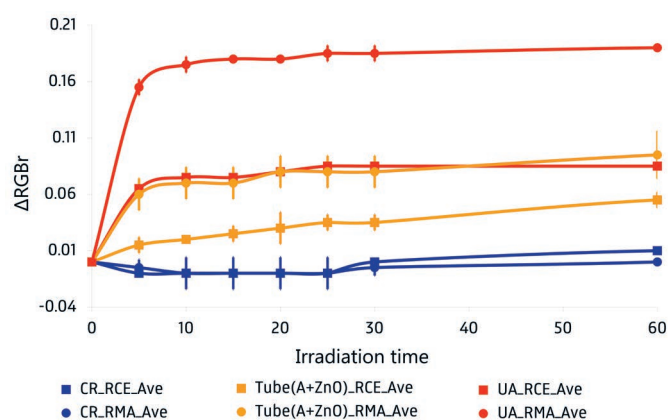
7.4.2. Measurement set-up

In this study the main sample set was evaluated with a microscope ('RMA') equipped with a stable LED light (aging magnification = 50x) and equipped with in-house color calibration software. To evaluate if this high quality set-up is required, we compared the qualitative classification when performed with a standard microscope, equipped with a halogen lamp and without color correction. This comparison was performed on a subset of 3 reference samples: photostable, photocatalytic and a mixed tube paint. These samples were chosen because they represent different speeds of degradation (no change/mid/high change). Figure 7.3, indicates that the same order of photocatalytic activity is obtained with both set-ups. The samples investigated on the 'RCE' microscope did show slower

color change. This is due to a difference in irradiation conditions. The samples on the ‘RMA’ microscope are irradiated with the UV light on the microscope with an intensity of 2.29 mW/cm². Alternatively the samples on the ‘RCE’ microscope were irradiated with an external UV source with an intensity of 1.4 mW/cm². This difference accounts for the different degradation rates:

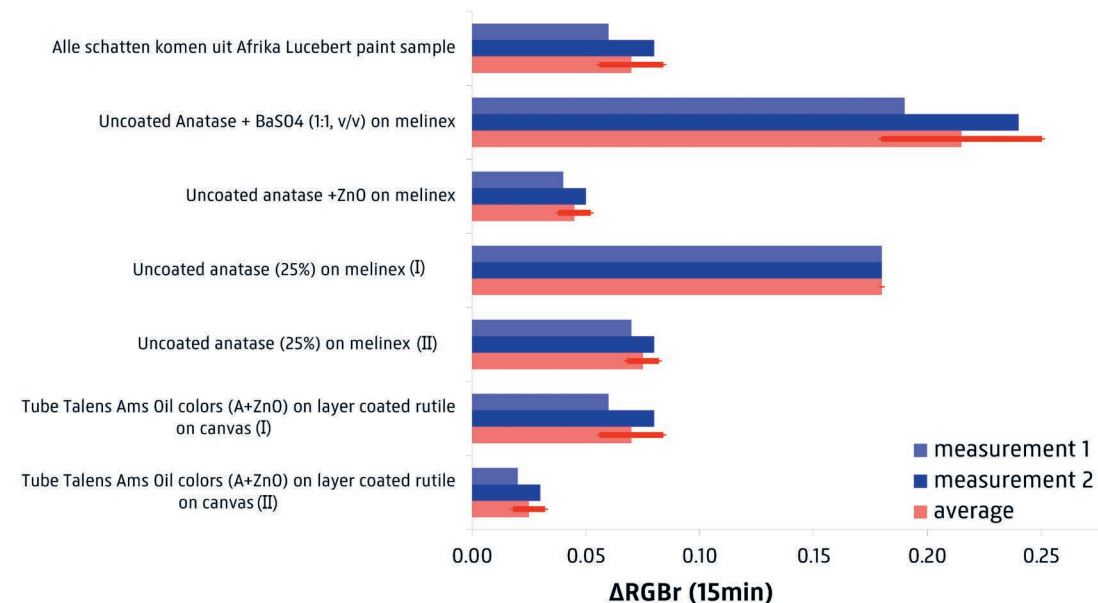
- $(RMA/(RMA+RCE))_{UV\ intensity} = 0.62$,
- $(RMA/(RMA+RCE))_{\Delta RGB_r(15min), Tube(A+ZnO)} = 0.74$ and
- $(RMA/(RMA+RCE))_{\Delta RGB_r(15min), UA} = 0.71$.

Figure 7.3 ΔRGB_r for stable, medium photocatalytic and high photocatalytic samples on both microscopes (RMA/RCE) indicating no color change, mid-range color change and high color change. The classified order is identical regardless of the measurement set-up.



7.4.3. Reproducibility

Figure 7.4 shows the difference between the two microscopes as well as the reproducibility of the measurements. Again, we present subset of the data, in this case only looking at samples containing active pigments. To repeat a measurement the blue ink or remainder of the ink is polished of the surface. If the ink had penetrated deeply into the sample (such as into the canvas, [uncoated anatase, Figure 7.2]), it will remain present. Fortunately, this only occurred for canvas/ground layers (probably due to the porosity) and not for paint layers. Depending on the amount of active material present at the polished surface, on the exact amount of ink applied and on the accuracy of the area selection to extract RGB values, variability will be introduced. Despite these variable factors the reproducibility of the test is quite good for both microscopes.



7.4.4. Classification of all samples based on changes in RGB values.

Figure 7.5 displays the full dataset collected under standard conditions (‘RMA’ microscope, UV 10%, aging magnification: 50x). In this figure we show the ΔRGB_r for each time point (0-90 min). An accurate classification of photocatalytic materials can already be made after five minutes of irradiation. This results confirms the speed benefit of this test reported by Mills et al. (2005-2017) on a paint cross-section (microscopic system).

Generally, the rate of color change can be divided into four categories: the stable pigments, causing no change or a negative ΔRGB_r (A); the pigments causing a minor and immediate (within the first 5 min) change (B); the mixtures, causing a noticeable change (C) and the highly photocatalytic pigments causing a major change (D). All but two samples follow the observed trends. These exceptions are organically coated anatase (here classified as highly photocatalytic) and zinc oxide (here only causing minor and immediate change).

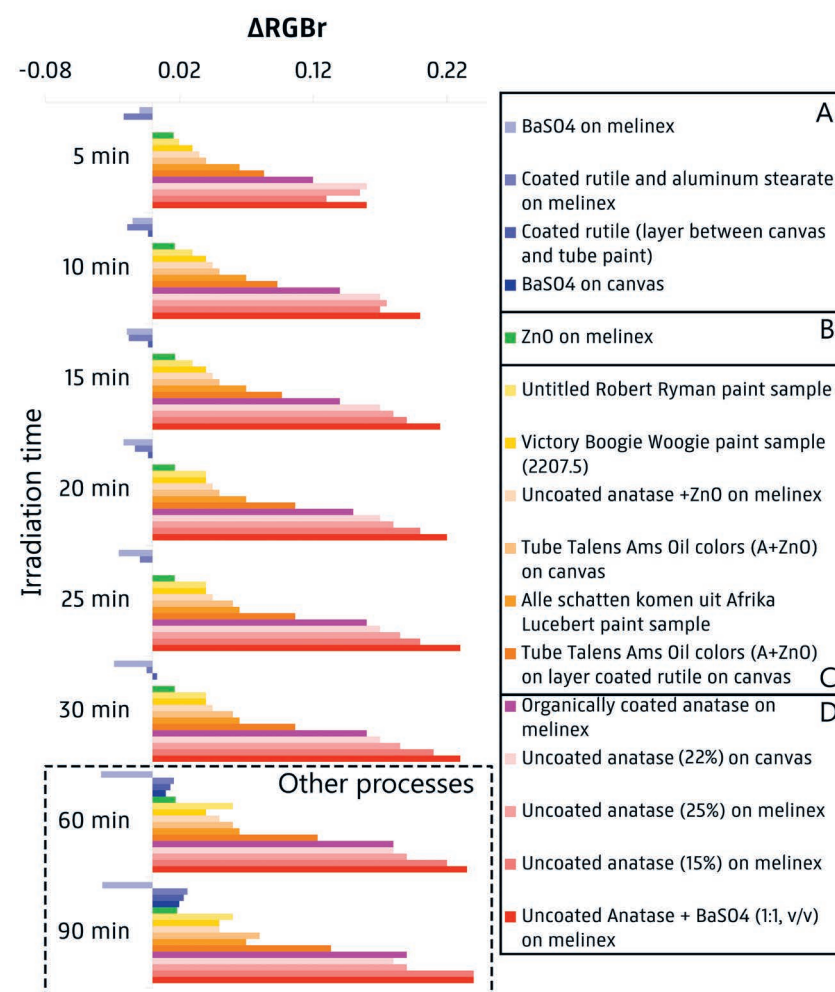
The behavior of ZnO was unexpected because artificial aging studies have shown (van Driel et al. 2017c) that zinc oxide causes similar photocatalytic degradation (loss of gloss) as uncoated anatase upon UV exposure. Here, we present several hypotheses for the unexpected behaviour of ZnO during PAII staining. These hypothesis are based on the difference between aging under a

Figure 7.4 Reproducibility of samples containing photocatalytic pigments. Several samples on either microscopes that have been repeated $\Delta RGB_r(15min)$ is presented for measurement 1, measurement 2 and the average, including standard deviation.

broad or narrow UV source, on the interaction with atmospheric oxygen and on the electronic structure and of ZnO.

First of all the irradiation conditions may play a role. In the artificial aging study (van Driel et al. 2017c), as well as in a study looking into the photocatalytic efficiency of ZnO and TiO₂ towards Acid Brown 14 degradation (Sakthivel et al. 2003), a broad irradiation source was used (300–400 nm and sunlight respectively). On the other hand, in the present study, as well as a study looking into the photocatalytic efficiency of ZnO and TiO₂ towards the decomposition of acetaldehyde (Kobayashi and Kalriess 1997), a narrow irradiation source was used (365 and 360 nm respectively). The studies by Saktivel and van Driel show similar photocatalytic activities or even a higher efficiency for ZnO than for TiO₂. Sakvitel assigns this difference to the larger amount of photons able to be absorbed by ZnO. Alternatively the study by Kobayashi shows lower photocatalytic efficiency for ZnO than for TiO₂.

Figure 7.5 Complete dataset acquired via standard procedure (ΔRGB, at all the different time intervals: 5, 10, 15, 20, 25, 30, 60, 90 min). If the sample was repeated, the average is projected. Four categories can be identified: A, stable; B, minor change; C, medium change; D, major change. At longer irradiation times (60, 90 min) other processes start to play a role and paint samples with stable paints also start to show discoloration of the PAII.



An alternative or supplementary hypothesis is that atmospheric oxygen can react with the photogenerated electron. This scavenged electron is therefore not capable to reduce the dye, inhibiting the color changing reaction. The reaction with atmospheric oxygen was described as an inhibiting factor for PAII tests on other semiconductors such as CdS, WO₃ and C₃N₄ (Mills, Wells, and O'Rourke 2017). This inhibition (competition between degradation of the dye and reaction with O₂) process could, to some extent, take place in the TiO₂ sample, however, it is possibly more influential for ZnO.

Additionally, ZnO has a strong green emission upon UV (360 nm) excitation (Artesani et al. 2016). This emission is a characteristic effect of recombination processes occurring in the ZnO. If recombination is faster than hole scavenging by glycerol, this could reduce the amount of photogenerated electrons accessible for the ink reduction process.

It is clear that the real life degradation process (break down of the binding medium) can be different from the effect measured in the PAII staining test. In case of ZnO, this results in a compromised classification. Nevertheless, the test does classify it as photocatalytic and can thus be used to provide a qualitative 'yes' or 'no' answer. Since the aim is to have a classification, that correlates with real degradation behaviour, we propose to carry out the PAII test on ZnO with a different (broad) irradiation source and/or covered with a transparent tape to prevent the reaction with oxygen to improve classification (Mills, Wells, and O'Rourke 2017).

Organically coated anatase reacts faster than expected. While this pigment is a photocatalyst causing binder degradation (thus the correct 'yes' or 'no' answer is provided) (van Driel et al. 2017b), the classification too severe. This may be due to the fact that the pigment is coated with a soft organic coating, possibly removed during sample preparation (polishing). At this moment, it is unclear if this could also occur with inorganically (SiO₂/Al₃O₂) coated pigments, which could result in false positives, hence further references with coated pigments should be investigated.

As expected, the method is not accurate enough to indicate minor changes such as those corresponding to a range of different pigment volume concentrations of anatase (category D). Variability can be related to several factors such as the amount of active material present at the polished surface, the paint porosity (related to composition, binding medium and age), the exact amount of ink applied and on the accuracy of the area selection to extract RGB values.

In category A (photostable and inert pigments), a small negative ΔRGB_r is presented (0-30 min), followed by a positive ΔRGB_r (60-90 min). The negative ΔRGB_r is not visually noticeable in the microscopic photographs. This change is not completely understood but could be due to the process of extraction of the RGB values, to the absorption or drying process of the ink in the support and/or to the measurement error induced by the low hiding powder of barium sulfate. The positive ΔRGB_r , on the other hand, is visible in the microscopic photographs and is suggested to be caused by other processes which take place. These could be photolysis or dye sensitization processes causing direct photodegradation of the ink at longer irradiation times (Mills, Wells, and O'Rourke 2017). These processes clearly take place at a much slower time scale and don't compromise successful 'yes' or 'no' classification. The final change remains much smaller than the change recorded in category C or D (photocatalytic pigments). While classification in this study was straight forward, it is possible that a minor amount of photocatalytic material or a low photocatalytic activity material remains unnoticed (false negative). However, these false negative are also unlikely to cause damage to the paint. The presented results indicate a successful first step towards introducing the use of photocatalytic activity indicator inks to determine the presence of photocatalytic material in a paint sample. Additionally, as photocatalytic activity is often related to the anatase crystal structure it can be used to suggest the anatase crystal structure when color change is observed. Unfortunately, the other way (relating 'no color change' to rutile and with that tentative dating) is not possible as between 1935 and 1940, anatase pigments for exterior use appeared on the market with inorganic surface treatments to improve chalk resistance (photocatalytic activity) (Stieg 1985). While these pigments may have not found their way into artist paints until later in the century, it makes the assignment of the rutile crystal structure based on PAII staining require additional analysis.

7.4.5. Real paint samples

Figure 7.6 shows the photographic results for the three samples from real paintings that were investigated (RGB results are presented in Figure 7.5). All samples show a degree of color change and thus contain photocatalytic material. The PAII staining method provides an unambiguous and spatially resolved characterization, which is confirmed by the absence of a coating (analysed by STEM-EDX).

Table 7.3 provides an overview of the supporting analysis for the paint samples. This shows that in the Robert Ryman and Lucebert

paintings, ZnO and Anatase are present, both possibly photocatalytic and thus causing the inks color change. The test successfully predicts the presence of photocatalytic and likely harmful material in the paintings. The expected reactivity, as indicated by XRF, XRD and STEM-EDX is thus confirmed by this easy-to-use test. It also indicates the importance of doing such test because based on their date (1960 and 1985 respectively), one may suppose the use of more developed pigments present on the market such as a coated rutile.

Painting	XRF	XRD	STEM-EDX	Other
Untitled, Robert Ryman, 1960	(S), (Ca), Ti, Ba, Zn, Sr	ZnO, Anatase, BaSO ₄ , SrSO ₄	BaSO ₄ (Sr associated), TiO ₂ , ZnO, Zn-organic (soap? Needle like structure), Al (0.3at%) and Si(0-0.1at%) associated with TiO ₂	n/a
Alle schatten komen uit Afrika, Lucebert, 1985	(Ca), Ti, Ba, Zn, (Pb), (Sr), (Nb), (Zr)	Anatase, ZnO	n/a	n/a
Victory Boogie Woogie, Mondriaan, 1944 (Sample 2207/05)	n/a	Anatase and rutile were both found (original vs. overpaint?)	Zn (spread out, does not look like particles), Ca, Ti uncoated (Ti/Ca possibly composite), Ba, clay, Al (spread out).	SEM-EDX: 3 layers containing Ca (1), Ti + (Ca) (2) + Ti + Ba + Zn + S FTIR: wood fibers (from frame)

Table 7.3 Supporting analysis on real oil paint samples.

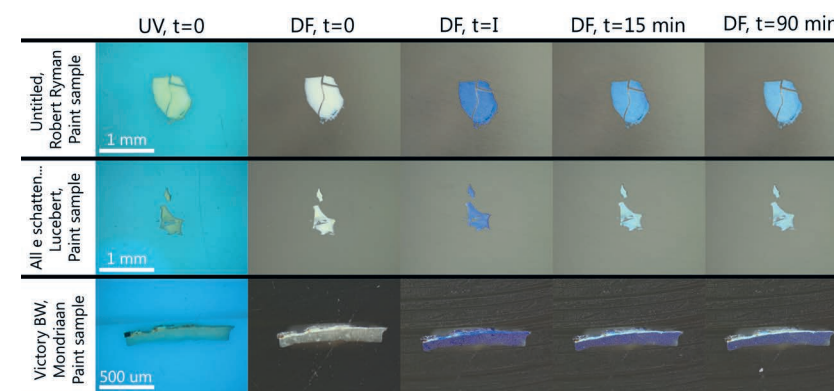


Figure 7.6 Photographs of real paint samples under investigations at t=0 (UV and DF), when the ink is applied (t=I) and after 15 and 90 min of UV irradiation.

The material from the Victory Boogie Woogie, sample 2207/05, was classified by van den Berg et al. (2012) as a sample from the frame due to the presence of wood fibres. This sample is present as a flake (used for STEM-EDX) and as an embedded sample (embedded during the research into the Victory Boogie Woogie, 2012). STEM-EDX suggest an association with calcium carbonate, possibly indicating a composite pigment. Whatever the exact type of pigment, it is clear from PAII staining that one layer in this

paint sample (between the wood and the top layer) contains photocatalytic material. Because the paint layer is located between two other layers and is not reached by UV light, the risk of photocatalytic degradation of the material in this layer (TiO₂ or ZnO based) is minimal. The PAII staining method provides an unambiguous and spatially resolved characterization, which is confirmed by the absence of a coating (analysed by STEM-EDX). Practically, the test will be often assessed visually using photographs such as those presented in Figure 7.6. This method is completely valid but less useful for comparison of a set of sample. For comparison extraction and comparison of RGB values is more practical.

7.5. Conclusion & Outlook

In this study we demonstrated the successful use of BB66 PAII staining for the determination of the presence of photocatalytic material in paint cross-sections. The method shows a good qualitative classification within five minutes, with good reproducibility, regardless of measurement set-up (type of microscope and UV source).

The test, despite the known variabilities, is successful and can already be used to provide information about the photocatalytic activity of TiO₂ pigments in cross-sections. Nevertheless, in an effort to work towards a more quantitative methods, further research is required. This research is challenged by the fact that each paint sample is unknown, inhomogeneous and different. Further research should involve investigation into the polished surface, the porosity of the ink support, the different binding media, the influence of the environment (pH?), the influence of other components in the paint (additives, driers) and the interaction with other semiconductor pigments. Concrete questions, that came up during this study, also need to be investigated. These included photolysis processes that play a role at longer time scales as well as the predictive power of the test for organically coated titanium dioxide or zinc oxide containing samples. Initial studies could investigate different irradiation conditions or prevent the contact with O₂. Additionally, inorganically coated TiO₂ pigments should be investigated in terms of sample preparation to check if the coating is not polished away during sample preparation, which could yield false positives. This chapter is the first step towards implementation of this method in conservation practice and further development into a fully validated and possibly commercial method. Cross-sections are widely available in studios and laboratories across the world. Applying this method, on these cross-sections, in a standardized manner, would reveal valuable and immediately applicable

information about the risk of degradation of those paintings. With a processing rate of four samples a day, 1000 paint samples may be evaluated in under a year time. Data processing (RGB value extraction) can, with some effort, be automated thus freeing more time for analysis.

New developments by Mills et al. include the production of photocatalytic indicator labels, which could be interesting for conservation as well. Using the labels would address the variability induced by the manual (and thus unreproducible) application of ink on each sample. Furthermore, reactions may be more pronounced and specific due to the absence of O₂. If these labels would be minimalized and easy to remove, one could even envision applicability on the actual paint surface without taking a sample rendering the method non-invasive.

Additionally, cross-section PAII staining may be possible with just a mobile phone and a UV source. While color measurement apps are already available (Wess 2017; Mills and Wells 2015), this was not usable on the microscale. Recently, researchers transformed an Iphone into a 'cheap yet powerful microscope'^{7.6} (Smith et al. 2011) opening the tantalizing possibility of easy-to-use determination of photocatalytic activity using only a mobile phone.

Acknowledgements

This work has been analytically and financially supported by AkzoNobel and hosted by the Rijksmuseum Amsterdam. Brenda Rossenaar and Wilma Ravesloot (AkzoNobel) are especially acknowledged for STEM-EDX sample preparation and analysis. Additionally, Tony Davies and Martijn Smout (AkzoNobel) provided important council during this study.

The authors acknowledge Caroline Coffrie (Bouwfonds kunstcollectie), the Cultural Heritage Agency of the Netherlands (RCE) and Lise Steyn (RCE/UvA, CMOP) for providing real paint samples).

Furthermore, we are indebted to Susan Smelt and Katrien Keune for their involvement in fruitful discussions and the support in the supervision of S.R. van der Meer. The authors acknowledge Muriel Geldof, Han Neevel and Luc Megens at the Cultural Heritage Agency of the Netherlands for the training on the microscope and for useful advice. Finally, Prof. P.J. Kooyman is acknowledged for the involvement in van Driels Ph.D. research.

- Anaf, Willemien, Stanislav Trashin, Olivier Schalm, Dennis van Dorp, Koen Janssens, and Karolien De Wael. 2014. "Electrochemical Photodegradation Study of Semiconductor Pigments: Influence of Environmental Parameters." *Analytical Chemistry* 86 (19):9742-8. doi: 10.1021/ac502303z.
- Artesani, A., S. Bellei, V. Capogrosso, A. Cesaratto, S. Mosca, A. Nevin, G. Valentini, and D. Comelli. 2016. "Photoluminescence properties of zinc white: an insight into its emission mechanisms through the study of historical artist materials." *Applied Physics A* 122 (12):1053. doi: 10.1007/s00339-016-0578-6.
- Baudys, M., J. Krýsa, and A. Mills. 2017. "Smart inks as photocatalytic activity indicators of self-cleaning paints." *Catalysis Today* 280, Part 1:8-13. doi: <http://dx.doi.org/10.1016/j.cattod.2016.04.041>.
- Baudys, M., J. Krýsa, M. Zlámal, and A. Mills. 2015. "Weathering tests of photocatalytic facade paints containing ZnO and TiO₂." *Chemical Engineering Journal* 261:83-7. doi: <https://doi.org/10.1016/j.cej.2014.03.112>.
- Benedix, Roland, Frank Dehn, Jana Quaas, and Marko Orgass. 2000. "Application of titanium dioxide photocatalysis to create self-cleaning building materials." *Lacer* (5):157-68.
- Braun, Juergen H., Andrejs Baidins, and Robert E. Marganski. 1992. "TiO₂ pigment technology: a review." *Progress in Organic Coatings* 20 (2):105-38. doi: [http://dx.doi.org/10.1016/0033-0655\(92\)80001-D](http://dx.doi.org/10.1016/0033-0655(92)80001-D).
- Ceresa, Emiliano Mello, Leo Burlamacchi, and Mario Visca. 1983. "An ESR study on the photoreactivity of tio₂ pigments." *Journal of Materials Science* 18 (1):289-94. doi: 10.1007/BF00543837.
- Christensen, P. A., A. Dilks, T. A. Egerton, and J. Temperley. 1999. "Infrared spectroscopic evaluation of the photodegradation of paint Part I The UV degradation of acrylic films pigmented with titanium dioxide." *Journal of Materials Science* 34 (23):5689-700. doi: 10.1023/A:1004737630399.
- Christensen, P. A., A. Dilks, T. A. Egerton, and J. Temperley. 2000. "Infrared spectroscopic evaluation of the photodegradation of paint Part II: The effect of UV intensity & wavelength on the degradation of acrylic films pigmented with titanium dioxide." *Journal of Materials Science* 35 (21):5353-8. doi: 10.1023/A:1004898913140.
- Collins, T. J. (2007). "ImageJ for microscopy". *Biotechniques*, 43(1 Suppl), 25-30.
- Daneshvar, N., D. Salari, A. Niaei, and A. R. Khataee. 2006. "Photocatalytic degradation of the herbicide erioglaucine in the presence of nanosized titanium dioxide: comparison and modeling of reaction kinetics." *J Environ Sci Health B* 41 (8):1273-90. doi: 10.1080/03601230600962302.
- Dozzi, Maria Vittoria, Cosimo D'Andrea, Bunsho Ohtani, Gianluca Valentini, and Elena Sellì. 2013. "Fluorine-Doped TiO₂ Materials: Photocatalytic Activity vs Time-Resolved Photoluminescence." *The Journal of Physical Chemistry C* 117 (48):25586-95. doi: 10.1021/jp4095563.
- Gunnarsson, Sverrir G. 2011. "Self-Cleaning Paint: Introduction of photocatalytic particles into a paint system." PhD, DTU.
- Irick, Gether. 1972. "Determination of the photocatalytic activities of titanium dioxides and other white pigments." *Journal of Applied Polymer Science* 16 (9):2387-95. doi: 10.1002/app.1972.070160917.
- Johansson, Leena-Sisko. 1991. "Analysing coated powders with XPS." *Surface and Interface Analysis* 17 (9):663-8. doi: 10.1002/sia.740170910.
- Klaas Jan Van den Berg, Costanza Miliani, Aldo Aldrovandi, Bruno G. Brunetti, Suzan de Groot, Kenza Kahrim, Metthijs de Keijzer, et al. 2012. "Chapter 7: The Chemistry of Mondrian's paints in Victory Boogie Woogie." In *Inside Out Victory Boogie Woogie*, edited by M.R. van Bommel, H. Janssen, R. Spronk and Haags Gemeentemuseum. Amsterdam University Press.
- Kobayashi, Masaru, and William Kalriess. 1997. "Photocatalytic Activity of Titanium Dioxide and Zinc Oxide." In *Cosmetics & Toiletries magazine* 83-5.
- Laver, Marilyn. 1997. "Titanium White." In *Artists' Pigments: A Handbook of their History and Characteristics* 295-355.
- Luo, Zhenghao, and Qing-Hua Gao. 1992. "Decrease in the photoactivity of TiO₂ pigment on doping with transition metals." *Journal of Photochemistry and Photobiology A: Chemistry* 63 (3):367-75. doi: [http://dx.doi.org/10.1016/1010-6030\(92\)85202-6](http://dx.doi.org/10.1016/1010-6030(92)85202-6).
- Mills, A., and N. Wells. 2015a. "Smart, reusable labels for assessing self-cleaning films." *Chemical Communications* 51 (20):4161-3. doi: 10.1039/C4CC09734C.
- Mills, A., and N. Wells. 2015b. "Indoor and outdoor monitoring of photocatalytic activity using a mobile phone app. and a photocatalytic activity indicator ink (paii)." *Journal of Photochemistry and Photobiology A: Chemistry* 298 (Supplement C):64-7. doi: <https://doi.org/10.1016/j.jphotochem.2014.10.019>.
- Mills, Andrew, James Hepburn, David Hazafy, Christopher O'Rourke, Josef Krysa, Michal Baudys, Martin Zlamal, et al. 2013. "A simple, inexpensive method for the rapid testing of the photocatalytic activity of self-cleaning surfaces." *Journal of Photochemistry and Photobiology A: Chemistry* 272:18-20. doi: <http://dx.doi.org/10.1016/j.jphotochem.2013.08.004>.
- Mills, Andrew, James Hepburn, David Hazafy, Christopher O'Rourke, Nathan Wells, Josef Krysa, Michal Baudys, et al. 2014. "Photocatalytic activity indicator inks for probing a wide range of surfaces." *Journal of Photochemistry and Photobiology A: Chemistry* 290:63-71. doi: <http://dx.doi.org/10.1016/j.jphotochem.2014.06.007>.
- Mills, Andrew, Claire Hill, and Peter K. J. Robertson. 2012. "Overview of the current ISO tests for photocatalytic materials." *Journal of Photochemistry and Photobiology A: Chemistry* 237:7-23. doi: <http://dx.doi.org/10.1016/j.jphotochem.2012.02.024>.
- Mills, Andrew, and Stephen Le Hunte. 1997. "An overview of semiconductor photocatalysis." *Journal of Photochemistry and Photobiology A: Chemistry* 108 (1):1-35. doi: [http://dx.doi.org/10.1016/S1010-6030\(97\)00118-4](http://dx.doi.org/10.1016/S1010-6030(97)00118-4).
- Mills, Andrew, and Mark McGrady. 2008. "A study of new photocatalyst indicator inks." *Journal of Photochemistry and Photobiology A: Chemistry* 193 (2-3):228-36. doi: <http://dx.doi.org/10.1016/j.jphotochem.2007.06.029>.
- Mills, Andrew, Christopher O'Rourke, and Nathan Wells. 2014. "A smart ink for the assessment of low activity photocatalytic surfaces." *Analyst* 139 (21):5409-14. doi: 10.1039/C4AN01375A.
- Mills, Andrew, Christopher O'Rourke, Katherine Lawrie, and Sofia Elouali. 2014. "Assessment of the Activity of Photocatalytic Paint Using a Simple Smart Ink Designed for High Activity Surfaces." *ACS Applied Materials & Interfaces* 6 (1):545-52. doi: 10.1021/am4046074.
- Mills, Andrew, Jishun Wang, Soo-Keun Lee, and Morten Simonsen. 2005. "An intelligence ink for photocatalytic films." *Chemical Communications* (21):2721-3. doi: 10.1039/B501131K.
- Mills, Andrew, Nathan Wells, and Christopher O'Rourke. 2014. "Correlation between ΔAbs, ΔRGB (red) and stearic acid destruction rates using commercial self-cleaning glass as the photocatalyst." *Catalysis Today* 230:245-9. doi: <http://dx.doi.org/10.1016/j.cattod.2013.11.023>.
- Mills, Andrew, Nathan Wells, and Christopher O'Rourke. 2016. "Correlation between the photocatalysed oxidation of methylene blue in solution and the reduction of resazurin in a photocatalyst activity indicator ink (Rz Paii)." *Journal of Photochemistry and Photobiology A: Chemistry* 330:86-9. doi: <http://dx.doi.org/10.1016/j.jphotochem.2016.07.020>.

- Mills, Andrew, Nathan Wells, and Christopher O'Rourke. 2017. "Probing the activities of UV and visible-light absorbing photocatalyst powders using a resazurin-based photocatalyst activity indicator ink (Rz Paii)." *Journal of Photochemistry and Photobiology A: Chemistry* 338:123-33. doi: <http://dx.doi.org/10.1016/j.jphotochem.2017.01.030>.
- Mills, Andrew, Dilidaer Yusufu, Nathan Wells, and Christopher O'Rourke. 2016. "Assessment of activity of 'transparent and clear' and 'opaque and highly coloured' photocatalytic samples using a fluorescent photocatalytic activity indicator ink, FPaii." *Journal of Photochemistry and Photobiology A: Chemistry* 330:90-4. doi: <http://dx.doi.org/10.1016/j.jphotochem.2016.07.019>.
- Morsch, Suzanne, Birgit A van Driel, Klaas Jan van den Berg, and Joris Dik. 2017. "Investigating the Photocatalytic Degradation of Oil Paint using ATR-IR and AFM-IR." *ACS Applied Materials & Interfaces* 9 (11):10169-79.
- Ohno, Teruhisa, Koji Sarukawa, and Michio Matsumura. 2002. "Crystal faces of rutile and anatase TiO₂ particles and their roles in photocatalytic reactions." *New Journal of Chemistry* 26 (9):1167-70. doi: 10.1039/B202140D.
- Phenix, A., K.J. van den Berg, A. Soldano, and B. A. van Driel. 2017. "The Might of White: formulations of titanium dioxide-based oil paints as evidenced in archives of two artists' colourmen mid-twentieth century." In *ICOM-CC Triennial conference 2017, Under review Copenhagen*
- Rauf, M. A., and S. Salman Ashraf. 2009. "Fundamental principles and application of heterogeneous photocatalytic degradation of dyes in solution." *Chemical Engineering Journal* 151 (1-3):10-8. doi: <http://dx.doi.org/10.1016/j.cej.2009.02.026>.
- Sakthivel, S., B. Neppolian, M. V. Shankar, B. Arabindoo, M. Palanichamy, and V. Murugesan. 2003. "Solar photocatalytic degradation of azo dye: comparison of photocatalytic efficiency of ZnO and TiO₂." *Solar Energy Materials and Solar Cells* 77 (1):65-82. doi: [https://doi.org/10.1016/S0927-0248\(02\)00255-6](https://doi.org/10.1016/S0927-0248(02)00255-6).
- Sandu, Irina Crina Anca, Stephan Schäfer, Donata Magrini, Susanna Bracci, and Cecilia A. Roque. 2012. "Cross-Section and Staining-Based Techniques for Investigating Organic Materials in Painted and Polychrome Works of Art: A Review." *Microscopy and Microanalysis* 18 (4):860-75. doi: 10.1017/S1431927612000554.
- Schiller, Michael, Franz Werner Müller, and Cornelia Damm. 2002. "Photo-physics of surface-treated titanium dioxides." *Journal of Photochemistry and Photobiology A: Chemistry* 149 (1-3):227-36. doi: [http://dx.doi.org/10.1016/S1010-6030\(02\)00009-6](http://dx.doi.org/10.1016/S1010-6030(02)00009-6).
- Scialfani, A., and J. M. Herrmann. 1996. "Comparison of the Photoelectronic and Photocatalytic Activities of Various Anatase and Rutile Forms of Titania in Pure Liquid Organic Phases and in Aqueous Solutions." *The Journal of Physical Chemistry* 100 (32):13655-61. doi: 10.1021/jp9533584.
- Smelt, S., and R. Erdmann. "A system for scientific microscope color calibration at the Rijksmuseum for the Paint Sample Database." Presented at Technart2017 Bilbao.
- Smith, Zachary J., Kaiqin Chu, Alyssa R. Espenson, Mehdi Rahimzadeh, Amy Gryshuk, Marco Molinaro, Denis M. Dwyre, Stephen Lane, Dennis Matthews, and Sebastian Wachsmann-Hogiu. 2011. "Cell-Phone-Based Platform for Biomedical Device Development and Education Applications." *Plos ONE* 6 (3):e17150. doi: 10.1371/journal.pone.0017150.
- Stieg, Fred B. 1985. "Opaque White Pigments in Coatings." In *Applied Polymer Science*, 1249-69. American Chemical Society.
- T.G., Smijd, and Pavel S. 2011. "Titanium dioxide and zinc oxide nanoparticles in sunscreens: focus on their safety and effectiveness." *Nanotechnology, Science and Applications* 4:95-112. doi: <http://dx.doi.org/10.2147/NSA.S19419>
- Umar, Muhammad, and Hamidi Abdul Aziz. 2013. "Photocatalytic Degradation of Organic Pollutants in Water." In *Organic Pollutants - Monitoring, Risk and Treatment*, edited by M. Nageeb Rashed, Ch. 08. Rijeka: InTech.
- van Driel, BA, TA Wezendonk, KJ van den Berg, PJ Kooyman, J Gascon, and J Dik. 2017a. "Determination of early warning signs for photocatalytic degradation of titanium white oil paints by means of surface analysis." *Spectrochimica Acta Part A: Molecular and Biomolecular Spectroscopy* 172:100-8.
- van Driel, B.A., K.J. van den Berg, J.Dik, L.Steyn, and B.Rossenaar. 2017b. "Visualizing the invisible " In. *Preprints ICOM-CC triennial conference Copenhagen (Poster)*.
- van Driel, B.A., K.J. van den Berg, M. Smout, N.Dekker, P.J.Kooyman and J.Dik. 2017c. "introducing Design of Experiments (DoE) – For the investigation of the effect of artists' paint formulation on degradation rates of TiO₂-based oil paints." Under Review.
- van Driel, BA, PJ Kooyman, KJ van den Berg, A Schmidt-Ott, and J Dik. 2016. "A quick assessment of the photocatalytic activity of TiO₂ pigments— From lab to conservation studio!" *Microchemical Journal* 126:162-71.
- Werner, A.J. 1969. "Titanium dioxide pigment coated with silica and alumina." In.: Google Patents.
- Wess, T. 2017. "Smartphone citizen science: can a conservation hypothesis be tested using non specialist technology?" *Heritage Science* 5 (1):35. doi: 10.1186/s40494-017-0148-z.
- Xu, Nanping, Zaifeng Shi, Yiqun Fan, Junhang Dong, Jun Shi, and Michael Z. C. Hu. 1999. "Effects of Particle Size of TiO₂ on Photocatalytic Degradation of Methylene Blue in Aqueous Suspensions." *Industrial & Engineering Chemistry Research* 38 (2):373-9. doi: 10.1021/ie980378u.
- Yang, Rui, P. A. Christensen, T. A. Egerton, and J. R. White. 2010. "Degradation products formed during UV exposure of polyethylene-ZnO nano-composites." *Polymer Degradation and Stability* 95 (9):1533-41. doi: <http://dx.doi.org/10.1016/j.polymdegradstab.2010.06.010>.
- Zangeneh, H., A. A. L. Zinatizadeh, M. Habibi, M. Akia, and M. Hasnain Isa. 2015. "Photocatalytic oxidation of organic dyes and pollutants in wastewater using different modified titanium dioxides: A comparative review." *Journal of Industrial and Engineering Chemistry* 26 (0):1-36. doi: <http://dx.doi.org/10.1016/j.jiec.2014.10.043>.

CONCLUSIONS, SCIENTIFIC OUTLOOK AND IMPACT ON SOCIETY

G	TITANIUM WHITE, FRIEND OR FOE? GENERAL CONCLUSIONS	283
G.1	PART I, Characterization of the use and properties of titanium white pigments	283
G.2	PART II, Understanding and monitoring the degradation	285
G.3	PART III, Predicting degradation	289
H	SCIENTIFIC OUTLOOK – WHAT’S NEXT?	291
H.1	General trends	291
H.2	Detailed suggestions	292
I	THE IMPLICATIONS FOR CONSERVATION PRACTICE AND COLLECTION CARE STRATEGIES	295
I.1	Where are we now?	295
I.2	Risk analysis and management	296
J	IN THE CONTEXT OF CONSERVATION SCIENCE AND BEYOND...	301
J.1	The playing field	301
J.2	Value vs. research endeavours	305
J.3	Institutes vs. private practice	307
J.4	The future	308

G TITANIUM WHITE FRIEND OR FOE? GENERAL CONCLUSIONS

Section G presents an overview of the most important conclusions of the dissertation for each of the three parts.

G.1. PART I, Characterization of the use and properties of titanium white pigments.

The main goal of part 1 was to investigate the extent of the use of titanium white in 20th century Netherlands. This was attained by the collection of a large number of pXRF spectra at modern art collections. Based on a large amount of analytical data, it was additionally possible to determine interesting features about these pigments, such as the occurrence of trace element markers in specific types of TiO₂ pigments. Chapter 1 illustrates the benefit of medium-sized datasets obtained under similar measurement conditions. As many institutes nowadays own or have access to a portable XRF instrument, it is advisable to introduce a standard measurement setting. Continuous analysis at different collection will, over time, result in a deeply informative dataset {H, I}.

In support of the XRF dataset, information was obtained from several archives. The work on titanium white paint formulations in the Weber (Permalba) and Talens archives was reported in the ICOM-CC paper '*The Might of White: formulations of titanium dioxide-based oil paints as evidenced in archives of two artists' colourmen mid-twentieth century*'.³⁴ The archival study, was an important reference in this dissertation and has, among others, inspired the paint compositions chosen for the Design of Experiments study {chapter 5}.

In the second chapter of part 1, the complex photoluminescence behavior of titanium white pigments was explored.

Additionally, during the project, I had access to STEM-EDX equipment at AkzoNobel, which was used to characterize the pigments under investigation in chapter 2. Paint fragments {chapter 1} were also analysed with STEM-EDX, and the results were presented on a poster at ICOM-CC 2017 (available upon request). Thus, the main conclusions of this study will also be briefly discussed, mainly to illustrate the applicability of STEM-EDX for pigment characterization.

34 Phenix, A., et al. (2017). The Might of White: formulations of titanium dioxide-based oil paints as evidenced in archives of two artists' colourmen mid-twentieth century. ICOM-CC Triennial conference, Copenhagen.

35 Phenix identified anatase in a Permalba paint likely to be from around the 1970s (Personal communication).

36 Unpublished research, XRD by B. van Driel at the RCE.

G.1.1. The occurrence of titanium white pigments in artists paints in the Netherlands

The pXRF survey indicates the slow rise of titanium white in the Netherlands. Titanium white were found in paint mixtures starting in the 1950s. However, it is only widely used starting in the 1970s. This corresponds to the titanium white production of Talens, where titanium white oil paint is first produced in a test batch in 1937, but it is not advertised until after 1951.³⁴

Pure titanium white is mostly present in non-oil binders. This could be due to the incompatibility of other white pigments in emulsion paints. On the other hand, a lot of pure zinc white oil paints have been found. These paints are, among others, used by artists from the CoBrA group.

The absence of titanium white in early 20th century Dutch oil paintings and its presence in late 20th oil paintings is positive: TiO₂ pigments are mostly present in paintings from a time when stable pigments were on the market. However, it is important to keep in mind that the artist's colors are only a niche market. Furthermore, artist's color makers continued to use anatase far after rutile was developed³⁵. In fact, it is still used in the Talens gouache today³⁶. Chapter 1 focusses on the Netherlands based on practical reasons. However, the results presented in the remainder of the dissertation are applicable to 20th century oil paintings from other geographical areas as well. Literature suggests that the rise of titanium white was much faster, for example in the United States. Therefore, there is a necessity to survey collections further: the more we know, the better we can assess the risks.

G.1.2. Trace element markers

In chapter 1 several elemental markers are described that are of interest for the investigation of titanium white pigments. The markers of interest are niobium and zirconium. The presence of niobium indicates the use of the sulfate process. Thus, its absence, under measurement settings optimized for niobium, characterizes the use of the chloride process, which points to a 'post 1959' date and a rutile-based pigment. Zirconium can originate from the paint drier or the pigment coating, and while conclusive statements cannot be made at this stage, further study of reference paints could elucidate the origin of zirconium.

G.1.3. Complex TRPL behaviour

The time resolved photoluminescence study, performed on fourteen historical and contemporary titanium white pigments, is a first, well balanced, explorative campaign. This study shoes agreement with literature for the general emission shape, but it also indicates an increased complexity for pigments compared to nanoparticles and single crystals. In a more general sense, the Ph.D. research indicates that while dealing with the same material, findings from nano-TiO₂ research (which is the bulk of the available literature) cannot always be extrapolated to pigment research. The increased complexity of pigments influences the shape and intensity of the PL-emission, mostly due to the presence of coating material and the niobium impurity in anatase. At this stage, a relation between photoluminescence and photocatalytic activity (mostly related to pigment coating) could not be determined. Due to its characteristic emission in the NIR (850 nm) photoluminescence can be used as a method to identify traces of rutile in a non-invasive manner.

G.1.4. STEM-EDX characterization

The coating on titanium white pigments can be hard to identify. STEM-EDX proved to be useful for the detection of inorganic coating material. On the other hand, the organic material cannot be conclusively detected. Py-GC-MS is probably a suitable method for detection³⁷. The results of STEM-EDX investigation show the inhomogeneity of these coatings (mainly Al/Si based) and show that the coating material can sometime, be found detached from the pigment. This can be imaged for pure pigments {chapter 2} and for pigments trapped in a paint sample {poster}.

G.2. PART II, Understanding and monitoring the degradation.

The second part of my research was performed to understand titanium white-catalysed degradation of oil paints. More specifically, the aim was to find early warning signs of degradation, detectable before visual changes occur. On the other hand, this part of the research was also intended to explore uncommon methods and approaches for the field of cultural heritage research. This approach resulted in three different chapters:

One chapter about the morphological changes taking place at the paint surface analysed by AFM, XPS and gloss analysis (in collaboration with T. Wezendonk at the chemical engineering department of TU Delft).

37 Unpublished work, further investigated by C. R. de Salis Gomes and C. B. da Costa Ferreira at the Cultural Heritage Agency of the Netherlands (2017-2018).

38 Master thesis done by E. van Dam – While the method was promising (published elsewhere) this research was not pursued further for TiO₂ paints.

39 In collaboration with K. Rasmussen at the European Space Agency.

One chapter about the changes taken place in the organic (oil) binder (in collaboration with S. Morsch at the AkzoNobel corrosion lab at the University of Manchester).

One chapter about the degradation rates of mixtures, evaluated using a Design of Experiments approach (in collaboration with AkzoNobel).

Next to the methods that resulted in a publication, I also evaluated a range of other methods such as LC-MS³⁸, electron spin resonance³⁹, Raman spectroscopy, AFM-Raman (in collaboration with AkzoNobel), Hirox imaging and IR microscopy. However, the methods reported in this thesis resulted in the most promising results for the detection of early warning signs.

G.2.1. Early warning signs of photocatalytic degradation

Chapter 3 and 4 describe the degradation phenomenology of titanium white containing oil paints, monitored with different techniques to identify specific early warning signs of degradation. An early warning sign can be detected by chemical analysis before the damage is visible by eye. The methods to detect early warning signs can be split into those focussing on the inorganics (TiO₂ surfacing) or those focussing on the organics (oil degradation). The outcome of the research presented in chapter 3 and 4, is summarized in the scheme presented in Figure 19. The degradation phenomenology of TiO₂-photocatalyzed degradation of oil paint essentially starts with an intact paint film and ends with a chalked paint film. The chalking stage is clearly distinguishable by eye but can also be imaged nicely in SEM or AFM. The changes occurring between the intact state and the chalked state are illustrated in the Figure 19 (and Figure 22) and can be classified as chemical changes, morphological changes and visible changes. Based on the results, I identified two distinct stages between the intact paint and the chalked paint: the stage of initial oil breakdown and the stage of TiO₂ surfacing. The step between stage 1 and 2 can be clearly imaged with AFM analysis and gloss analysis (morphological changes) as well as analysed with FTIR or AFM-IR analysis (chemical changes). The step between stage 2 and 3 is characteristic for the surfacing of the pigment, which can be determined by XPS. This is the final stage before visible and mechanical change occurs and the oil paint is unacceptably damaged.

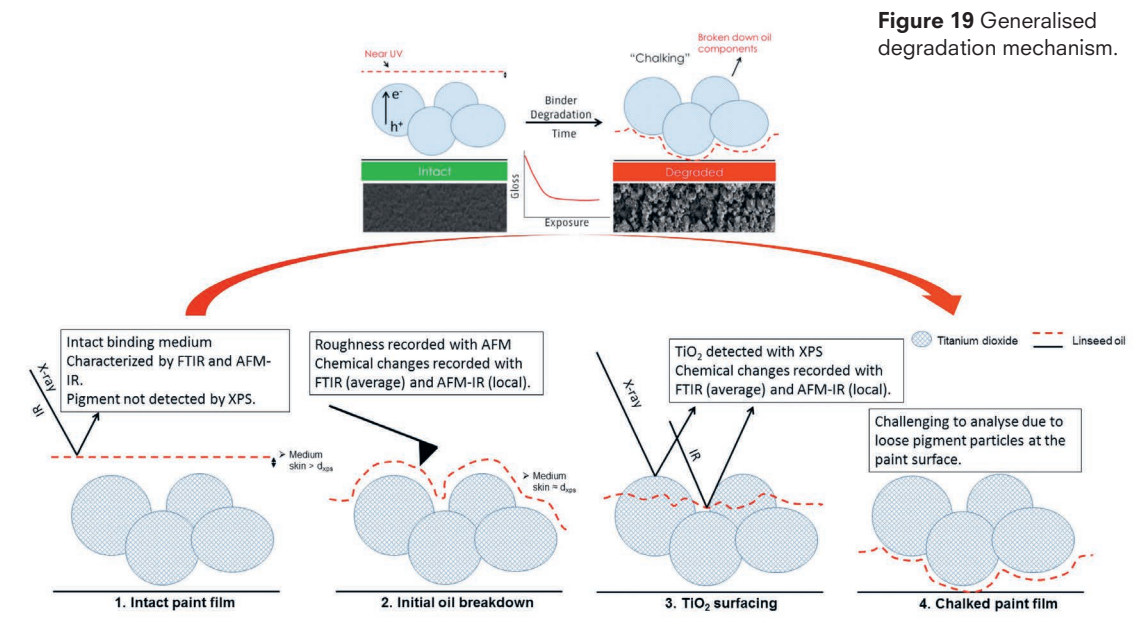


Figure 19 Generalised degradation mechanism.

G.2.1.1. Changes in morphology at the paint surface during aging

AFM and gloss analysis are good methods to monitor degradation over time. However, they are not absolute methods and have to be used comparatively. AFM and gloss analysis are directly correlated, which proves that gloss can be used as a good measure for binder degradation {chapter 5}. XPS, a relatively uncommon method in the field of cultural heritage, is suitable to use as an absolute method of early warning sign detection. Given its limited penetration depth, an oil paint that is in good condition will only have detectable organic components from the binder. As soon as degradation starts taking place, and the pigment begins to surface, the pigment becomes detectable (stage 3, Figure 19). Several things need to be considered:

- The method has only been confirmed for low PVC paints.
- Sampling requires great care because XPS needs to be performed on the paint surface.
- The method is based on the assumption that a layer of medium skin⁴⁰ is present.
- The method has not been tested on paints with other binders.

40 As proposed by K.J. van den Berg and illustrated by the absence of a TiO₂ signal in XPS analysis of the intact paint.

G.2.1.2. Changes in the organic binder during aging

Investigating the organic changes in an oil paint film is traditionally done by IR methods. However, as the changes are minor and mostly confined to the broad carbonyl band, traditional ATR-FTIR was combined with AFM-IR to characterize the changes further. The use of these two methods on anatase and rutile pigmented paints provided valuable information, due to the different resolution and different measurement depth of both techniques. The study shows the formation of lactones at the paint surface directly upon UV irradiation. This formation is clearest in AFM-IR, which is sensitive to the surface. We propose a dynamic surface layer, as the lactone peak stabilizes during aging. In ATR-FTIR, which has a larger measurement depth than AFM-IR, the continuous growth of the peaks is interpreted as the presence of other degradation products such as acids, aldehydes, and ketone, below the surface. Thus, this comparison elucidates degradation indicators in the bulk of the paint. The hypothesis of a lactone-containing surface layer and other degradation product deeper into the bulk of the material is validated by the analysis of an anatase-based paint cross-section. The increased understanding of changes in the binder, opens the possibility to use portable non-invasive IR spectroscopy systems to monitor the state of the paint over time.

G.2.2. The influence of paint formulation on degradation rate of TiO₂ containing oil paints

Chapter 5 shows the influence of paint formulation on degradation rates. Firstly, the type of pigment is found to be highly relevant. The order of PC activity by artificial aging correlates with the order found in the dye degradation test {part 3}, which confirms the validity of both methods. It is interesting to note that the application of an inorganic coating is more efficient for the reduction of photocatalytic activity than a change in the crystal structure from anatase to rutile. Other interesting conclusions are:

- The protective effect of inorganically coated rutile is significant and can even protect paint from chalking in certain mixture ratios with photocatalytic uncoated anatase.
- Zinc oxide can be as photocatalytic as uncoated anatase and has a similar interaction with coated rutile. The relation between ZnO photocatalysis and saponification should be investigated.
- Aluminium stearate has a significant, but still badly understood, effect on the degradation rate. As this is a common additive in 20th century paintings, further investigation is necessary.

- The ratio between active material (pigment) and degradable material (oil) has an important effect on the degradation rate.
- Extenders have an important effect on degradation rate, which is partly due to an increased UV penetration depth due to the low hiding power of the extenders. The effect of extenders should be investigated in more depth considering most titanium white paints contain extenders.

Chapter 5B comments on the application of DoE and the added value that can be gained during formulation/reconstruction studies. To introduce DoE to conservation science five guidelines were formulated.

- You get what you design for (Crap in = Crap out).
- Think about the question you want to answer.
- Gather information about the system and the responses. Sometimes optimal use of DoE is not possible simply because it is not practical (e.g. aging each sample in a separate oven run). In these cases, DoE is still very useful but it is important to be aware of the consequences.
- Stay critical - Everything can be modeled but it has to physically make sense.
- Successful use of DoE requires statistical insight as well as material/system specific knowledge.

G.3. PART III, Predicting degradation

The aim of part three was to build a bridge to conservation practice. In other words, to develop an easy-to-use method to determine if a painting is likely to degrade or if a pigment is likely to cause degradation. This goal is achieved by the development of two different tests: one suitable for powder material or paint scrapings {chapter 6} and one suitable for paint cross-sections {chapter 7}. Additional work was done to investigate the use of an electrochemical method⁴¹. However, we found that this method (amperometry) is too sensitive to unrelated effects and thus not applicable for the investigation of TiO₂ photocatalytic activity.

G.3.1. Predicting photocatalytic activity of powders

The dye degradation test described in chapter 6, can be used to test the photocatalytic activity of pigment powders. This requires several adjustments of the traditional test developed for catalytic powders. The adjustments are necessary to deal with the coatings present on pigment particles and with the size difference of pigments versus catalysts. Furthermore, it is important to always include a photocatalytic and a photostable standard during a test

as benchmark samples. The inks, used to test photocatalytic activities of pigments in cross-sections {chapter 7}, are being investigated further by Mills et al. for their use on powders, and may in time be more suitable as a test method.

G.3.2. Predicting photocatalytic activity of pigments in a paint cross-section

The cross-section staining PAII test can be implemented directly in modern art conservation studios. The test is easy-to-use and provides an accurate 'yes' or 'no' answer. Follow up studies should be carried out for validation on mixed materials, the effect of zinc white, cross-section with non-oil binders and powder materials⁴².

H SCIENTIFIC OUTLOOK – WHAT'S NEXT?

This dissertation provides information about titanium white oil paint degradation and explores several techniques for the field of conservation science. However, it should not stop here. In this outlook, I will discuss how I think the research should continue in terms of detailed suggestions, related to the specific chapters in this dissertation, as well as general recommendations.

H.1. Detailed suggestions

The pXRF study provides an overview of the use of white pigments and illustrates the discovery of one interesting trace element. However, further data-mining on the present dataset with different data-analysis methods could yield further interesting insights. One approach would be to look at the complete spectra, rather than deconvoluted peak heights. Another approach could be to analyse all individual spectra, related to their specific location, rather than analysing painting averages. Furthermore, the dataset should be extended by doing analysis at other collections or on paintings from different geographical regions.

Chapter 2, indicates the complexity of the photoluminescence behaviour of TiO₂ pigments. Future research should focus on the separation of the different effects of coating, impurity etc. by investigating well controlled pigments from an identical parent material.

The pXRF survey indicates that most pure titanium white paints are prepared in non-oil binders. Thus degradation phenomenology (early warning signs) and rates of TiO₂ in non-oil binders such as acrylics and gouache should be investigated. Ideally, those studies, as well as other artificial aging/formulation studies are carried out using Design of Experiments as this proved to be a very effective method {chapter 5}. Further formulation studies should be carried out to elucidate the processes behind the effects identified in chapter 5. It is of specific interest to focus on extenders, aluminium stearate and zinc oxide since they are common components in titanium white paint. In the case of zinc oxide, which is well known for its degradation problems related to saponification, the relation between photocatalytic activity and soap formation is of research interest. Furthermore, all studies in this research were performed with continuous UV irradiation. The relation between continuous UV aging and other irradiation modalities (e.g. cyclic lighting or day light) should be investigated to better estimate the timeframe of the expected changes. This research focussed on white paints. Nevertheless, it is also important

43 Unpublished work by the author in collaboration with C. Gervais, M.A. Languille and E. Nazarenko

44 Summary Paper ICCROM Forum 2013, supplement 2 to Studies in conservation Volume 60, A. Heritage and S. Golfomitsou "Conservation Science: Reflections and future perspectives."

to research the combination of titanium white with colored pigments as these degradation processes may be faster since they do not require the breakdown of an oil network, but only the destruction of smaller organic components or the reduction of metal ions. The sensitivity of Prussian blue to anatase (even under normal lighting)⁴³ was observed during my studies and this could be an important avenue to pursue.

Finally, the PAII staining test should be validated and implemented in real practice. The test can already be valuable for samples of oil paints, but further research is required to test its applicability on paint samples with, for instance, other binder media. Furthermore, research is required to better understand the results, especially those of samples containing zinc oxide and organically coated anatase.

H.2. General recommendations

The summary paper⁴⁴ of the ICCROM forum in 2013 states that important goals for the future are:

- *'Improving methods, minimizing errors in experimental processes and making use of standardized methodologies will also enhance the quality of scientific data.'*
- *'An important advance would be the creation of shared tools for planning and implementing evaluation studies (e.g. survey questionnaires, data sets, and protocols). Common tools would also enable a 'big data' approach to the analysis of surveys, opening the way towards the collection of comparative data, benchmarking and the development of indicators for the field, and in turn provide a quantifiable basis to support strategy development.'*

In line with these goals and in my personal view, the conservation field should move towards a more preventive and predictive approach, in which we try to understand, predict and prevent degradation. This can be achieved using several ideas from my dissertation such as:

- The development and introduction of easy testing methods into conservation studios.
- Surveying collections.
- Applying systematic approaches (DoE) to artificial aging studies.
- Regularly monitoring the aging of objects using established diagnostic techniques, which focusses on early warning sign detection.

Firstly, the PAII staining test {chapter 7} should be implemented in conservation studios for modern art, following a standard measurement protocol (Figure 20, left), as soon as possible. Simultaneously, the PAII test should be further investigated, professionalized and commercialized. I am convinced that easy-to-use methodologies are the bridge between theory and practice in conservation science. Furthermore, I believe that smartphones will play a big role in the introduction and availability of such methods. An online protocol is already available to build a microscope on your smartphone for under \$20, which was proposed for the detection of Malaria⁴⁵. Furthermore, smartphone technologies are investigated for their use as cheap multispectral imaging tools⁴⁶, which was already reported for skin diagnosis.⁴⁷ Even without microscope capabilities smartphones can play a role using apps such as those for colorimetric analysis. Wess questions if citizen science⁴⁸, which uses non-specialized technology, is beneficial to the field and if it can be used to test conservation hypotheses. I would like to argue that we should embrace this type of citizen science. Even though, it may not be wise to use non-specialized technology for fundamental scientific studies; the development of easy tests using simple equipment, is the step we need to take to move conservation science out of the elite institutes and into the real work field {J}.

Secondly, with the introduction of MA-XRF, I notice a devaluation of pXRF. However, the value of comparative pXRF on a medium-sized set of paintings was demonstrated in this thesis {chapter 1}. If a large national or international group of XRF users can agree on a measurement set-up (always performed next to the measurement performed to answer the specific question), a large dataset can be build, Figure 20 (right). This dataset may grow rapidly and become an important source of information for researchers and conservators. Such a data gathering procedure should be broader than only for TiO₂ pigments. Ideally it is applied for all types of materials. Where possible, it is advisable to focus on impasto paints, as this removes that stratigraphy concerns in XRF interpretation. Survey studies are most valuable when supported with archival information and appropriate metadata. While several archives are available^{49,50}, most archives lack the organization and digitization, which is needed to make efficient use of the information. Thus, simultaneously, efforts should be undertaken to achieve accessibility of organized archives.

Furthermore, the use of DoE is strongly recommended, especially when it comes to reconstruction/artificial aging studies. The introduction of the DoE approach was immediately received with much enthusiasm in the Ateliergebouw. For example, following

45 <https://www.tudelft.nl/2017/3me/using-microscope-technology-on-mobile-phones-to-trace-malaria-quickly-and-cheaply/>, accessed 11-12-2017

46 www.eigenimaging.com/learn-more/smartphone-multispectral-imaging

47 www.ncbi.nlm.nih.gov/pmc/articles/PMC5175570.

48 Wess, T., Smartphone citizen science: can a conservation hypothesis be tested using non specialist technology? Heritage Science, 2017. 5(1): p. 35.

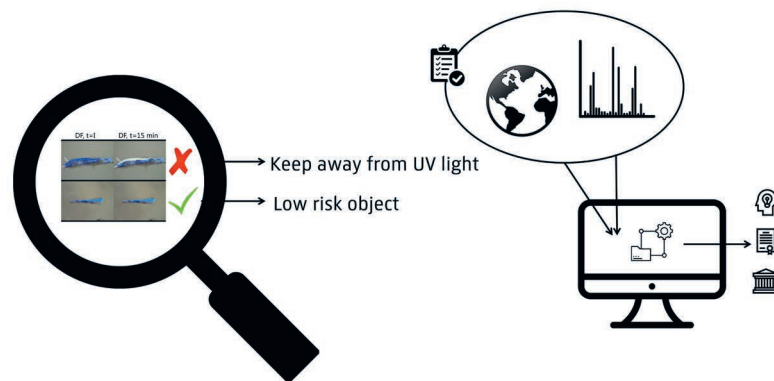
49 Burnstock, A., Jan van den Berg, K., van Gorp, F., Bayliss, S., & Ovink, K. (2016). ". In S. Eyb-Green, J. H. Townshend, K. Pilz, S. Kroustallis, & I. van Leeuwen (Eds.), Sources in Art Technology, Back to Basics (pp. 43-50). Archetype. (2016). "Making paint in the 20th Century: the Talens Archive."

50 Phenix, A., et al. (2017). The Might of White: formulations of titanium dioxide-based oil paints as evidenced in archives of two artists' colourmen mid-twentieth century. ICOM-CC Triennial conference, Copenhagen.

my study, I performed a DoE analysis on data by Kate van Lookeren, who investigated the properties of different ceramics compositions. This resulted in a successful analysis of a historical data set. The analysis did point out that application of the DoE approach from the start, would have resulted in a study containing fewer samples while gaining more information. For the future, it is my advice to use Design of Experiments for reconstruction studies and studies into formulations. Furthermore, the DoE basics need to be implemented in the curriculum of conservation and technical art history students.

Finally, methods to monitor change and to detect early warning signs were developed (AFM, IR, XPS). These methods were validated on mock-up paint samples. To truly use them for the determination of early warning signs and for the assessment of real degradation rates; these methods should be validated on real paintings in real environments. This type of investigation requires a long term commitment, because natural aging instead of accelerated aging will be monitored. Nevertheless, this knowledge is essential to estimate an acceptable 'UV budget' for artworks containing titanium white.

Figure 20 Left: Infographic for citizen based conservation science more specifically the PAII staining test. Right: Infographic on pXRF data gathering principle.



I THE IMPLICATION FOR CONSERVATION PRACTICE AND COLLECTION CARE STRATEGIES.

The main question raised in the Ph.D. research is 'Titanium white, friend or foe?'. As described in this dissertation, titanium dioxide is a material with variable PC activity (vulnerability). Thus the correct answer to that question is 'it depends'. Nevertheless, it is an important question, that collection care takers need to be aware of and about which they need to start thinking now, in order to prevent future problems.

The risk scenario (impact) under investigation in this thesis is: the occurrence of visible TiO₂-photocatalyzed paint degradation during display.

Whether titanium white is a friend or a foe to the painting in which it is contained ('good' or 'bad'), depends on the paint compositions and the pigment's photocatalytic activity, which in turn depends on pigment characteristics. Furthermore, whether degradation will occur and how fast it will occur, depends on the exposure conditions.

I.1. Where are we now?

Figure 22 illustrated the changes that take place in an oil paint with 'bad' titanium white upon exposure to UV irradiation. This figure is an integration of multiple results and observation from my studies {chapter 3-5}. From the figure, it becomes clear that waiting for the sudden and intense visible change is not advisable. My studies have shown that degradation can be detected at an earlier stage by measuring the chemical or morphological changes. Thus, an important question for risk management is: 'Where are we on the change curve?'. Unfortunately, again, the answer is not straightforward: calculations based on research outcome (Table 1) indicate a time frame between 50 and 1000 years of continuous exposure. The exact time until visible change depends on the type of pigments, the amount of pigment and the exposure conditions and is thus difficult to predict⁵¹. This time frame is quite broad. However, it does indicate that it can happen, and in some cases, in a relatively short amount of time.

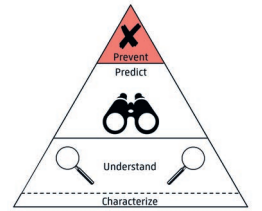
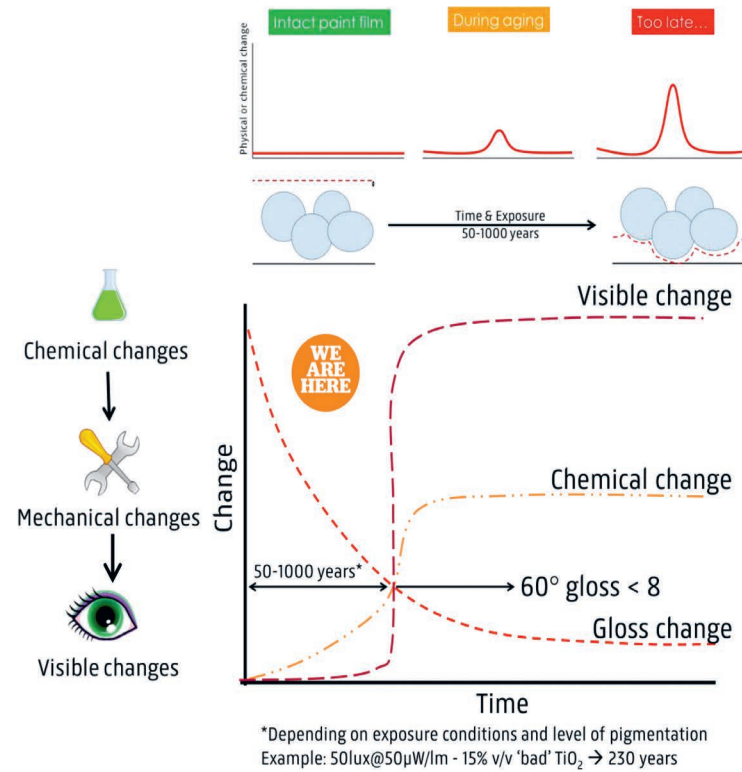


Figure 21 Thesis triangle.

51 Only pure TiO₂-Binder paints were taken into account for the calculations.

Figure 22 Changes which occur during TiO₂-mediated degradation.



I.2. Risk analysis and management

Recall that, in this study, we distinguish the ‘potential risk of impact’ of the object and the ‘risk of impact’ once exposure conditions are taken into consideration. The potential risk is a combination of value and vulnerability of the object. Before any risk management can be performed the potential risk of the object has to be classified {F}. Each star on the value-vulnerability diagram (Figure 23, left) represents an art object in a collection. Thus an assessment of the value and vulnerability of each object needs to be made to fill out a value-vulnerability diagram. The value, based on financial and cultural importance, can be determined by all stakeholders. The vulnerability, is presently often unknown. Therefore the first step in risk assessment is to determine the vulnerability of art objects to TiO₂-mediated degradation. This can be done for instance by analysing the elemental composition of the paint via non-invasive methods such as pXRF {chapter 1} and by measuring the photocatalytic activity of the TiO₂ pigments {chapter 7}. If the pigment is not TiO₂, collection care takers should be aware of other degradation phenomena, such as soap formation, and act accordingly. Here I

present a vulnerability assessment based only on TiO₂-catalyzed degradation. In the future it would be sensible to extend such an assessment with degradation processes caused for instance by other pigments. If the pigment is TiO₂, the important question is: ‘Is it good or bad TiO₂?’ ‘Is it a Friend or a Foe?’. This answer can be obtained by performing the ink test {chapter 7}. I suggest to do this test continuously as a standard procedure, as paintings come into the studio. Additionally, the test can be performed on collections of cross-sections already taken from paintings in earlier conservation or research campaigns. If the pigment is ‘good’ titanium white, the object has low vulnerability. However, if the pigment is ‘bad’ titanium white, the object has high vulnerability.

Based on two samples from chapter 5, other samples range between these ‘dose to chalk’ values.

			10%	vol% TiO ₂	15%			
Office*	Museum*	Working areas with minimal visual tasks*				Working areas with minimal visual tasks*	Museum*	Office*
500@150	50@50	100@100				100@100	50@50	500@150
75000	2500	10000				10000	2500	75000
75	0.25	1				1	0.25	75
						8246		
						1806		
						1.81E+09		
1.10E+08	3.30E+10	8.25E+09				1.81E+09	7.22E+09	2.41E+07
1.83E+06	5.50E+08	1.37E+08				3.01E+07	1.20E+08	4.01E+05
3.05E+04	9.16E+06	2.29E+06				5.02E+05	2.01E+06	6.69E+03
1273	4.E+05	1.E+05				20903	83611	279
3.5	1045.9	261.5				57.3	229.1	0.8

In Figure 23 (left), I randomly filled out a value-vulnerability diagram for a fictional collection which results in a ‘collection composition’ (Figure 23, right). Private or company collections likely have a different collection composition than museum collections. This is related to differences in collection strategies, in display conditions, in the age of the collections and in the acquisition budgets.

Depending on the collection composition and the current exposure situation, the target situation can be determined based on the mission/aim/value of the collection which can be display,

52 Egerton, T. A. and C. J. King (1979). “The influence of light intensity on photoactivity in TiO₂ pigmented systems.” J. Oil Col. Chem. Assoc 62: 386-391.

Table 1 Exposure calculations.

*Equipped with Incandescent lamps, halogen incandescent lamps or fluorescent lamps. LED lamps have a UV content of <5µW/lm significantly reducing the dose.

** Calculations were performed as if the reciprocity principle applies. We know that generally photocatalysis follows a power law relation to intensity.⁵²

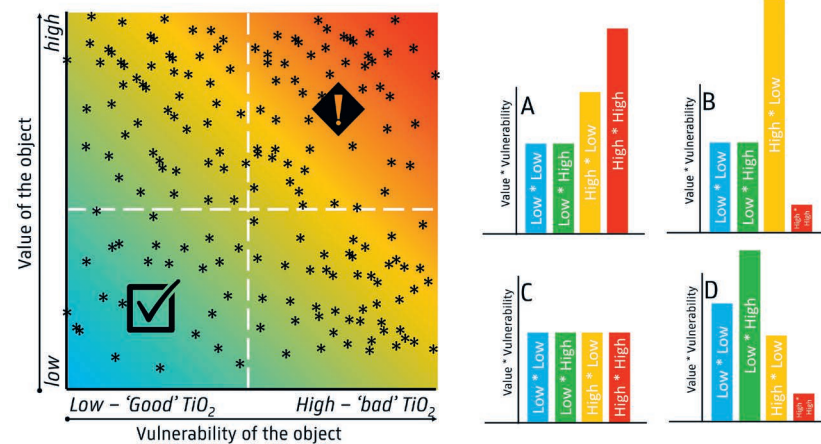
*** Calculations relate to continuous exposure, experiments with cyclic exposure were not performed.

**** Calculations are based on pure TiO₂/oil paints, not taking into account different formulations.

53 These are not necessarily strategies that I support.

preservation or something else. The difference between the current situation and the target situation can be evaluated (gap analysis) and cost-benefit analysis can be carried out to determine the preferred risk strategy. This strategy can be to accept, transfer or mitigate risk by implementing corrective actions. Some of these strategies require significant resources. Thus it is important to have all the information from the first step (a minor continuous investment) before spending the resources.

Figure 23 Left: Value-Vulnerability diagram. Right: Composition of fictional collections.



Possible risk management strategies/corrective actions are⁵³:

- Accept:
 - Write off the object(s) or collection over a defined period of time.
 - Sacrifice one object in a series.
 - Write off the objects but monitor the degradation (sacrifice in exchange for information about degradation rates/ UV budget).
 - Write off the objects but develop a treatment for powdery paints (sacrifice in exchange for test object to evaluate developed treatments).
 - Transfer:
 - Sell/store high vulnerability objects and buy low vulnerability objects for display.
 - Insurance (for instance during loan).
 - Charge if the painting is on loan for used 'UV budget'.
 - Monitoring degradation is required to determine the UV budget.
- Mitigate:
 - Store in the dark.
 - Display a copy.
 - Remove UV irradiation.

- On building level.
- On room level.
- On object level.
- Monitor the degradation to determine 'UV budget' – Distribute UV irradiation over display time before visible change and store in the dark afterwards.

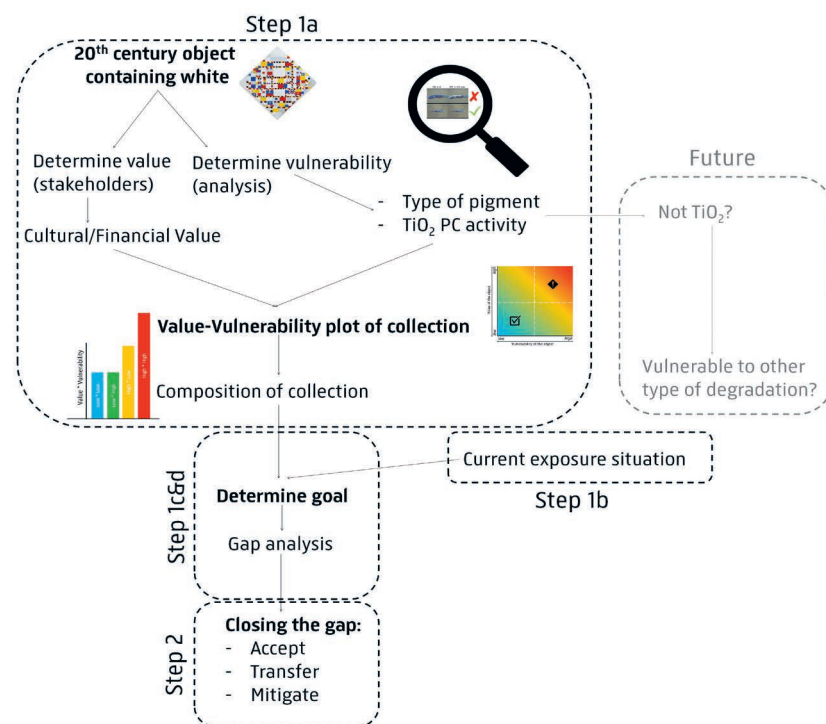
Which risk strategy is preferred depends among others on the composition and aim of the collection, which are significantly different for museum-, private- and company collections. I will present some fictional examples to illustrate possible applications of the proposed risk management strategy:

- A collection which contains a lot of high potential risk objects (Figure 23 right A) and aims to display the objects: -> Remove UV on a building level [mitigate].
- A collection which contains a lot of high potential risk objects (Figure 23 right A) and aims to preserve the objects without display: -> Store objects in the dark and possible obtain information on 'UV' budget available for occasional display [mitigate].
- A collection which contains several high potential risk objects (Figure 23 right B or D) and aims to display the objects: -> Remove UV on an object level [mitigate].
- A collection which contains several high potential risk objects (Figure 23 right B or D) and is considered a private investment: -> Store the high potential risk objects in the dark [mitigate]. -> Sell/Store high vulnerability objects and buy low vulnerability objects for display [transfer].
- A collection with an even distribution of low and high risk objects (Figure 23 right C) and the aim to display the collection: -> UV removal on building level or object level [mitigate].
- A collection with a lot of low value, high vulnerability objects (Figure 23 right D) and the aim to display objects and to contribute to conservation science: -> Sacrifice in exchange for information (monitoring degradation/test object for potential treatments) [accept].
- A collection with some high value, high vulnerability objects (Figure 23 right B, C or D), the aim to display but a good argument against putting the high risk object behind glass: -> Monitor degradation to determine 'UV budget' – Distribute UV budget over display time before visible change and store in the dark afterwards [accept/mitigate].

To summarize the proposed risk strategy has two main steps: assessment and management, illustrated in Figure 24:

1. Assessment (minor, long-term commitment):
 - a. Fill out the value-vulnerability diagram & determine composition of collection.
 - i. Determine vulnerability of objects.
 1. pXRF {chapter 1}
 2. Ink test {chapter 7}
 3. Other analysis (e.g. photoluminescence, Raman, XRD) {chapter 2}
 - ii. Stakeholder meeting to determine value.
 - b. Assess current exposure situation/identify unusual UV exposure situations (loans?).
 - c. Determine the target situation.
 - d. Gap analysis: difference between current situation and the target situation.
2. Management (possibly a major commitment):
 - a. Determine strategy/corrective actions (cost-benefit analysis): accept, transfer or mitigate.
 - b. Close the gap (carry out strategy).
3. Re-evaluate.

Figure 24 Risk management strategy.



J. IN THE CONTEXT OF CONSERVATION SCIENCE...

When I started my Ph.D., the topic for the project described in this thesis was not crystallized yet. The research proposal assumed that TiO_2 pigments were a problem, and an acute one at that. The unsuccessful search for case studies to build the research on, in a traditional conservation science way, was a setback. But I did not let it get me down. Instead, I used this to adjust my research approach. The resulting approach could be described as a preventive approach. Because of my background in engineering, I am also tempted to describe my approach as an engineering approach. This approach is characterized by the role of the end user and therefore the bridge between theory and practice. It is illustrated by the following quotes:

‘Engineering is the art of modelling materials we do not wholly understand, into shapes we cannot precisely analyse so as to withstand forces we cannot properly assess, in such a way that the public has no reason to suspect the extent of our ignorance.’

– Dr. AR. Dykes⁵⁴

‘Engineering problems are under-defined, there are many solutions, good bad and indifferent. The art is to arrive at a good solution. This is a creative activity, involving imagination, intuition and deliberate choice.’ – Ave Arup⁵⁵

During my research, I started to question the relevance and applicability of research performed in conservation science, a young but mature research field. I found it very insightful to zoom out from the molecular level to the real world. Following this train of thought, I would like to use this part of my dissertation to shed some light on the relevance and impact of my study in the context of the history and future of conservation science.

J.1. The playing field

Since the mid-20th century, the Netherlands has been and continues to be a leading player in the field of conservation science. The Netherlands Organisation for Scientific Research (NWO) has supported multiple research programs (Molart, de Mayerne, Science4Art, NICAS) to deepen the understanding of the behaviour of cultural heritage materials. Presently, in Europe, the breadth of conservation science is illustrated by Iperion-CH, JPI-CH, INCCA and many other initiatives. The field exists under different names such as conservation science, heritage science, heritage preservation or art scientific studies illustrating that its objectives are dynamic. In Europe and North America, the term

⁵⁴ <https://javigon.com/like/>
⁵⁵ <https://nl.pinterest.com/pin/208713763954297615/>

All URL's were accessed on 19-01-2018

56 ICROMM Forum 2013, <http://www.iccrom.org>, accessed 19-01-2018

57 Groen, C. M. (2011). *Paintings in the laboratory: scientific examination for art history and conservation*. Martin Heinrich Klaproth (1743-1817) performed studies on objects from antiquity in Berlin.

58 https://en.wikipedia.org/wiki/Rathgen_Research_Laboratory, accessed 19-01-2018

59 Bewer, F. G. (2010). *A Laboratory for Art: Harvard's Fogg Museum and the Emergence of Conservation in America, 1900-1950*, Harvard Art Museum

60 Groen, C. M. (2011). *Paintings in the laboratory: scientific examination for art history and conservation*

61 Cardinali, M. (2017). *Technical Art History and the First Conference on the Scientific Analysis of Works of Art (Rome, 1930)*. *History of Humanities*, 2(1), 221–243. <https://doi.org/10.1086/690580>

62 <http://www.iccrom.org/wp-content/uploads/Survey-of-Conservation-Literature-final-web.pdf> <http://www.iccrom.org/conservation-literature-2/> - features and interactive plot. Accessed 11-12-2017.

63 <http://www.iccrom.org/wp-content/uploads/Survey-of-Conservators-final-web.pdf>, accessed 11-12-2017.

heritage science is becoming increasingly popular⁵⁶. This term is used to describe the combination of several fields such as archaeological science, technical art history, and conservation science, thus creating a field of study with a larger critical mass dealing with similar problems. While, it is often regarded as a young field, scientific studies of artworks have been performed for a long time. Research started on archaeological objects in the 18th century⁵⁷. At the end of the 19th century, the first ever chemical laboratory in a museum was founded (1888) in the Kaiser Friedrich Museum of the Königlichen Museen in Berlin with Friedrich Rathgen as the first chemist working in a museum⁵⁸. The goals of this new founded research were mainly to detect forgeries, to develop durable materials (commonly carried out by industrial chemists) and to address concerns related to the physical changes of works of art⁵⁹. The second lab that opened was in the British museum in 1922⁶⁰, followed by the Louvre in 1923⁶¹. Simultaneously, in the early 20th century, pioneer E.W. Forbes was taking the first steps towards the development of a research department at the Fogg Museum in the United states, which opened in 1928. In 1934, the first national institute was set up in Belgium (IRPA). This initiative that was followed in the Netherlands in 1963 (Centraal Laboratorium voor Onderzoek van Voorwerpen van Kunst en Wetenschap)⁶⁰. The foundation of museum laboratories led to the first ever conservation science conference in 1930 in Rome, organized by the International Museum Office (IMO). Attendees of the conference aimed to place the preservation of works of art on a solid scientific basis. It is interesting that topics on the agenda in 1930, such as raising standards and gathering more reliable data, are still relevant today⁶². A committee of 5 art historians, 5 restorers, 2 chemists and 1 consulting physicist was formed after this meeting to write a manual on easel paintings. This effort can be regarded as the first professional and interdisciplinary collaboration in the field, laying the groundwork for many to come⁵⁹.

In the past decades, a shift in contributors to conservation science can be observed. Universities started to play a major role, and government institutes moved their focus away from fundamental studies⁶². Dissemination and transfer of knowledge remains an important goal⁵⁹ and conservators indicate that they are influenced by scientific publications⁶³. Due to the increased role of universities, access to publications became an issue. With the option of Open Access publication now available, this option should always be considered, especially for topics that have a direct influence on conservation practice. When submitting my work for publication, I consciously decided which papers should published with Open Access. Papers that were in my view directly applicable in practice

{chapter 1, 5 and 6} were submitted to journals that allow Open Access. Publishing cost was shared between the institutions {chapter 6} or covered by the TUDelft Open Access fund {chapter 1 and 5}, which illustrates the joint sense of responsibility.

As described by Iperion-CH, heritage science is a ‘*Cross-cutting domain embracing a wide range of research disciplines supporting the various aspects of tangible and intangible Cultural Heritage conservation, interpretation and management*’⁶⁴. The field shows its maturity through a range of well visited themed conferences (such as the Gordon Research Conference for scientific methods in Cultural Heritage), a prominent spot on the European agenda and the establishment of dedicated professional journals. The place of my study within the field of research is illustrated by my contributions to these conferences and journals. Collaborations between museum professionals, academics and industry have been of high importance since Forbes’ time⁵⁹, and while some projects reach true interdisciplinarity (e.g. the restoration of Rembrandt’s Marten and Oopjen at the Rijksmuseum), this is not always achieved. Some art historians misunderstand how science can contribute to art history or conservation and are therefore hesitant to use it. On the other hand, others may expect science to solve everything. However, this will never be the case. In fact, scientific studies usually raises more questions⁶⁵, based on an increased understanding. Presently, problem holders and knowledge holders come together in temporary projects, for acute problems and solutions. As noted in the NICAS white paper, in the Netherlands, conservation science professionals strive for ‘*mutually-beneficial collaborations between museums, scientists, cultural heritage caretakers and industry that help identify and realize like-minded goals*’. Here I would like to underline the words ‘mutually-beneficial’: it is a start for a museum to provide access to artworks but to make progress the aim should be to achieve true mutual-beneficial collaborations. With the commitment of modern art museums in the Netherlands, my Ph.D. may have a real impact and I hope that next to providing access to the collection, collection caretakers will carefully take account of my dissertation and apply it to conservation and collection care.

Many problems of the future, like the TiO₂ problem, lack a problem holder. The 2005 report ‘*a public trust at risk: the heritage health index report on the state of America’s collection*’ makes the following, in my opinion important, recommendations:

Every institution must assign responsibility for caring for collections to members of its staff.

64 <http://www.iperionch.eu/about/>

65 Ondoordingbaar groen en blauw: de praktijk van het verrichten van natuurwetenschappelijk technisch onderzoek. Arie Wallert in gesprek met J.R.J. van Asperen de Boer. Door: Anna-Maria van Egmond. (2014)

66 https://heritagescienceresearch.com/2015/11/17/theory_heritagescience/ Nov 2015. Accessed 11-12-2017.

67 Stokes, D. E. (1997). *Pasteur's Quadrant: Basic Science and Technological Innovation*, Brookings Institution Press. https://en.m.wikipedia.org/wiki/Pasteur%27s_quadrant, accessed 21-01-2018.

Individuals at all levels of government and in the private sector must assume responsibility for providing the support that will allow these collections to survive.

In 1920 at a meeting of the College of Art Association (CAA) Forbes similarly stated that: '*Neglecting to take responsibility for the preservation of cultural heritage, was tantamount to a crime against civilization*'⁵⁹. Within this context, which is still relevant after nearly a century, any modern art collection must assume responsibility for the upcoming titanium white problem and act accordingly. The Stedelijk Museum in Amsterdam, a leading museum for modern art in the Netherlands, neglected to do exactly that by refusing cooperation for this dissertation.

Matija Strlic states that heritage science is '*inherently biased*.' This statement stems from the idea that by researching an object, value is added to it. However, while the investigation of blockbuster pieces can be scientifically relevant, it is also a means to raise awareness, attention and thus funding. This funding may then be used to do less popular research, such as surveying collections for possible problems {I}. Furthermore, another statement by Strlic is that '*heritage science can be neither fundamental nor experimental*'⁶⁶, because work is done on one of a kind objects which makes it difficult or even impossible to rigorously follow the scientific method. This is a premise I don't agree with. Conservation science, in the manner that is described by Strlic, is not the type of conservation science that research endeavours and resources should go towards. Whenever possible, conservation science should follow the scientific method as rigorously as possible. In my opinion three different approaches in conservation science can be discerned, in analogy with healthcare, namely: a fundamental approach to increase understanding, a diagnostic approach which should preferably be non-invasive and used for decision making processes and lastly a treatment approach, focussed on the active preservation of objects. My research uses the two first approaches and can be described as: understanding the use {chapter 1} and properties {chapter 2} of materials, understanding processes taking place in those materials {chapter 3-5} as well as predicting {chapter 1, 6 and 7} and preventing damage {I}. The combination of the three different approaches can also be classified as 'use-inspired basic' research (Pasteur's quadrant)⁶⁷. Scientific research is traditionally motivated by either fundamental understanding of nature (exemplified by the work of Niels Bohr) or by the aim to find solutions for immediate problems (exemplified by the work of Thomas Edison). Research described by the Pasteur's quadrant falls between the two and has the goal to enhance knowledge and utility. Typically this type of research is characteristic for interdisciplinary research fields such as conservation science.

J.2. Value versus research endeavours

The value of cultural heritage objects is very difficult to determine and is dependent on many parameters such as economic, social and cultural value. Subsequently, these values are related to supply and demand and to the taste of a particular time and place. Presently, in terms of financial value the impressionists dominate the market (35%), followed by post-war and contemporary artists (27%), Chinese painting and calligraphy (17%) and finally the old masters (13%)⁶⁸. While old master pieces contribute to a decreasing share of the art market,^{69,70} there is still a block buster appeal to them in museum collections. Also old masterpieces do not come to auction very often and when they do they are sold for astronomical values, such as da Vinci's *Salvator Mundi*⁷¹ (Table 2). It is interesting to note that the da Vinci was sold at the post-war and contemporary auction evening, an economically savvy move to raise the price.⁷²

Table 2 reports the 15 most expensive paintings ever (according to Wikipedia's list of 50). In addition to the astronomical prices of these artworks (most of which were produced in the 20th century), it is interesting to note that no less than seven of these paintings were made by painters known to have used titanium white. Furthermore, all of these seven paintings were purchased by private collectors, possibly unaware of the risks {I}. Remembering Forbes' words in 1920, these private collector should, similar to museums, be held responsible for the preservation of these artworks, and hence invest in research.

As an additional complication, modern art objects were produced in a time of technological development, and are thus composed of highly complex materials and formulation. Therefore, the chance of such a painting falling apart is significant. Some examples of problems with modern paintings are the dripping paintings by Frank van Hemert⁷³, the problem of water sensitivity in modern oil paints⁷⁴ and the wide variety of problems occurring in paintings by Karel Appel⁷⁵ and other CoBrA artists. Furthermore, the processes that cause the degradation of modern paintings are less well understood since it is incorrect to just extrapolate what is known from traditional painting materials. This complication was already noted almost a century ago by Forbes who was aware that '*Artist' experiment with materials and methods untested by tradition could result in the deterioration of their work at an unprecedented pace*.'⁵⁹ and by Church who notes: '*But not only were the conditions under which the painters of Titan's time worked simpler than those of the 19th century, but grounds, paints oils and varnishes were generally prepared in the studios of the artists and, under their own superintendence, so that the chances of going wrong were comparatively limited. And it is*

68 Percentage of the 100 most expensive artists at auctions URL: <https://www.artsy.net/article/artsy-editorial-the-100-most-expensive-artists>.

69 <https://www.nytimes.com/2016/08/29/arts/design/can-the-old-masters-be-relevant-again.html>

70 <https://www.artsy.net/article/artsy-editorial-the-10-most-important-takeaways-from-the-2016-tefaf-art-market-report>

71 <https://www.theguardian.com/artanddesign/2017/nov/16/salvator-mundi-leonardo-da-vinci-most-expensive-painting-ever-sold-auction>

72 <https://www.theguardian.com/artanddesign/2017/nov/15/leonardo-da-vinci-masterpiece-salvator-mundi-christies>

73 <https://eenvandaag.avrotros.nl/item/de-druipende-schilderijen-van-frank-van-hemert/>, accessed 11-12-2017.

74 <https://www.incca.org/articles/water-sensitive-oil-paints-project>, accessed 11-12-2017.

75 <https://www.nrc.nl/nieuws/2016/05/11/het-gaat-niet-goed-met-de-schilderijen-van-karel-appel-a1407332>, accessed 11-12-2017.

All URL's were accessed on 19-01-2018.

76 Copied from Wikipedia https://en.wikipedia.org/wiki/List_of_most_expensive_paintings

77 <http://www.christies.com/features/The-Private-Sale-of-Rembrandt-Van-Rijn-Portrait-of-Oopjen-Coppit-and-Maerten-Soolmans-7044-1.aspx>

Table 2 The 15 most expensive paintings ever according to Wikipedia⁷⁶.

Price in millions \$	Painting	Artist	Year	Buyer
450.3	Salvator Mundi	Leonardo da Vinci	~1500	Abu Dhabi Department of Culture & Tourism
304	Interchange	Willem de Kooning	1955	Kenneth C. Griffin
270+	The card players	Paul Cézanne	1892/93	State of Qatar
213	Nafea Faa Ipoipo	Paul Gauguin	1892	State of Qatar
~203	Number 17A	Jackson Pollock	1948	Kenneth C. Griffin
190	No. 6 (Violet, Green and Red)	Mark Rothko	1951	Dmitry Rybolovlev
182	Pendent portraits of Marten Soolmans and Oopjen Coppit ⁷⁷	Rembrandt	1634	Dutch and French government
181.7	Les Femme d'Alger	Pablo Picasso	1955	Hamad bin Jassim bin Jaber Al Thani
172.6	Nu Couché	Amedeo Modigliani	1917/18	Liu Yiquan
164.5	No. 5, 1948	Jackson Pollock	1948	David Martinez
165	Masterpiece	Roy Lichtenstein	1962	Steven A. Cohen
161.6	Woman III	Willem de Kooning	1953	Steven A. Cohen
161.5	Le Rêve	Pablo Picasso	1932	Steven A. Cohen
158.7	Portrait of Adele Bloch-Bauer I	Gustav Klimt	1907	Ronald Lauder, Neue Galerie
137.7	Portrait of Dr. Gachet	Vincent van Gogh	1890	Ryoei Saito

not to be denied that better acquaintance with the nature of materials, which many of the old masters employed would have caused their works to be handed down in sounder preservation to future generations.⁷⁸ Furthermore, for modern art we are currently on the steep part of the kinetic curve, thus at this moment in time there is still a lot to gain⁷⁹. The kinetic curve describes a universal transformation curve from the initial state towards the final thermodynamic equilibrium between an object and its environment. The steep part of the curve is where most processes of change take place prior demise or stabilization.

The extend of the 'modern art problem' is only partly reflected by research endeavours. Currently, several large projects and consortiums are in place such as CMOP (Cleaning of Modern Oil paint), MORC (Modern Oils Research Consortium), Project Plastics⁸⁰ (following 'Modern Art, Who cares?'), COMPLEX⁸¹ and others. In the Netherlands, the SBMK (Stichting behoud modern kunst/Foundation for the conservation of contemporary art), and its professional (international) network (INCCA) were established to meet the need for knowledge and information exchange concerning modern art⁸². Thus, research efforts are undertaken, but 'is it enough?' and 'is it balanced compared to research towards traditional materials?'. The scientific output is disproportional with the amount of projects reported on the internet. This suggests that it isn't enough and that it isn't balanced. While numbers are difficult to find when it comes to the investigation of traditional materials versus modern materials, a quick investigation into the publications in Heritage Science indicates that only 7.5% of papers between 2013 and 2017 deals with modern materials. However, according to Brokerhof⁸³, as science in the case of heritage science contributes to society, its impact should not be measured by counting publications, but rather by its real impact on society (and practice), as well as public engagement. While I agree, at the moment, publications are the easiest way to get an idea about impact. Furthermore, publications are an important channel to disseminate research outcome and are used as a source of information by conservators.

J.3. Institutes vs. private practice

Another challenge of applied research (research in the Pasteur's quadrant), is the translation between research and practice, especially to smaller museums or private conservators. Conservation science, while well established in the Netherlands, remains for the elite. Initiatives such as Molab, 'research on demand' offered

78 Church, A. H. (1890). The Chemistry of Paints and Painting, Seeley.

79 Artioli G. (2010). Scientific methods and cultural heritage. An introduction to the application of materials science to archaeometry and conservation science. Oxford. Page 261-262.

80 Identification and conservation of plastics in The Netherlands.

81 Project led by UCL (The degradation of complex modern polymeric objects in Heritage collections: a system dynamics approach).

82 The appreciation for this platform is clear by its growth from 23 members in 1999 to currently 100+ members from 50 institutes in 14 countries.

83 Position Paper ICCROM Forum 2013, supplement to Studies in conservation volume 60, A. Brokerhof "How can science connect with and contribute to conservation? Recommendations and reflections".

by the Cultural Heritage Agency of the Netherlands (RCE), private research initiatives such as JAAP enterprise and the involvement of private conservators in NICAS projects are important to connect both groups. I think that my engineering approach, has led to some concrete ideas directly useful for conservation practice at museum or private level. I think that my research illustrates the Pasteur's quadrant⁶⁷ because it contains both the relation with the end user {chapter 1, 6 and 7} as well as outward looking research with the aim to increase understanding and explore new methods and approaches for the field of heritage science {chapter 2-5}.

J.4. The future

Present and future conservation science in the Netherlands is represented by the Netherlands Institute for Conservation Art and Science (NICAS). I fully agree with the white paper when it states that *'we only analyse the present, while it is necessary to understand the past and to predict the future'*. In conjunction with the NICAS vision, the approach used in this Ph.D. thesis {B}, aims to understand (*'Material dynamics'* *'diagnostics'*, *'a new type of art history'*), predict (*'diagnostic'*) and prevent (*'conservation treatment'*) degradation. And this is precisely what I was motivated to do during my Ph.D. study and what was made possible by the collaboration between the Rijksmuseum, Delft University of Technology, the Cultural Heritage Agency of the Netherlands and AkzoNobel.

Not finding any case studies for titanium white degradation proved to be an opportunity to explore other approaches of conservation science moving into preventive conservation or even, I dare say, predictive conservation.



van Driel at TEDxDelft Award Finals. Photo credit: Jaap van Driel

BACK MATTER

- List of acronyms
- List of descriptions & additional information
- Link to supplementary material of (accepted) papers and description of their content.
- Dissemination of research
- TEDxDelft award talk
- Acknowledgements
- Curriculum Vitae

List of acronyms

A = Anatase
AB9 = Acid Blue 9
AFM = Atomic Force Microscopy
AFM-IR = Atomic Force Microscopy couple with InfraRed
AlSt = Aluminum Stearate
AO7 = Acid Orange 70
ATR-FTIR = Attenuated Total Reflectance – Fourier Transform InfraRed
BB66 = Basic Blue 66
BET = Brunauer-Emmett-Teller
B-PL = Blue PhotoLuminescence
C = Coated
CA(inorg) = Coated Anatase with inorganic and organic coating.
CA(org) = Coated Anatase with organic coating
CMOP = Cleaning of Modern Oil Paints
cPVC = critical Pigment-Volume-Concentration
CR = Coated Rutile with inorganic and organic coating
CR(inorg) = Coated Rutile with inorganic and organic coating
CR(org) = Coated Rutile with organic coating
DF = Dark Field
DoE = Design of Experiments
EDX = Energy Dispersive X-rays
ESR = Electron Spin Resonance
GC-MS = Gas Chromatography, Mass spectrometry
GPC = Gel Permeation Chromatography
G-PL = Green PhotoLuminescence
HEC = Hydroxyl Ethyl Cellulose
ICP-OES = Inductively Coupled Plasma – Optical Emission Spectrometry
IR-PL = InfraRed PhotoLuminescence
I_x = Irradiation step
kT = KiloTon
MA-XRF = Macro X-ray fluorescence (XRF scanner)
MB = Methylene Blue
MORC = Modern Oil paints Research Consortium
MT = Mega Ton
NICAS = Netherlands Institute for Conservation, Art and Science
NIST = National Institute of Standards and Technology
NMR = Nuclear Magnetic Resonance
OFAT = One Factor at a Time
PAII = Photocatalytic Activity Indicator Ink
PC = PhotoCatalysis / PhotoCatalytic *OR* Principal Component

PC activity = Photocatalytic activity
PCA = Principal Component Analysis
PE = PolyEthylene
PL = PhotoLuminescence
PS = PolyStyrene
PVA = (Poly)Vinyl Alcohol
PVC = Pigment-Volume-Concentration *OR* PolyVinylChloride
pXRF = portable X-ray fluorescence
Py-GC-MS = Pyrolysis Gas Chromatography – Mass Spectrometry
PyMCA = Python Multi Channel Analyzer
R = Rutile
RCE = Rijksdienst voor het Cultureel Erfgoed / Cultural Heritage Agency of the Netherlands
Ref = reference
RGB = Red, Green, Blue
RMA = Rijksmuseum Amsterdam
ROI = Region of Interest
R-PL = Red PhotoLuminescence
Rz = Resazurin
S = Supplementary Information
SBMK = Stichting Behoud Moderne Kunst
SEM = Scanning Electron Microscopy
SI = Supplementary Information
STEM = Scanning Transmission Electron Microscopy
TEM = Transmission Electron Microscopy
TRPL = Time-Resolved PhotoLuminescence
TUD = Delft University of Technology
U = Uncoated
UA = Uncoated Anatase
UV = UltraViolet
UVA = UltraViolet
UvA = University of Amsterdam
UV-VIS = UltraViolet-Visible Light Spectroscopy
XPS = X-ray Photoelectron Spectroscopy
XRD = X-Ray Diffraction
XRF = X-Ray fluorescence

List of descriptions and additional information

Additives: Chemical species that are added in low amounts to formulations, such as paints, to adjust their properties. Additives can be added to extend the shelf-life, adjust the viscosity, improve fire-resistance, absorb UV light and many other properties.

Anatase (A): TiO₂ can occur in three different crystal structures (Anatase, Rutile and Brookite) of which only anatase and rutile are used as pigments. Both anatase and rutile are TiO₂ octahedra with different distortions and assembly patterns [1]. The distances between titanium atoms are significantly different in both structures (3.79/3.04 Å in anatase, 3.57/2.96 Å in rutile) and so is the distance between titanium and oxygen atoms (1.934/1.980 Å in anatase, 1.949/1.980 Å in rutile). Furthermore, the amount of neighboring octahedrons is 10 for rutile and 8 for anatase. These lattice differences cause differences in mass densities and electronic band structures of the crystal phases. Both crystal phases have a slightly different bandgap (3.03 eV for rutile and 3.20 eV for anatase).

Artificial aging: Also called accelerated aging. Process in which the aging process is accelerated by high light intensity, temperature, relative humidity, pollutants or others. These experiments are performed if the effect under investigation is slow (many years) {chapter 3-5}.

Atomic Force Microscopy (AFM): Scanning probe microscopy with nanometer resolution. AFM uses an ultra-fine needle attached to a cantilever to 'feel' the surface and produce a height image {chapter 3}.

Atomic Force Microscopy coupled Infrared Spectroscopy

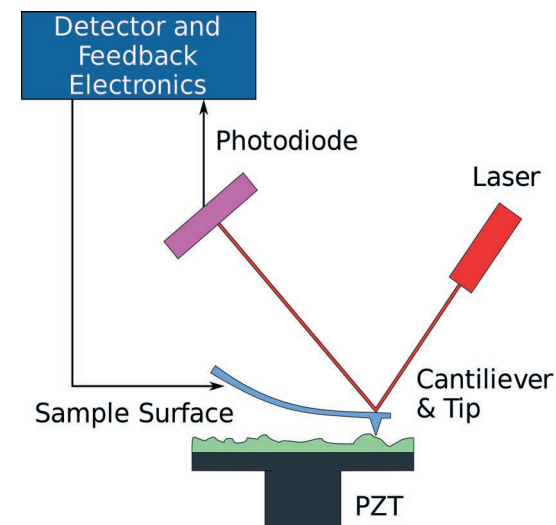


Illustration of AFM, https://upload.wikimedia.org/wikipedia/commons/1/1a/Atomic_force_microscope_block_diagram.png

(AFM-IR): AFM (See above) coupled with infrared spectroscopy. The IR source induces thermal expansion of the sample detected by the deflection of the AFM cantilever {Scheme 3, chapter 4}.

Attenuated Total Reflectance Fourier Transformed Infrared Spectroscopy (ATR-FTIR): Attenuated total reflection is a sampling technique used coupled to infrared spectroscopy. This sampling technique is suitable to measure surface properties with a penetration depth of a few micron {chapter 4}.

Binder: The binder is the component of the paint that holds the pigments together. It is also the component that starts in liquid form and needs to dry (chemically or physically) to a solid film. In this study we focus on linseed oil. However many other binders are available such as plastics. Plastics are synthetic organic macromolecules. In view of a wide range of (petroleum) based starting materials, a wide variety of plastics have been on the market. Crystallinity of a polymer determines if it is opaque or transparent; however polymers are seldom fully opaque and require fillers and pigments to achieve this. Most plastics also contain additives such as plasticizers, hindered amine light stabilizers, fire retarders and light stabilizing pigments [2]. Research has been done on the degradation of certain plastics pigmented with titanium dioxide such as polyvinylchloride (PVC), polyethylene and polystyrene [3-6].

Charge carrier: A mobile particle that carries an electric charge such as a negatively charged electron or a positively charged hole.

Coating or surface treatment: A modification of the pigment surface to adjust its properties {C.2.3}.

Organic: Organic coatings are often used to make pigments suitable for their end application (affiliation to the binder).

Inorganic: Inorganic coatings are most often based on metal oxides and in the case of titanium white they decrease photocatalytic activity by forcing electron-hole recombination.

Composite pigments: Early titanium white pigments composed of a co-precipitate of titanium white with other materials such as calcium carbonate or barium sulfate.

Defect: A structural imperfections in a crystal lattice such as point defect (vacancies) or line defects (dislocations).

Degradation: Unwanted change.

Design of Experiments (DoE): Statistical approach to plan an experiment, with an optimum number of runs, to find significant factors and factor interactions describing the variation in the response {chapter 5B}.

Diffusion: Movement of molecules driven by a concentration gradient.

Einstein's diffusion equation can be used to determine diffusion coefficients:

$$D = \frac{\overline{X^2}}{t}$$

D = Diffusion coefficient [cm^2sec^{-1}]

$\overline{X^2}$ = Average of diffusion distance squared [cm^2]

t = Diffusion time [sec]

The values of the diffusion coefficients of oxygen through several polymers have been investigated and most values are between $2 \cdot 10^{-9}$ and $2 \cdot 10^{-7} cm^2sec^{-1}$. These values correspond to a diffusion time between 0.05 and 5 seconds [7] and show that catalytic degradation is probably not limited by diffusion. The permeability for water is up to 1000 time greater than that of oxygen and is therefore also not limited [7, 8]. It is important to realize that these numbers and conclusions are system specific.

Drier: Metal ions added to oil paints to facilitate the drying process of drying oil. In this study we use a drier obtained from P. Keune composed of cobalt and zirconium compounds.

Drying oil: see linseed oil.

Dummy reaction: A simple chemical reaction meant to mimic the behaviour of a much more complex system. In this study this refers to investigating the degradation rate of dyes rather than of complex macromolecules.

Dye degradation test: A specific type of dummy reaction which entails monitoring the photocatalytic degradation of a dye by TiO_2 to determine the photocatalytic activity {chapter 6}.

Early warning sign: A measurable change that is characteristic for an ongoing degradation process which is not yet visible {chapter 3 and 4}.

Electron Spin Resonance Spectroscopy (ESR): A spectroscopic method to investigate paramagnetic species. The concepts of the method are analogous to NMR. Any paramagnetic species has two spin states: $+1/2$ and $-1/2$. When a magnetic field (G) with a field strength of B_0 is applied the magnetic moments align in a parallel or antiparallel fashion. The energy that separates the two spin states (ΔE) depends on the field strength. A paramagnetic species can move between the both states by either emitting or absorbing the exact right amount of energy. The movement of the species causes a net absorption of microwaves, which is the measured quantity in ESR [9].

Embrittlement: Process of becoming brittle. This can for instance

happen to polymers when they reach a high degree of cross-linking.
Extenders: Also called fillers. Cheap materials added to paints as replacement for the binder or for more expensive pigments. Alternatively, extenders can be added to adjust the tinting strength of colored paints. They are often added to student quality paints.

Formulation: Paint recipe.

Gloss: Gloss is an optical property that describes the reflection of a surface. Gloss can be measured at different angles {chapter 3 and 5}.

Hole: See charge carrier.

Photocatalytic activity test: Test to measure photocatalytic activities of photocatalyst under specific condition {E, Part 3}.

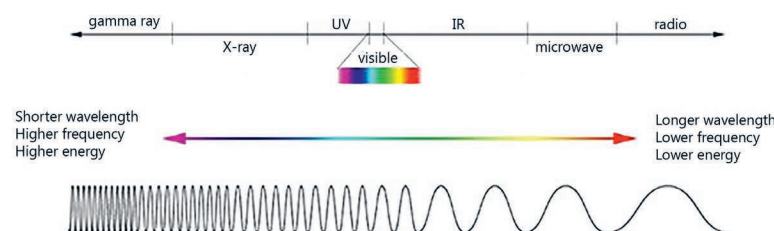
Direct PC activity test: Measures entities directly formed in the semiconductor or on its surface such as electrons, holes and radicals.

Indirect PC activity test: Monitors a reaction caused by the formed radicals. See dummy reaction/dye degradation test.

Inductive Coupled Plasma-Optical Emission Spectrometry (ICP-OES): A quantitative analytical technique used for the detection of chemical elements at trace levels. The technique uses the inductively coupled plasma to produce excited atoms and ions that have a characteristic emission {chapter 2}.

Light: Light represents electromagnetic radiation of a certain wavelength. We distinguish visible light, as what is visible by human eyes (roughly between 400 and 800 nm). Other types of 'light' irradiation are infrared light and UV-light. UV-light is the radiation at the lower boarder of the visible light (lower wavelength/higher energy).

Electromagnetic spectrum, https://imagine.gsfc.nasa.gov/Images/science/EM_spectrum_compare_level1_lg.jpg



A model by Egerton and King leads to the relation (at high intensities) [9]:

$$Rate = K \cdot I^{0.5}$$

$$K = ((k_3^2 \cdot k_1) / k_2)^{0.5}$$

k_1 : reaction speed coefficient of acetone formation

k_2 : reaction speed coefficient of hole and electron formation, assuming $e^- = h^+$

k_3 : reaction speed coefficient of electron-hole recombination, assuming $e^- = h^+$

At low UV intensities recombination is negligible which caused the solution of the model to yield a directly proportional relation between the intensity and the rate of degradation.

Units & typical exposure

Unit	Abbreviation	Meaning	Important relations
Lux	Lx	Illuminance based on visible light (luminous flux per unit area)	1 Lux = 1 Lumen/m ²
Lumen	lm	Illuminance - amount of visible light emitted by a light source	1lm=1cd*sr (1 candela across an angel of 1 steradian)
Candela	cd	Luminous intensity	A common candle emits light with a luminous intensity of approximately 1 candela
Radiant flux / power		Power of all electromagnetic waves emitted by a source	Watt, Watt/nm
Joule	J	Energy	
Quanta		Amount of photons, 1 photon = 1 quantum of light. Usually used in quanta/m ² s	5.44*10 ⁻¹⁹ J/photon of 365 nm (E= hc/λ) Not SI unit
Einstein	E	Energy of 1 mole of photons	1 mol = 6.022*10 ²³ not an SI unit
Photon flux	μmol /m ² s	SI unit for term to be avoided such as quanta or Einstein	Can be related to radiant flux by knowing the energy of 1 photon of a certain λ. (E= hc/ λ)
Watt	W	Energy per unit time μW/lumen often used for UV-content	1 Watt = 1 J/sec

Light source	UV-content (μW/lm)
Daylight	400-1500
Incandescent	70-80
Halogen incandescent	40-170
Fluorescent lamp	30-100
Metal halogen lamp	160-700
LED	<5

Surrounding	Illumination (lux =lm/m ²)
Sunlight	10.000
Overcast day	1.000
Public areas with dark surroundings	20-50
Museum	50-150
Working areas where visual tasks are only occasionally performed	100-150
Warehouses/homes/theaters/archives	150
Easy office work, classes	250
Normal office work, PC work, study, library, Show room, Lab	500
Mechanical workshops, office landscapes	750
Detailed drawing or mechanical work	1500-2000

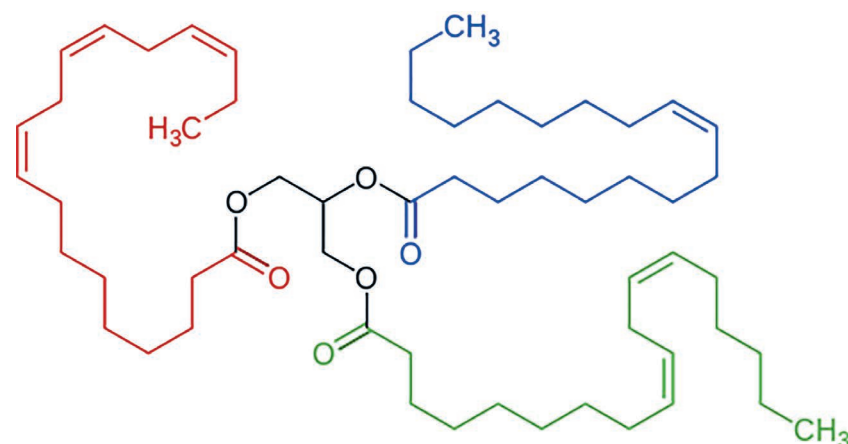
Light and radiation units and conversion factors.

UV-content of different light sources. Reproduced from [10].

Illumination in different environments – Adapted from [11].

Structure of linseed oil,
https://commons.wikimedia.org/wiki/File:Triglyceride_unsaturated_Structural_Formulae_V2.svg

Linseed oil: Drying oil (based on triglycerides) used in paintings. During the drying process the oil polymerizes to a solid film.
Metal stearate: Metal salt/soap of a metal ion (e.g. zinc) and stearic acid.



Permalba: Brand name of titanium white paint by Weber. Marketed in the United States.

Photocatalytic activity (PC activity): Photocatalysis is the acceleration of a process due to the presence of a catalyst and its interaction with light.

Photocatalytic Activity Indicator Ink (PAII): An ink used to identify the presence of a photocatalyst via a color changing reaction {chapter 7}.

Photoconductivity: The mobility of charges due to interaction with light.

Photoluminescence (PL): The emission of light after the absorption of photons {chapter 2}.

Pigment: Solid material that changes the color of a coating/paint by wavelength selective absorption.

Pigment volume concentration: $V_{\text{pigment}}/V_{\text{total}}$.

Principal component analysis (PCA): A type of statistical analysis that uses orthogonal transformation to convert the coordinate system of multivariate data to the axis of largest variation {chapter 1}.

Reciprocity principle: The concept that intensity and time equality contribute to irradiation dose.

Recombination (surface/bulk): The process by which mobile charge carriers are eliminated.

Reconstructions: Reconstructions of for instance a paint to understand its properties and behaviour {chapter 3-5}.

Royal Talens: Dutch paint manufacturer based in Apeldoorn.

Rutile (R): Crystal structure of TiO_2 , see Anatase.

Scanning Transmission Electron microscopy coupled with Energy Dispersive X-ray spectroscopy (STEM-EDX): Type of transmission electron microscopy {chapter 1 and 2}. Images are formed by scanning an electron beam over a thin enough sample for transmission mode. Energy Dispersive X-ray Spectroscopy is coupled to the TEM and is used for elemental analysis of the sample based on the emission of characteristic X-rays.

Self-Cleaning: Surfaces with the ability to degrade pollutants (e.g. by photocatalysis).

Metal soaps: Metal salts, see metal stearates.

Time Resolved Photoluminescence Spectroscopy (TRPL): Analytical technique that analysed the time dependent photoluminescence behaviour of materials {chapter 2}.

Ultraviolet (UV): Light with wavelengths between 10 and 400 nm. See Light.

Weber: Paint manufacturer from the United States, see Permalba.

Winsor & Newton: Company that produces fine art products. Founded in 1832. Based in London.

X-ray diffraction (XRD): An analytical technique used to determine the crystal structure of a material. The material is irradiated with X-ray that diffract in a certain pattern related to the specific structure {chapter 1}.

X-ray Fluorescence Spectrometry: Analytical technique that uses the emission of secondary X-rays from a material to detect the elements present {chapter 1}.

MA-XRF: XRF scanner that has a x-y stage to collect a grid of spectra which can be transformed into elemental images.

pXRF: portable XRF device.

X-ray Photoelectron Spectroscopy (XPS): A surface sensitive and quantitative analytical techniques that uses X-rays to analyse elemental composition and chemical state of a sample {chapter 3}. Under X-ray irradiation the kinetic energy and number of electron that escape from the surface of the material are analysed.

References for the list of descriptions

1. Linsebigler AL, Lu G and Yates JT. Yates, Photocatalysis on TiO₂ Surfaces: Principles, Mechanisms, and Selected Results. Chem Rev. 1995. 95(3): p. 735-758.
2. Painter PC and Coleman MM. Essentials of Polymer Science and Engineering. 2009. DEStech Publications, Inc. ISBN: 978-1-932078-75-6.
3. Gesenhues U. Influence of titanium dioxide pigments on the photodegradation of poly(vinyl chloride). Polym Degrad Stabil. 2000; 68(2): 185-196.
4. Shang J, Chai M and Zhu Y. Solid-phase photocatalytic degradation of polystyrene plastic with TiO₂ as photocatalyst. J Sol State Chem. 2003; 174(1): 104-110.
5. Zhao X, Li Z, Chen Y, Shi L and Zhu Y. Solid-phase photocatalytic degradation of polyethylene plastic under UV and solar light irradiation." J Mol Cat A. 2007; 268(1-2): 101-106.
6. Day RE. The role of titanium dioxide pigments in the degradation and stabilisation of polymers in the plastics industry. Polym Degrad Stabil. 1990; 29(1): 73-92.
7. Sullivan WF. Weatherability of Titanium-Dioxide-Containing Paints. Prog Org Coat. 1972; 1: 157-203.
8. Völz HG, Kaempf G, Fitzky HG, Klaeren A. The Chemical Nature of Chalking in the Presence of Titanium Dioxide Pigments. ACS Photodegrad Photostabil Coat. 1981; 151: 163-182.
9. Lund A, Shimida S and Shiatani M. Principles and Applications of ESR Spectroscopy, Springer. 2011.
10. Szabo F, Csuti P and Schanda J. Solid State Light sources in museum lighting - lighting reconstruction of the sistine chapel in the Vatican. Presentation from Virtual Environments and Imaging Technologies Research Laboratory, University of Pannonia, Veszprem, Hungary.
11. Light levels. URL: http://www.engineeringtoolbox.com/light-level-rooms-d_708.html. Accessed 2015.

Description of supplementary material

Supplementary information with chapter 1

The supplementary information is available at:

https://static-content.springer.com/esm/art%3A10.1186%2Fs40494-018-0183-4/MediaObjects/40494_2018_183_MOESM1_ESM.pdf

The supplementary information contains:

- Table with pigment compositions in the 1920s and 1940s.
- Description of the datasets (paintings and references).
- Figure with spectral changes caused by the use of the Al/Ti Filter.
- PyMCA deconvolution details.
- Threshold values.
- Deconvolution results.
- Guidelines for spectra interpretations based on reference paint outs.
- Additional supporting results.
 - Coloring figure 4.
 - Scatterplots involving barium/calcium.
 - Spectra of paints containing niobium.

Supplementary information with chapter 2

The supplementary information if available at: <https://www.sciencedirect.com/science/article/pii/S0143720817325469>

The supplementary information contains:

- Raman spectra of all investigated TiO₂ powders.
- EDX spectra relating to phase deconvolution of the STEM-EDX maps.
- Full ICP-OES results.
- Full decay kinetics tables.

Supplementary information with chapter 3

The supplementary information is available at: <http://www.sciencedirect.com/science/article/pii/S1386142516302013?via%3Dihub#ec0010>

The supplementary information contains:

- Schematic of intact paint film.
- Scheme of sample preparation.
- Pictures of the samples.
- AFM results of UA-2.
- Additional XPS full survey spectra and C1s core level spectra.

Dissimination of research

Publications as part of this dissertation

- **van Driel, B. A.**, Kooyman, P.J., van den Berg, K.J., Schmidt-Ott, A. and Dik, J. (2016). ‘A quick assessment of the photocatalytic activity of TiO₂ pigments — From lab to conservation studio!’ *Microchemical Journal* **126**: 162-171.
- **van Driel, B.**, Wezendonk, T.A., van den Berg, K.J., Kooyman, P.J., Gascon, J. and Dik, J. (2017). ‘Determination of early warning signs for photocatalytic degradation of titanium white oil paints by means of surface analysis.’ *Spectrochimica Acta Part A: Molecular and Biomolecular Spectroscopy* **172**: 100-108.
- Morsch, S., **van Driel, B.A.**, van den Berg, K.J. and Dik, J. (2017). ‘Investigating the Photocatalytic Degradation of Oil Paint using ATR-IR and AFM-IR.’ *ACS Applied Materials & Interfaces* **9**(11): 10169-10179.
- **van Driel, B.**, van den Berg, K.J., Smout, M., Dekker, N. and Dik, J. (2018) ‘Investigation the effect of artists’ paint formulation on degradation rates of TiO₂-based oil paints. *Heritage Science* **6**:21.
- **van Driel, B.**, van den Berg, K.J., Gerretzen, J. and Dik, J. (2018) ‘The white of the 20th century – An explorative survey into Dutch modern art collections. *Heritage Science* **6**:16.
- **van Driel, B.**, van der Meer, S., van den Berg, K.J. and Dik, J. ‘Determining the presence of photocatalytic titanium white pigments via paint sample staining: a proof of principle.’ *Under review at Studies in Conservation*.
- **van Driel, B.**, Artesani, A., van den Berg, K.J., Dik, J., Mosca, S., Rossenaar B.D., Hoekstra J.U., Davies, A.N., Nevin, A., Valentini, G. and Comelli, D. (2018) ‘New insights into the complex photoluminescence behaviour of titanium white pigments’. *Dyes&Pigments* **155**: 14-22.

Publication in close connection to this dissertation

- Phenix, A., van den Berg K.J., Soldano, A., **van Driel, B.A.** (2017). *The Might of White: formulations of titanium dioxide-based oil paints as evidenced in archives of two artists’ colourmen mid-twentieth century*. ICOM-CC Triennial conference 2017, Copenhagen.

Posters as part of this dissertation

- **van Driel, B.A.**, van den Berg, K.J., Smout, M. and Dik, J. (2016) ‘Comparing the degradation rate of titanium white

- paint formulations by means of a design of experiments (DoE)'. ChemCH, Brussels, Belgium.
- **van Driel, B.**, van den Berg, K.J., Kooyman, P.J. and Dik, J. (2016) 'Determining photocatalytic activity of titanium white in a paint cross-section'. Gordon Research Conference, Scientific methods in cultural heritage, Sunday River, USA.
 - **Van Driel, B.**, van den Berg, K.J., Steyn, L., Rossenaar, B.D. and Dik, J. (2017) 'Visualizing the invisible – Detection of the inorganic surface coating on TiO₂ pigments, inside a paint.' ICOM-CC Triennial conference Copenhagen.

Other publications

- Van der Snickt, G., Martins, A., Delaney, J., Janssens, K., Zeibel, J., Duffy, M., McGlinchey, C., **van Driel, B.** and Dik, J. (2016). 'Exploring a hidden painting below the surface of René Magritte's Le Portrait.' *Applied Spectroscopy* **70**(1): 57-67.
- Martins, A., Coddington, J., Snickt, G., **van Driel, B.**, McGlinchey, C., Dahlberg, D., Janssens, K. and Dik, J. (2016). 'Jackson Pollock's Number 1A, 1948: a non-invasive study using macro-x-ray fluorescence mapping (MA-XRF) and multivariate curve resolution-alternating least squares (MCR-ALS) analysis.' *Heritage Science* **4**(1): 33.
- Milosevic, I., Jayaprakash, A., Greenwood, B., **van Driel, B.**, Rtimi, S. and Bowen, P. (2017). 'Synergistic Effect of Fluorinated and N Doped TiO₂ Nanoparticles Leading to Different Microstructure and Enhanced Photocatalytic Bacterial Inactivation.' *Nanomaterials* **7**(11): 391.
- Milosevic, I., Rtimi, S., Jayaprakash, A., **van Driel, B.**, Greenwood, B., Aimable A., Senna, M. and Bowen, P. (2018). 'Synthesis and characterization of fluorinated anatase nanoparticles and subsequent N-doping for efficient visible light activated photocatalysis.' *Colloids and Surfaces B: Biointerfaces*.
Under review.

Conferences

- Synchrotron Radiation and Neutrons in Art and Archaeology. 2014, Paris, France. Participant.
- Technart. 2015, Catania, Italy. Oral presentation & publication special issue.
- Colloquium spectroscopicum internationale. 2015, Figueira da Foz, Portugal. Oral presentation & publication special issue.
- Metal soaps in Art. 2016, Amsterdam, The Netherlands. Participant.

- Chemistry for Cultural Heritage. 2016, Brussels, Belgium. Poster presentation.
- Gordon Research Seminar Scientific Methods for Cultural Heritage. 2016, Sunday River, USA. Oral presentation.
- Gordon Research Conference Scientific Methods for Cultural Heritage. 2016, Sunday River, USA. Poster presentation.
- Technart. 2017, Bilbao, Spain. Oral presentation.
- ICOM-CC triennial conference. 2017, Copenhagen, Denmark. Poster presentation (Scientific working group) and co-author on a paper (Art Technological Source Research working group).

Other public appearances

- 'Schitterend wit', speaker at a symposium at the Stedelijk museum Schiedam (connected to the Schoonhoven Exhibit).
- XRF Bootcamp organized by Stichting Restauratie Atelier Limburg. Participant.
- Finalist TEDxDelft Award, February 2016.
- IPERION-CH Summerschool Madrid. Participant.
- Young talent meeting in conjunction with Erasmus-Descartes conference: Cultural heritage & innovation. 2016, Paris, France. Participant.
- NICAS colloquium (2x)
- Speaker at the NICAS project day, November 13th 2017.

List of co-authors for the publications that were part of this dissertation

Alessia Artesani, Politecnico di Milano (chapter 2)
Andreas Schmidt-Ott, Delft University of Technology (chapter 6)
Antony Davies, AkzoNobel (chapter 2)
Austin Nevin, Consiglio Nazionale della Ricerche (Istituto di Fotonica e Nanotecnologie) (chapter 2)
Brenda Rossenaar, AkzoNobel (chapter 2)
Daniela Comelli, Politecnico di Milano (chapter 2)
Gianluca Valentini, Politecnico di Milano (chapter 2)
Jan Gerretzen, AkzoNobel (chapter 1)
Johan Hoekstra, AkzoNobel (chapter 2)
Jorge Gascon, Delft University of Technology (chapter 3)
Joris Dik, Delft University of Technology (chapter 1-7)
Klaas Jan van den Berg, Cultural Heritage Agency of the Netherlands and the University of Amsterdam (chapter 1-7)
Martijn Smout, AkzoNobel (chapter 5)
Niels Dekker, AkzoNobel (chapter 5)
Patricia Kooyman, University of Cape Town (chapter 3-6)

Sara Mosca, Politecnico di Milano (chapter 2)
Sharon van der Meer, Hogeschool Utrecht (chapter 7)
Suzanne Morsch, University of Manchester (chapter 4)
Tim Wezendonk, Delft University of Technology (chapter 3)

TEDx Delft award talk

In February 2016, TU Delft organized a competition to win a speaking slot for TEDxDelft event. This competition consisted of three rounds. In the first round, a visualization of your idea was required. For my submission, I produced a 'facebook page' of my research. The second round consisted of a workshop and the five finalist were selected based on a one minute pitch. In the final round, we were assigned a TEDx speaking coach, who helped me to prepare my 9 minute TEDxDelft award talk. I presented this talk to an audience of 300 students, universities employees, friends and family. Even though I did not win, I would like to share this talk with you because working on this talk with my coach and colleagues had a big impact on the way I think about my research and on the choices I made during the remainder of my Ph.D.

Note
This is a spoken text.

Good evening

When I was 17, in my final year of high school, I took a trip to Rome. During this trip I visited the Sistine chapel and, as anyone who's ever been to the Sistine chapel will know, they told us not to use the flash on our cameras but they never told me why...

This made me so curious that, for my final high school project, I decided to investigate the influence of the use of camera flash on the frescoes of the Sistine chapel. Through an traditional paint manufacturer near where I lived I got my hands on traditional pigments and fresh wet plaster. They taught me how to make frescoes and when I got home I made frescoes with 6 different pigments. I then exhausted the flash of my dad's camera by flashing it more than a thousand times at my reconstructed frescoes. And I monitored the color change using my dad's camera. What I found out was that after as little as a few thousand flashes (I say little because even though I exhausted the flash and almost injured my index finger it is very little compared to the 15.000 visitors in the Sistine chapel on a daily basis) I already noticed fading of the colors: the paint was degrading!

And that's when I realised that the degradation of works of art is inevitable and we should do something about it, because imagine a world without the gigantic legacy of Picasso? A world without Monet's Lilies? A world without Piet Mondriaan?

You may realise I've jumped a few centuries between the Sistine chapel and Picasso, Monet and Mondriaan. I've done this because I would like to focus your attention to art of 19th and 20th centuries. The 19th and 20th centuries were centuries of great

discoveries and technological advancement. Among others, a range of new materials were brought on the market and used by artists, all kind of plastics, dyes, and synthetic pigments were used and unfortunately these materials happen to be even more unstable than Michelangelo's frescoes. So wouldn't it be great if we could understand, predict and prevent the degradation that is inevitably upon us? The degradation that will cause a huge decrease in cultural, aesthetical and financial value of art objects?

We apply the 'understand, predict, prevent' methodology in a lot of aspects of our daily life. For instance, we go to the dentist regularly to have our teeth checked in order to prevent them from rotting and falling out. The dentist may use an X-ray photo to find a cavity before it causes a toothache, and his understanding of the dental system allows him to determine a suitable procedure to prevent more damage.

Why don't we use the same principle to understand, predict and prevent art degradation. Let me show you a way to do this.

First I need to give you a quick chemistry lesson. Paintings are very complex systems and therefore many different types of damaging processes may occur. A simple paint contains pigments particles which gives the paint the color and a binder to keep the pigment together. A more complex paint includes other pigment and a range of fillers and additives. On top of that, paintings are mostly made in a layered way therefore they contain layers of all sorts of different paints making them very complex chemical systems. For simplicity let's focus on one process of deterioration: the degradation of the binding medium caused by titanium white pigments.

Titanium white is one of the new materials that reached the market in the 20th century and it was quick to be used as a replacement for the toxic lead white. Titanium white was used by Picasso, by Jackson Pollock, by Schoonhoven and by many other 20th century painters, and it was also found in the painting that the Dutch state paid 37 million for in 1997, a painting that president Obama called fabulous: Mondriaan's Victory Boogie Woogie.

Titanium white pigments used today have been improved to a very stable form. However the early titanium white pigments—those used by Mondrian have the ability to attack the material around them, such as binding medium, when the work of art is exposed to near UV light.

So back to the chemistry.

When a painting is intact generally a small layer of binding medium is present on top of the pigments resulting in a glossy appearance. But when the painting degrades due to the presence of these early titanium white pigments the binding medium is broken down into small chemical species that can evaporate from the painting. This causes the pigment particles to appear on the painting's surface causing first a decrease in gloss and finally an effect called chalking: at this moment the pigment is unbound at the painting's surface and your fingers will turn white if you touch it, much like chalk on a chalkboard (hence the name).

So now, why don't we do the same thing the dentist does? Why don't we try to understand, predict and prevent this degradation phenomenon? Why don't we use analytical tools, such as x-ray methods to show us this problem before it is too late? Before the visual value is affected? Well that is exactly what I am proposing: I call it detection of early warning signs.

In the system I just explained to you I found that X-rays actually offer the best solution. Instead of taking an X-ray image like the dentist we do something called X-ray photoelectron spectroscopy or XPS. This technique measures chemical elements but has a very small penetration depth. Therefore an intact paint film — recall that there is a small layer of binding medium at the surface of the painting, does not show any titanium signal but a degrading paint film, even in the very first stages of degradation, starts to show a titanium signal which is an early warning sign. Before it is too late.

Of course, as scientists, we like to support this with another technique, in this case a microscopic technique, so that we can complement the chemical information of XPS with morphological information, meaning information about the roughness of the surface. Atomic force microscopy or AFM can detect very small height differences at a very high resolution.

Here we see the degradation in a more visual way than with XPS, the images shown are the surface roughness of an area that is 40 to 80 times smaller than the cross area of a human hair. Together, these techniques allow us to see degradation before it is visible to the naked eye. And once we know that degradation is occurring we can stop it by our understanding of the process. In the case of titanium white degradation: remove of limit exposure to near UV light.

Now, does this type of detection require high tech equipment? Yes, Does this type of detection require a high level of understanding about the different degradation processes? Yes, But is it worth it to detect, predict and prevent art degradation? Yes it is. You would not go to a dentist using 100 year old equipment either. So this means we must make these techniques routinely available to the field of art conservation by collaborations between art institutions, universities and industrial partners. Furthermore the field of conservation science needs to grow to support more research. Several steps have already been taken in the right direction but we are not there yet.

So if we go to the dentist to prevent cavities,

and if we do regular checks on our Dutch water defence systems to prevent floods,

why don't we monitor our precious art works to prevent them from falling apart?

If we start changing the view on art conservation to a more prevention based approach we will be able to understand, predict and prevent art degradation and with that protect our art and our history!

Then people in the year 2500 will be able to enjoy the works of Picasso, Monet, and Mondrian just as I have enjoyed the Sistine chapel when I was 17.

Thank you.

Acknowledgements

As I am reading through the acknowledgements in other dissertations for inspiration, I notice that the acknowledgement are usually the final thing to be put on paper. In that sense, it may be strange that I am starting to write this on November 22nd, 2017 – possibly still six months away from my defence. However, the people who know me, and have worked with me, should not be too surprized by this. This is the time and place to put into words the gratitude that I have for all the people that were there along the way leading up to my Ph.D. defence. People who were there to help, to supervise, to correct, to criticize, to brainstorm with, to drink with, to laugh with, to complain to, to travel with, to collaborate with and so much more.

Let me start by thanking the Rijksmuseum and AkzoNobel for their long term collaboration which led to two research projects, one of which is my Ph.D research. Financially the project was made possible by AkzoNobel, for which I am very grateful. A special thanks goes out to **Robert van Langh** (Rijksmuseum) for making this project possible and for his support and belief in me along the way. I am thankful to **Irma Boom** and especially **Jan van der Kleijn** for designing as well as **Lenoirschuring** for printing the dissertation. Other people that I would like to thank for supporting and arranging the project are **Apas Zwart**, **Jacobien Schneider**, **Francine Heijmans**, **Hanneke Beijnen** and **Laura Huijgen** from the Rijksmuseum, **Sara Keur-O'neill** and **Ans van de Bovenkamp** from AkzoNobel and **Saskia van der Meer** from Delft University.

Secondly, I could not have concluded this Ph.D. without my supervisory team: **Joris Dik** (TU Delft), **Klaas Jan van den Berg** (RCE) and **Tony Davies** (AkzoNobel).

Joris, from the day I wrote you an email expressing an interest in doing a bachelor thesis in conservation science, I always felt you supported me. Looking back at my high school 'profielwerkstuk', I found out that I referenced your work already during that project. Perhaps you've been influencing me for the past 13 years... Your trust in me and my capabilities has been a great support and catalyst for my personal development, and perhaps the reason that I am now confident enough to pursue a career outside academia ;-).

Note Each chapter includes a chapter specific acknowledgements.

Klaas Jan, when I started my Ph.D., I had a clear opinion of what I wanted to do, and to your regret it was not organic chemistry... Eventually you realized that my (engineering) approach wasn't all that bad and we were a great team. I am very grateful for our fruitful discussions, for the times you joined me to do XRF, for the time you joined me to Milano, for the times you read and corrected my papers and for your encouragement for presentations. In other words, thanks for your kind and dedicated supervision – it was a joy to work with you.

Tony, I am glad you became an active member of my supervisory team. Thanks to you, the collaboration with AkzoNobel extended from a financial commitment to active collaboration. You were always present at my progress meetings and always managed to ask the right questions. Additionally, you arranged my participation in the DoE course and introduced me to **Gill**, **Brenda** and **Martijn**, who have always kindly received me in Deventer and have actively contributed to the research! And it did not stop there, since they put me in contact with **Niels**, **Johan**, **Marian**, **Wilma** and **Jan** who all performed analysis for me, helped me with data processing and Design of Experiments, or co-authored my papers.

I thank the three of you for supervising me, putting up with me and for being part of my committee.

A word of thanks for the rest of my committee:

Ana, I first met you in 2013 at MoMA, when Joris sent me to go with the MA-XRF. It was my first experience working in a real conservation lab and more importantly with real art objects. In the month I was there, you introduced me to the world of heritage science and specifically of pigments. Together, we scanned Mondriaan, Pollock and van Gogh paintings, you showed me around New York and you let me profit from your MoMA shop discount. After my time in New York, we stayed in touch and you were always interested in my work. I am very glad you are a part of my committee today.

Ella, I met you during my time at the Ateliergebouw and you always showed interest in my work. I did some analysis for you on TiO₂ containing retouches from van Gogh paintings, which gave insight into the date of the restoration. As a conservator you represent a very important and relevant group for the evaluation of my dissertation which is why I very much appreciate you being a part of my committee.

Ian Richardson, **Costanza Miliani** and **Jilt Sietsma**, as respected expert in your fields, I thank you for taking the time to read and evaluate my thesis.

Patricia, like Joris, you already supervised me during my bachelor thesis and you continued the work we started with other students, in my absence. When I came back, it was only logical to involve you in my supervisory team. You always ask the right questions and are very thorough when it comes to correcting papers, which comes in handy, considering that I am a sloppy writer. When you moved to South Africa, your supervision became less regular, but we kept in touch and you still had a big impact on editing chapter 5. Thank you for staying involved and I hope you will be present at the defence.

Katrien, even though you were not technically my supervisor, you were in some way my boss within the Rijksmuseum and I had my evaluations with you. Additionally, you attended a few of my progress meetings in the final years and assisted me with chapter 4. Finally, you referred a student to me, Sharon van der Meer, who was of great help for chapter 7. I want to thank you for being there for me during this project.

The seven papers on which this thesis is based were written with many co-authors. I am grateful to all of them: **Klaas Jan** and **Joris**, who co-authored all papers as well as: **Jan Gerretzen** {chapter 1}, **Alessia Artesani**, **Daniela Comelli**, **Sara Mosca**, **Brenda Rossenaar**, **Tony Davies**, **Johan Hoekstra**, **Gianluca Valentini** and **Austin Nevin** {chapter 2}, **Patricia Kooyman**, **Tim Wezendonk** and **Jorge Gascon** {chapter 3}, **Suzanne Morsch** {chapter 4}, **Patricia Kooyman**, **Martijn Smout** and **Niels Dekker** {chapter 5}, **Patricia Kooyman** and **Andreas Schmidt-Ott** {chapter 6}, **Sharon van der Meer** {chapter 7} and **Alan Phenix** and **Alexia Soldano** for the ICOM-CC paper (not included as a chapter).

Other people that I am grateful to for contributing to the papers in other ways are **Marian** and **Wilma** (AkzoNobel, ICP and TEM), **Marcel Bus** (AFM, TUDelft), **Muriel** and **Han** (RCE, PAII brainstorm), **Maartje** and **Luc** (review chapter 5), **Henk van Keulen** and **Ineke Joosten** (RCE, GC-MS, SEM-EDX), **Arie Pappot** (Rijksmuseum, PyMCA) and **Rob Erdmann** (Rijksmuseum, PCA, Python), all the people (**Klaas Jan van den Berg**, **Rose Heaton**, **Maranthe Lamers**, **Rika Pause**, **Lise Steyn**, **Nathalie de Vries**, **Annelies van Hoesel**) that assisted

me while doing XRF at collections and all the students (**D. van den Berg, I. du Fossé, R. Verheijen, F. van Dockum, E. Remmelts** and **S. Pahud de Mortange**) that were involved in the experiments for chapter 6. Furthermore, I would like to acknowledge everyone who supplied samples during this projects {all chapters} and all the collections interested in collaborating {chapter 1}. Also, I would like to acknowledge the people I worked with, which did not lead to publication. Thanks to **K. Rasmussen** at ESA-ESTEC for trying out the applicability of ESR spectroscopy for my project. Thanks to **Elena Nazarenko** and **Claire Gervais** for including me in research concerning the degradation of Prussian blue when mixed with white pigments.

I am especially grateful to **Lydia Beerkens** and **Marjan de Visser** who've shown great interest in my work over the past four years and have given me an insight into the practice of modern art conservation.

I am grateful to **Agnes Brokerhof** for her help with the risk management parts of this dissertation.

Since I was working in a collaboration with three institutes, I had many colleagues supporting me along the way. The whole Conservation and Restauration department of the Rijksmuseum, the PaInT group, other students, Ph.D.s and postdocs: **Eliane, Joen, Alessa, Lise, Selvin, Lambert, Victor, Sofia, Maranthe, Rose, Janneke, Annelies, Ana** and the RCE colleagues especially those I briefly shared an office with (**Art, Luc, Annelies, Ana** and **Han**). Whether just by chit-chat at the coffee machine, having a few beers at Mankind, enjoying the Rijksmuseum garden or Christmas party, in-depth discussions, having lunch, sharing an office or sharing work/building frustrations; you have all made my time in the Ateliergebouw more enjoyable.

As a loud person, people usually expect me to like public speaking. However, unfortunately, this is absolutely not the case. But practice it the best cure. Thus, I want to thank everyone for accepting my abstracts and inviting me to speak at international conferences, NICAS meetings, AkzoNobel meetings and other events. Participating in the TedX Delft award was one of the most rewarding public speaking experiences for me. **Lise, Tim** and **Yvonne**, I still remember the anger you felt when I did not win, thank you for feeling that for me, I was so proud I overcame my fear I did not have time to be angry ;-). I want to especially thank **Jonathan Talbot** for coaching me for the TedX Delft award. I still think about what I learned during that process each time I am asked to do a presentation.

Going way back, I want to acknowledge **Lenneke** and **Edwin** (College Hageveld) who supervised my 'profielwerkstuk' and nurtured my dual interest in arts and science.

But while studying and working played an important role in where I am today, so did the people in my personal life. I am grateful to all the flatmates I've lived with and all the people I studied with, whether in Delft, Brussels, Lausanne or Basel, between 2006 and now. At DHS NBNGB and at the Technologisch Gezelschap, I made friends for life. **Thijs** (huisgenoot, bestuursgenoot, bijna echtgenoot ;)), **Guus** (wat was het fijn toen jij ook naar Amsterdam verhuisde) & **Ed** (NixChicks, even our parents call us by our 'guy' names), **Tim de Wees** and by extension **Nicole & Soof** (wat een mooie dingen hebben wij samen beleefd, teveel om op te noemen), **Boob, Ari, Maus, Taco & Baco** (sinds Buisco 2012, meidenkamer), alle andere Nixers en TGers; I can't imagine my life without you guys. We did more crazy things than I can recall and most should not be put in writing, so I won't. Also at the Coenderstraat (**Charlotte P.**), Rue van Orley (**Eva, Philip, Barbie, Nina Sara** and so many more), Avenue Recordon (**Gabrielle** & your awesome pizza recipe, **Poussin, David** and my other EPFL friends), Hofackerstrasse (**Aga, Willy**), Falkensteinerstrasse (**Greg**), Chassestraat (**Hans**) and Haarlemmer Houttuinen (**Yv**); I lived with and met amazing people. **Yvonne**, you were my flatmate during most of my Ph.D., thanks for all the endless conversation about career choices, our (disappointing) dating life and our shared love for wine, cheese and Italian food. **Charlotte C.**, from the moment we were dancing on the table of Café Stiels, I knew we would become successful ;), thanks for sticking around. Thanks to all of you for helping me maintain my social life during my Ph.D. and for celebrating with me now that it's over.

My paranyms: **Thijs** en **Guus**, my male and female BFF ;), I am so happy that you will stand next to me during the defence. I am sure that if I faint, you are the perfect combination of creativity, engineering and 'slap gelul' to answer the questions of my opponents. I met both of you at the Nix Boven Negen more than a decade ago. Out of the nearly eleven years, I've known you both, we lived together for five. We've seen each other at our best and at our worst, we've laughed with each other (and at each other), and yelled at each other, we went on holidays and to festivals together and spent more drunken nights that I can remember together. Thank you for sharing this day with me.

I also want to thank my brother **Jacob** and sister **Hedwig**. Growing up with these brainiacs, I was never the smartest, but it taught me to work hard and smart. I learned how to study early on in my life, which I always profited from. I am grateful for all the challenging conversations, games, trips and shared experiences (the good and the bad). Also Jacob, thanks for travelling with me to Indonesia, when I really needed a holiday but was too scared to travel alone (a fear that I overcame just recently by travelling to Colombia alone). Finally, I want to thank my parents for supporting me in everything I do. Thank you for always encouraging me in all my foreign adventures and for moving all my stuff across Europe multiple times. **Mom**, thanks for dragging us in and out of museums for a good part of our childhood. I'm sure it played some role in my love of art. **Dad**, thanks for sitting with me until I finally understood the basics of physics, if you hadn't I probably would not have gone to TU Delft in the first place.

Thank you all!

Curriculum Vitae

Birgit Anne van Driel was born in Heemstede in 1988. After attending several elementary schools in the Netherlands, France, and Morocco, she attended Atheneum College Hageveld from 2000 to 2006. She got her 'VWO' degree in the natural science direction ('Natuur en gezondheid') with additional courses in French, History, and Arts. For her final project ('profielwerkstuk') on why the use of flash is prohibited in the Sistine chapel, she received the school price for best project in the science category.

Birgit originally started studying Industrial Design at Delft University of Technology (TUD) in 2006. She switched to Molecular Science and Technology (MST) at the same university the next year. During her bachelor, she followed 30 ECTS in Arts Science and Archaeology at the Free University of Brussels (VUB), and she spent one year on the board of the study association for chemical engineering. She concluded the bachelor (majoring in chemical engineering) in March 2012, with a bachelor thesis project researching titanium white, under the supervision of Joris Dik (graded 9/10). Before starting her Master, Birgit worked at the European Patent Office as a patent examiner assistant. Birgit did a in Masters Materials, Science & Engineering at the Ecole Polytechnique Fédérale de Lausanne (EPFL) between September 2012 and March 2014. During this time she participated in a research project (graded 6/6) about photocatalytic titanium dioxide, which in 2017 resulted in a paper. She also participated and won, the EPFL 'lab-in-a-tube' competition, in which a flexible sensor for blood temperature and flow had to be developed within a multidisciplinary team (graded 6/6). Furthermore, she did an internship at the Museum of Modern Art working with the M6 Jetstream MA-XRF, and she conducted the research for her master thesis at BASF in Basel working on microfluidics (graded: 6/6). In May 2014, Birgit started her Ph.D. project on titanium white containing oil paints at the Rijksmuseum, in collaboration with and under the supervision of Delft University, the Cultural Heritage Agency of the Netherlands (RCE) and AkzoNobel. During her Ph.D., Birgit supervised multiple students (high school, BSc., MSc), presented her work at international conferences and published several papers. Additionally, she participated in the TedXDelft Awards in 2016, in which she reached the finals.

Outside of work, Birgit likes to cook, eat (cheese), travel the world (with a backpack), hike or bike, read and binge watch Netflix. During her Ph.D. she visited Indonesia, Cuba, and Colombia.

Birgit aims to pursue a career outside of academia.



